# DEVELOPMENT OF SILVER CATALYSTS FOR THE HETEROCYCLIZATION REACTIONS OF ALKYNES

## WONG HUI LIN VALERIE

## NATIONAL UNIVERSITY OF SINGAPORE

## 2014

# DEVELOPMENT OF SILVER CATALYSTS FOR THE HETEROCYCLIZATION REACTIONS OF ALKYNES

## WONG HUI LIN VALERIE
*(B.Sc.,(Hons.), NUS)*

## A THESIS SUBMITTED FOR THE DEGREE OF DOCTOR OF PHILOSOPHY

## DEPARTMENT OF CHEMISTRY

## NATIONAL UNIVERSITY OF SINGAPORE
## 2014

# DECLARATION

I hereby declare that this thesis is my original work and it has been written by me in its entirety, under the supervision of Prof. Hor Tzi Sum Andy, Chemistry Department, National University of Singapore, and Dr. King Kuok (Mimi) Hii, Chemistry Department, Imperial College London, between 08/2010 and 07/2014.

I have duly acknowledged all the sources of information which have been used in the thesis.

This thesis has also not been submitted for any degree in any university previously.

The content of the thesis has been partly published in:

1) Valerie H. L. Wong, T. S. Andy Hor and King Kuok (Mimi) Hii. *Chem. Commun.* **2013**, *49*, 9272–9274.


| | | |
|---|---|---|
| Name | Signature | Date |

# Summary

This PhD thesis describes work undertaken to develop efficient silver(I) catalysts for the intramolecular reactions of alkynes with nitrogen and oxygen containing nucleophiles for the synthesis of heterocycles. The introductory chapter provides an overview of recent advances in silver-catalyzed heterofunctionalization reactions of alkynes, with a focus on reactions involving C-N and C-O bond formations. A summary of the catalytic applications of silver(I) NHC catalysts in the literature, which will be explored in Chapter 4, is also provided.

Chapter 2 begins with the screening of silver salts as catalysts for the intramolecular hydroamination of alkynes with trichloroacetimidates. A strong counteranion effect on selectivity was observed. The impact of employing silver(I) complexes with variety of *P*- and *N*- donor ligands on catalytic activity was also explored, where pyridine-ligated silver salts showed superior activity and selectivity. Reaction optimization was undertaken, and 1-bromoalkyne substrates were effectively cyclized with catalytic loadings as low as 1 mol%.

In Chapter 3, the application of the pyridine-ligated silver salts developed in Chapter 2 as catalysts for the cycloisomerization of propargyl amides is described. A broader substrate scope was observed compared to the previously reported $AgSbF_6$ catalyst and a mechanism for the reaction is proposed based on

experimental observations. In Chapter 4, the synthesis and characterization of a new class of silver(I) NHC carboxylate complexes are presented. The activity towards the cycloisomerization of propargyl amides was investigated, and they showed complementary reactivities compared to the pyridine-ligated silver catalysts in Chapter 3. In Chapter 5, an overall conclusion and future work are discussed.

The last Chapter contains experimental procedures and characterization data of all the compounds synthesized during the course of this project.

# Acknowledgements

I would like to thank my supervisors, Prof. Andy Hor and Dr. Mimi Hii, for their guidance and patience throughout my PhD. Without them, the completion of this thesis would not have been possible. I would also like to thank my lab mates from both NUS and the Barton Lab at Imperial. It is my pleasure to work in such an encouraging and positive environment. I am also grateful to the following staff from the department of chemistry at Imperial College for their help: Dr. Andrew White for his X-ray crystallography analysis; Mr. Dick Sheppard and Mr. Peter Haycock for their NMR service; and Dr. Lisa Haigh for her mass spectrometry service. Lastly, financial support in the form of the NUS research scholarship is gratefully acknowledged.

# Table of Contents

# List of Tables

# List of Figures

# List of Abbreviations

| | |
|---|---|
| Ar | aryl |
| Bn | benzyl |
| $^{n}$Bu | primary butyl |
| $^{t}$Bu | tertiary butyl |
| bpy | 2,2'-bipyridine |
| CSD | Cambridge Structural Database |
| DABCO | 1,4-diazabicyclo[2.2.2]octane |
| DBU | 1,8-diazabicyclo[5.4.0]undec-7-ene |
| DCE | 1,2-dichloroethane |
| DMAP | 4-dimethylaminopyridine |
| DMF | *N*,*N*-dimethylformamide |
| DMSO | dimethyl sulfoxide |
| FABA | *tetrakis*(pentafluorophenyl)borate) |
| IAd | 1,3-*bis*(1-adamantyl)imidazol-2-ylidene |
| IMes | 1,3-*bis*-(2,4,6-trimethylphenyl)imidazol-2-ylidene |
| IPent | 1,3-*bis*(2,6-di(3-pentyl)phenyl)imidazol-2-ylidene |
| IPr | 1,3-*bis*(2,6-diisopropylphenyl)imidazol-2-ylidene |
| $^{i}$Pr | isopropyl |
| MOM | methoxymethyl |
| NHC | *N*-Heterocyclic Carbene |
| OAc | acetate |
| OBz | benzoate |
| phen | 1,10-phenanthroline |
| PMP | 4-methoxyphenyl |
| PTSA | *p*-toluenesulfonic acid |
| Py | pyridine |
| SIMes | 1,3-*bis*-(2,4,6-trimethylphenyl)imidazolin-2-ylidene |
| SIPr | 1,3-*bis*(2,6-diisopropylphenyl)imidazolin-2-ylidene |
| TBDPS | *tert*-butyldiphenylsilyl |
| Tf | trifluomethanesulfonate |
| TFA | trifluoroacetate |
| THF | tetrahydrofuran |
| TLC | thin-layer chromatography |
| TMAO | Trimethylamine *N*-oxide |
| TMS | trimethylsilyl |
| tol | 4-methylphenyl |
| Ts | *p*-toluenesulfonyl |
| XPS | X-ray photoelectron spectroscopy |

# List of Publications and Conference Presentations

1. <u>Wong, V. H. L.</u>; Hor, T. S. A.; Hii, K. K. "Silver-catalyzed intramolecular hydroamination of alkynes with trichloroacetimidates" *Chem. Commun.* **2013**, *49*, 9272–9274.

2. <u>Wong, V. H. L.</u>; White, A. J. P.; Hor, T. S. A.; Hii, K. K. "Ligand Effect and Control of *E*- and *Z*-Selectivity in the Silver-Catalyzed Synthesis of 4-Bromooxazolines" *Org. Lett.* **2015**, Manuscript submitted.

3. <u>Wong, V. H. L.</u>; Hii, K. K. "Silver(I)-Catalyzed Intramolecular Hydroamination of Alkynes with Trichloroacetimidates" 18th European Symposium on Organic Chemistry (ESOC), Marseille, France, July 2013.

4. <u>Wong, V. H. L.</u>; Hii, K. K. "*N*-Heterocyclic Carbene-Silver(I) Carboxylate Complexes: Synthesis and Catalytic Application" VII International School on Organometallic Chemistry, Universitat Autònoma de Barcelona (UAB), Spain, June 2014.

# Chapter 1 Introduction

## 1.1 The Role of Silver Salts in Gold Catalysis

Over the last decade, gold compounds have been extensively studied due to their superior catalytic activity in various organic transformations. [1] In particular, cationic gold(I) complexes bearing *N*-heterocyclic (NHC) carbene or phosphine ancillary ligands have shown remarkable reactivity in various organic transformations compared to classic "neutral" gold salts. [2,3] Their superior catalytic efficiency is apparent in several processes, such as the electrophilic activation of alkynes towards nucleophiles, where good chemoselectivities and yields can be obtained with low catalytic loadings of 0.1 to 1 mol%. On the other hand, the use of neutral gold salts often requires a higher loading (1−10%) and, in some cases, elevated temperatures to achieve similar conversions.[4]

Currently, the preparation of these cationic species is achieved predominantly by the treatment of gold(I) and gold(III) chloride salts or complexes with the corresponding silver salt, which effectively introduces a new, weakly coordinated and thus labile anion on the gold center. Silver salts have often been viewed as innocent anion exchange agents for the generation of cationic gold catalysts, as long as the silver salts cannot catalyze the reaction. Furthermore, it has also been assumed that the silver chloride byproduct formed as a result of the anion metathesis reaction precipitates out of solution quantitatively, and a filtration step will remove it completely from the reaction mixture.
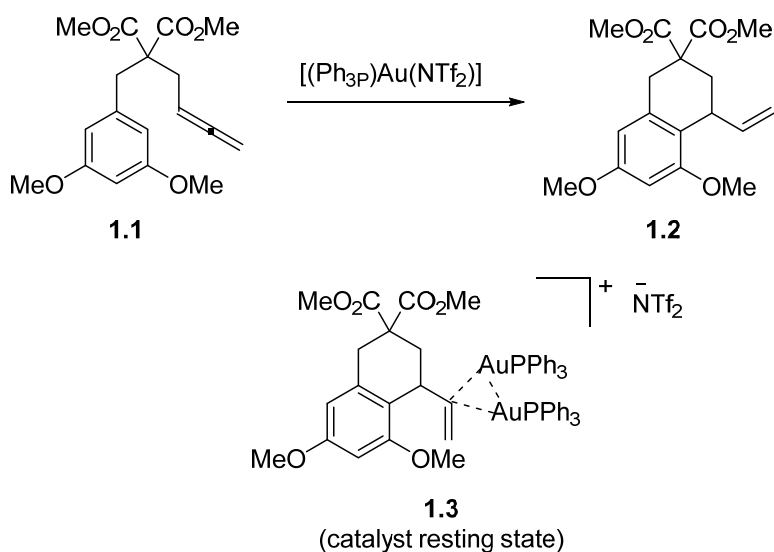
**Scheme 1.1.** Digold catalyst resting state in the intramolecular hydroarylation of allenes catalyzed by [(Ph₃P)Au(NTf₂)]
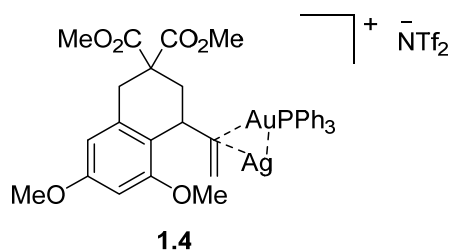


**Fig. 1.1.** Proposed mixed Au-Ag intermediate **1.4** formed in the intramolecular hydroarylation of allenes catalyzed by [(Ph₃P)AuCl]/AgNTf₂

However, the role of silver in gold-catalyzed reactions has recently been questioned. Known as the "silver effect" in gold catalysis, experimental evidence have shown a distinct influence of silver on gold-catalyzed reactions. In 2009, Gagné and co-workers reported the observation of a digold catalyst resting state **1.3** in the catalytic intramolecular hydroarylation of allene **1.1** to give **1.2** (Scheme 1.1).[5] However, when the catalyst was generated *in situ* from a 1:5 mixture of Ph₃PAuCl/AgNTf₂ (5 mol%/25 mol%), the reaction proceeded just as efficiently, although a different catalyst resting state was

observed.[6] It was formulated as the mixed Au–Ag species **1.4** (Fig. 1.1), based on $^1$H and $^{31}$P NMR spectroscopic data. It was also found that **1.3** could be converted to **1.4** in the presence of 3 equivalents of AgNTf$_2$, hinting at the possibility of Ag(I) ions intercepting Au(I) catalytic intermediates in the reaction mixture, with a possible impact on reaction kinetics. Indeed, at a catalytic loading of 5 mol% of [(Ph$_3$P)Au(NTf$_2$)], the rate of reaction was significantly decreased when a three-fold excess of AgNTf$_2$ was added to the reaction mixture, showing that the mixed-metal dinuclear species may have their own unique reactivity.
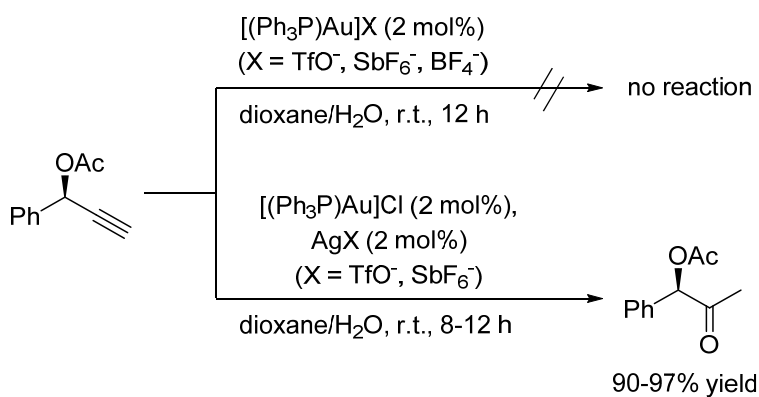


**Scheme 1.2.** Hydration of propargyl esters

Shi and co-workers also obtained conflicting results with those previously reported by Sahoo *et al.*[7] with regards to the ability of cationic gold(I) catalysts [(Ph$_3$P)Au]X to promote the hydration of propargyl esters[8] (Scheme 1.2). They found that when an additional step involving filtration of the [(Ph$_3$P)AuCl]/AgX (X = TfO$^-$, SbF$_6^-$, BF$_4^-$) catalytic mixture through Celite was taken prior to addition of the substrate, the catalytic reaction did not proceed. However, if the mixture of [(Ph$_3$P)AuCl]/AgX was used directly, the reaction proceeded in good yields. Analysis of the catalytic mixtures after

Celite filtration by X-ray photoelectron spectroscopy (XPS) revealed the absence of any silver, implying that in certain cases, a combination of both gold and silver was essential to make catalysis possible. Further evidence for the formation of different species in solution in the presence of silver ions was provided by ^{31}P NMR.
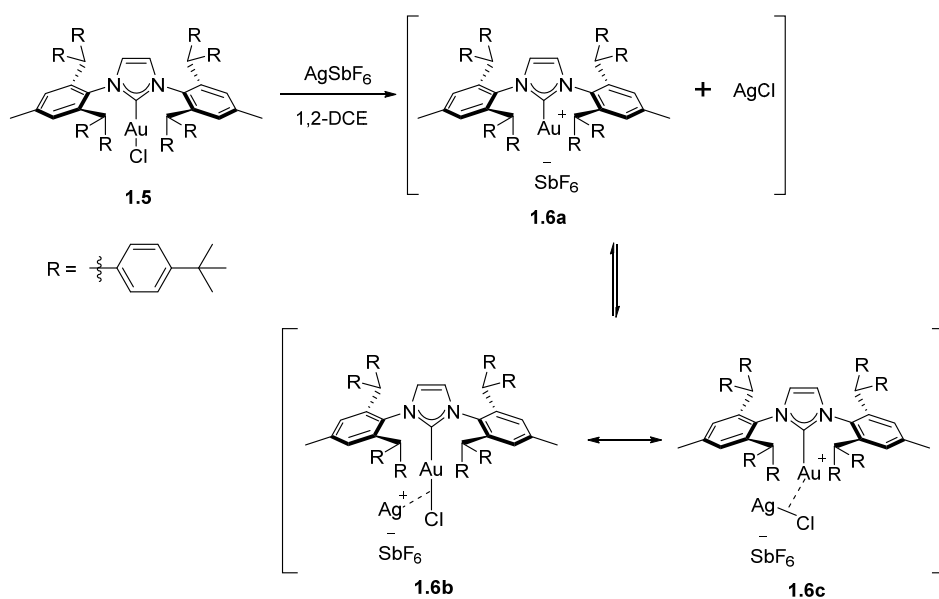


**Scheme 1.3.** Preparation of the IPr**AuCl–AgSbF$_6$ intermediate

Having successfully prepared an extremely bulky *N*-heterocyclic carbene ligand, IPr**, and its corresponding gold(I) chloride complex (**1.5**), Straub and co-workers took advantage of the steric shielding of the IPr** ligand to probe the structure of cationic gold(I) intermediates generated from chloride abstraction by silver salts.[9] A solution of complex **1.5** in DCE was added to AgSbF$_6$, and the mixture was filtered through Celite was carried out to remove the AgCl. Removal of the solvent *in vacuo* yielded a colorless solid, which was crystallized from CD$_2$Cl$_2$. Single crystal X-ray diffraction studies of crystals grown from the filtrate revealed the formation of a silver(I)-

4

coordinated gold(I) chloride complex with a triangular Ag–Cl–Au fragment (Scheme 1.3, compounds **1.6b** and **1.6c**). This result shows that silver cation-gold chloride adducts which are soluble in organic solvents may form during the chloride abstraction step, which can result in the retention of small amounts of silver in solution even after filtration through Celite – a procedure previously thought to remove all traces of silver ions in solution. More importantly, these adducts may account for the observed differences in activity and selectivity of catalyst reaction mixtures generated by the different protocols.
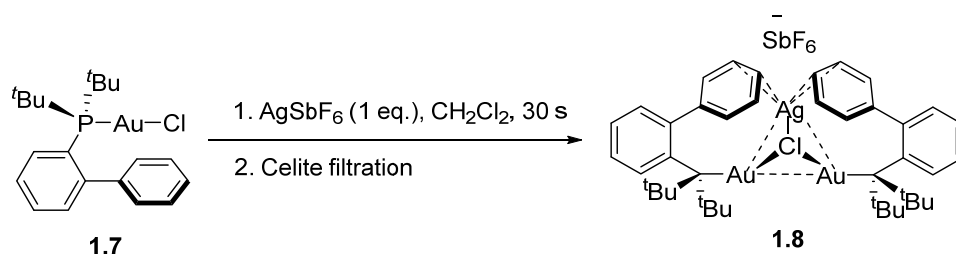


**Scheme 1.4.** Preparation of $[\{Au(JohnPhos)\}_2(\mu\text{-Cl})Ag][SbF_6]$

The interference of silver(I) in gold(I) catalysis was also recently demonstrated by the isolation of a chloride-bridged trimetallic dication with a bimetallic gold/silver core (**1.8**) generated from a mixture of the neutral complex [(JohnPhos)AuCl] (**1.7**) and AgSbF$_6$, followed by a quick filtration through Celite (Scheme 1.4).[10] It was also found that the precipitation of AgCl is a slow process: Little to no AgCl precipitates when the filtration is done immediately; approximately half is removed if filtration is done within 5 minutes; and a trace (1-3%) remains even after stirring for 20 h. The solid state structure of **1.8** gives a snapshot of the early stages of halide abstraction and possibly provides clues to the mechanism by which silver can be

5

reincorporated into catalyst structures. It is possible that the formation of **1.8** is driven by the instability of the initially formed [(JohnPhos)Au]SbF$_6$, which is stabilized by coordination to remaining [(JohnPhos)AuCl] to give the binuclear structure in **1.8**.



**Fig. 1.2.** Gold complexes that do not require activation by silver salts

R$^1$ = R$^2$ = Mes (**1.15a**)
R$^1$ = R$^2$ = $^t$Bu (**1.15b**)
R$^1$ = Me, R$^2$ = Et (**1.15c**)

**1.16**

**1.17a**          **1.17b**
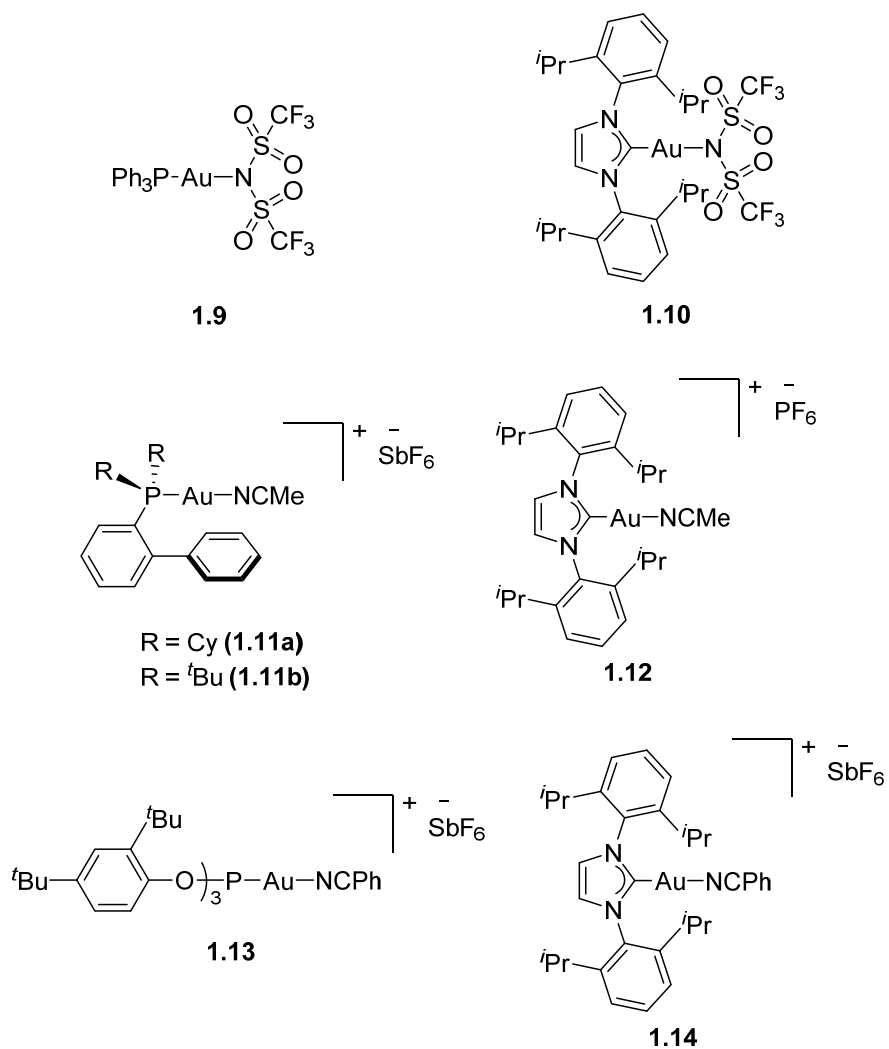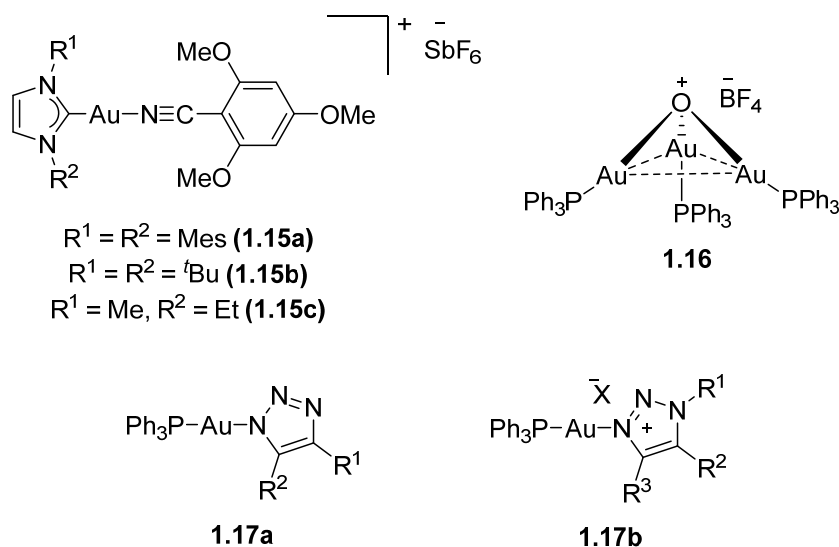
**Fig. 1.2. cont'd** Gold complexes that do not require activation by silver salts.

Driven by the ambiguous role of silver ions in gold catalysis, there is a growing trend towards the development of alternative routes for 'silver-free' gold catalysis. As a result, several cationic Au(I) complexes have been prepared (Fig. 1.2) that are stabilized by an inner sphere counteranion[11,12] (**1.9** and **1.10**), solvent molecule[13,14] (**1.11a,b** and **1.12**), benzonitrile ligands[15] (**1.13**, **1.14**, **1.15a-c**), oxonium center[16,17] (**1.16**) or triazole ligand[18] (**1.17a,b**), and do not require activation by silver salts. They have also demonstrated good catalytic efficiency towards organic transformations. However, the preparation of these complexes still require the use of a silver salt, and more economically viable methods that would completely eliminate the use of silver salts in both the synthesis and activation steps are needed.

$$[(R_3P)AuMe] + CH_3SO_3H \longrightarrow [(R_3P)Au][CH_3CO_3] + CH_4$$
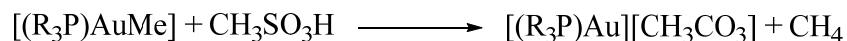
**Scheme 1.5.** Activation of a phosphine gold(I) methyl complex by a strong acid

To date, only three such alternative methods have been developed, and they each have their limitations and disadvantages. The first strategy involves the protonation of phosphine Au(I) methyl complexes [R$_3$P-Au-Me] with strong acids such as methanesulfonic acid,[19] to liberate methane and the cationic complex (Scheme 1.5). The resulting cationic catalysts are robust and stable to air and moisture, and show good activities towards the intermolecular addition of alcohols to alkynes. However, the harsh acidic conditions required are incompatible with organic transformations that involve acid-sensitive substrates.
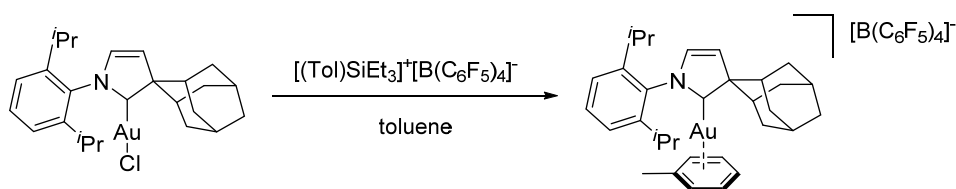


**Scheme 1.6.** Activation of a carbene gold(I) chloride complexes by a silylium salt

The second method involves using alternative halide abstracting reagents. Bertrand and co-workers have used the silylium salt [(Tol)SiEt$_3$]$^+$[B(C$_6$F$_5$)$_4$]$^-$ (Tol = toluene)[20,21] to obtain the cationic gold(I) complex of the cyclic (alkyl)(amino)carbene (CAAC) ligand (Scheme 1.6).[22] The resulting cationic complex is indefinitely stable in solution and in the solid state, and shows good activity towards the cross-coupling of enamines and alkynes. The only disadvantage is the non-trivial synthesis of the silylium reagent.
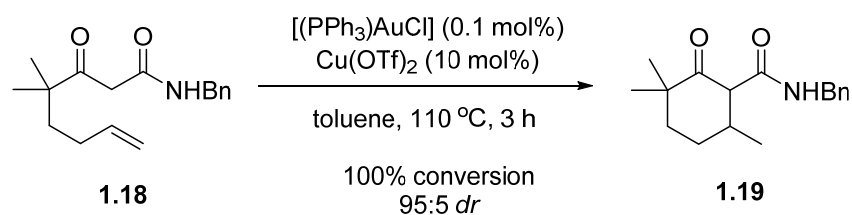
**Scheme 1.7.** Intramolecular hydroalkylation of ene-$\beta$-ketoamides catalyzed by [(Ph$_3$P)AuCl]/Cu(OTf)$_2$

Bezzenine and Gandon have also recently reported that Lewis acids such as the triflate salts of Cu(I), Cu(II), Zn(II), In(III) and Bi(III), and trimethylsilyl triflate can act as activators.[23,24,25] The use of Cu(OTf)$_2$ as an activator was compatible with the use of chiral phosphine, phosphite and NHC complexes of gold(I) and various reaction media, including water.[24] Surprisingly robust catalytic species can result, which outperform gold(I)/silver(I) combinations.[23] For instance, in the intramolecular hydroalkylation of ene-$\beta$-ketoamides, complete conversion of substrate **1.18** occurred at high reaction temperatures and low catalytic loadings (Scheme 1.7), while only 28% conversion was achieved with AgOTf as the activator under identical conditions. However, the success of the Au(I)/Cu(II) catalytic system is highly dependent on the reaction being catalyzed; in certain instances silver salts are still better.[24] Moreover, the exact role of Cu(OTf)$_2$ in the reaction is still unknown, although the authors propose that it acts as a halide scavenger and undergoes slow anion metathesis with chloride of the gold(I) complex, delivering small amounts of cationic gold(I) catalytic species at a time, thus preventing fast decay of these highly reactive species. There is also the possibility of cooperative Au(I)/Cu(II) catalysis, which has not been ruled out. However, a disadvantage is the need to employ five- to ten-fold excess of the Lewis acid activator compared to silver salts, which were usually used in equal amounts or two-fold excess.
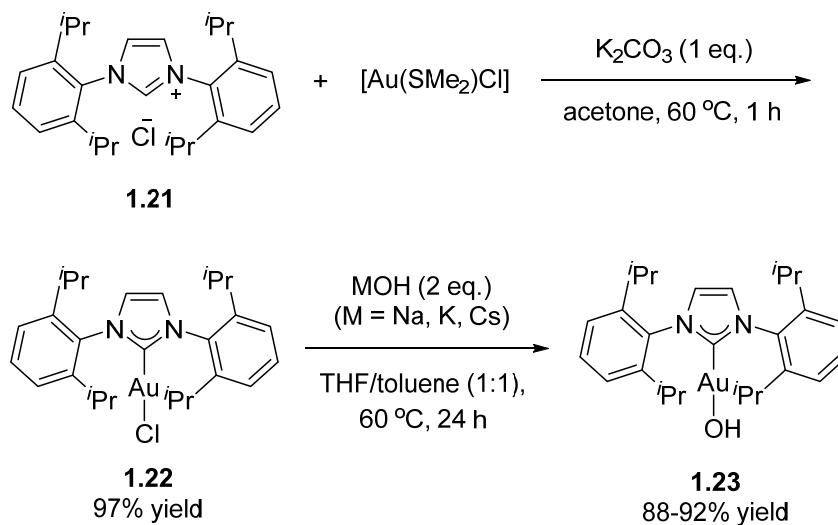
**Scheme 1.8.** Synthesis of [(IPr)Au(OH)] (**1.23**)

The third method involves the use of the "golden synthon" [(IPr)Au(OH)] (**1.23**) developed by the group of Nolan, which is an excellent precursor to several organogold compounds due to the presence of a basic hydroxide ligand (Scheme 1.8).[26] The synthesis of **1.23**[26] is simple and high yielding, and does not require an inert atmosphere.
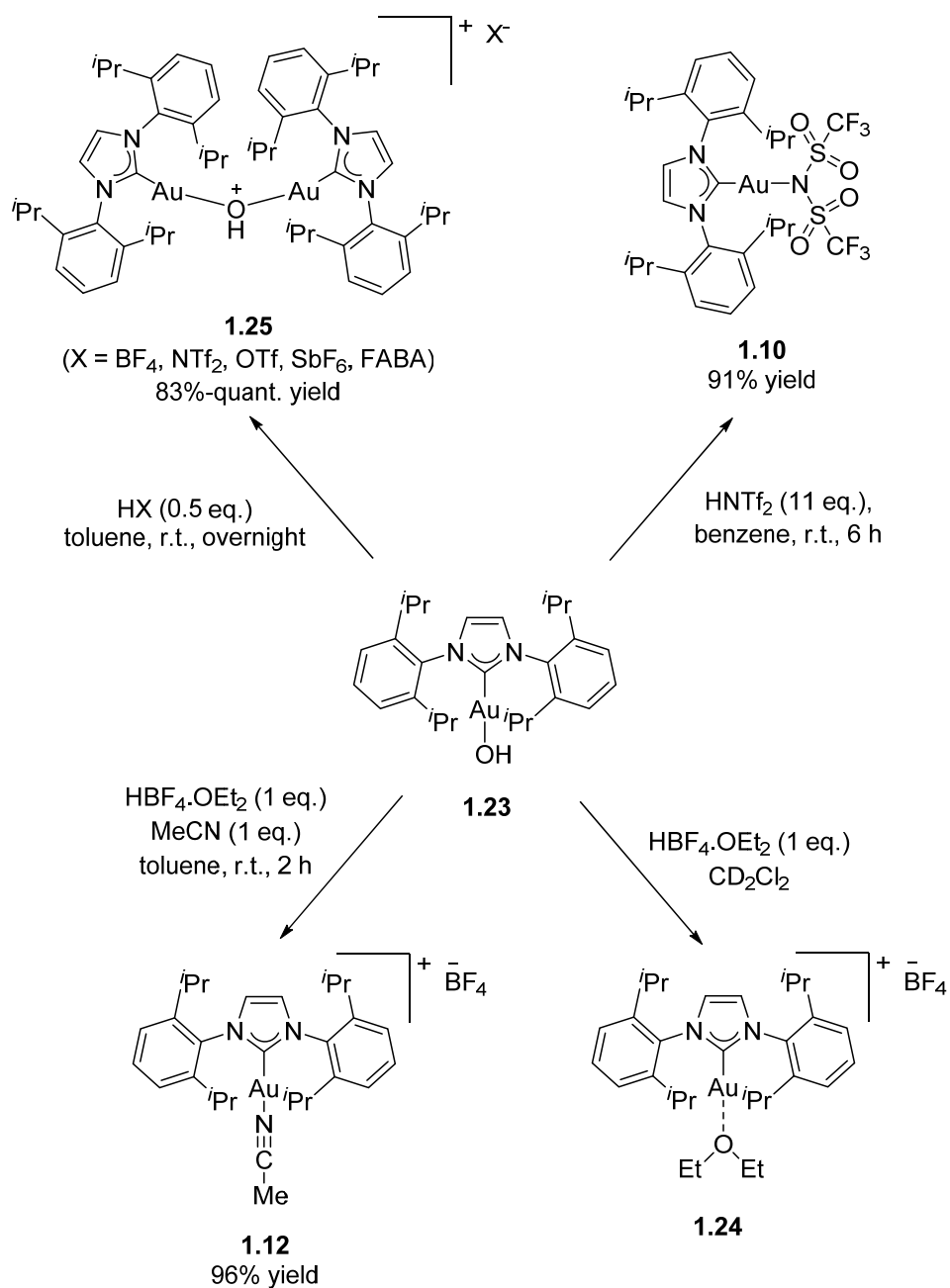
**Scheme 1.9.** Activation of [(IPr)Au(OH)] (**1.23**) by reaction with acids

Complex **1.23** is basic in nature, having a pK$_a$ value between 29 and 31. Thus, it can be activated by protonolysis with acids (Scheme 1.9). The reaction of **1.23** with trifluoromethanesulfonimide (HNTf$_2$) enabled access to complex **1.10** via a silver-free synthetic route in excellent yield. The solvent-stabilized cationic Au(I) complexes [(IPr)Au(solv)][BF$_4$] (solv = Et$_2$O (**1.24**), MeCN

(**1.12**)) can also be generated *in situ* by the reaction of **1.23** with HBF$_4$·OEt$_2$, and have shown good activities in the 3,3'-rearrangement of allylic acetates and Beckmann-type rearrangement reaction of aldoximes.[27] If an aqueous solution of HBF$_4$ is used, the $\mu$-hydroxy-bridged dinuclear species [{Au(IPr)}$_2$($\mu$-OH)][X] (X = BF$_4$, NTf$_2$, OTf, SbF$_6$, FABA) **1.25** are formed. The stability of these complexes in aqueous media has been exploited in gold-catalyzed reactions involving water, such as the hydration of nitriles and alkynes.[28] Although **1.23** provides an elegant silver-free approach to the synthesis of [(IPr)Au]$^+$, it is not a general strategy that can be easily extended to other ligands than IPr. At this point, the stability of Au(I) hydroxide complexes of other ancillary ligands such as phosphines, or even similar NHC ligands are yet unknown. Thus, if enantioselective gold catalysis is the aim and chiral ligands are required, activation by silver salts might still be the best method to generate the catalytically active cationic gold species.

## 1.2 Silver-Catalyzed Heterocyclization Reactions of Alkynes

While homogeneous gold catalysis has emerged as one of the most powerful tools in organic synthesis in the last decade, the use of silver catalysts in organic synthesis is also well-documented.[29] However, the utility of silver in the field of chemical catalysis has largely been overshadowed by the success of gold, and it has mainly assumed the role of a co-catalyst/halide scavenger in gold-catalyzed transformations. However, the recent revelations of the non-innocent role of silver in gold catalysis have had an impact on the interpretation of the results of gold-catalyzed reactions. Indeed, the silver salt employed for the generation of cationic gold species may sometimes act as a

catalyst in its own right. Indeed, as we will discuss in this section, silver salts are active catalysts for the addition of nucleophiles of alkynes, and also sometimes exhibit different reactivity patterns from gold catalysts.

The study of heterocycles constitutes one of the largest areas of research in organic chemistry, due to their immense importance in biological systems and in industry, where they are frequently found as key structural units in pharmaceuticals and agrochemicals. Much effort has thus been devoted to developing new and efficient methods for their synthesis, including the application of metal-catalyzed processes. [30] The metal-catalyzed heterocyclization of alkynes provides an efficient and atom-economical route for the assembly of heterocycles.
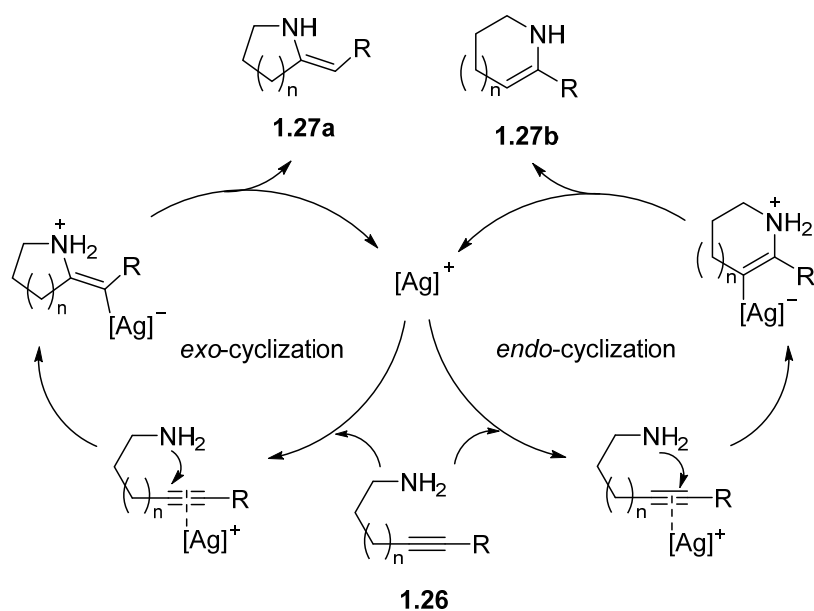


**Scheme 1.10.** General mechanism of a silver(I)-catalyzed intramolecular hydroamination reaction

13

Silver(I) species, which are good π-Lewis acids,[31] form favorable interactions with unsaturated systems such as alkynes. The generally accepted mechanism for these transformations is illustrated using the intramolecular hydroamination reaction as an example in Scheme 1.10. This involves the initial interaction of the alkyne (**1.26**) with the π-acidic silver catalyst, which reduces the electron density of the triple bond, rendering it electrophilic and susceptible to nucleophilic attack by the heteroatom to generate an organosilver intermediate, which then undergoes protodemetallation to give the heterocyclic product. It is important to note that the issue of regioselectivity can arise in the cyclization step, as the nucleophile can add to either carbon atom of the alkyne to give the *exo-* or *endo-*cyclized product **1.27a** and **1.27b,** respectively. The heteroaddition usually proceeds in an *anti* manner, such that only the *Z*-diastereoisomer of the *exo-*cyclized product **1.27a** is obtained.

In the following sections, silver(I)-catalyzed reactions of O- and N-nucleophiles with alkynes will be presented, based on literature reviews[32,33,34,35] and recent publications. The next section will be divided into two parts; the first devoted to the reactions involving oxygen nucleophiles, and the second to those with nitrogen nucleophiles. Mechanisms of these reactions will only be discussed only if they are significantly different from the general mechanism presented in Scheme 1.10, or if the cyclization step precedes another transformation, for instance, in tandem reactions. If the same reaction has been reported with gold catalysts, the differences between the two catalytic systems will be highlighted.

## 1.2.1 Oxygen nucleophiles

The various functional groups that can acts as oxygen nucleophiles are summarized in Fig. 1.3. These include alcohols, carboxylic acids, carbonates, and phosphates that contain $sp^3$-hybridized oxygen atoms; and aldehydes, ketones, amides and pyrimidine nucleobases that contain $sp^2$-hybridized oxygen atoms.
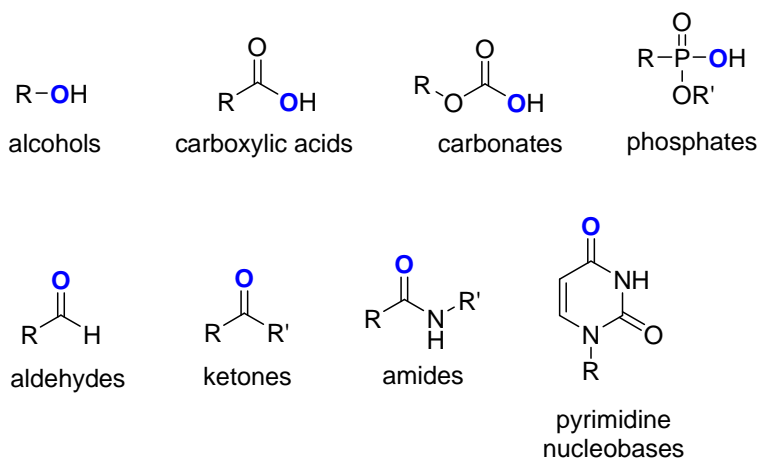


**Fig. 1.3** Functional groups containing nucleophilic oxygen atoms

### 1.2.1.1 Alcohols
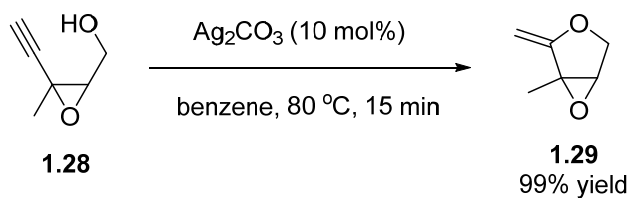


**Scheme 1.11.** Cyclization of acetylenic alcohol **1.28** to the functionalized 2-methylene oxolane **1.29**

The first example of a silver-catalyzed intramolecular cyclization of alcohols was reported in 1987 by Pale and Chuche.[36] The acetylenic epoxy alcohol **1.28**

15

was effectively cyclized to the functionalized 2-methylene oxolane **1.29** in the presence of silver carbonate (Scheme 1.11). Subsequently, it was found that only silver salts having a basic counteranion, such as acetate, oxide and carbonate, were effective towards the transformation. In contrast, silver nitrate was inactive, while the more electrophilic silver tetrafluoroborate only led to decomposition. The reaction also proceeded well in most solvents, except protic solvents, which cause degradation of the product. The cyclization process was also regiospecific for the 5-*exo-dig* product. However, it was found that linear acetylynic alcohols without the epoxy group did not react, suggesting that the cyclization was highly dependent on the substrate, requiring that the hydroxyl and acetylenic units to be held in close proximity. Silylated alkynes also reacted poorly, unless a stoichiometric amount of catalyst was employed.[37]



$$R^1 = H$$
$$R^2 = OH, OMe, OMOM, O^tBu, OTBDPS$$
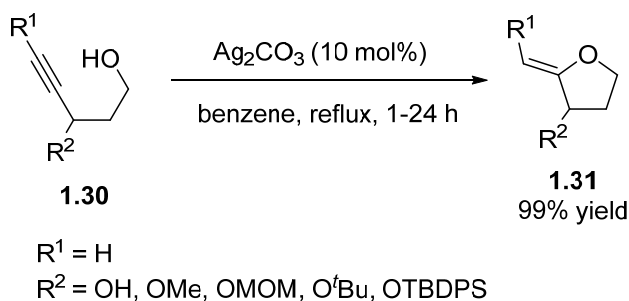
**Scheme 1.12.** Cyclization of acetylenic alcohols **1.30** with ether groups in the propargylic position (MOM = methoxymethyl, TBDPS = *tert*-butyldiphenylsilyl)

Ether groups at the propargylic position were found to lead to a dramatic acceleration of the cyclization rate (Scheme 1.12), possibly by altering the adjacent π-system through hyperconjugation. No reaction took place in their

absence or if they were replaced by an electron-withdrawing group such as acetate.[38]
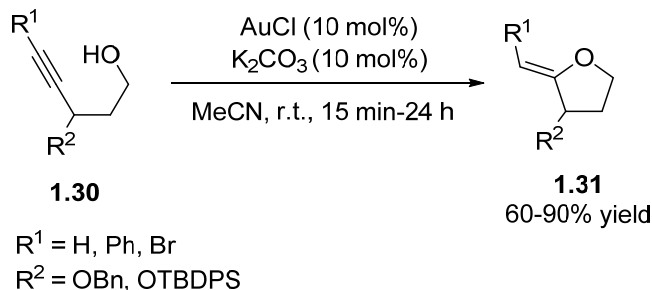


**Scheme 1.13.** Gold(I) chloride catalyzed cyclization of acetylenic alcohols **1.30**

It was later found that gold(I) chloride could also catalyze the reaction at 10 mol% catalytic loading in the presence of potassium carbonate (Scheme 1.13).[39] Neither gold(III) chloride nor the triphenylphosphine gold(I) complex [(Ph₃P)AuCl] were suitable catalysts. Similar to the silver-catalyzed reaction, oxygenated substituents in the propargylic position were required for good yields. Internal alkyne substrates where $R^1$ = Ph and Br also cyclized in good yields, but no reaction was observed when $R^1$ = TMS.
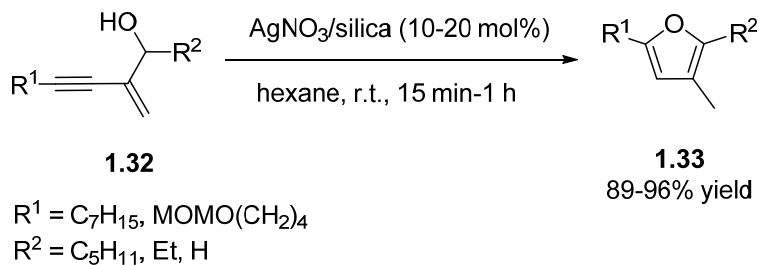


**Scheme 1.14.** Cyclization of β-methylene acetylenic alcohols **1.32** to furans **1.33**

The related *β*-methylene acetylenic alcohols **1.32** also undergo 5-*endo-dig* cyclization and aromatization to the corresponding furans **1.33** in the presence of silver nitrate adsorbed on silica (Scheme 1.14).[40] Other silver salts such as AgOTf, AgBF$_4$ and AgTFA also afforded the products in good yields, but AgNO$_3$ adsorbed on silica has the added advantage of recyclability. Non-polar solvents such as hexane were superior, as they increased the affinity of the polar alcohol towards the silica gel surface.
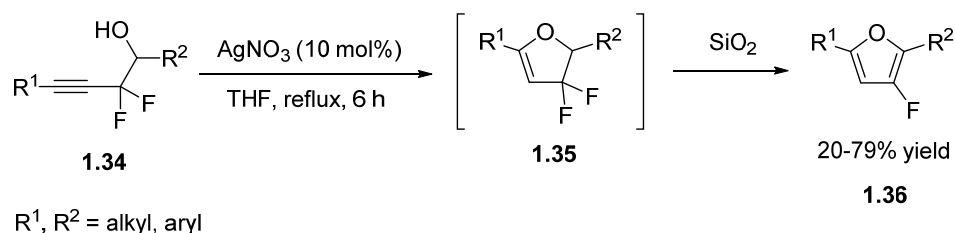


**Scheme 1.15.** Cyclization of *gem*-difluoropropargyl substituted acetylenic alcohols

The cyclization of *gem*-difluoropropargyl substituted acetylenic alcohols **1.34** using AgNO$_3$ enabled the formation of fluorinated furan derivatives. [41] Interestingly, gold(I) and gold(III) catalysts resulted in unsatisfactory yields and were unable to activate the electronically deficient triple bond. The reaction presumably proceeds via 5-*endo-dig* cyclization to the difluoro-4,5-dihydrofuran **1.35**, which aromatizes spontaneously to the more stable 4,5-dihydrofuran **1.36** after elution through silica gel. Both electron-withdrawing and electron donating aliphatic and aromatic groups are tolerated at R$^2$, but internal alkynes resulted in low to moderate yields.
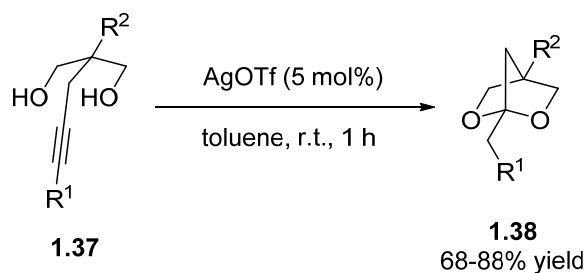
**Scheme 1.16.** Oxacyclization of homopropargylic diols to bicyclic ketals
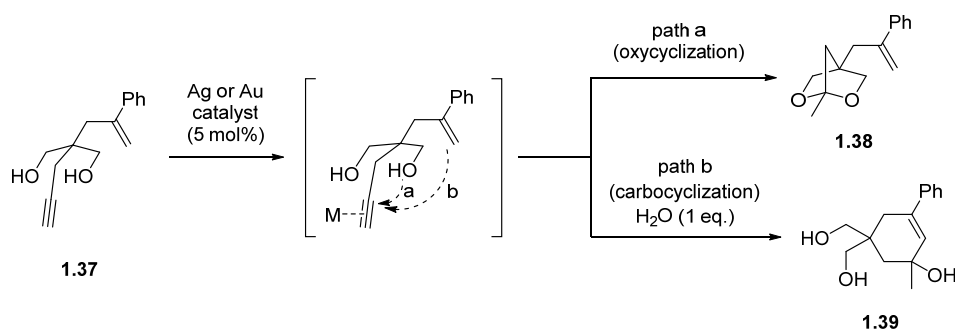


**Scheme 1.17.** Different reactivities of silver and gold catalysts towards the cyclization of homopropargylic diol **1.37**

Although the formation of five-membered rings seems to be preferred in most of the silver-catalyzed cyclization of acetylenic alcohols, conveniently chosen substrates can lead to six-membered heterocycles, as shown in Scheme 1.16.[42] AgOTf catalyzes the oxacyclization of homopropargylic diols **1.37**, providing convenient access to bicyclic ketals **1.38** bearing a functionalizable side chain. In comparison, cationic gold(I) and gold(III) catalysts generated *in situ* in the presence of AgOTf, however, resulted in low yields of the bicyclic ketals **1.38** in DCE. Addition of one equivalent of water to the reaction mixture, however, furnished the carbocyclized product **1.39** exclusively (Scheme 1.17). This observed difference in chemoselectivity was attributed to the higher Lewis acidity of gold(I) and gold(III) cations which resulted in activation of the alkyne towards nucleophilic attack by the softer alkene nucleophile. This is an

example of where the stronger π-Lewis acidity of gold complexes can be detrimental and result in undesired byproducts. In fact, this difference in π- and σ-Lewis acidity between silver(I) and gold(I) has recently been recognized and harnessed in the development of new cascade reactions.[43]



Reaction conditions for Ag(I)-mediated cyclization: AgOAc (1.26 eq.), Et$_3$N (1 eq.), acetone, r.t.
Reaction conditions for Au(III)-catalyzed cyclization: AuCl$_3$ (5 mol%), PTSA (10 mol%), CH$_2$Cl$_2$, r.t.
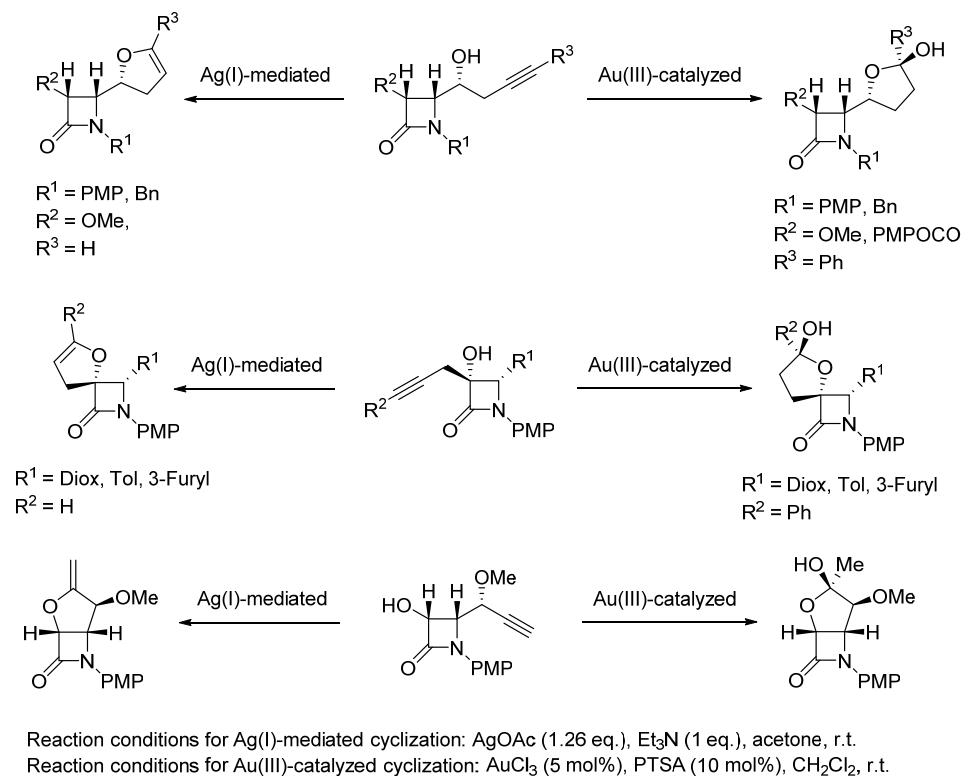
**Scheme 1.18.** Cyclization of 2-azetidinone-tethered alkynols. (Diox = (*S*)-2,2-dimethyl-1,3-dioxolan-4-yl, Tol = 4-MeC$_6$H$_4$

The differences in reactivity between Ag(I) and Au(III) is reinforced in the study by Alcaide and co-workers[44], who described the AgOAc and AuCl$_3$-mediated cyclization of 2-azetidinone-tethered alkynols to give different tetrahydrofuran-based *β*-lactams (Scheme 1.18). The reaction required a stoichiometric amount of AgOAc under basic conditions, while the reaction using AuCl$_3$ was carried out with a 5 mol% catalytic loading under acidic

20

conditions. Due to the higher Lewis acidity of AuCl$_3$ and the presence of the Brønsted acidic PTSA, intramolecular hydroalkoxylation, followed by hydration of the resulting alkene, was always observed with the Au(III) catalytic system.
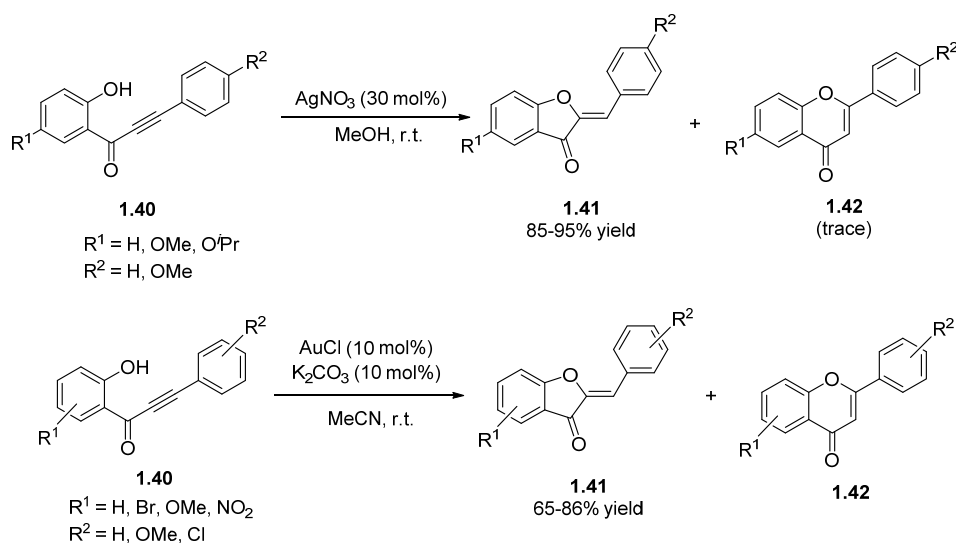


**Scheme 1.19.** Comparison of silver and gold catalysts in the cyclization of *o*-alkynoylphenols to aurones

*o*-Alkynoylphenols **1.40** may be cyclized to the corresponding aurones **1.41** in the presence of catalytic amounts of AgNO$_3$ in methanol (Scheme 1.19). The reaction proceeds with good regioselectivity towards the 5-*exo-dig* cyclized aurone products, as only traces of the 6-*endo-dig* cyclized flavones **1.42** were detected.[45] In the corresponding gold-catalyzed reaction reported several years later,[46] the aurone products were obtained in good yields and regioselectivities at a lower catalytic loading of 10 mol%. However, the addition of 10 mol% of K$_2$CO$_3$ was essential to deprotonate the phenol before it can participate as a nucleophile in the reaction. Other more soluble and Lewis acidic gold catalysts

such as $(Ph_3P)AuCl$, $(Ph_3P)AuCl/AgSbF_6$ and $AuCl_3$ were less effective than AuCl, resulting mainly in degradation products.

## 1.2.1.2 Carboxylic Acids
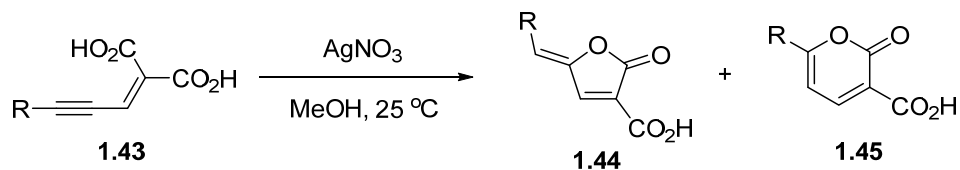


**Scheme 1.20.** Silver nitrate-mediated cyclization of acetylenic acids

The silver-mediated cyclization of acetylenic acids was first reported in 1958 by Castañer and Pascual (Scheme 1.20).[47] They observed that phenylpropargylidene malonic acid (**1.43**, R = Ph) could be converted to γ-benzylidene-α-carboxybutenolide (**1.44**, R = Ph) in the presence of stoichiometric amounts of silver nitrate at room temperature. Although aromatic propargylidene malonic acids afforded exclusively the butenolides **1.44**, their alkyl analogues (R = Me, $^{n}$Bu) resulted in mixtures of butenolides **1.44** and α-pyrones **1.45** in a variable ratio.[48]
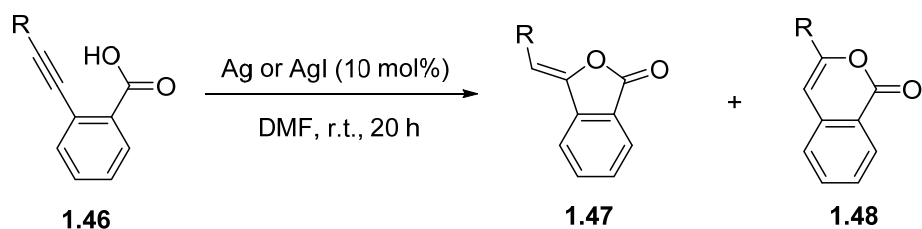
| R | Ratio of 1.47/1.48 |
|---|---|
| $^n$Hex | 86/14 |
| Cy | 90/10 |
| $^t$Bu | 98/2 |
| Ph | 100/0 |



| R | Ratio 1.50/1.51 |
|---|---|
| $^n$Hex | 96/4 |
| Cy | 97/3 |
| $^t$Bu | 98/2 |
| Ph | 98/2 |
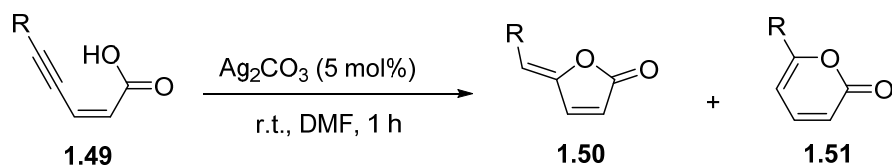
**Scheme 1.21.** Cyclization of $\alpha,\beta$-unsaturated acetylenic acids to furanones and pyranones using silver catalysts

Interest in the five-membered furanone-derivatives arising from their biological activities has stimulated research in the development of efficient methods to prepare these compounds. An example is the silver-catalyzed cyclization of $\alpha,\beta$-unsaturated acetylenic acids **1.46** and **1.49** (Scheme 1.21), which could potentially afford both the five-membered furanones **1.47** and **1.50** or six-membered pyranones **1.48** and **1.51**. Although factors affecting the pyranone/furanone ratio have not been clearly established, it is known that the ratio between the two products is strongly dependent on the substrate structure, the nature of silver salt employed, and the solvent.[49] Depending on

the substrate, the selectivity towards the five-membered furanone product may be increased by using either AgI or Ag in DMF at high dilutions,[50] or $Ag_2CO_3$ in DMF.[51]
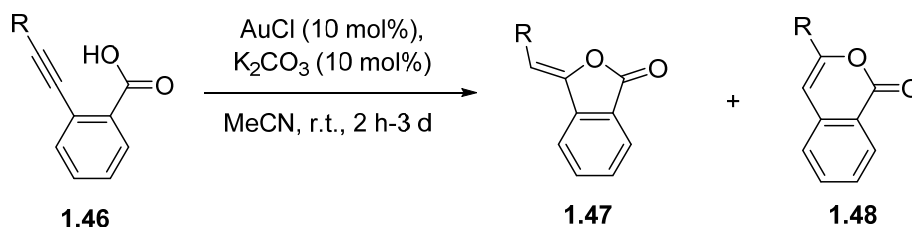


**Scheme 1.22.** Cyclization of $\alpha,\beta$-unsaturated acetylenic acids to furanones and pyranones using gold(I) chloride

The cyclization of **1.46** has also been attempted with AuCl (Scheme 1.22).[52] Although a direct comparison of the selectivities and yields with the silver-catalyzed reaction is not possible due to the different substrate scope examined, it appears that the use of AuCl does not offer much advantage over the use of silver salts. Similar to the silver-catalyzed reaction, 10 mol% of catalyst was also required; and in addition, a basic additive such as $K_2CO_3$ was also essential.
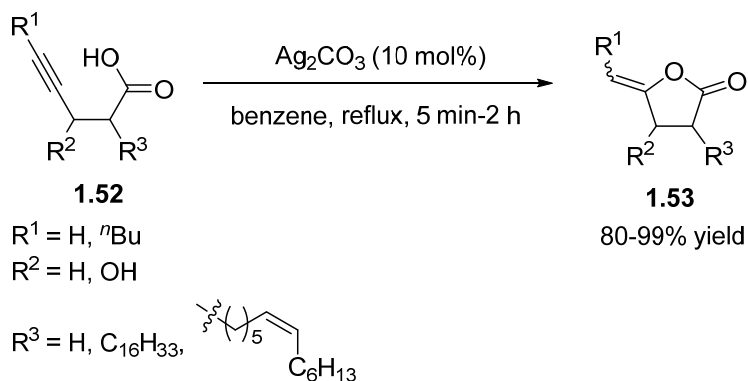


**Scheme 1.23.** Cyclization of saturated acetylenic acids to enol lactones using silver carbonate
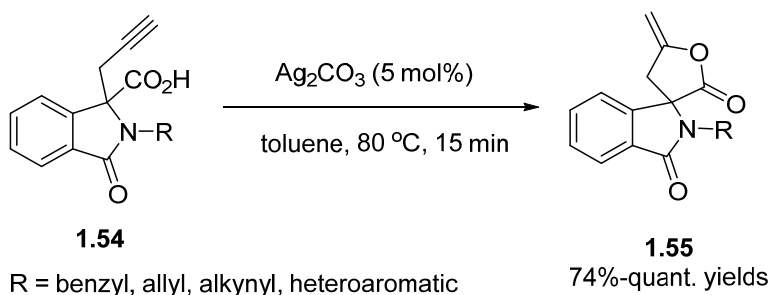
**Scheme 1.24.** Silver-catalyzed synthesis of γ-spirobutyrolactone derivatives

For the cyclization of saturated acetylenic acids **1.52**, the use of $Ag_2CO_3$ as a catalyst in aromatic solvents has proven to be most effective[37] (Scheme 1.23). The presence of oxygen-containing propargylic substituents also favored the cyclization.[39] The protocol can also be extended to the synthesis of γ-spirobutyrolactone derivatives **1.55** (Scheme 1.24).[53] Gold catalysts were recently employed for the same reaction. Using a gold(III) *N*-heterocyclic carbene (NHC) complex, 4-pentynoic acid (**1.52**, $R^1$, $R^2$, $R^3$ = H) was cyclized to the corresponding enol lactone **1.53** in quantitative yield (Scheme 1.25), as was previously obtained with $Ag_2CO_3$.[54] A lower catalytic loading of 2.5 mol% was sufficient for the gold-catalyzed reaction, and the reaction could be effected at room temperature. In comparison, the use of $AuCl_3$ and $AuCl$ salts only resulted in yields of 90% and 70% respectively under the same conditions, which highlights the ability of the NHC ligand to improve the reactivity of the gold catalyst.
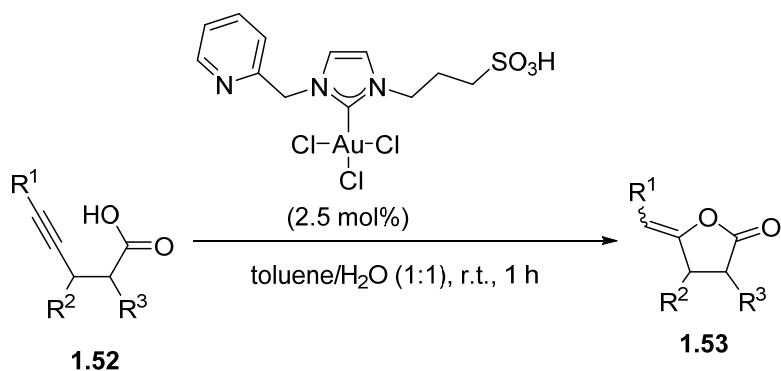
**Scheme 1.25.** Cyclization of saturated acetylenic acids to enol lactones using a gold(III) NHC catalyst.

### 1.2.1.3 Carbonates
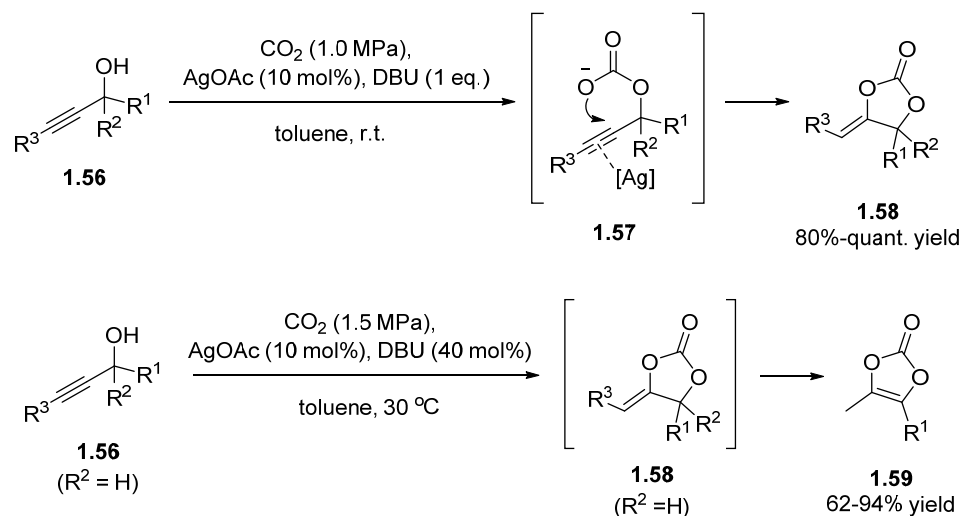


**Scheme 1.26.** Synthesis of cyclic carbonates **1.58** and vinylene carbonates **1.59**

In addition to acetylenic alcohols and carboxylic acids, acetylenic carbonates can also be used in heterocyclization reactions. In the presence of 10 mol% of silver acetate and 1 equivalent of DBU, acetylenic carbonates **1.57**, produced *in situ* by the incorporation reaction of carbon dioxide with tertiary propargylic alcohols **1.56**, afford the corresponding cyclic carbonates **1.58** in quantitative yields (Scheme 1.26).[55,56] Most of the silver salts were efficient in promoting this reaction. It is worth noting that gold was inactive for the

26

reaction, while copper salts only produced trace amounts of the cyclic carbonate. When a secondary propargylic alcohol **1.56** ($R^2 = H$) was used, reducing the amount of DBU could result in the sole formation of vinylene carbonates **1.59**, the more stable isomerized product of the cyclic carbonate **1.58** ($R^2 = H$).[57]
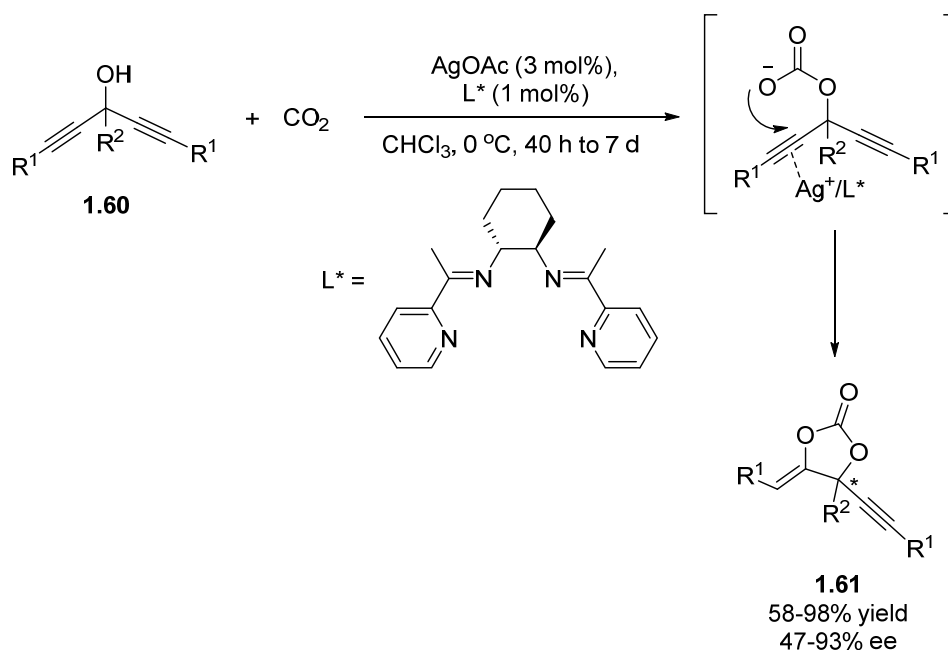


**Scheme 1.27.** Enantioselective carbon dioxide incorporation into bispropargylic alcohols, followed by silver-catalyzed cyclization

As an extension of this work, the combined catalyst system of AgOAc with a chiral Schiff base ligand (L*) achieved the asymmetric carbon dioxide incorporation into *bis*-propargylic alcohols **1.60** with desymmetrization to afford the corresponding cyclic carbonates **1.61** in good yields and enantiomeric excesses (Scheme 1.27).[58] However, long reaction times were required. DBU was not necessary for the reaction, as it results in a racemic product if added to the reaction mixture, presumably by blocking coordination

of the chiral ligand to the silver catalyst. ^{1}H NMR spectroscopic analysis suggested that the silver acetate and chiral ligand would form a corresponding 2:1 complex.

### 1.2.1.4 Phosphates
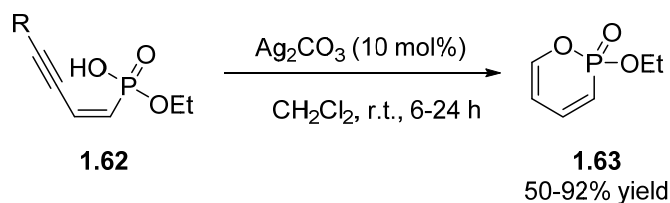


**Scheme 1.28.** Cyclization of acetylenic phosphonic acids to 2-pyrones

The cyclization of acetylenic phosphonic acids **1.62** to 2-pyrones **1.63** (Scheme 1.28) was reported for the first time in 2005, [59] with high regioselectivity and good yields in the presence of catalytic amounts of $Ag_2CO_3$. $AgNO_3$ gave comparable yields, but AgI was ineffective.

### 1.2.1.5 Aldehydes, Ketones and Amides
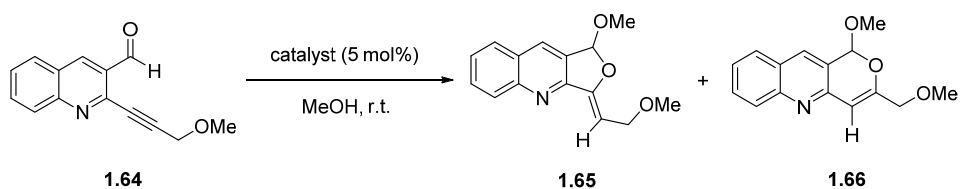


**Scheme 1.29.** Gold(I)- and silver(I)-catalyzed cyclization of *ortho*-alkynyl formylquinoline in the presence of methanol

28

**Table 1.1.** Comparison of the furoquinoline (**1.65**) to pyranquinoline (**1.66**) product ratio in the cyclization of *ortho*-alkynyl formylquinoline by various gold and silver catalysts

| Entry | Catalyst | Ratio 1.65/1.66 |
|-------|----------|-----------------|
| 1 | $AuCl_3$ | no conversion |
| 2 | [(Ph$_3$P)AuCl] | 0/100 |
| 3 | [(Ph$_3$P)AuCl]/AgSbF$_6$ | 0/100 |
| 4 | AgSbF$_6$ | 0/100 |
| 5 | AgPF$_6$ | 0/100 |
| 6 | AgOTf | 0/100 |
| 7 | AgNO$_3$ | 0/100 |
| 8 | Ag$_2$SO$_4$ | 5/95 |
| 9 | AgF | 5/95 |
| 10 | AgOCN | 40/60 |
| 11 | AgOAc | 48/52 |
| 12 | Ag$_2$CO$_3$ | 100/0 |
| 13 | Ag$_2$O | 100/0 |
| 14 | AgO | 100/0 |

The oxygen atoms of the carbonyl group in aldehydes and ketones can act as nucleophiles, forming cationic intermediates that can be trapped by protic nucleophiles such as alcohols, thus formally constituting an O-H addition to the alkyne. For instance, Belmont *et al.* have reported a comparative study of gold(I) and silver(I) catalysts in the cyclization of *ortho*-alkynyl formylquinolines **1.64** in the presence of methanol to give furoquinolines **1.65** or pyranquinolines **1.66** (Scheme 1.29).[60] It was observed that AuCl$_3$ did not catalyze the reaction (entry 1), while [(Ph$_3$P)AuCl] resulted in a poor conversion of 25% to the pyranoquinoline **1.66** (entry 2). The more reactive [(Ph$_3$P)Au][SbF$_6$] generated *in situ* by using AgSbF$_6$ provided **1.66** with a high conversion of >95% (entry 3). Screening of silver salts in the same reaction (entries 4 to 14) revealed an interesting correlation of the p$K_a$ of the counteranion used with the regioselectivity, where the selectivity towards the 5-*exo-dig* product **1.65** increased with increasing p$K_a$ of the counteranion.
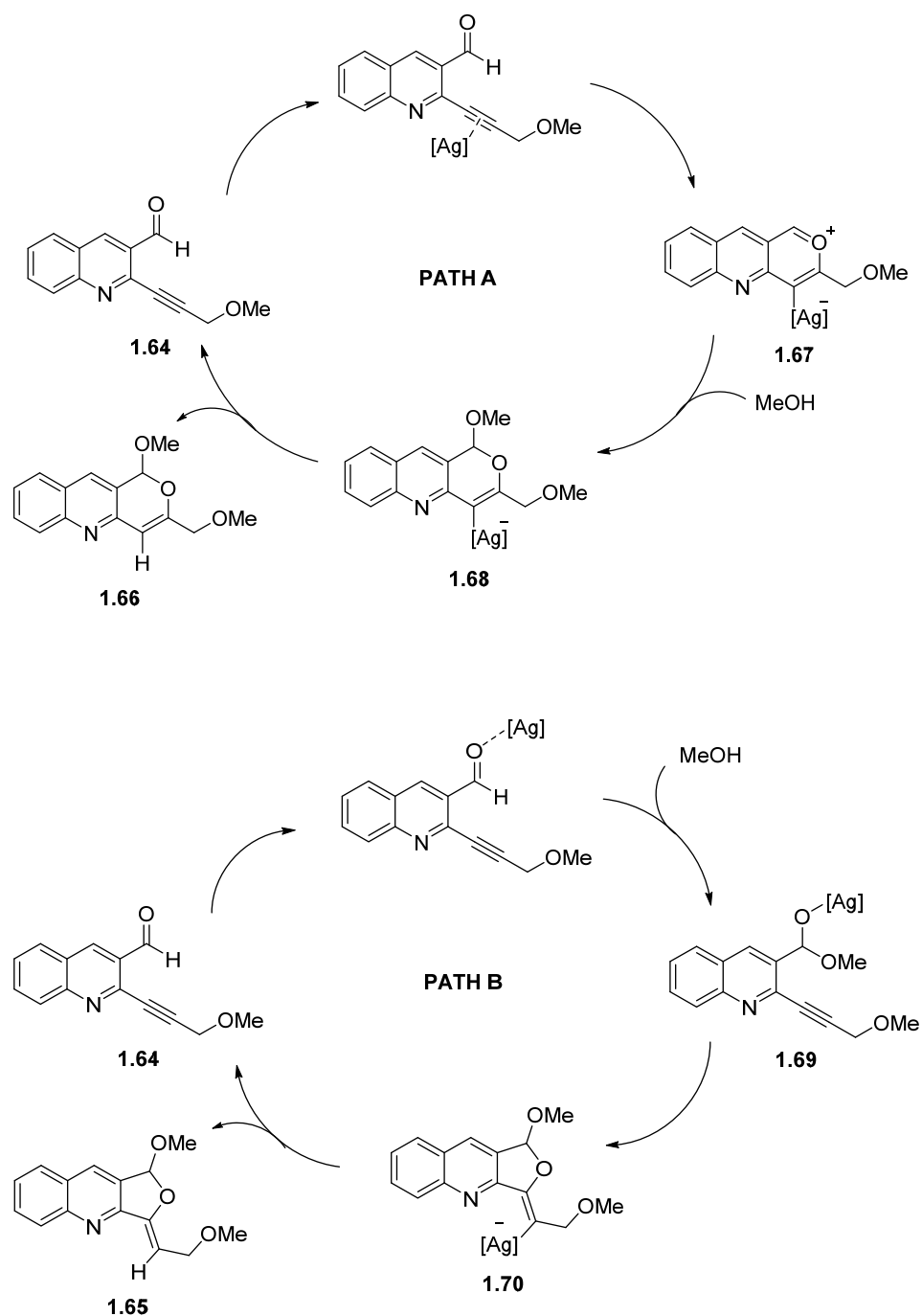
**Scheme 1.30.** Proposed mechanistic pathways for the cyclization of *ortho*-alkynyl formylquinoline

The observed counteranion effect was rationalized according to the Lewis

acidity and oxidizing ability of the compounds, which resulted in two different

modes of activation of the substrate. AgSbF$_6$, AgPF$_6$, AgOTf, AgNO$_3$, AgF

and $Ag_2SO_4$ (Scheme 1.30, path A), known for their ability to form π-complexes with alkynes, activate the alkyne towards nucleophilic attack by the carbonyl group, forming the zwitterionic complex **1.67** which is attacked by MeOH to give the intermediate **1.68**. Protodemetallation occurs to release product **1.66** and regenerate the catalyst. $Ag_2CO_3$, $Ag_2O$, and AgO (Scheme 1.30, path B), on the other hand, tend to interact mainly with the aldehyde functionality due to their higher oxidative abilities. Nucleophilic attack of MeOH at the aldehyde function results in the formation of the acetyl derivative **1.69**, which then cyclized to give intermediate **1.70**. Protodemetallation then occurs to give the product **1.65** and regenerate the catalyst. The remaining two compounds, AgOCN and AgOAc (Table 1.1, entry 10 and 11) exhibit poor regioselectivities due to hybrid activation of both the alkyne and aldehyde functionalities in the substrate.



R¹, R² = alkyl and aromatic substituents
R³OH = primary and secondary alcohols
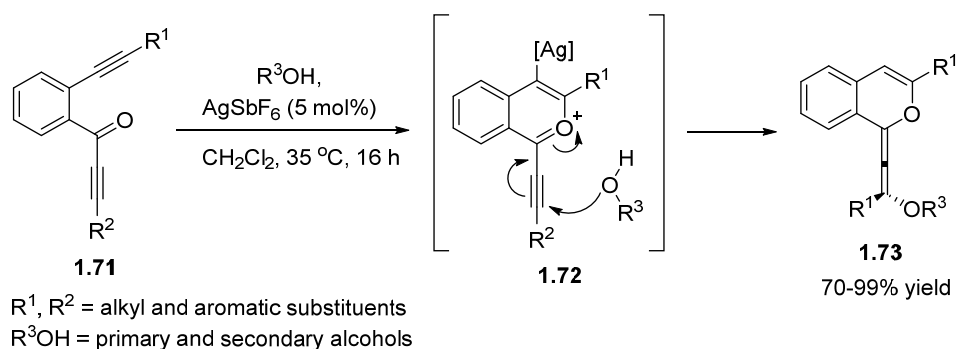
**Scheme 1.31.** Silver-catalyzed cyclization of alkynones in the presence of alcohols

In a similar fashion, the silver(I)-catalyzed reaction of alkynones **1.71** with alcohols has been used as a tool for the synthesis of 1-allenyl isochromenes **1.73** (Scheme 1.31). [61] The reaction most probably proceeds through a benzopyrylium cation **1.72** formed by the nucleophilic attack of the carbonyl

oxygen to the silver-coordinated alkyne. The subsequent addition of an alcohol molecule led to the formation of the allene system. Notably, the use of AuCl$_3$ as a catalyst did not afford any of the desired products. Notably, a counteranion effect of the silver salts was observed; AgSbF$_6$ gave the highest yields for the transformation, while AgClO$_4$, AgBF$_4$, and AgPF$_6$ were not as effective. Ag$_2$SO$_4$ did not promote the reaction at all.



$R^1$ = Me, Et, $^t$Bu, Bn, -CH=CH-Me, (CH$_2$)$_3$Cl, Ph, 4-O$_2$NC$_6$H$_4$
$R^2$ = Me, Et, -(CH$_2$)$_5$-
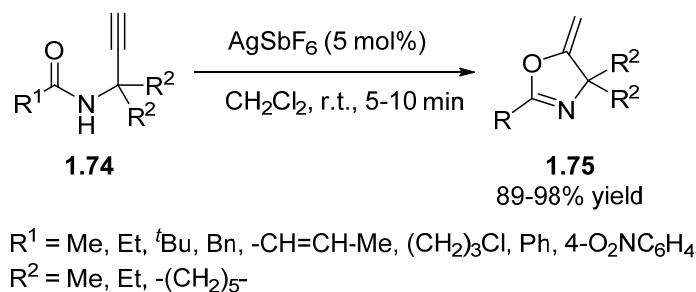
**Scheme 1.32.** Cyclization of *N*-propargyl amides

The silver-catalyzed cyclization of *N*-propargyl amides **1.74** to 5-methyleneoxazolines **1.75** was reported by Harmata *et al.* in 2008 (Scheme 1.32).[62] Unlike the aldehyde and ketone examples described above, the addition of a protic nucleophile was not necessary, as the amide moiety provides the proton necessary for protodemetallation and regeneration of the catalyst. *N*-propargyl amide substrates with *gem*-dialkyl substitution at the propargylic position cyclized in excellent yields, presumably due to the Thorpe-Ingold effect.[63] Sterically hindered and electron-withdrawing alkyl and aryl groups were also tolerated at the position beside the carbonyl carbon. However, only one substrate without the *gem*-dimethyl substitution was reported, and the effect of substitution at the terminal positon of the alkyne

was not investigated. We have thus studied this reaction in greater detail, and the results will be reported in Chapters 3 and 4.

### 1.2.1.6 Pyrimidines
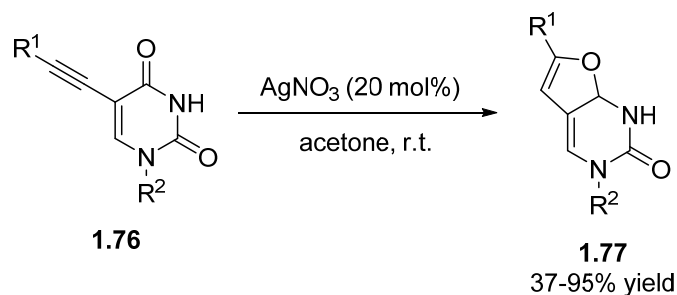


$R^1 = C_5H_{11}, C_8H_{17}, PhC_5H_{11}, Ph$
$R^2 = $ ether groups

**Scheme 1.33.** Silver-catalyzed synthesis of furanopyrimidine nucleosides

Another example of the versatility of silver salts as catalysts is in the synthesis of substituted furanopyrimidine nucleosides.[64,65] Upon treatment of 5-alkynyl uracil derivatives **1.76** with a catalytic amount of AgNO$_3$, substituted furanopyrimidine nucleosides **1.77** were obtained in quantitative yields (Scheme 1.33). This represents an improvement over the previously reported protocol which involves a stoichiometric amount of CuI in triethylamine/ methanol at reflux,[66] as higher yields were obtained under milder reaction conditions.

## 1.2.2 Nitrogen Nucleophiles

A diverse range of functional groups can act as nitrogen nucleophiles, as illustrated in Fig. 1.4. Other than differences in hybridization of the nitrogen atom ($sp^3$ or $sp^2$), some of these functional groups also contain more than one nitrogen atom.
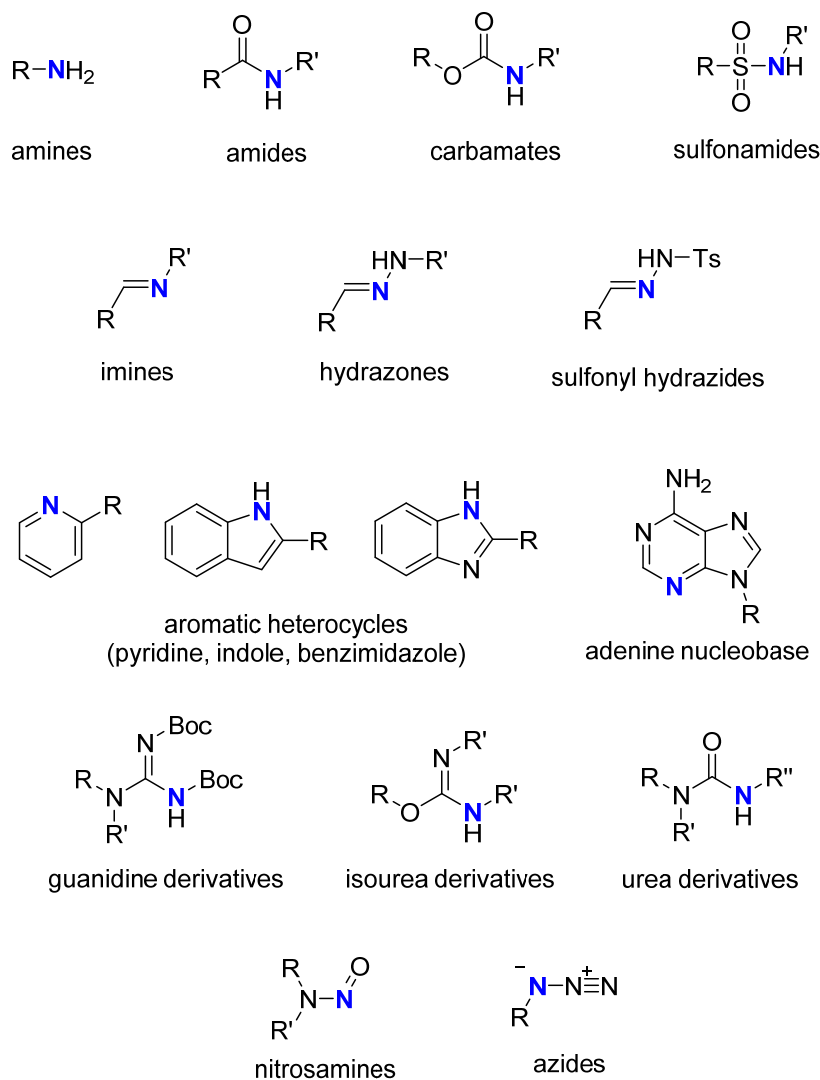


**Fig. 1.4** Functional groups containing nucleophilic nitrogen atoms

## 1.2.2.1 Amines
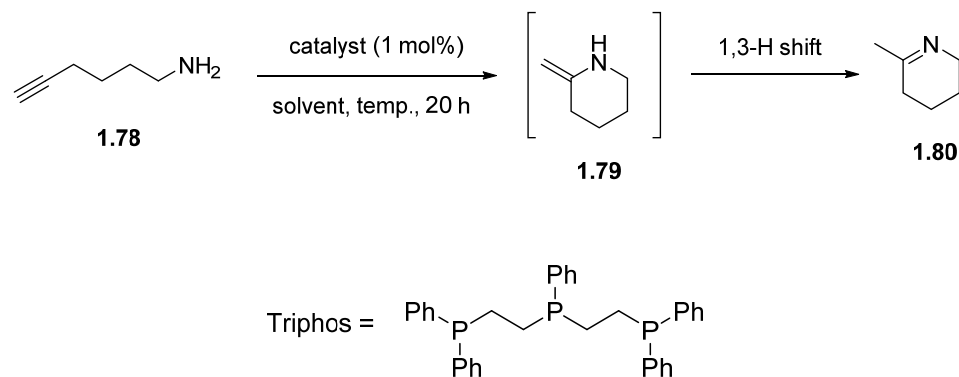


Triphos =



| Catalyst | Solvent | Temp. | Yield |
|---|---|---|---|
| AgBF$_4$ | CH$_2$Cl$_2$ | 40 °C | 69 |
| [Ag(Triphos)]BF$_4$ | toluene | 111 °C | 75 |
| AuCl$_3$ | MeCN | 82 °C | 71 |
| AuCl$_3$/Triphos (1:1 molar ratio) | CH$_2$Cl$_2$ | 40 °C | 49 |

**Scheme 1.34.** Intramolecular hydroamination of 6-aminohex-1-yne using silver(I) and gold(III) catalysts

In a study encompassing a screening of twenty group 8 to 12 transition metal catalysts, Müller and co-workers found that AgBF$_4$ and the silver complex, [Ag(Triphos)]BF$_4$, are active catalysts for the intramolecular hydroamination of 6-aminohex-1-yne **1.78**. [67] The reaction proceeds via the enamine intermediate **1.79**, which undergoes a 1,3-hydrogen shift to give the more stable cyclic imine product **1.80** (Scheme 1.34). Au(III) catalysts could also catalyze the reaction, while the Au(I) complex [(Ph$_3$P)AuCl], did not give any conversion. The result is significant as this is the first report of a structurally well-characterized silver(I) complex being applied in the heterocyclization reactions of alkynes, as only simple silver salts have been used previously. General trends in the effect of counteranions on the same reaction were also revealed in a later study. [68] The highest rates were observed when anions derived from sulfonic acids are used ($^-$OTs, $^-$OTf), medium rates were

observed for $CF_3CO_2^-$, $NO_3^-$ and the non-coordinating ions ($ClO_4^-$, $BF_4^-$, $PF_6^-$); whereas very low rates are observed for the more basic anions ($CH_3CO_2^-$, $PhCO_2^-$, and $CO_3^{2-}$).
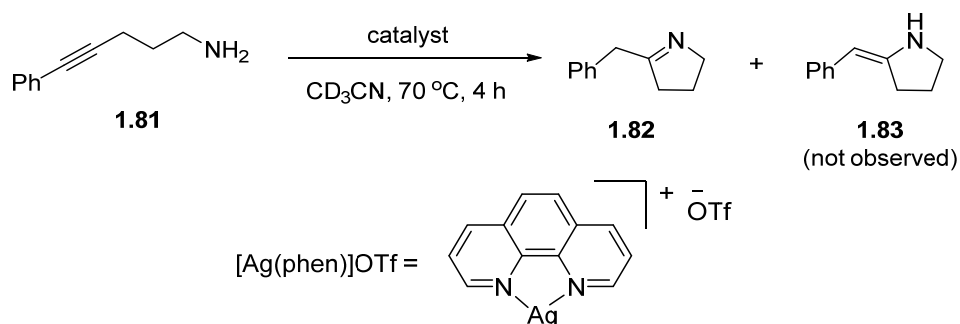


| Catalyst | Yield / % |
|----------|-----------|
| AgOTf | 55 |
| [Ag(phen)]OTf | 95 |
| NaAuCl$_4$ | 46 |

**Scheme 1.35.** Intramolecular hydroamination reaction of 5-phenyl-4-pentyn-1-amine using silver and gold catalysts

More recently, Helquist and co-workers have demonstrated that the silver(I) phenanthroline complex is an efficient catalyst for the intramolecular hydroamination of 5-phenyl-4-pentyn-1-amine **1.81** (Scheme 1.35).[69] Other silver and gold catalysts screened under the same conditions furnished the cyclic imine **1.82** as the sole product, albeit in lower yields. The higher yields obtained with [Ag(phen)]OTf compared to AgOTf showed the ability of the phenanthroline ligand to stabilize the catalytically active metal center during the reaction. The [Ag(phen)]OTf complex also has the added advantage of being stable towards air and moisture compared to silver salts, which tend to be hygroscopic.
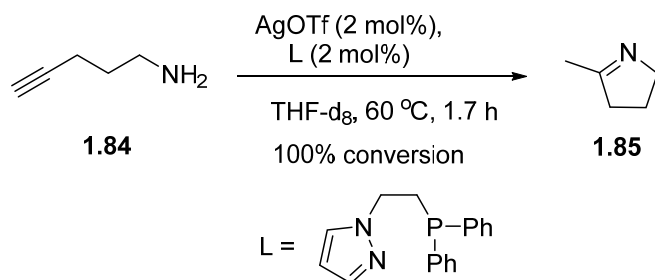
**Scheme 1.36.** Intramolecular hydroamination reaction of 4-pentyn-1-amine

Inspired by the ability P- and N-donor ligands to improve the stability and catalytic efficiency of silver in hydroamination reactions, Messerle and co-workers investigated a series Ag(I) complexes prepared *in situ* from AgOTf and a series of bidentate *N,N*-, *P,N*- and *P,P*-donor ligands as catalysts towards the intramolecular hydroamination of 4-pentyn-1-amine **1.84**.[70] The best result was obtained with the pyrazole-phosphine ligand shown in Scheme 1.36.



X = Y = CH, R = *o*-NH$_2$, *o*-OMe, *p*-NO$_2$
X = CH, Y = N, R = H
X = N, Y = CH, R = H
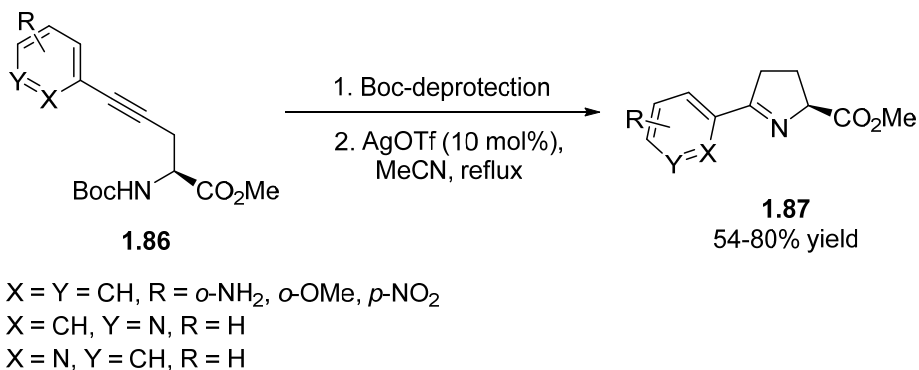
**Scheme 1.37.** Synthesis of 2,5-disubstituted pyrrolines

Enantiomerically pure 2,5-disubstituted pyrrolines **1.87** can be prepared from enantiopure propargyl glycines **1.86** by a Ag-catalyzed intramolecular hydroamination reaction (Scheme 1.37).[71] AgOTf was found to be the best catalyst compared to other group 11 metal salts such as NaAuCl$_4$ and Cu(OTf)$_2$.
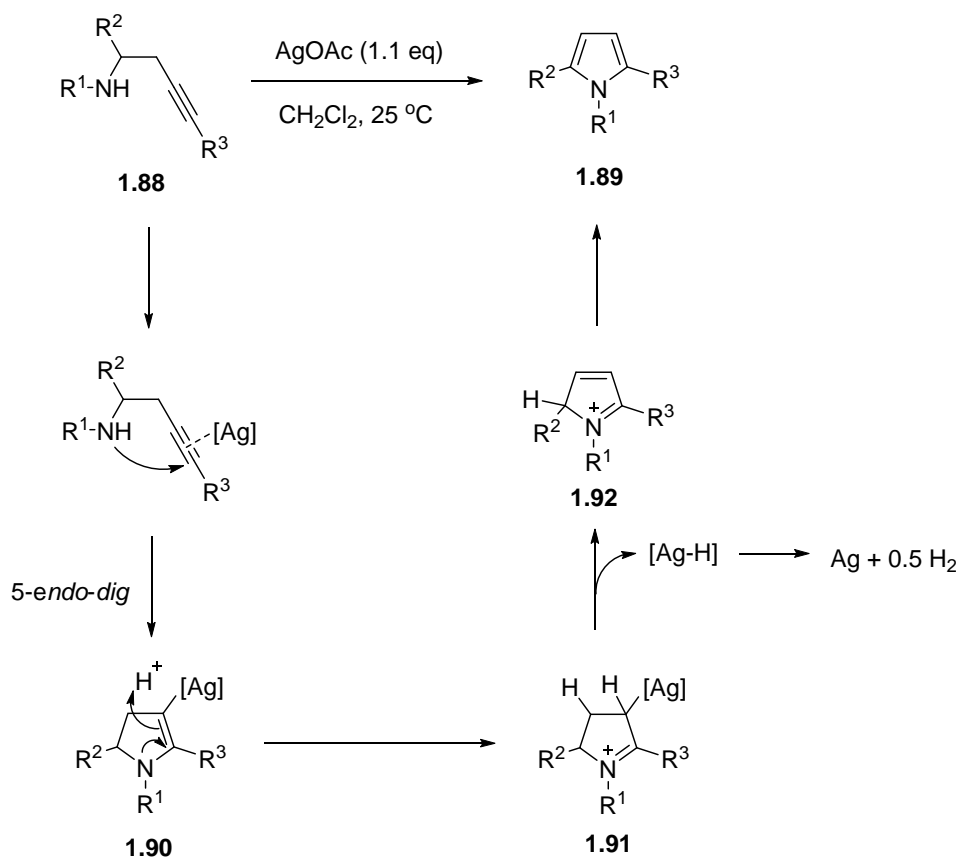
**Scheme 1.38.** Silver-promoted oxidative cyclization of homopropargylamines

Knölker and coworkers has also reported the synthesis of pyrroles via the cyclization of homopropargylamines **1.88**.[72] The reaction involves an oxidative cyclization process, which necessitates stoichiometric amounts of silver salt to be used. The proposed mechanism is represented in Scheme 1.38. The coordination of the alkyne to the silver cation activates the alkyne group of **1.88** towards intramolecular nucleophilic attack of the amine leading to intermediate **1.90**. Protonation of **1.90** affords the iminium ion **1.91**, which on subsequent $\beta$-hydride elimination generates the pyrrylium ion **1.92** and metallic silver. Finally, deportonation of **1.92** provides pyrrole **1.89**.
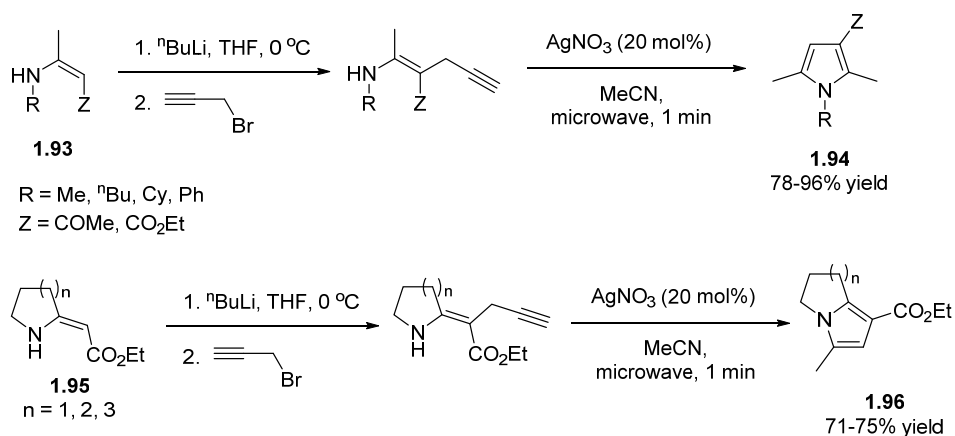
**Scheme 1.39.** Synthesis of functionalized pyrroles

As an interesting extension of the work by Knölker, Dovey *et al.*, the synthesis of functionalized pyrroles **1.94** was described in two steps: the propargylation of secondary enaminones **1.93**, followed by an AgNO$_3$ catalyzed intramolecular hydroamination (Scheme 1.39).[73] The hydroamination step can be accelerated by microwave irridation, resulting in a drastic reduction in reaction times from 16-20 h to 1 min. The reaction was also extended to the synthesis of the bridgehead pyrroles **1.96** from **1.95**.[74]
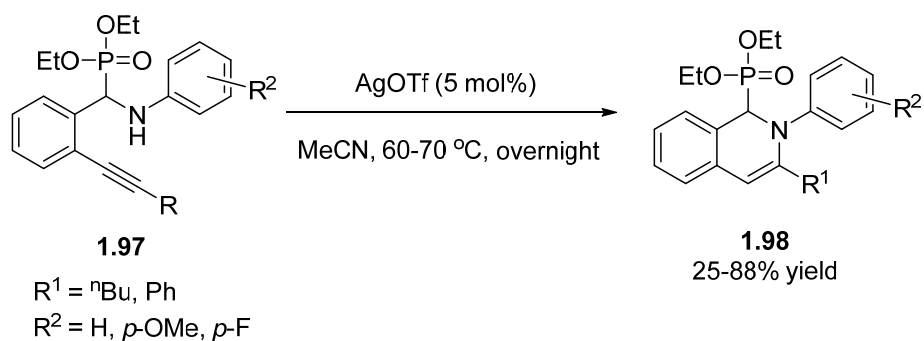


**Scheme 1.40.** Cyclization of alkynylaminophosphonates

Alkynylaminophosphonates **1.97**, analogues of amino acids, can also be cyclized in the presence of silver triflate to obtain 1,2-dihydroisoquinolines **1.98** in high yields (Scheme 1.40).[75]

### 1.2.2.2 Amides
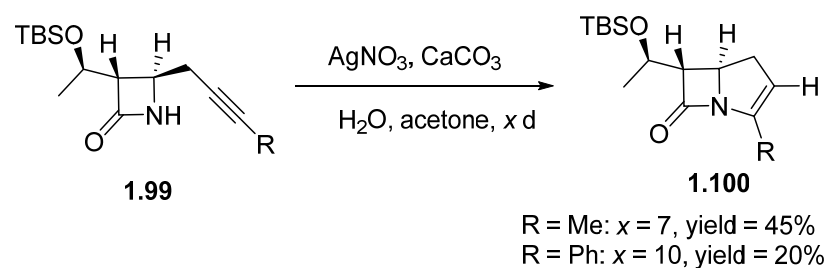


**Scheme 1.41.** Cyclization of 4-propargyl azetidinones

The first example of silver-mediated addition of amides to alkynes was reported by Liebeskind and Prasad in 1988,[76] which involves the cyclization of 4-propargyl azetidinones **1.99** (Scheme 1.41). However, a stoichiometric amount of AgNO$_3$ was required, the reaction time was long, and only substrates bearing Me and Ph groups at the alkyne could be cyclized.



**Scheme 1.42.** Cyclization of alkynyl amides

A decade later, Nagasaka *et al.* reported another example of the cyclization of alkynyl amides **1.101** (Scheme 1.42).[77] In this case, strong basic conditions

were required for the deprotonation of the amide, and the reaction conditions were quite harsh.

### 1.2.2.3 Carbamates



**1.103**

R = PhCO, MeCO, MeCH=CHCO
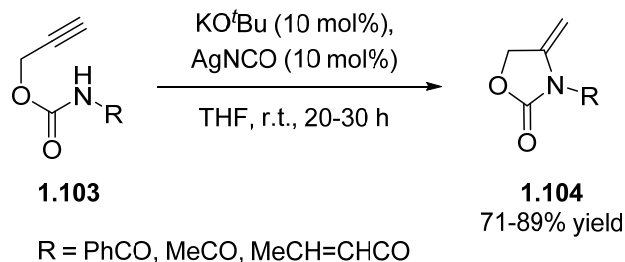
**1.104**
71-89% yield

**Scheme 1.43.** Cyclization of *O*-propargyl carbamates with silver isocyanate

The nitrogen atom of *O*-propargyl carbamates **1.103** can also act as nucleophiles, providing convenient access to 4-methylene-2-oxazolidinones **1.104**. The transformation has been reported to be catalyzed by Ag(I) isocyanate, but the reaction was only demonstrated with a somewhat limited substrate scope of three examples (Scheme 1.43).[78] A later report showed that with 5 mol% AuCl and 5 mol% of either Et$_3$N or KO$^t$Bu as base, internal alkyne substrates can also be cyclized in good to moderate yields.[79]

### 1.2.2.4 Sulfonamides



**1.105**

R$^1$ = alkyl, aryl
R$^2$ = Me, F
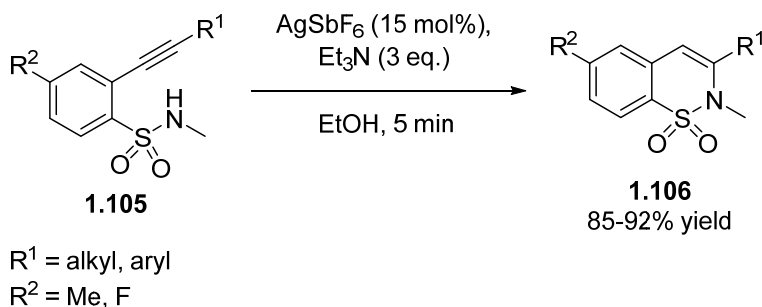
**1.106**
85-92% yield

**Scheme 1.44.** Cyclization of benzenesulfonamides

Benzenesulfonamides **1.105** can also be cyclized by silver salts, giving 1,1-dioxo-2*H*-1,2-benzothiazines **1.106** (Scheme 1.44) selectively.[80] Silver salts (AgNO$_3$, AgF, AgSbF$_6$) were better than copper salts (CuI and CuCl) as catalysts for this reaction. The addition of triethylamine to the reaction mixture also resulted in an acceleration of the reaction, and this was attributed to the ability of triethylamine to form hydrogen bonds with the sulfonamide group (S–N–H·····NEt$_3$), enhancing its nucleophilicity. The reaction proceeded in with good chemoselectivity without any of the *O*-cyclization product; and also with good regioselectivity, as none of the isomeric five-membered ring product was detected. A plausible explanation for the regioselectivity is that the longer S-N bond length favored *endo* ring closure due to the lower geometric constraint. The broad generality of this approach was also evident from the variety of electron-donating and electron withdrawing alkyl and aryl groups on the alkyne that were tolerated under the reaction conditions.
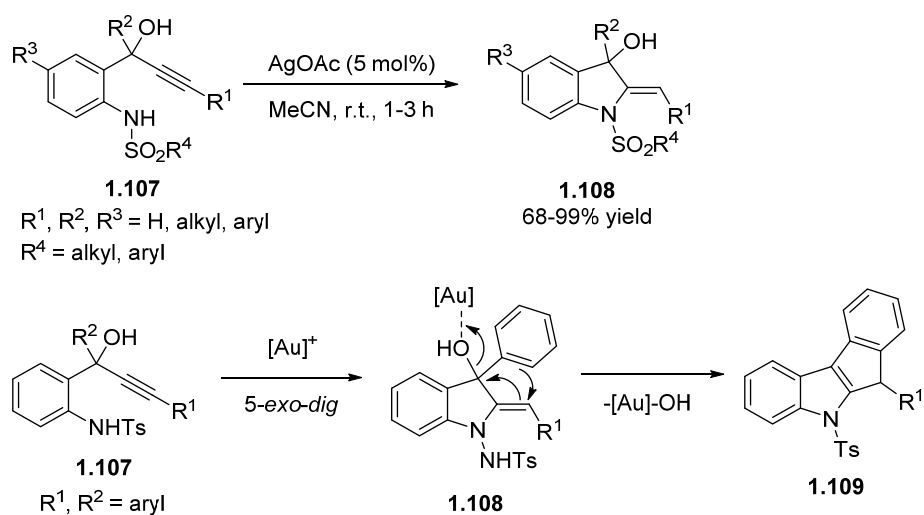


**Scheme 1.45.** Silver and gold-catalyzed intramolecular hydroamination of 1-(2-(sulfonylamino)phenyl)prop-2-yn-1-ols

Chan *et al.* have also reported that AgOAc catalyzes the intramolecular hydroamination of 1-(2-(sulfonylamino)phenyl)prop-2-yn-1-ols **1.107** to afford (*Z*)-2-methylene-1-sulfonylindolin-3-ols **1.108** in excellent yields under mild reaction conditions and with low catalytic loadings.[81] The reaction also proceeded with good regioselectivity, as no side products arising from 6-*endo-dig* cyclization were detected. It is interesting to note that the reaction produces only the 5-*exo-dig* cyclized product when silver catalysts are employed. When cationic gold catalysts were used, the 5-*exo-dig* cyclized product **1.108** further underwent an intramolecular Friedel-Crafts alkylation when $R^1$ and $R^2$ = Ar to afford the indenyl-fused indoles **1.109**.[82]



R¹, R² = H, alkyl, aryl
R³ = H, Br, Cl, Me, OMe
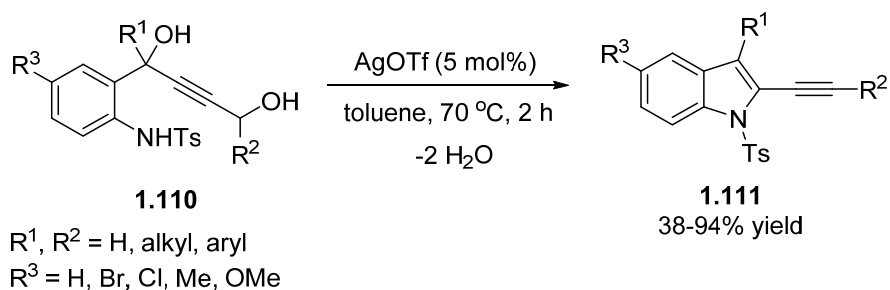
**Scheme 1.46.** Tandem cyclization/alkynylation reaction of 1-((2-tosylamino)aryl)but-2-yne-1,4-diols

With the structurally similar 1-((2-tosylamino)aryl)but-2-yne-1,4-diols **1.110**, tandem cyclization/alkynylation can occur under silver catalysis to afford the 2-alkynyl indoles **1.111** (Scheme 1.46).[83] The proposed mechanism for the transformation is shown in Scheme 1.47.
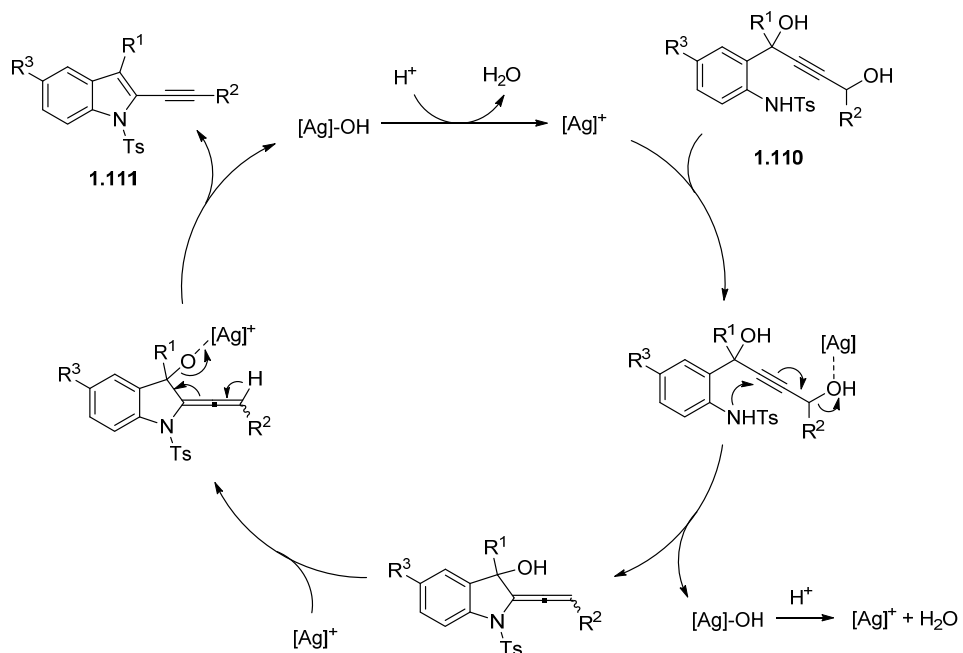
**Scheme 1.47.** Proposed mechanism for the tandem cyclization/alkynylation reaction of 1-((2-tosylamino)aryl)but-2-yne-1,4-diols

## 1.2.2.5 Imines



X = CH, N
R = alkyl, aryl, alkenyl
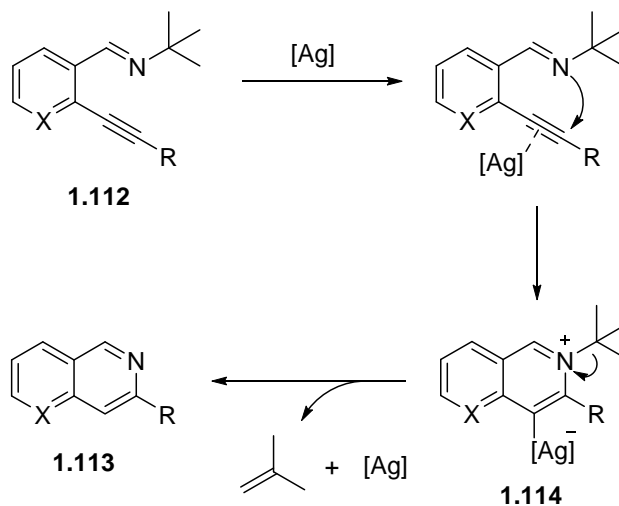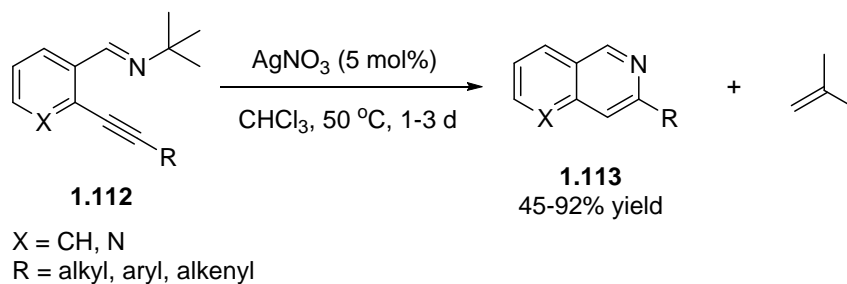


**Scheme 1.48.** Synthesis of isoquinolines via cyclization of iminoalkynes

In reactions similar to those of *o*-alkynyl benzaldehydes (Scheme 1.29), imines derived from these substituted benzaldehydes can also be cyclized in the presence of silver salts (Scheme 1.48).[84] In the presence of $AgNO_3$, the attack of the imino nitrogen atom on the activated alkyne triple bond of **1.112** results in the formation of an isoquinolinium intermediate **1.114**. Cleavage of the C-N bond affords a *tert*-butyl carbocation, which supplies the proton for regeneration of the catalyst and release of the isoquinoline product **1.113**.



**1.115**

R¹ = ⁿBu, Ph, Bn, allyl

R² = ⁿBu, Ph, 1-cyclohexenyl

**1.117**

**1.116**

42-93% yield
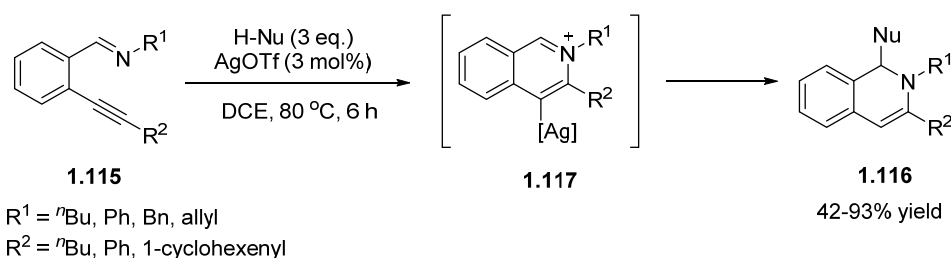
**Scheme 1.49.** Synthesis of 1,2-dihydroisoquinoline derivatives

In a similar manner, Yamamoto *et al.* have reported the synthesis of functionalized 1,2-dihydroisoquinoline derivatives **1.116** through trapping of the iminium intermediate **1.117** produced in the cyclization step by various pro-nucleophiles, such as $MeNO_2$, $EtNO_2$, $CH_2(COMe)_2$, $CH_2(CO_2Me)_2$, $CH_2(CN)_2$, acetone, MeCN and even alkynes (Scheme 1.49).[85] $Cu(OTf)_2$ can also catalyze the reaction, but with slightly lower yields. AuCl, however, was ineffective.
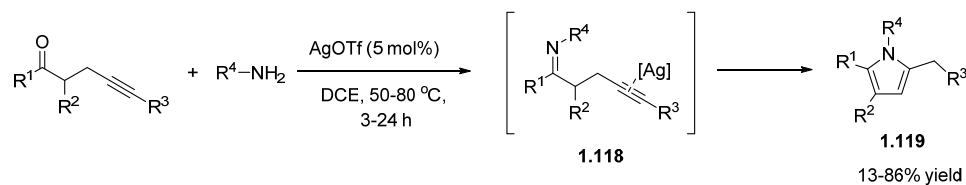
**Scheme 1.50.** Synthesis of pyrroles from imines

AgOTf catalyzes the intramolecular reaction between imines **1.118** (formed *in situ* from condensation of ketone and amine) and alkynes to yield functionalized pyrroles **1.119** (Scheme 1.50).[86] The reaction was tolerant of various substituents on the amine (*i.e. n*-pentyl, allyl, benzyl, *p*-methoxybenzyl, phenyl, *p*-methoxyphenyl, *p*-toluenesulfonyl) and cyclic ketones were also possible substrates. Comparisons were also made with the AuCl/AgOTf/PPh₃ catalytic system where 5 mol% of each component was used. The AgOTf-catalyzed reactions were faster and similar yields were obtained with both catalysts, except in reactions that require higher temperatures. Higher yields were obtained with the AuCl/AgOTf/PPh₃ combination in those cases, possibly due to the higher thermal stability of the catalyst. Attempts to characterize the active catalytic species in the AuCl/AgOTf/PPh₃ catalytic system were largely unsuccessful.

### 1.2.2.6 Hydrazones and Hydrazides
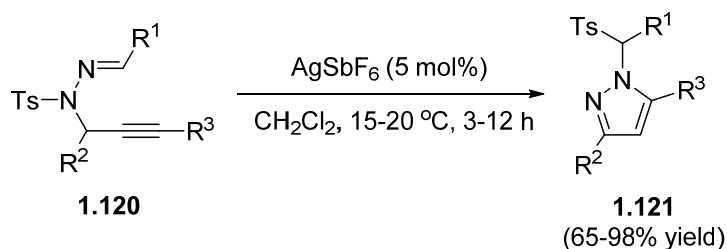


**Scheme 1.51.** Cyclization of propargyl *N*-sulfonylhydrazones

The cyclization of propargyl *N*-sulfonylhydrazones **1.120** allows the efficient and regioselective synthesis of 1,3- and 1,5-disubstituted and 1,3,5-pyrazoles **1.121**. [87] Silver salts (AgSbF$_6$, AgBF$_4$, AgOTf, AgPF$_6$, AgClO$_4$) were generally effective at promoting the reaction, although AgSbF$_6$ gave the highest yields. The gold complex [Au(PPh$_3$)$_2$]SbF$_6$ was inactive. The sulfonyl group (tosylate and mesylate) on the hydrazone was essential for the reaction to occur, and it migrates from N to C during the reaction. Based on crossover experiments and deuterium labeling studies, a plausible mechanism was proposed, as outlined in Scheme 1.52. Coordination of the alkyne to silver activates it towards nucleophilic attack by the hydrazone, and gives rise to intermediate **1.122**. Deprotonation and cleavage of the N-Ts bond results in the formation of the ion pair **1.123**. An attack of the tosyl anion to the electron-deficient imine carbon followed by protodemetallation gives the product **1.121** and regenerates the silver catalyst.
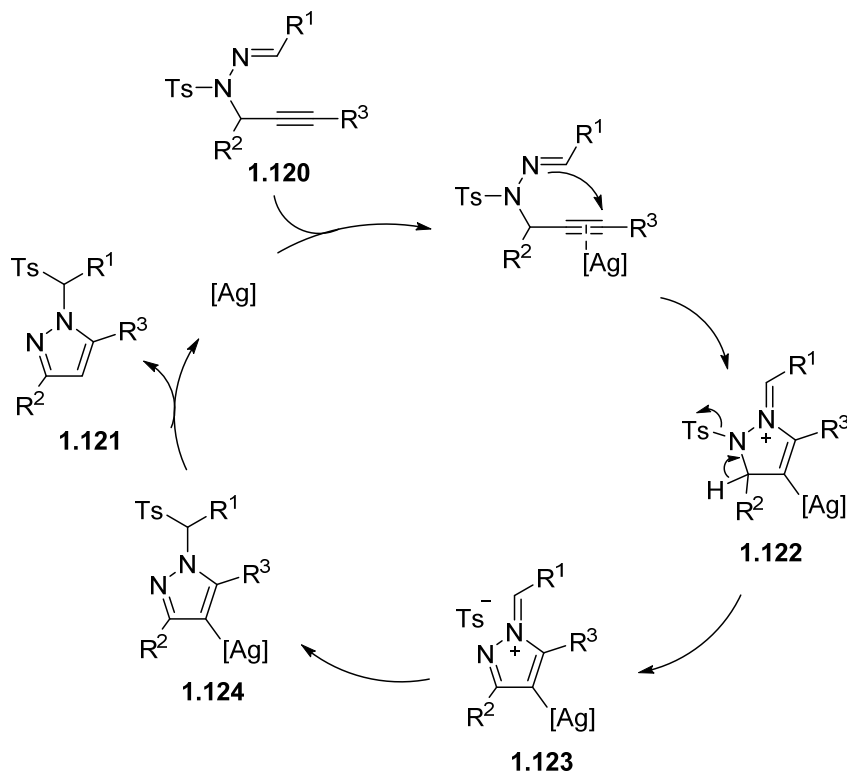
**Scheme 1.52.** Plausible mechanism for the cyclization of propargyl *N*-sulfonylhydrazones
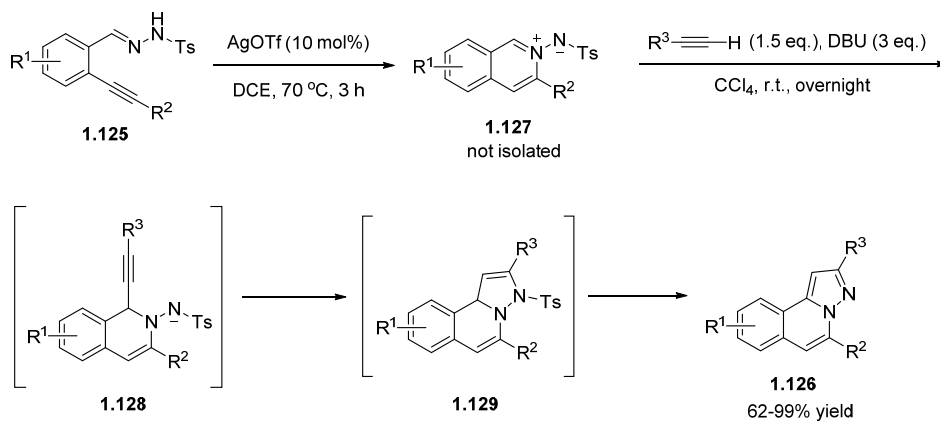


**Scheme 1.53.** Silver triflate catalyzed tandem reaction of *N'*-(2-alkynylbenzylidene)hydrazide with alkynes

Wu *et al.* have developed an efficient tandem reaction of *N'*-(2-alkynylbenzylidene)hydrazide **1.125** with alkynes catalyzed by AgOTf, which generated the highly functionalized fused 1,2-dihydroisoquinolines **1.126** in

good to excellent yields.[88] The proposed mechanism for the transformation involves activation of the alkyne in substrate **1.125** by AgOTf, followed by nucleophilic attack by the hydrazide to form the isoquinolium intermediate **1.127**. Nucleophilic attack by the acetylide ion formed *in situ* from a mixture of alkyne and DBU on **1.127** afforded the corresponding product **1.128**, which then undergoes intramolecular 5-*endo* cyclization, leading to **1.129**, followed by aromatization to generate the product **1.126**.

### 1.2.2.7 Nitrogen-containing heterocycles



$R^1$ = H, Me
$R^2$ = H, Me, Ph
X = O, S, Se
$Y^1$ = H, Cl
$Y^2$ = H, OMe, Me, Cl, CN, $CO_2Me$, $SO_2Me$
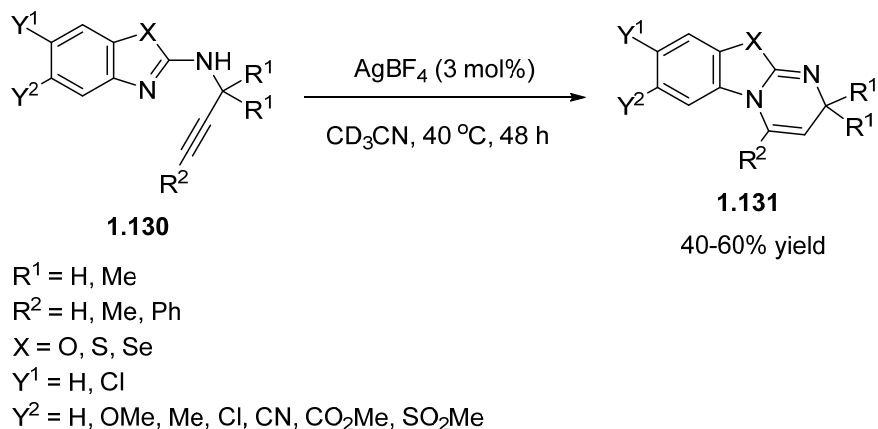
**Scheme 1.54.** Synthesis of *N*-fused heteroaromatic compounds

In a similar way to imine nucleophiles, $sp^2$ nitrogen atoms embedded in aromatic compounds also reacted with alkynes to give *N*-fused heteroaromatic compounds via an intramolecular cyclization reaction catalyzed by $AgBF_4$ (Scheme 1.54).[89] Moderate yields of 40-60% were obtained. Electron-donating groups on the benzene ring accelerate the reaction, while electron-withdrawing groups slow down the reaction. AgTFA, on the other hand, only resulted in low conversions. This could have been due to the deprotonation of the terminal alkyne proton by the weakly basic trifluoroacetate anion, and the

formation of the corresponding silver acetylide which could not take part in the cyclization reaction. In comparison, the Au(I) complexes [(Ph$_3$P)AuCl] and KAu(CN)$_2$ were inactive as catalysts for the reaction, while the Au(I) bis(tetrahydrothiopyran) salt [Au(C$_5$H$_{10}$S)$_2$]BF$_4$ showed a similar reaction rate to AgBF$_4$. However, the formation of a gold mirror was also observed – an indication of the reduction of the Au(I) ion by the dihydropyrimidine cyclized product. No reduction to Ag(0) was observed in the silver-catalyzed reactions, which was attributed to the slightly lower reduction potential of Ag(I) compared to Au(I).



X = CH$_2$, O
R$^2$ = H, alkyl, aryl
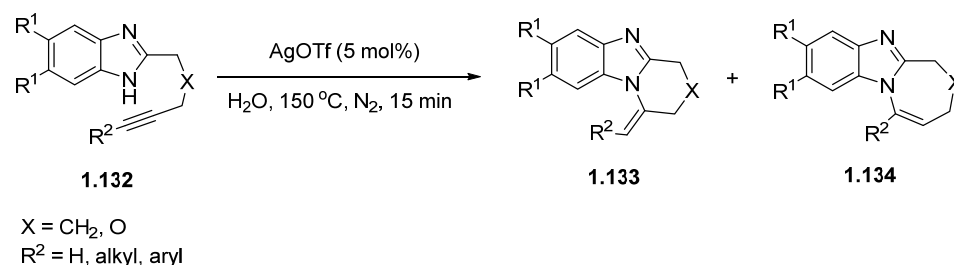
**Scheme 1.55.** Synthesis of fused tricyclic benzimidazoles

A similar strategy was reported for the preparation of fused tricyclic benzimidazoles using silver salts (Scheme 1.55).[90] Among the eight silver salts screened, AgOTf showed the highest efficiency. Water could be used as the solvent and microwave irradiation enabled higher yields in shorter reaction times. Complete selectivity towards the 6-*exo-dig* product **1.133** was always obtained, except when X = O and when R$^2$ is an aromatic group. In these cases, almost equal amounts of the 7-*endo-dig* product were also observed, possibly due to the π–π conjugative effect between the alkyne and the aryl groups,

which results in a similar propensity of the benzimidazole nitrogen attacking either carbon of the acetylene bond.
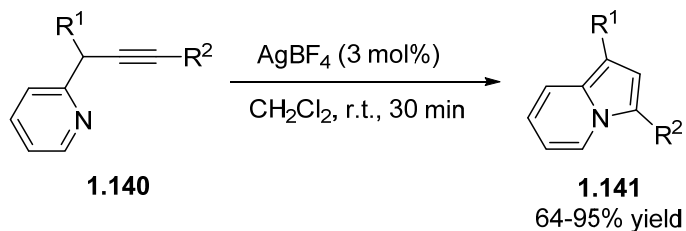


**Scheme 1.56.** Synthesis of fused pyrrole-containing heterocycles

Gevorgyan *et al.* developed a mild and base-free protocol for the synthesis of fused pyrrole-containing heterocycles **1.141** which involves the silver-catalyzed 5-*endo-dig* cyclization of propargyl-containing pyridines **1.140** (Scheme 1.56).[91] An initial screening of catalysts showed that $AgBF_4$ and $AgPF_6$ led to nearly quantitative yields of the product in 30 min, while copper and gold catalysts were also efficient, although the yields obtained were slightly lower (See Table 1.2). The reaction also showed a broad substrate scope, as several substituents were tolerated at the propargyl position and at the alkyne, and their corresponding products were obtained in good yields of 64-95% yield.

**Table 1.2.** Initial screening of catalysts for the cyclization of **1.140**

| Entry | Catalyst | Time / h | Yield / % |
|-------|----------|----------|-----------|
| 1 | AgBF$_4$ | 0.5 | >99 |
| 2 | AgPF$_6$ | 0.5 | >99 |
| 3 | AgSbF$_6$ | 0.5 | 52 |
| 4 | CuI | 3 | 77 |
| 5 | CuCl | 0.5 | 83 |
| 6 | AuI | 3 | 95 |
| 7 | AuCl$_3$ | 0.5 | 71 |
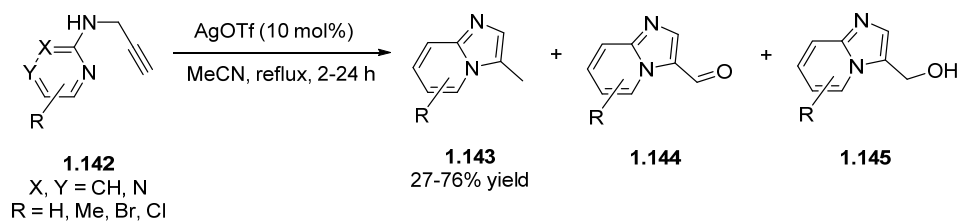


**Scheme 1.57.** Cyclization of alkynyl pyridin-2-amines

Similarly, silver salts also catalyze the cyclization of alkynyl pyridin-2-amines to give imidazo[1,2-*a*]pyridines (Scheme 1.57).[92] However, higher catalytic loadings (10 mol%), and harsher reaction conditions were required for the transformation. Extra caution had to be taken to keep oxygen out of the reaction mixture to minimize the formation of the side products **1.144** and **1.145**. AgOTf was the best catalyst for the reaction, and it was found that methyl substituents on the pyridine ring resulted in short reaction times, while bromo- or chloro- substituents slowed down the reaction significantly. Other heterocyclic ring systems, such as imidazole or pyrazine also underwent smooth cyclization to the corresponding azo-fuzed heterocycles.
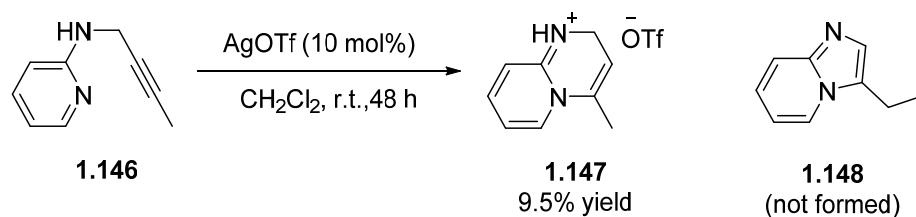
**Scheme 1.58.** Cyclization of the internal alkyne substrate **1.146**

Interestingly, with the internal alkyne substrate **1.146** (Scheme 1.58), the expected product resulting from 5-e*xo-dig* cyclization was not observed. Instead, the corresponding triflate salt **1.147** resulting from 6-*endo-dig* cyclization, was obtained in poor yield. However, when a stoichiometric amount of AgOTf was used, product **1.147** could be isolated in 92% yield after a short reaction time of 30 minutes.
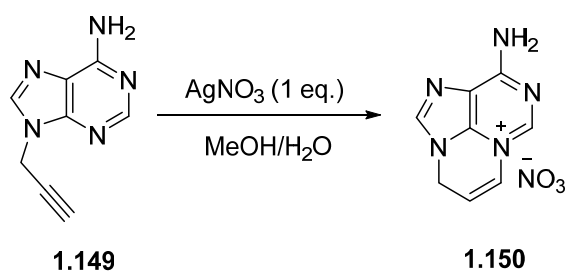


**Scheme 1.59.** Cyclization of 9-propargyladenine

Verma and co-workers observed an unexpected silver-mediated cyclization of 9-propargyladenine **1.149** (Scheme 1.59) when they attempted to prepare the corresponding silver(I) complex.[93] The product was the cationic tricyclic purine derivative **1.150**.

## 1.2.2.8 Guanidine derivatives
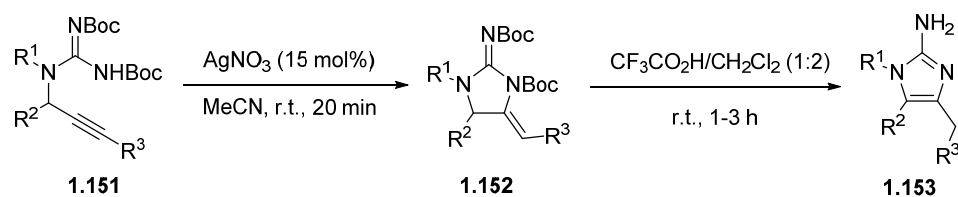


**Scheme 1.60.** Cyclic guanidines as precursors to 2-aminoimidazoles

Eycken and co-workers envisaged that the cyclic guanidines **1.152**, prepared via cyclization of propargyl guanidines **1.151**, would be suitable precursors for the preparation of 2-aminoimidazoles **1.153** (Scheme 1.60).[94] The screening of several Lewis acid catalysts led to the discovery of AgNO$_3$ as the most efficient catalyst for the transformation, leading to near quantitative conversions in acetonitrile at room temperature after 20 minutes. Comparable results were obtained with AgOTf, while other catalysts, such as AuCl$_3$, CuCl, CuBr, and Cu(OTf)$_2$ were inefficient.
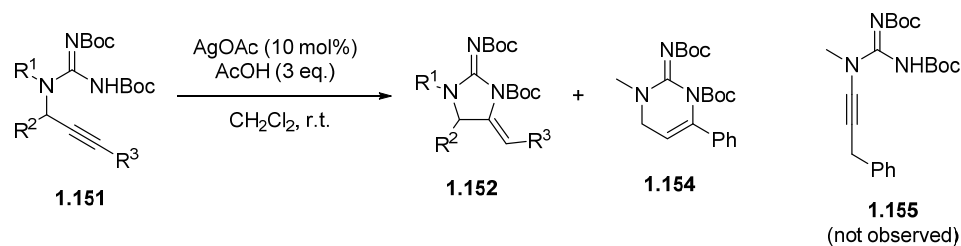


**Scheme 1.61.** Cyclization of di-Boc-protected propargylguanidine under acidic conditions

Looper *et al.* later found that silver salts catalyze the same transformation under acidic conditions with good selectivity for the 5-*exo-dig* cyclized product **1.152** (Scheme 1.61).[95] Au(III) salts were less efficient, and tended to afford the 6-*endo-dig* cyclized product **1.154**, while Cu(OTf) resulted in the

formation both cyclization products and **1.155**, which results from a [1,3]-prototropic shift and isomerization of the alkyne. By varying the propargylic substituent and the alkyne substituent, it was found that selectivity towards the 5-*exo-dig* product was the greatest when the electronic differences between the two substituents are large.

### 1.2.2.9 Isourea derivatives
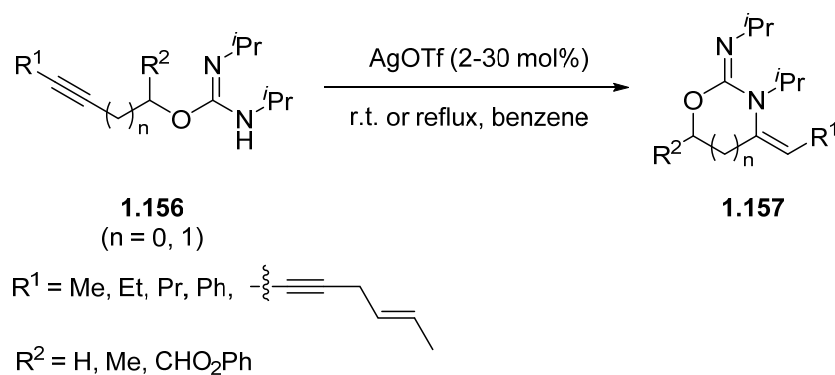


**Scheme 1.62.** Cyclization of acetylenic isoureas

The structurally similar acetylenic isoureas **1.156** afforded oxazolidines **1.157** ($n = 0$) or oxazines **1.157** ($n = 1$) when treated with silver triflate (Scheme 1.62).[96] The reaction proceeded at room temperature with 2-5 mol% of AgOTf with the *O-α*-acetylenic isoureas **1.156** ($n = 0$); however, higher catalytic loadings of 25-30 mol% and higher reaction temperatures were required for the *O-β*-acetylenic isoureas **1.156** ($n = 1$). Yields and reaction times were not reported in this publication.

## 1.2.2.10. Urea Derivatives
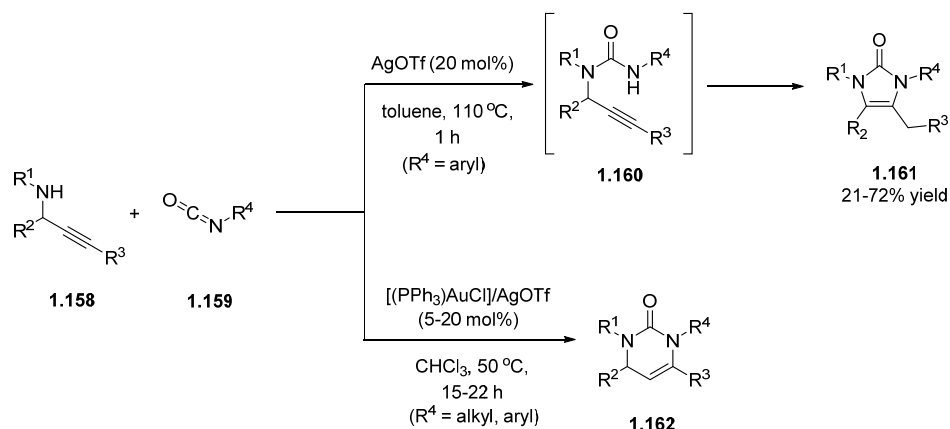


**Scheme 1.63.** Synthesis of 2-imidazolones **1.161** and tetrasubstituted 3,4-dihydropyrimidin-2(1*H*)-ones **1.162** from secondary propargylamines and isocyanates
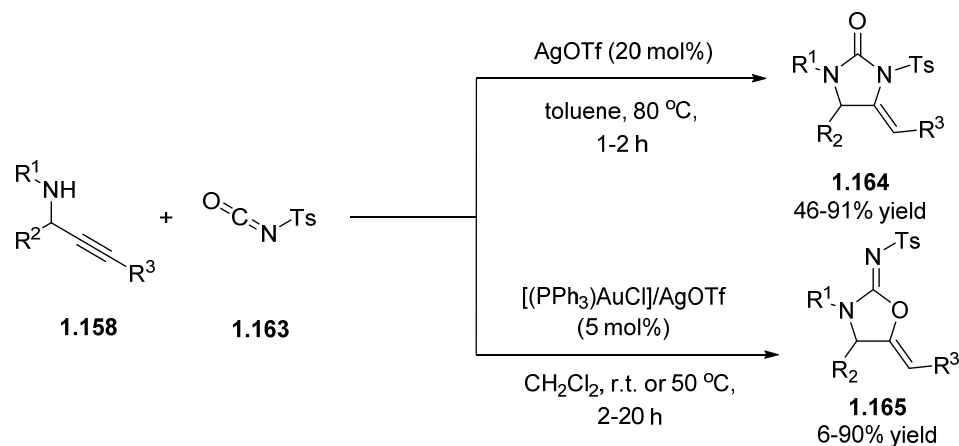


**Scheme 1.64.** Synthesis of imidazolin-4-ones **1.164** and oxazolidin-2-imines **1.165** from secondary propargylamines and tosylcyanates

Eycken has reported the synthesis of 2-imidazolones **1.161** from secondary propargylamines **1.158** and isocyanates **1.159** by a one-pot acylation, followed by Ag(I)-catalyzed cycloisomerization, via the propargylic urea intermediate **1.160** (Scheme 1.63).[97] Recently, cationic gold catalysts were employed for the reaction, and interestingly, the reaction afforded mainly the 6-*endo*-cyclized product **1.162**.[98] The reaction with tosylcyanates **1.163** also resulted

in different products when silver and gold catalysts were employed (Scheme 1.64) – the AgOTf-catalyzed reaction favors the *N*-cyclized imidazolin-4-ones **1.164**, while the gold-catalyzed reaction resulted in the *O*-cyclized oxazolidin-2-imines **1.165**.[99]

In an attempt to rationalize the differences in behavior between the two catalysts, triphenylphosphine was added as a ligand in the AgOTf-catalyzed reaction between *N*-methylpropargyl-amine **1.158** ($R^1$ = Me, $R^2$ = $R^3$ = H) and tosyl isocyanate **1.163**, with the hope of observing an effect on the selectivity brought about by the reduced Lewis acidity of the silver metal center. Indeed, an improved stability of the catalyst and a greater selectivity towards the *N*-cyclized product was observed. Pearson's concept of hard and soft acid and bases (HSAB) was invoked to explain the chemoselectivity difference observed between the silver and gold catalytic systems in the reaction of tosylcyanates. The authors thus propose that in the [(Ph₃P)AuCl]/AgOTf-catalyzed process, the triflate counteranion is pushed outside the primary coordination sphere, resulting in a completely aurated alkyne triple bond that is a hard acid and would preferably react with the harder carbamide oxygen nucleophile. In the AgOTf-catalyzed process, however, AgOTf does not dissociate completely and exists as a contact ion-pair which would form a highly polarized soft π-complex with the alkyne triple bond and preferably react with the softer amide nitrogen. The differences in regioselectivity observed with the alkyl and aryl isocyanates, on the other hand, appear to be more susceptible to kinetic and thermodynamic control rather than the choice of catalytic system. The higher temperatures and higher catalytic loadings of

the AgOTf-catalyzed process indicate that the 5-*exo*-cyclization could be kinetically-favored, while the cationic Au(I) process which occurs under milder conditions could be under thermodynamic control.

### 1.2.2.11 Azides



$R^1 = p$-Cl, $m$-Me
$R^2 = $ H, Et, $^n$Bu, Ph
$R^3 = $ $^n$Pent, various aromatic substituents
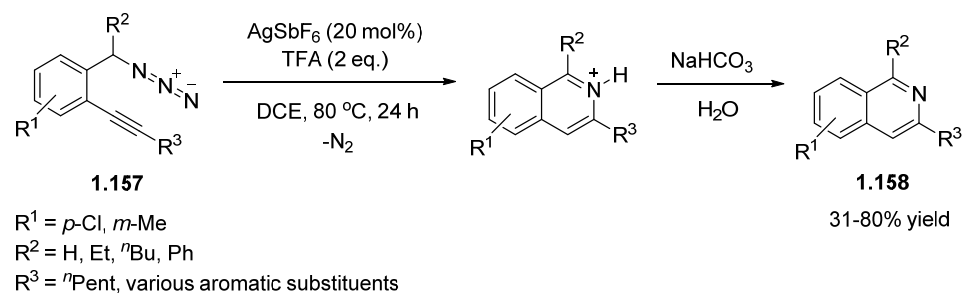
**Scheme 1.65.** Cyclization 2-alkynyl benzyl azides

Other than the cyclization of imines (see Schemes 1.48 and 1.49), the cyclization 2-alkynyl benzyl azides **1.157** can also provide access to substituted isoquinolines **1.158** (Scheme 1.65).[100] The reaction proceeds with high regioselectivity as only the 6-e*ndo-dig* cyclization product was formed. Higher yields were also obtained with substrates with electron-withdrawing substituents on the phenyl ring. However, this reaction requires high catalyst loading (20 mol%), trifluoroacetic acid additive and high temperatures to obtain decent yields.

### 1.2.2.12 Nitrosamines
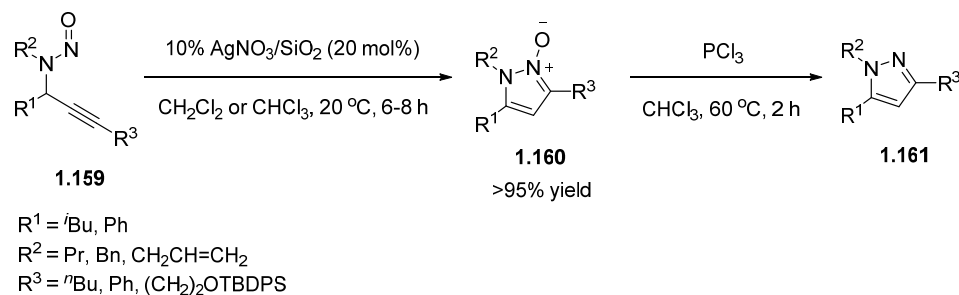


**Scheme 1.66.** Cyclization of *N*-nitrosamines

Building on the success of the AgNO$_3$/silica catalyst in the cyclization of $\beta$-methylene alkynols to furans (see Scheme 1.14), Knight and co-workers applied the same catalyst to the cyclization of *N*-nitrosamines **1.159** to afford pyrazole-*N*-oxides **1.160** in nearly quantitative yields (Scheme 1.66).[101] Deoxygenation of the pyrazole-*N*-oxides with PCl$_3$ gives the corresponding *N*-substituted pyrazoles **1.161**.

## 1.3 Catalytic Applications of Silver(I) NHC Complexes

During the past decades *N*-heterocyclic carbenes (NHCs) have emerged as a versatile class of ligands in coordination chemistry, particularly in the field of homogeneous catalysis. The first silver NHC complex was synthesized by Arduengo and co-workers in 1993.[102] However, it was left to Wang and Lin to demonstrate their capability as versatile carbene transfer agents that the chemistry of silver NHCs was explored.[103] Since then, they have been widely employed in transmetallation reactions.[104] However, their application catalysis remains largely unexplored. In this section, a summary of all the catalytic applications of silver NHCs reported to date will be provided, with particular emphasis on the important structural features of the NHC ligands that

influence the catalytic activity of the resulting silver complex. This would be appropriate before a discussion of the structures and reactivity of NHC silver(I) acetate complexes provided in Chapter 4. Instead of describing the examples in chronological order as previous reviews have done [105,106], the discussion will be broadly divided into three sections based on the type of reaction being catalyzed.

## 1.3.1. Reactions Involving Alkenes
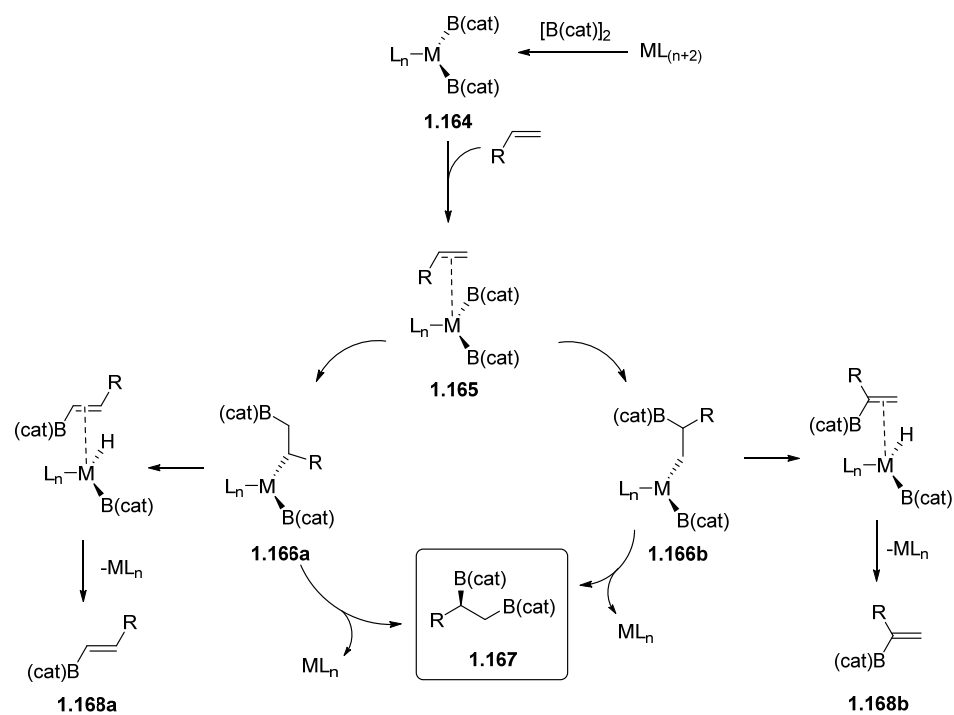


**Scheme 1.67.** General mechanism for the diboration of alkenes

The diboration of alkenes presents two inherent issues of chemoselectivity and enantioselectivity that can be tackled with the proper design of metal catalysts. As can be seen from the general mechanism[107] in Scheme 1.67, a successful catalyst must first be able to into the B–B σ bond of the diboron reagent in order to form the intermediate metal *bis*(boryl)complex **1.164**. Subsequent

60

alkene coordination to form **1.165** and insertion into the M–B bond provides

intermediates **1.166a** and **b**, which can then undergo reductive elimination to

generate the desired 1,2-*bis*(boronate)ester product **1.167**. It should be noted

that intermediates **1.166a** and **b** can also undergo a competitive *β*-hydride

elimination to give the undesired hydroboration products **1.168a** and **b**.
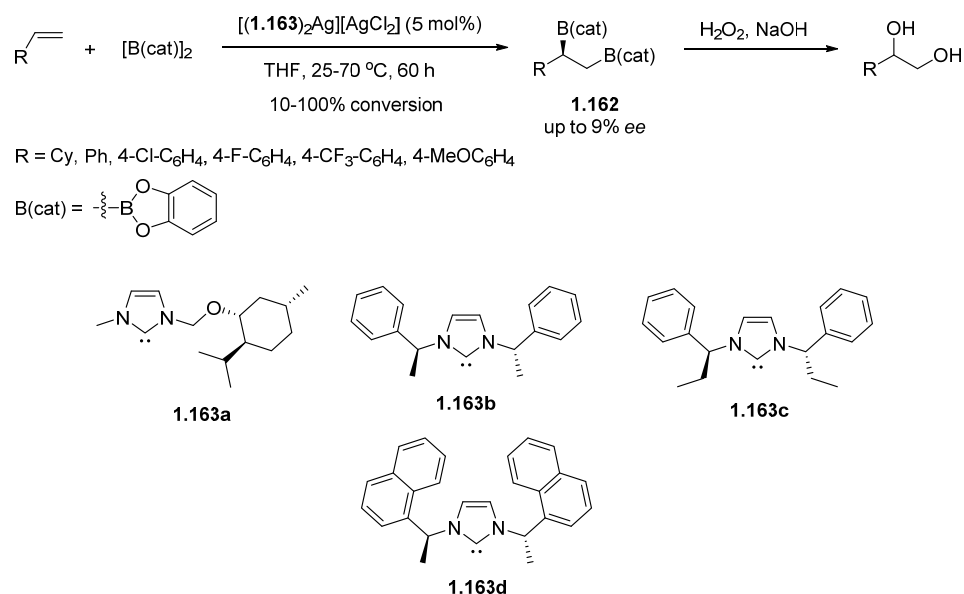


**Scheme 1.68.** Diboration of alkenes using silver(I) chiral NHC complexes

In 2005, Peris and Ferńandez reported that Ag(I) *bis*(NHC) complexes of the

menthol-derived ligand **1.163a** catalyzed the diboration of alkenes (Scheme

1.68). [108] They thought that Ag(I) NHC complexes combined requisite

electronic properties to ensure cleavage of the diborane, while low energy d-

orbitals minimize π-backbonding and thus β-hydride elimination. More

significantly, it provided the first example of Ag(I) NHC complexes being

applied in catalytic reactions. Disappointingly, the silver(I) complex of ligand

**1.163a** catalyzed the diboration reaction with limited scope, and no

asymmetric induction was observed, possibly due the lability of the Ag-C

bond, and that the chiral center lies far from the metal. Subsequently, other chiral NHC ligands **1.163b-d** were employed[109], but the *ee*s remained low, with the highest *ee* of 9% achieved by the complex of ligand **1.163c**, presumably due to the higher steric hindrance around the metal center upon coordination. In comparison, AgNO$_3$ and Ag(I) phosphine complexes were completely inactive under the same reaction conditions.
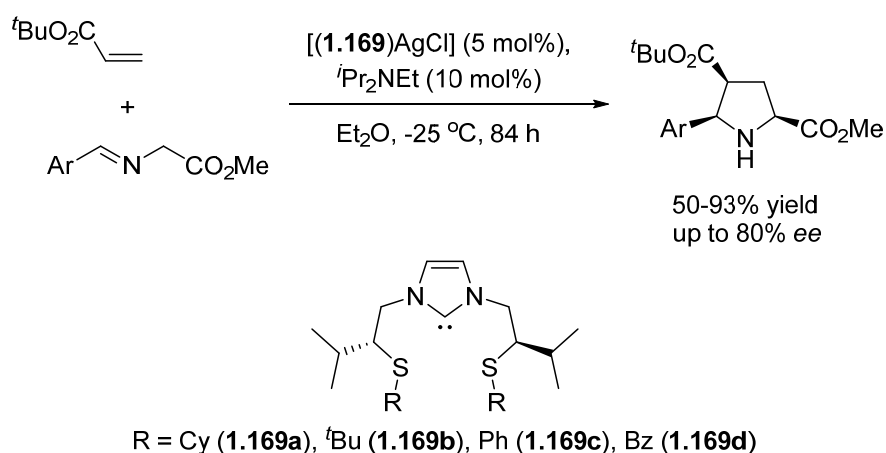


**Scheme 1.69.** Silver(I) NHC catalyzed 1,3-dipolar cycloaddition of azomethine ylides with acrylates

Later, Lassaletta, Ferńandez and co-workers reported that enantioselective catalysis by Ag(I) NHC complexes can be achieved using pincer type S/C(NHC)/S ligands, where the configuration of the sulfur atom is controlled by a neighboring stereogenic centre (Scheme 1.69). [110] Ligand **1.169a** produced the highest *ee*s of up to 80%. The authors attribute the successful chiral induction to the ability of the tridentate pincer ligands to stabilize the resulting complexes, and also to the hemilabile behavior of the thioether functionalities in the ligand.
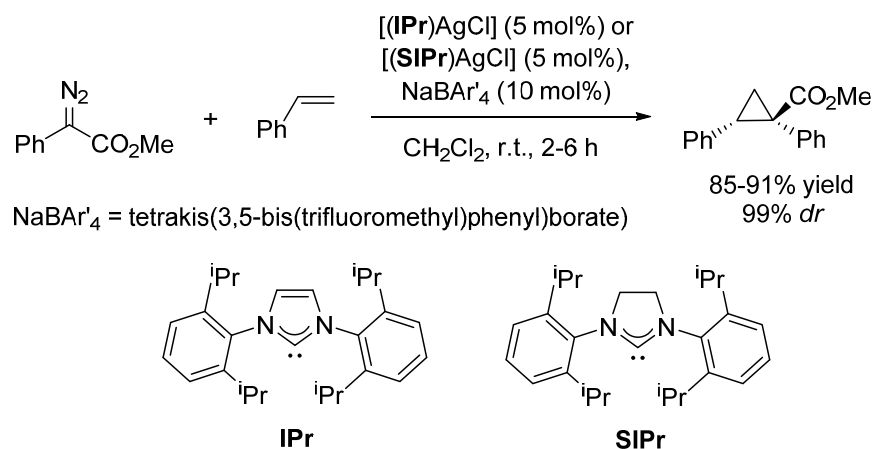
**Scheme 1.70.** Silver(I) NHC catalyzed cyclopropanation reaction between styrene and phenyldiazoacetate

In a comparative study of the ability of NHC complexes of group 11 metals to catalyze the cyclopropanation of olefins, Pérez and Echavarren reported that the Ag(I)-NHC chloride complexes of IPr and SIPr were able to catalyze the cyclopropanation reaction between styrene and phenyldiazoacetate, although they were less active than their gold and copper analogues (Scheme 1.70).[111]

## 1.3.2. C-C Bond Forming Reactions
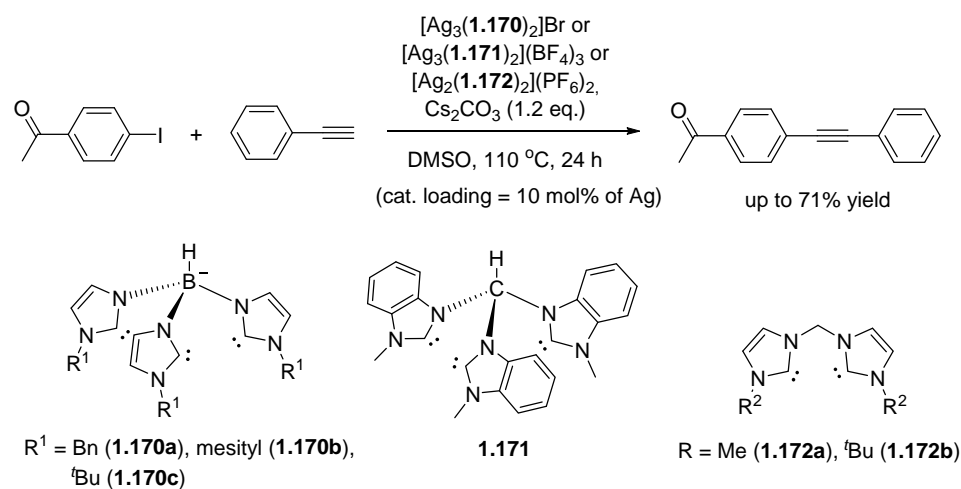


**Scheme 1.71.** Silver(I)-NHC catalyzed Sonogashira coupling reaction

The group of Biffis employed Ag(I) complexes of scorpionate-type triscarbene ligands and biscarbene ligands in the Sonogashira coupling of phenylacetylene and 4-iodoacetophenone (Scheme 1.71). [112] Despite the harsh reaction conditions, the yields were generally poor, and even lower than that of AgI (yields >90%)[113] under similar reaction conditions.
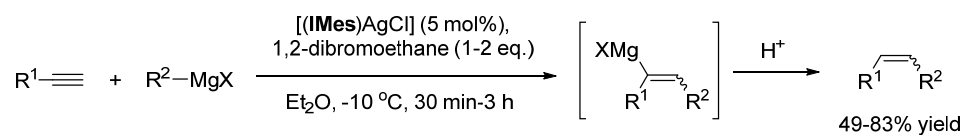
$R^1$ = aryl, 3-thienyl, PhMe$_2$Si
$R^2$ = $^n$Bu, $^s$Bu, $^t$Bu, $^n$Oct
X = Cl, Br
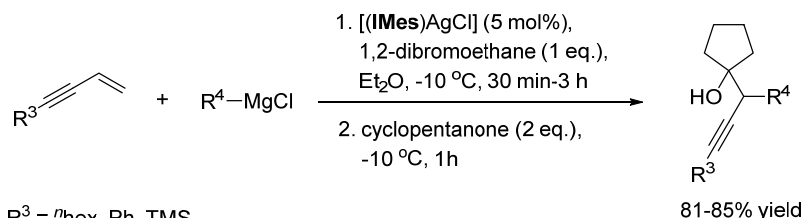
$R^3$ = $^n$hex, Ph, TMS
$R^4$ = $^s$Bu, $^t$Bu

**IMes**
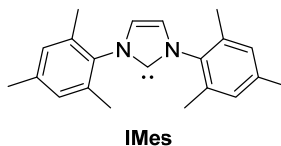
**Scheme 1.72.** Silver(I) NHC catalyzed carbomagnesiation reactions of alkynes and enynes with alkyl Grignard reagents
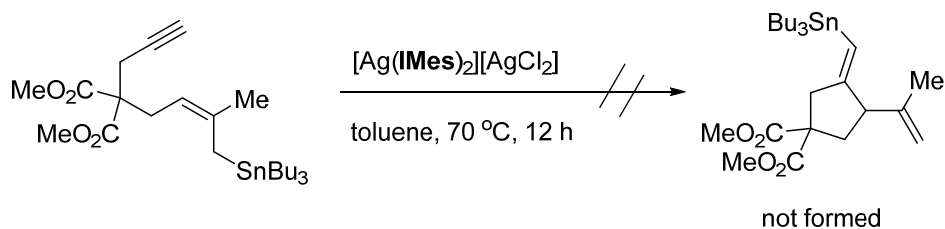
**Scheme 1.73.** Unsuccessful use of a silver(I) *bis*(NHC) complex in the carbostannylation reaction of alkynes

Terao and Kambe *et al.* have also reported that the [(IMes)AgCl] catalyzes the carbomagnesiation of terminal alkynes efficiently in the presence of 1,2-dibromoethane as an oxidant. Compared to AgOTs or combinations of AgOTs/phosphine, [(IMes)AgCl] generally gave better yields, except when *sec*-butylmagnesium was used.[114] The reaction could also be extended to conjugated enynes, provided an electrophile, such as cyclopentanone, was used to trap the intermediate organomagnesium species formed. In the somewhat related carbostannylation reaction of alkynes (Scheme 1.73), silver salts (AgOTf, AgBF$_4$ and AgSbF$_6$) and the triphenylphosphine complex [(Ph$_3$P)AgOTf] were active catalysts, while the cationic Ag(I) *bis*(NHC) complex of IMes could not catalyze the reaction.
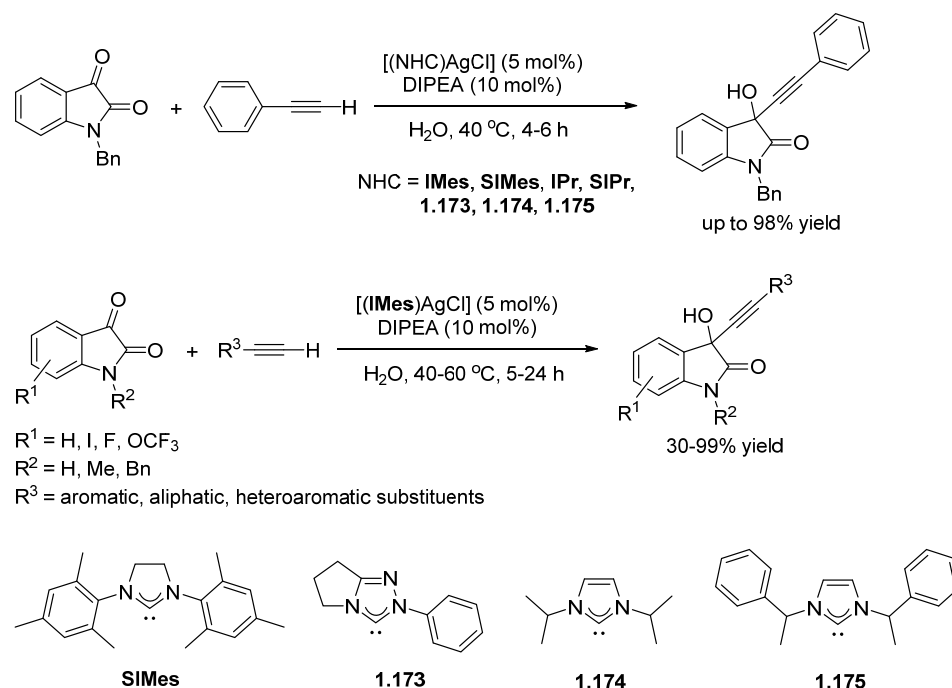


**Scheme 1.74.** Silver(I) NHC-catalyzed alkynylation reactions of isatins

65

Liu, Li and co-workers have reported the first silver(I) NHC-catalyzed reaction performed in water.[115] Using the reaction of *N*-benzylisatin with phenylacetylene as a model reaction (Scheme 1.74), the activity of seven Ag(I)-NHC chloride complexes were screened. Interestingly, they found that the NHC ligand employed had a profound effect on the outcome of the reaction – complexes of imidazole-derived NHC ligands with aromatic substituents on nitrogen (IMes, SIMes, IPr and SIPr) gave excellent yields of 92-98%, while complexes of the triazole derived NHC ligand **1.173**, and imidazole-derived NHC ligands with alkyl substituents on nitrogen **1.174** and **1.175** showed poor activity (0-10% yield). Using the most effective IMes complex, the substrate scope was explored. The reaction was found to be insensitive to substitution at the alkyne, while the substitution at the *N*-atom of the isatins influenced the reactivity and the product yield strongly. The use of water as the solvent was crucial for obtaining good yields, and the reaction could also be run in air. The authors propose that excellent activity of the catalysts was due to the high stability of the complexes and corresponding silver acetylide catalytic intermediates.
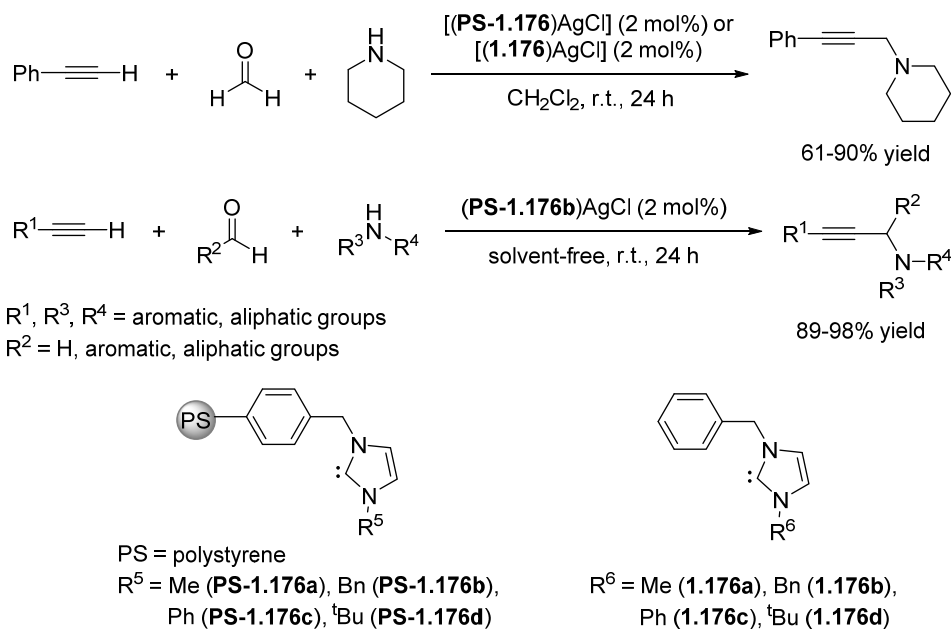
**Scheme 1.75.** The first silver(I) NHC catalyzed $A^3$-coupling reaction reported by the group of Wang

The three-component coupling of aldehyde, alkyne, and amine ($A^3$-coupling) is probably the most widely studied catalytic reaction employing Ag(I)-NHC catalysts, first reported by the group of Wang in 2008. [116] They have demonstrated that Ag(I)-NHC complexes and polystyrene-supported Ag(I)-NHC complexes are efficient catalysts for the reaction (Scheme 1.75). In both the polystyrene-supported and non-polystyrene supported complexes, the *N*-substitution on the NHC ligand was found to influence the catalytic efficiency in the order: Bn > Ph > $^t$Bu > Me, which approximately correlates with the size of the substituents. The polystyrene supported complexes also showed slightly higher activities compared to the non-polystyrene supported complexes (69-90% vs. 61-80% yield), and can be recycled for over 12 cycles without significant leaching.
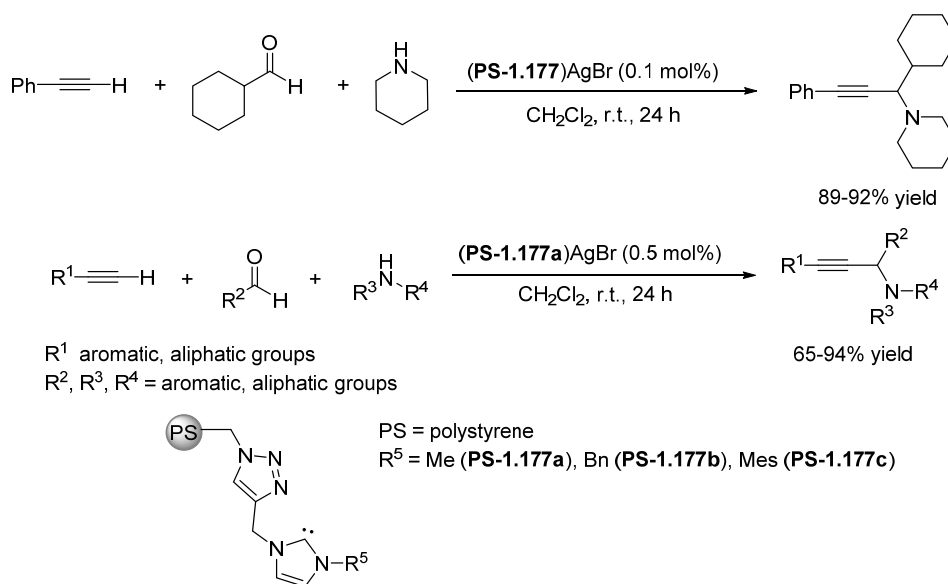
**Scheme 1.76.** Catalytic activity of polystyrene-supported silver(I) NHC complexes synthesized by the group of Cai

The use of polystyrene-supported Ag(I) NHC complexes for the $A^3$ reaction was further investigated by Cai *et al.* (Scheme 1.76).[117] Instead of using a benzyl linker group to tether the NHC moiety to polystyrene, they used a 1,2,3-triazole linker group, which was constructed *via* click chemistry. In contrast to the catalysts previously reported by Wang, the activity of this series of catalysts was not affected by the *N*-substitution of the NHC ligands. The presence of the potentially coordinating triazole group also appeared to be beneficial to the catalytic efficiency of the complexes, as good yields could be obtained at reduced catalytic loadings of 0.5 mol%. The catalysts can also be recycled for 5 cycles without significant loss in activity.
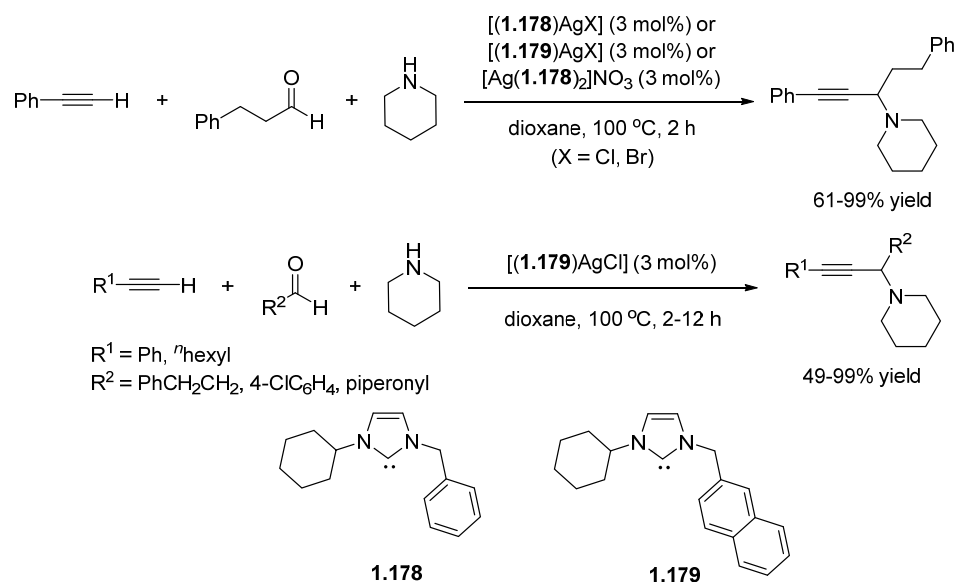
**Scheme 1.77.** Catalytic activities of well-defined silver(I) NHC complexes

Zou and co-workers prepared chloro-, bromo- and *bis*(NHC) complexes of the ligands **1.178** and **1.179**, and unambiguously confirmed their structure in the solid state via single crystal X-ray crystallography.[118] Screening for their catalytic activity towards the $A^3$ reaction, it was found that complexes of the more sterically hindered ligand **1.179** were superior, and the chloride complexes showed better yields than the corresponding bromide and *bis*(NHC) complexes (Scheme 1.77). The larger steric hindrance of ligand **1.179** presumably results in more stable complexes that do not undergo exchange readily in solution, while the observation that the chloride complexes were more active than their bromide counterpart suggests that the first step of the catalytic cycle involves the coordination of the alkyne to the complex, which is more favorable with a smaller anion.

However, these complexes were less active than the polystyrene supported catalysts reported by Wang *et al.*, as adopting the same reaction conditions

reported by Wang ($CH_2Cl_2$ at room temperature) in the reaction of phenylacetylene, 3-phenylpropionaldehyde and piperidine only furnished trace amounts of product. More forcing reaction conditions (dioxane at 100 °C) were adopted; and although respectable yields of 61-99% were obtained, it was found that AgCl also resulted in 80% yield of under the same reaction conditions. Complex [(**1.179**)AgCl] exhibited a near quantitative yield of 99% which surpassed that of AgCl, and it was used for subsequent investigation of the substrate scope.
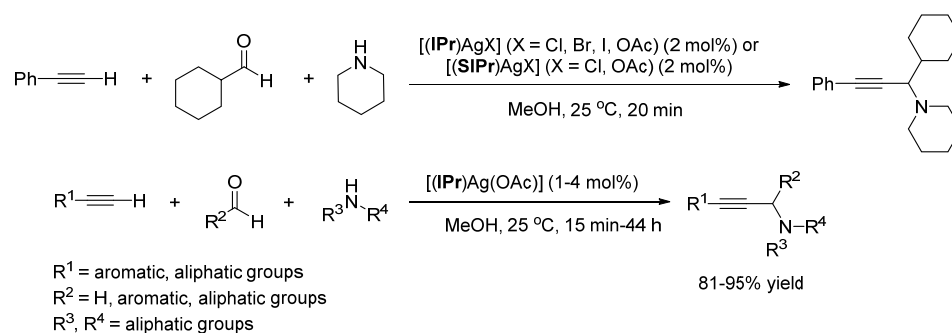


**Scheme 1.78.** Silver(I) NHC halide and acetate complexes as catalysts for the A[3] reaction reported by Navarro and co-workers

A similar effect of the size of the anionic ligand on silver was also observed by Navarro and co-workers.[119] In a comparative study of the complexes of silver(I) halide and acetate complexes of IPr and SIPr ligands (Scheme 1.78), it was found that the catalytic activity decreased in the order: OAc > Cl > Br ≫ I, and differences in activity between the IPr and SIPr complexes were minimal; lending support to Zou's proposal that the initiating step of the reaction involves displacement of halide ligand by the alkyne to form a silver acetylide intermediate.
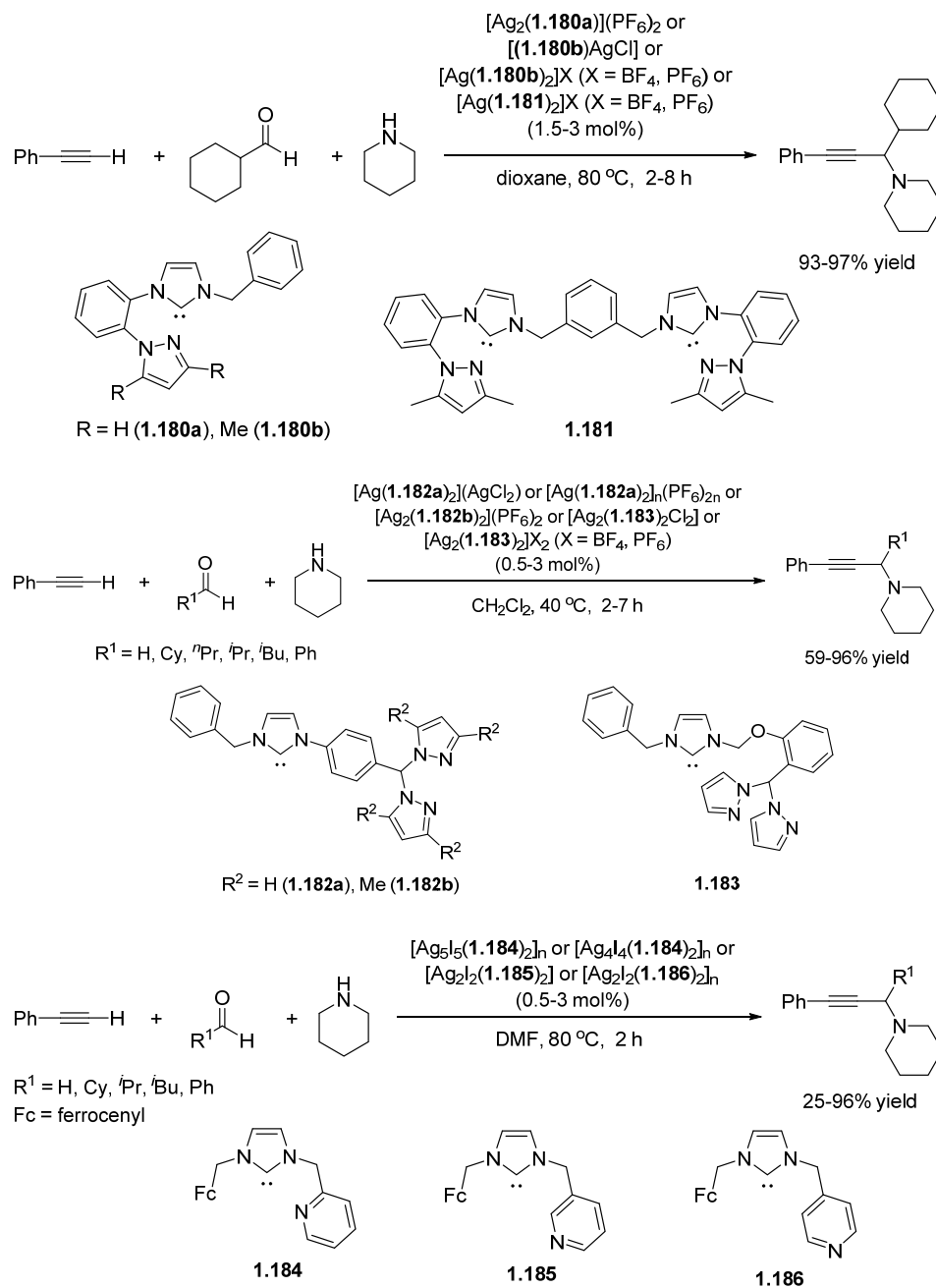
**Scheme 1.79.** Di- and polynuclear Ag(I)-NHC complexes synthesized by Tang's group

The three most recent reports by Tang's group[120,121,122] focused more on the structural features of the complexes than their catalytic activity, as there is little discussion on how the structure of the NHC impacts the catalytic activity of the resulting complexes. Nevertheless, in this work, the flexibility and

presence of multiple donor functionalities in the NHC ligands resulted in multinuclear and polymeric structures. These impose a negative effect on the efficiency of the resulting complexes as both higher reaction temperatures and catalytic loadings were required (Scheme 1.79).

### 1.3.3 Nucleophilic Addition Reactions to Alkynes
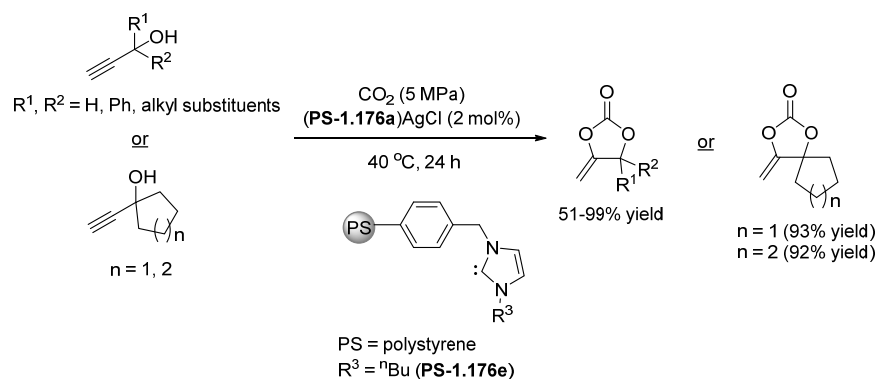


**Scheme 1.80.** Synthesis of cyclic carbonates

The synthesis of cyclic carbonates using homogeneous silver catalysts has been described previously (Scheme 1.26). Building on the success of Zhang's polystyrene-supported Ag(I) NHC complexes in the $A^3$ reaction, Qi, Jiang and co-workers prepared two of the polystyrene catalysts reported by Zhang's group, **PS-1.176a** and **PS-1.176b** (see Scheme 1.75), and a new polystyrene-supported Ag(I) complex of the same NHC ligand bearing an *n*-butyl group on nitrogen, **PS-1.176e** (see Scheme 1.80). The catalysts were tested for their activity towards the cyclization of carbonates,[123] and good yields were obtained at low catalytic loadings. The catalyst could also be recycled for up to 15 times without decrease in catalytic activity.
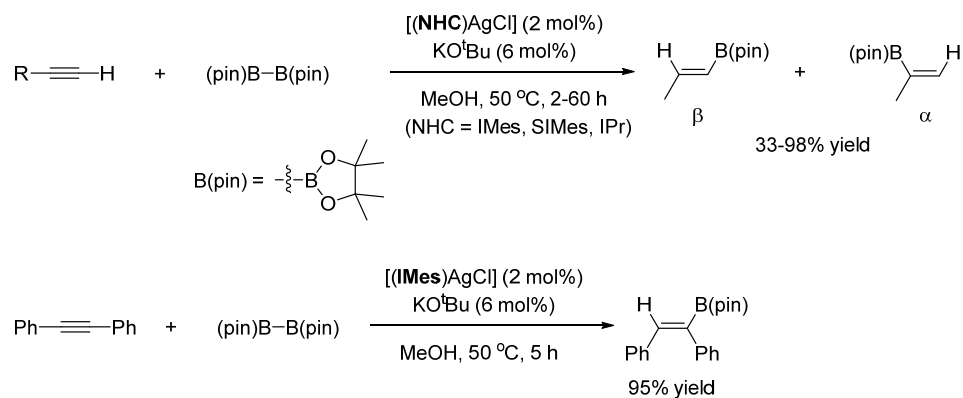
**Scheme 1.81.** Formal hydroboration of alkynes

The ability of Ag(I) to catalyze the formation of carbon-boron bonds was exemplified by the seminal work of Peris and Fernández[108] in the diborylation of alkenes with *bis*(catecholato)-diboron (Scheme 1.68). This prompted the group of Yoshida to carry out a preliminary screening of Ag(I)-NHC chloride complexes of IMes, SIMes and IPr to catalyze the addition of *bis*(pinacolato)-diboron to alkynes (Scheme 1.81).[124] It was found that a strong base was essential for the reaction to proceed in a protic solvent such as methanol. The IMes and SIMes complexes showed similar activities, while the reaction did not proceed with the complex of the more sterically demanding IPr. Using [(IMes)AgCl], the substrate scope was explored. In addition to the high regioselectivity towards the *β*-product, a variety acyclic and cyclic alkyl groups, functional groups such as cyano, halogen, silyl ether, and hydroxyl, were tolerated at the alkyne. The non-terminal alkyne, diphenylacetylene, also underwent the stereoselective hydroboration to afford (*Z*)-borylstilbene in 95% yield.

## 1.3.4. Nucleophilic addition reactions to aldehydes and imines
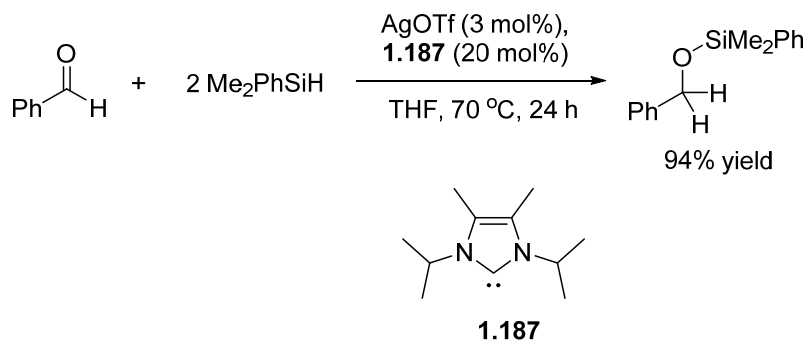


**Scheme 1.82.** Hydrosilylation of benzaldehyde

In 2006, Stradiotto and Wile reported the first application of silver compounds in the hydrosilylation of aromatic and aliphatic aldehydes to yield silyl ethers.[125] They found that AgOTf alone could catalyze the reaction, but the addition of appropriate ligands such as monodentate phosphines or NHC could result in cleaner reactions and improved yields. Only one example of a NHC ligand was used in this work (**1.187**, Scheme 1.82), and monodentate phosphines with non-sterically hindered substituents such as Et$_3$P, were still superior.
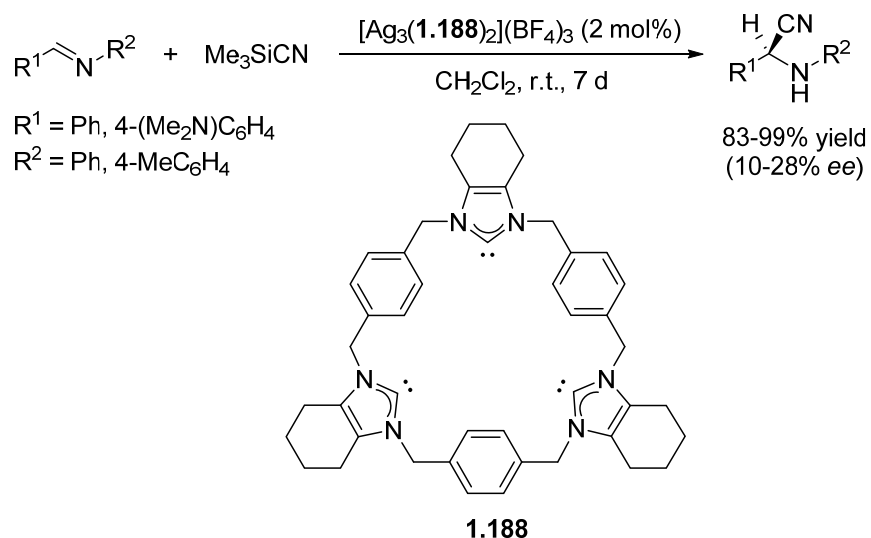
**Scheme 1.83.** Cyanosilylation of imines by a trisilver cationic cage

Zhang, Duan and co-workers synthesized a novel chiral trisilver cationic cage of the ligand **1.188**, which had a cylindrical shape with a diameter of approximately 1 nm (9.5 Å) (Scheme 1.83). When the complex was applied to the asymmetric cyanosilylation of imines, they found that the yields diminished with sterically hindered substrates bearing naphthyl groups, suggesting that the reactions took place within the cavity of the cylinder. The low levels of stereoinduction obtained were attributed to the linear geometry around the silver centers and the lack of steric hindrance to constrain the spatial geometry of products.[126]

## 1.4 Summary and Project Aims

The gold- and silver-catalyzed cycloisomerization reactions involving attack of a heteroatom nucleophile on alkynes is an attractive method for the synthesis of heterocycles. In the examples presented above, differences in reactivity between gold and silver catalysts are evident, and numerous

transformations where gold catalysts have previously proven to be efficient can be achieved by silver species, sometimes under slightly different reaction conditions. Although the slightly lower Lewis activity of silver(I) catalysts compared to gold(I) catalysts may require that higher catalytic loadings and harsher reaction conditions in certain instances, this property of silver may be harnessed when more than one nucleophilic site is present in the substrate and reaction of the weaker nucleophile with the alkyne is preferred; or when subsequent reactions of the double bond resulting from the cyclization reaction is to be avoided.

Lately, the role of silver salts in cationic gold(I) and gold(III) catalysts has also come under scrutiny, and the potential of silver salts to mediate some of these transformations, or to exhibit different reactivity patterns in the same transformation that complement that of gold catalysts is slowly being recognized. Moving beyond their role as halide abstractors in gold catalysis, a number of reports where silver catalysts have been employed at low catalytic loadings and mild reaction conditions, or even in tandem reactions, have been amply demonstrated. However, most of these early studies have primarily focused on the use of silver salts rather than silver complexes as catalysts. In the few cases where suitable ligands are employed, greater stability and efficiency of the catalyst was reported. However, very little is known about the active catalytic species in the reaction mixture in these cases.

Previous work in the KKH group[127] has also demonstrated the utility of silver(I) catalysts in the enantioselective heterofunctionalization reactions of

allenes, which offer a cost-effective alternative to gold-catalyzed reactions. Similarly, the objective of this work is to explore the catalytic utility of silver(I) salts and complexes in the heterocyclization reactions of alkynes, as a step towards the development of silver catalysts that are competitive with existing gold(I) complexes. This work began with the screening of simple silver salts to establish the counteranion effects on catalytic activity, followed by an investigation of the various P- and N-donor and NHC ligands on the catalytic activity. Given that there are few examples of silver(I) NHC complexes as catalysts for organic transformations, we believe that there is much room for exploration of these strong σ-donor ligands on the catalytic activity of the resulting silver complexes. Catalysts which show good activity will be optimized by varying the reaction conditions, e.g. the solvent, temperature and catalytic loading. Finally, a range of substrates will be synthesized and screened to determine the reaction scope and limitations of the catalyst.

# Chapter 2 Intramolecular Hydroamination Reaction of Trichloroacetimidates

In this chapter, the catalytic activity of silver(I) salts and their complexes with *P*- and *N*-donor ligands towards an intramolecular hydroamination reaction – specifically, the addition of trichloroacetimidates to alkynes, will be explored. As described in Chapter 1, previously reported examples of intramolecular silver(I)-catalyzed hydroamination reactions of alkynes have been limited to the addition of amine and amide substrates. It would thus be worthwhile to explore the possibility of expanding the scope to include imidates as nucleophiles, potentially affording *N,O*-heterocycles such as oxazoline, oxazole and oxazine products.
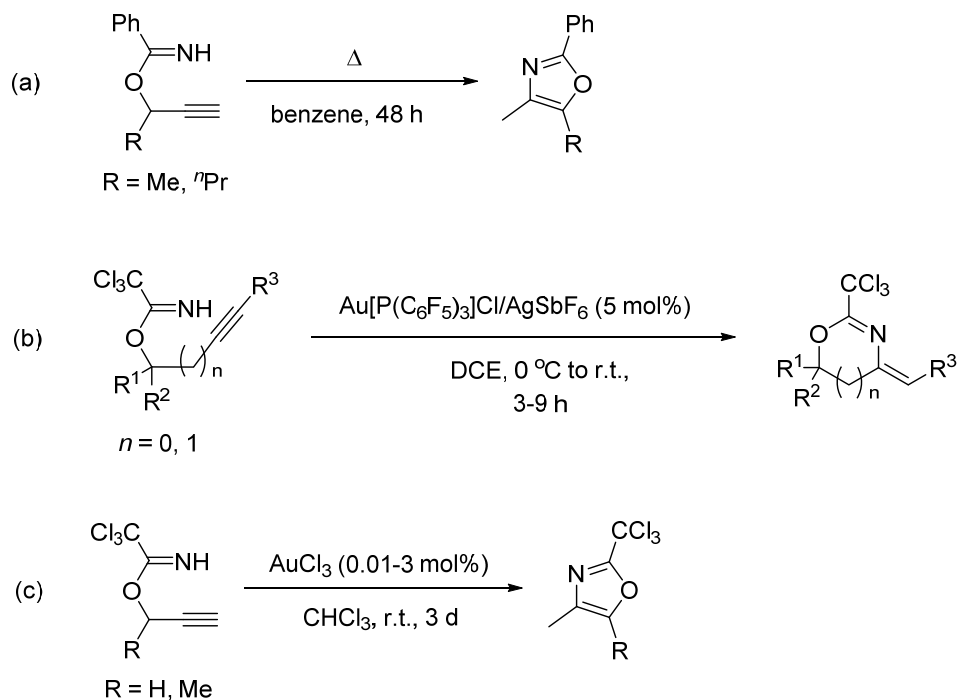
**Scheme 2.1.** Previous reports of intramolecular hydroamination of alkynes by imidate nucleophiles

The intramolecular addition of imidates to alkynes can occur without any catalyst *via* a thermal isomerization process, as shown in Scheme 2.1a.[128] Gold catalysts were later employed for the reaction, allowing it to proceed under milder reaction conditions: Shin and co-workers[129] were the first to report the use of a cationic phosphine–gold(I) complex to effect the cyclization of 16 acyclic substrates to *exo*-methylene substituted oxazolines and oxazines in good to excellent yields (Scheme 2.1b). Hashmi *et al.*[130] later reported that AuCl₃ could also promote the reaction, affording the oxazole products, but with a very limited substrate scope, consisting of only two examples (Scheme 2.1c).

## 2.1 Initial Screening of Silver Salts
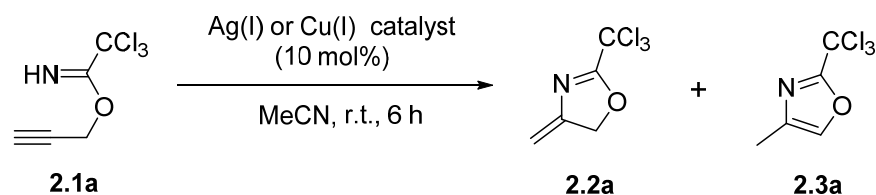


**Scheme 2.2.** Model reaction for the initial screening of Ag(I) and Cu(I) salts

The ability of various silver and copper salts to promote the intramolecular hydroamination reaction of the model substrate **2.1a** was first examined. The reaction could potentially afford the methylene oxazoline **2.2a** or the oxazole **2.3a** (Scheme 2.2). In the initial screening, a mixture of **2.1a** and 10 mol% of the silver or copper salt was stirred in acetonitrile at room temperature. After 6 h, TLC analysis showed that **2.1a** was completely consumed in certain cases.

Removal of the solvent *in vacuo* and subsequent $^1$H NMR analyses of the crude reaction mixtures in CDCl$_3$ indicated the absence of the alkyne resonance peak at 2.55 ppm, and the appearance of triplet of doublet resonances at 5.39 and 4.87 ppm, which correspond to the diastereomeric alkene protons of **2.2a**; and/or a triplet at 2.27 ppm which corresponds to the methyl protons in **2.3a**. The reactions were then repeated with a known amount of an internal standard (1,3,5-methoxybenzene) added to the NMR samples of the crude reaction products. The NMR yields of **2.2a** and **2.3a** can thus be calculated by comparing the integrals of the alkene protons of **2.2a** and the methyl protons of **2.3a** relative to the protons of 1,3,5-methoxybenzene. The results are tablulated in table 2.1; the corresponding pK$_a$ values of the conjugate acids of the counteranions of the silver and copper salts were also included in the analysis.

**Table 2.1.** Initial screening of Ag(I) and Cu(I) salts in the cyclization of **2.1a**[a]

| Entry | Catalyst | pK$_a$ of conjugate acid | Conversion[b] (%) | Yield[b] of 2.2a (%) | Yield[b] of 2.3a (%) |
|---|---|---|---|---|---|
| 1 | AgOAc | 4.8[131] | 36 | 8 | – |
| 2 | AgTFA | 0.2[131] | 100 | 76 | – |
| 3 | AgNO$_3$ | -1.3[132] | – | – | – |
| 4 | AgOTs | -2.8[133] | 91 | 9 | 8 |
| 5 | AgBF$_4$ | -4.9[134] | 100 | – | 16 |
| 6 | AgSbF$_6$ | -13[135] | 100 | 28 | – |
| 7 | AgOTf | -14[136] | 100 | 18 | 15 |
| 8 | AgPF$_6$ | -20[135] | 49 | 16 | – |
| 9 | Ag$_2$O | 15.7[137] | – | – | – |
| 10 | Ag$_2$CO$_3$ | 3.9[138] | – | – | – |
| 11 | Ag$_2$SO$_4$ | -3.0[132] | – | – | – |
| 12 | [Cu(OTf)]$_2$·C$_6$H$_6$ | -14[136] | 100 | 33 | – |
| 13 | TfOH | -14[136] | – | – | – |

[a] Reaction conditions: **2.1a** (0.4 mmol), catalyst (0.04 mmol, 10 mol%), 23 °C, MeCN (1 mL).
[b] Determined by $^1$H NMR spectroscopy, using 1,3,5-trimethoxybenzene as internal standard.

It was observed that some of the silver salts and copper(I) triflate were active for the transformation. However, although full conversion of **2.1a** was achieved in some cases, the yields of the products remained low, due to competitive formation of side products, which were also observed in the reaction mixture. Attempts to identify these products were unsuccessful. None of the di-silver salts $Ag_2O$, $Ag_2CO_3$ and $Ag_2SO_4$ were active (entries 9-11) and, with the exception of AgOAc, $AgPF_6$ and $AgNO_3$, all other AgX salts and $[Cu(OTf)]_2$ afforded quantitative conversion of **2.1a** within 6 h at room temperature (entries 2, 4-7 and 12). This indicated a strong counteranion effect on catalytic activity; in the order $CF_3CO_2^- > > TfO^- > SbF_6^- > BF_4^- > TsO^- > PF_6^- > CH_3CO_2^-$, which did not show any correlation with the $pK_a$ values of the conjugate acids. Notably, AgTFA gave the highest yield of **2.2a** in 76% yield after 6 h. To clarify that Brønsted acids were not involved in the reaction, a control experiment was performed using 10 mol% of triflic acid (the maximum amount of acid that could theoretically be formed in the reaction). No conversion of substrate **2.1a** was observed (entry 13).

The reaction was also conducted in various common organic solvents, such as $CH_2Cl_2$, DCE, acetone and THF, and the results are summarized in Table 2.2. It was postulated that the differing polarities and donor abilities of these solvents will affect the solubility of the catalysts and stability of reactive catalytic intermediates during the reaction, which could potentially allow cleaner reactions and improved yields of the products.

**Table 2.2.** Solvent study using silver salts[a]

| Entry | Catalyst | Solvent | Conversion[b] (%) | Yield[b] of 2.2a (%) | Yield[b] of 2.3a (%) |
|---|---|---|---|---|---|
| 1 | AgOAc | DCE | 51 | 21 | – |
| 2 | AgTFA | DCE | 100 | 14 | 15 |
| 3 | AgOTs | DCE | 100 | 5 | 26 |
| 4 | AgBF$_4$ | DCE | 100 | – | 16 |
| 5 | AgSbF$_6$ | DCE | 100 | 54 | – |
| 6 | AgOTf | DCE | 100 | – | 46 |
| 7 | AgPF$_6$ | DCE | 37 | 13 | – |
| 8 | AgOTf/PS[c] | DCE | 100 | 80 | – |
| 9 | AgOAc | acetone | 30 | 9 | – |
| 10 | AgTFA | acetone | 62 | 22 | – |
| 11 | AgOTs | acetone | 68 | 28 | – |
| 12 | AgBF$_4$ | acetone | 100 | 37 | 5 |
| 13 | AgSbF$_6$ | acetone | 82 | 37 | – |
| 14 | AgOTf | acetone | 100 | 40 | – |
| 15 | AgPF$_6$ | acetone | 27 | 5 | – |
| 16 | AgOAc | CH$_2$Cl$_2$ | 51 | 26 | – |
| 17 | AgTFA | CH$_2$Cl$_2$ | 100 | 10 | 28 |
| 18 | AgOTs | CH$_2$Cl$_2$ | 100 | – | 38 |
| 19 | AgBF$_4$ | CH$_2$Cl$_2$ | 100 | 12 | 22 |
| 20 | AgSbF$_6$ | CH$_2$Cl$_2$ | 100 | 13 | 35 |
| 21 | AgOTf | CH$_2$Cl$_2$ | 100 | – | 52 |
| 22 | AgPF$_6$ | CH$_2$Cl$_2$ | 40 | 15 | – |
| 23 | AgOAc | THF | 46 | 9 | – |
| 24 | AgTFA | THF | 73 | 15 | – |
| 25 | AgOTs | THF | 79 | 28 | – |
| 26 | AgBF$_4$ | THF | 57 | 16 | – |
| 27 | AgSbF$_6$ | THF | 77 | 35 | – |
| 28 | AgOTf | THF | 96 | 51 | – |
| 29 | AgPF$_6$ | THF | 26 | 3 | – |

[a] Reaction conditions: **2.1a** (0.4 mmol), catalyst (0.04 mmol, 10 mol%), 23 °C, solvent (1 mL). [b] Determined by $^1$H NMR spectroscopy, using 1,3,5-trimethoxybenzene as internal standard. [c] PS = proton sponge (5 mol%), 40 °C, 3 h.

In chlorinated solvents such as CH$_2$Cl$_2$ and DCE, complete conversion of **2.1a** was obtained with all the silver salts except AgOAc and AgPF$_6$, while acetone and THF afforded lower conversions but allowed the high selectivities towards the oxazoline product **2.2a**. Interestingly, the use of 10 mol% of AgOTf in CH$_2$Cl$_2$ and DCE afforded the aromatic oxazole product **2.3a** exclusively in

moderate yields (entries 6 and 21), while the formation of the oxazoline product **2.2a** was favored in acetone and THF.

The irreversible isomerization of methylene oxazolines to oxazoles has been reported to occur rapidly under acidic conditions.[129] Although it was found that TfOH is not catalytically active in the cyclization of **2.1a** (Table 2.1, entry 13), it was found that the aromatization of **2.2a** to **2.3a** was complete within 5 h in the presence of 5 mol% of TfOH. Suspecting that trace amounts of the Brønsted acid could be generated *in situ* and be responsible for the isomerization of **2.2a** to **2.3a**, a separate experiment was conducted whereby 5 mol% of 1,8-*bis*(dimethylamino)naphthalene (proton sponge) was added to the AgOTf-catalyzed cyclization of **2.1a**. Indeed, **2.2a** was formed exclusively in 80% yield (entry 8) with minimal side product formation, showing that selective formation of the *exo*-methylene product **2.2a** can be attained by Ag-catalysis, as long as the attendant Brønsted acidity can be suppressed.

## 2.2 Synthesis and Catalytic Activity of Ag(I) Complexes of *P*- and *N*-Donor Ligands

Encouraged by the above results, the effect of ligands on the activity of the silver catalysts was assessed, in an attempt to improve the performance of these silver(I) catalysts. Well-defined Ag(I) complexes of several *P*- and *N*-donor ligands were first prepared by reaction with AgOTf in the appropriate stoichiometric ratio (Scheme 2.2). Complexes **2.4**,[139] **2.5a**[140] and **2.7**[69] were prepared according to literature procedures, and characterized by comparisons

of their NMR data. Complex **2.6** was specifically prepared as a new entity in this work.

(a)  AgOTf  +  PPh$_3$  $\xrightarrow{\text{CH}_2\text{Cl}_2, \text{ r.t., 12 h}}$  [(PPh$_3$)Ag(OTf)]
                                                                        **2.4**

(b)  AgOTf  +  2 [pyridine]  $\xrightarrow{\text{MeCN, r.t., 6 h}}$  [py–Ag–py]$^+$ OTf$^-$

[Ag(py)$_2$]OTf
**2.5a**

(c)  AgOTf  +  2 [2,2'-bipyridine]  $\xrightarrow[\text{overnight}]{\text{MeCN, r.t.,}}$  [Ag(bpy)$_2$]$^+$ OTf$^-$

[Ag(bpy)$_2$]OTf
**2.6**

(d)  AgOTf  +  [1,10-phenanthroline]  $\xrightarrow[\text{r.t., 15 min}]{\text{MeOH/H}_2\text{O,}}$  [Ag(phen)]$_n$OTf
                                                                                (n = 1 or 2)
                                                                                **2.7**
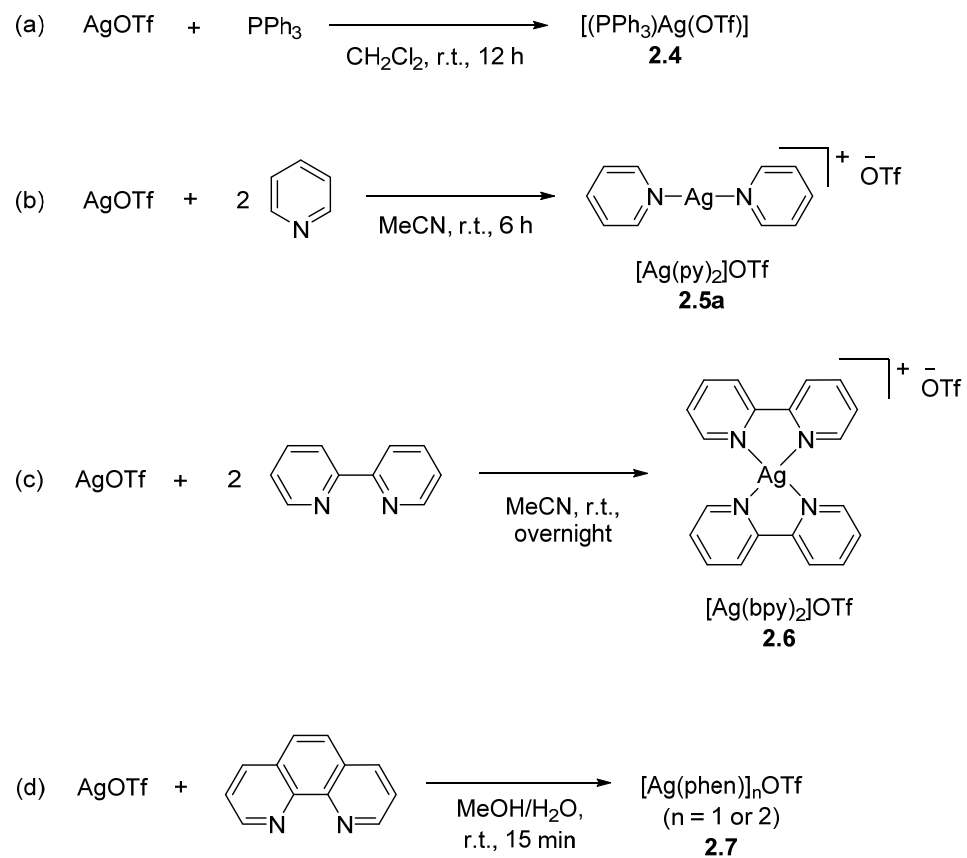
**Scheme 2.3.** Synthesis of Ag(I) complexes of (a) triphenylphosphine, (b) pyridine, (c) 2,2'-bipyridine and (d) 1,10-phenanthroline
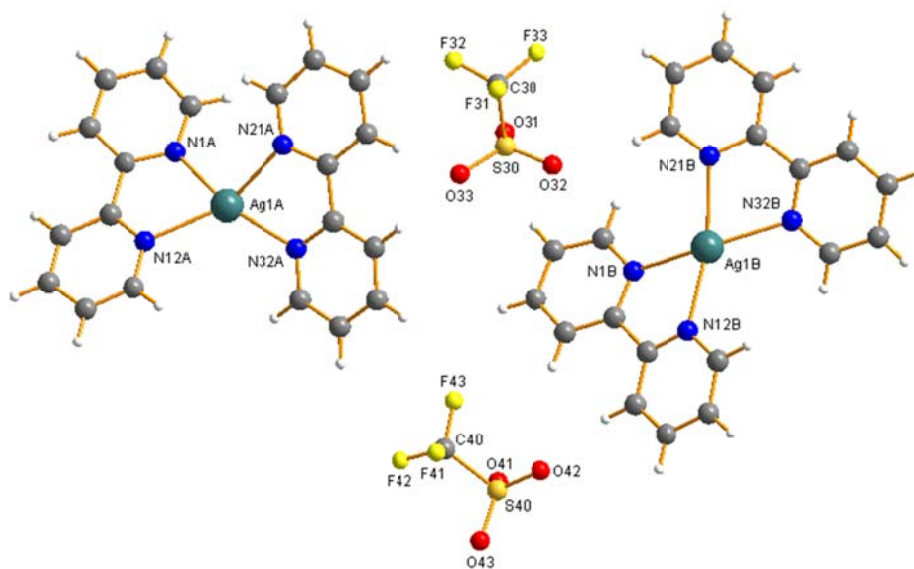
**Fig. 2.1.** Molecular structure of complex **2.6**, with two structurally distinct molecules in the asymmetric unit

**Table 2.3.** Selected bond lengths (Å) and angles (deg) for complex **2.6**

| | | | |
|---|---|---|---|
| Ag(1A)-N(1A) | 2.362(3) | Ag(1B)-N(1B) | 2.372(4) |
| Ag(1A)-N(12A) | 2.300(4) | Ag(1B)-N(12B) | 2.305(3) |
| Ag(1A)-N(21A) | 2.393(3) | Ag(1B)-N(21B) | 2.350(3) |
| Ag(1A)-N(32A) | 2.264(3) | Ag(1B)-N(32B) | 2.322(4) |
| N(1A)-Ag(1A)-N(12A) | 71.0(1) | N(1B)-Ag(1B)-N(12B) | 70.9(1) |
| N(21A)-Ag(1A)-N(32A) | 71.2(1) | N(21B)-Ag(1B)-N(32B) | 71.3(1) |

The structure of the *bis*(pyridine) complex **2.6** has been confirmed by X-ray structure analysis, and is depicted in Fig. 2.1, with relevant bond distances and angles given in Table 2.3. The asymmetric unit of complex **2.6** consists of two distinct $[Ag(bpy)_2]^+$ cations and two triflate anions, with slightly different bond distances and angles obtained for each. The Ag(I) ion adopts a distorted square planar geometry in the complex, through coordination with two chelating 2,2'-bipyridine ligands. The Ag−N bond lengths fall within the range of 2.264(3) and 2.393(3) Å, and the ligand N−Ag−N bite angles range from 70.93 to 71.34 °, typical for complexes of such ligands.[141] The two pyridyl

rings within each bipyridine ligand are roughly coplanar, with dihedral angles in the range of 9.15 to 15.33°, while the interplanar dihedral angles between pairs of ligands bonded to silver are 33.5° and 23.8°.

It is worthy to note that the 2,2'-bipyridyl ligand forms a *bis*-chelate complex with AgOTf, while a mono-chelate complex is formed with the 1,10-phenanthroline ligand. However, the actual metal-to-ligand ratio of the 1,10-phenanthroline silver(I) triflate complex remains ambiguous. In the adopted literature procedure[69] for the synthesis of the complex, a 1:1 metal-to-ligand ratio was assumed by analogy to a previously reported [Ag(phen)]NO$_3$ complex[142], and no spectroscopic data or elemental analysis results were provided. A literature search revealed that Ag(I) has a tendency to form *bis*-chelate complexes with 1,10-phenanthroline in the presence of weakly coordinating anions such as triflate,[141, 143] although different solvents and reaction conditions were used for the preparation of the complex. Although $^1$H and $^{13}$C NMR experiments on the complex revealed the presence of a single species in solution while C, H, and N microanalyses showed that the composition of the complex is closer to that of a *bis*-chelate complex than that of a *mono*-chelate complex. Attempts to crystallize the complex only afforded thin, poor quality needles that were unsuitable for X-ray single crystal diffraction. Despite this uncertainty, the complex was included in the catalyst screening since it was reported to be an active catalyst in intramolecular hydroamination reactions.

The isolated silver complexes **2.4-2.7** were evaluated as catalysts in the cyclization of the model substrate **2.1a** in a number of solvents (MeCN, DCE, acetone, CH$_2$Cl$_2$ and THF), and the results are shown in Table 2.4.

**Table 2.4.** Screening of catalysts for the cyclization of substrate **2.1a**[a]

| Entry | Catalyst | Solvent | Conversion[b] (%) | Yield[b] of 2.2 (%) | Yield[b] of 2.3 (%) |
|---|---|---|---|---|---|
| 1 | **2.4**[c] | MeCN | – | – | – |
| 2 | **2.5** | MeCN | 100 | 83 | – |
| 3 | **2.5** | DCE | 100 | 83 | – |
| 4 | **2.5** | acetone | 100 | 87 | – |
| 5 | **2.5** | CH$_2$Cl$_2$ | 100 | 83 | – |
| 6 | **2.5** | THF | 100 | 75 | – |
| 7 | **2.6** | MeCN | 32 | 13 | – |
| 8 | **2.6** | DCE | 44 | 22 | – |
| 9 | **2.6** | acetone | 69 | 46 | – |
| 10 | **2.6** | CH$_2$Cl$_2$ | 35 | 17 | – |
| 11 | **2.6** | THF | 49 | 21 | – |
| 12 | **2.7**[c] | MeCN | – | – | – |

[a] Reaction conditions: **2.1a** (0.4 mmol), catalyst (0.04 mmol, 10 mol%), 23 °C, solvent (1 mL). [b] Determined by $^1$H NMR spectroscopy, using 1,3,5-trimethoxybenzene as internal standard. [c] Changing the solvent failed to improve the conversion.

The triphenylphosphine complex **2.4** was found not to be catalytically inactive in any of the solvents employed (Table 2.4, entry 1). The failure of complex **2.4** to catalyze the reaction could be due to the reduced Lewis acidity of the metal center that arises from the stronger donating ability of triphenylphosphine towards Ag(I) compared to nitrogen-donor ligands. This higher affinity of Ag(I) towards phosphorous donors compared to nitrogen donors has been exemplified in the structural studies of Ag(I) complexes of 2-pyridylphosphine ligands, where it was found that coordination to the pyridine nitrogen to silver(I) is only involved when chloro or phosphorus coordination is insufficient for coordinative saturation.[144]

The Ag(I) *bis*(pyridine) complex **2.5** afforded **2.2a** regioselectively as the sole product in all solvents, and in higher yields than that obtained with AgTFA in MeCN (Table 2.4 entry 2 *vs* Table 2.1, entry 2). The solvent did not have a significant effect on the yield, although marginally higher yields were obtained when the reactions were conducted in acetone (Table 2.4, entries 2-6). The complete selectivity for the oxazoline product **2.2a** suggests that in addition to their ability to stabilize reactive catalytic species, the pyridine ligands could also serve as acid scavengers, preventing the isomerization of **2.2a** to **2.3a**.
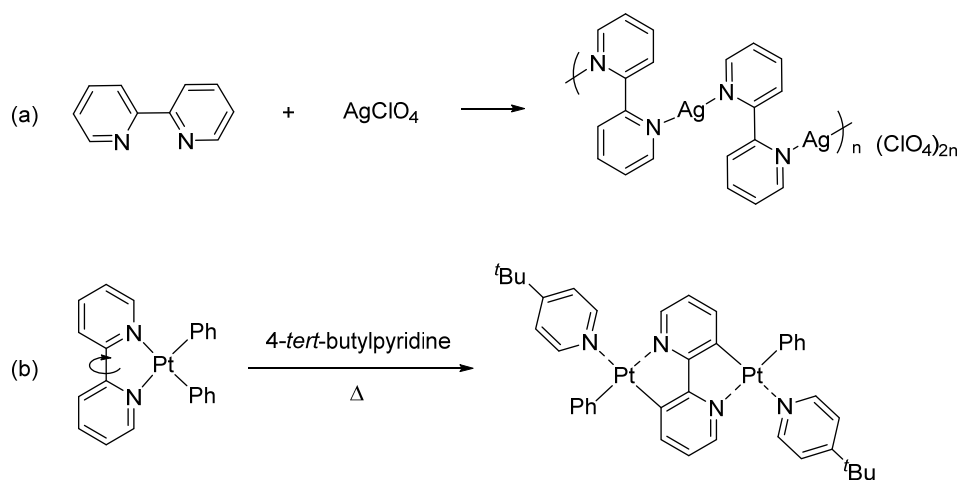


**Scheme 2.4.** (a) Synthesis of $[Ag(bpy)]_n(ClO_4)_{2n}$, which exists as one-dimensional polymer in the solid state; (b) An example of a Pt(II) 2,2-bipyridine 'roll-over' cyclometallated complex

Complex **2.7** is similar to **2.6** in that they both contain bidentate, chelating *N*-donor ligands. However, complex **2.6** catalyzed the reaction while complex **2.7** was inactive (entries 7-12). The observed difference in catalytic activity could be attributed to the poor solubility of complex **2.7** in the solvents

employed at room temperature, and the greater rigidity of the phenanthroline (phen) ligand compared to the bipyridine (bpy) ligand. Despite having a saturated square planar coordination sphere, rotation around the central bond of the bpy ligands in complex **2.6** can create vacant coordination sites for the coordination of incoming substrates. This flexibility of the bpy ligand is apparent from its ability to form one-dimensional ligand-bridged polymeric arrays[141] and 'roll-over' cyclometallated complexes by rotation around the central bond[145] (Scheme 2.3). In comparison, this rotational freedom is not possible for the phen ligand. If the structure of a *bis*-ligated complex is assumed, coordination of substrates will not be possible without the dissociation of a phen ligand from the metal center, which is less likely to occur given its strong chelating ability.

## 2.3 Reaction Optimization and Substrate Scope



$n = 0$ (**2.1**)
$n = 1$ (**2.8**)

$n = 0$ (**2.2**)
$n = 1$ (**2.9**)
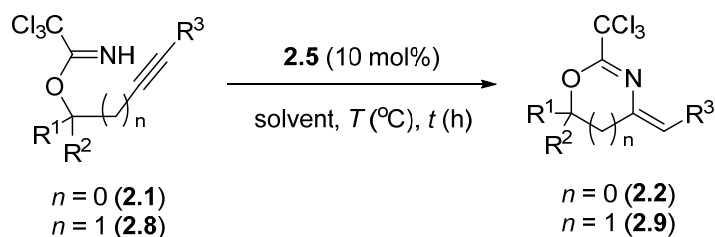
**Scheme 2.5.** 5- and 6-*exo-dig* cyclizations of (homo)propargylic trichloroacetimidate substrates **2.1** and **2.8**

The scope of complex **2.5** was subsequently investigated with a range of substrates, and the results were compared with those previously achieved using cationic gold complexes (Table 2.5).

**Table 2.5.** Substrate scope[a]

| Entry | R$^1$, R$^2$, R$^3$ | Solvent | $n$ | T (°C) | $t$ (h) | Prod. | Yield[b] | Yield[c] (Au cat.) |
|---|---|---|---|---|---|---|---|---|
| 1 | H, H, H | acetone | 0 | 23 | 6 | **2.2a** | 87 (67) | 98 |
| 2 | Me, H, H | acetone | 0 | 23 | 6 | **2.2b** | 85 (74) | |
| 3 | Et, H, H | acetone | 0 | 23 | 6 | **2.2c** | >99 (86) | |
| 4 | $^i$Pr, H, H | acetone | 0 | 23 | 6 | **2.2d** | 87 (82) | 74 |
| 5 | Ph, H, H | acetone | 0 | 23 | 6 | **2.2e** | –[d] | –[d] |
| 6 | Me, Me, H | acetone | 0 | 23 | 6 | **2.2f** | 89 (79) | |
| 7 | H, H, Me | acetone | 0 | 23 | 6 | **2.2g** | – | – |
| 8 | H, H, Ph | MeCN | 0 | 60 | 7 | **2.2h** | 29 | |
| 9 | H, H, CH$_2$Br | acetone | 0 | 23 | 6 | **2.2i** | – | |
| 10 | H, H, SiMe$_3$ | MeCN | 0 | 60 | 7 | **2.2j** | 82 (72) | |
| 11 | H, H, Br | acetone | 0 | 23 | 6 | **2.2k** | 77 (30) | |
| 12 | H, H, H | acetone | 1 | 23 | 6 | **2.9a** | 93 (76) | 91 |
| 13 | Me, H, H | acetone | 1 | 23 | 6 | **2.9b** | 97 (93) | |
| 14 | Et, H, H | acetone | 1 | 23 | 6 | **2.9c** | 99 (91) | |
| 15 | Ph, H, H | acetone | 1 | 23 | 6 | **2.9d** | 94 (90) | |
| 16 | 4-ClC$_6$H$_4$, H, H | acetone | 1 | 23 | 6 | **2.9e** | 96 (87) | 91 |
| 17 | 4-CF$_3$C$_6$H$_4$, H, H | acetone | 1 | 23 | 6 | **2.9f** | 73 (70) | |
| 18 | H, H, Ph | acetone | 1 | 56 | 7 | **2.9g** | 31 | |
| 19[e] | H, H, SiMe$_3$ | acetone | 1 | 56 | 8 | **2.9h** | 80 (71) | |

[a] Reaction conditions: Substrate (0.4 mmol), **2.5** (0.04 mmol, 10 mol%), solvent (1 mL).
[b] Determined by $^1$H NMR spectroscopy, using 1,3,5-trimethoxybenzene as internal standard. Isolated yields after purification by column chromatography are indicated in parentheses.
[c] Reported isolated yields according to ref. 129, under the following conditions: Au(PAr$_3$)Cl/AgSbF$_6$ (5 mol%), DCE, 0 °C then r.t., 10 min to 9 h (Ar = C$_6$F$_5$, C$_6$H$_5$).
[d] Mixture of unidentifiable products was obtained.
[e] 20 mol% of catalyst used.

All reactions proceeded with good regio- and diastereoselectivity; only the

*exo*-cyclized products and (*Z*)-double bond isomers were observed in all cases,

indicating that the *anti*-addition of the N-H occurs exclusively. The presence

of alkyl substituents at $R^1$ and/or $R^2$ for both propargyl ($n = 0$) and

homopropargyl substrates ($n = 1$) did not significantly alter the reactivity

(entries 1-4 and 12-14). However, propargylic substrate **2.1e** with a phenyl

group in the propargylic position, was not a viable substrate, as was the case

previously observed with the Au(I) cationic catalyst (entry 5). In this case, an

unidentifiable mixture of products were obtained. In contrast, the

homopropargylic substrates **2.8d-f** with aryl substituents at $R^1$ cyclized in

good yields (entries 15-17). The failure of **2.1e** to undergo clean cyclization

was attributed to the ability of the trichloroactimidate functionality to act as a

leaving group in the presence of Lewis acids – a property that has been

frequently been exploited in the generation of glycosidic linkages in the

synthesis of oligosaccharides[146] – it is thus postulated that an elimination

reaction could have occurred with substrate **2.1e** in the presence of the silver

catalyst, resulting in a resonance-stabilized benzylic carbocation as depicted in

Scheme 2.6. This reactive carbocation may then attacked by nucleophiles

present in the reaction mixture to give several side products. However,

attempts to identify these side products to support our hypothesis have been

unsuccessful.
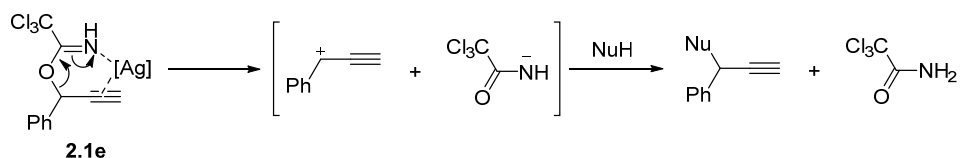


**Scheme 2.6.** Possible Ag(I)-promoted elimination of the trichloroacetimidate functionality in substrate **2.1e**

One of the limitations of the reported Au(I) and Au(III) catalysts was their inability to cyclize propargylic substrates containing non-terminal alkyne groups (n = 0, $R^3 \neq$ H), which limits its utility only to the synthesis of methylene oxazolines and methyl oxazoles. Remarkably, although substrates **2.1g** and **2.1i** containing alkyl groups at the alkyne terminus were inactive (entries 7 and 9) with the silver catalyst, good conversions were obtained with substrates that have trimethylsilyl and bromo substituents at these positions (entries 10 and 11). The phenyl-substituted substrate **2.1h** also showed a low level of conversion of 29% at an elevated temperature of 60 °C (entry 8). Similarly, the cyclization of homopropargylic substrates with non-terminal alkynes also proceeded in good conversions, albeit at elevated temperatures and higher catalytic loadings.

These results constitute the first example of a silver-catalyzed intramolecular hydroamination addition of trichloroacetimidates to alkynes, with comparable yields being obtained to that of previously reported cationic Au(I) catalysts. The fact that internal alkyne substrates can be cyclized to afford vinyl-bromide and silane products is particularly encouraging, as this extends the scope of the reaction beyond methylene oxazolines, with the potential to afford useful oxazoline and oxazole derivatives.

## 2.4. Investigation of Ligand Effects in the Cyclization of Bromoalkynes



AgOTf + 2 [pyridine with X substituent] → MeCN, r.t., overnight → [X-pyridine–Ag–pyridine-X]⁺ OTf⁻

X = OAc (**2.10a**) [Ag(Ac-Py)$_2$]OTf
OMe (**2.11a**) [Ag(MeO-Py)$_2$]OTf
NMe$_2$ (**2.12a**) [Ag(4-DMAP)$_2$]OTf
Me (**2.13a**) [Ag(Me-Py)$_2$]OTf
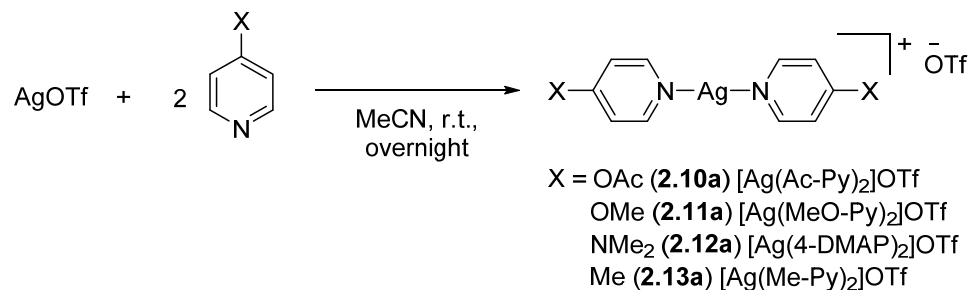
**Scheme 2.7.** Synthesis of Ag(I) *bis*(pyridine) triflate complexes

The facile cyclization of internal alkyne substrate **2.1k** (Table 2.5, entry 11) to afford the (*Z*)-4-(bromomethylene)-4,5-dihydrooxazole **(Z)-2.2k** at room temperature at 10 mol% catalytic loading attracted particular attention, as **2.2k** could potentially be subjected to further functionalization *via* cross-coupling of the vinyl bromide moiety, hence affording 4-substituted oxazoline derivatives. Hence, it was decided to investigate if the efficiency of the Ag(I) *bis*(pyridine) triflate catalyst **2.5a** could be further improved by fine-tuning of the ligand properties and counteranion. To this end, analogous complexes of pyridine ligands with electron-donating and electron-withdrawing substituents at the 4-position were prepared in a similar manner to complex **2.5a** (Scheme 2.7), and their 1:2 AgOTf:pyridine stoichiometry was confirmed by elemental analyses. Attempts to prepare the complex of the 4-trifluoromethylpyridine ligand failed, as it could not coordinate effectively to silver, due to its much-reduced Lewis basicity. The solid state structures of these complexes will be discussed in Section 2.6.

The conversion of the acyclic substrate **2.1k** in the presence of 1 mol% of the respective catalyst to the bromo-substituted oxazoline **2.2k** was monitored *in situ* by $^1$H NMR spectroscopy at room temperature (23 °C), using acetone-d$_6$ as the solvent (Scheme 2.8), and the results are shown in Fig. 2.2. The final conversions were recorded and are shown in Table 2.6.
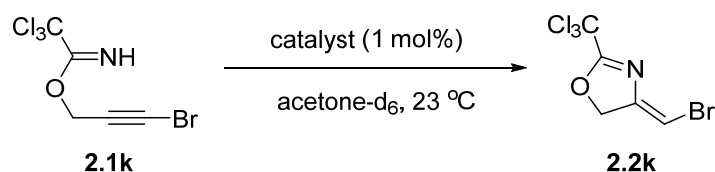


**Scheme 2.8.** Comparison of the catalytic activity of *bis*(pyridine) triflate complexes in the cyclization of substrate **2.1k** to **2.2k**.
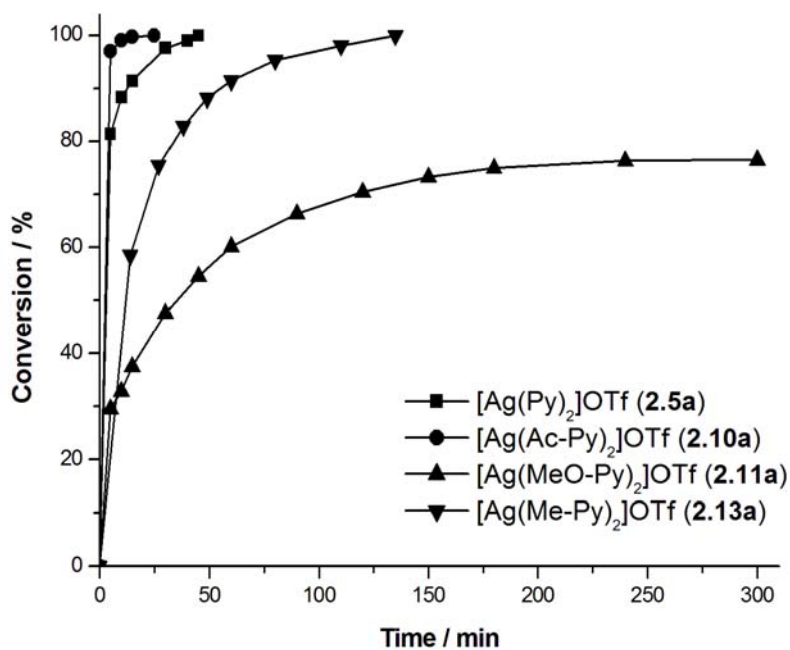


**Fig. 2.2.** Percentage Conversion of **2.1k** vs. time in the presence of 1 mol% of *bis*(pyridine) triflate complexes.

**Table 2.6.** Screening of various *bis*(pyridine) triflate catalysts for the cyclization of substrate **2.1k**

| Entry | Catalyst | Time | Conversion (%) |
|---|---|---|---|
| 1 | [Ag(Py)$_2$]OTf (**2.5a**) | 45 min | 100 |
| 2 | [Ag(Ac-Py)$_2$]OTf (**2.10a**) | 25 min | 100 |
| 3 | [Ag(MeO-Py)$_2$]OTf (**2.11a**) | 6 h | 77 |
| 4 | [Ag(4-DMAP)$_2$]OTf (**2.12a**) | 6 h | 0 |
| 5 | [Ag(Me-Py)$_2$]OTf (**2.13a**) | 2 h 15 min | 100 |

The presence of an electron-withdrawing acetyl group on the pyridine ligand in complex **2.10a** led to a dramatic enhancement in reaction rate, and complete conversion of **2.1k** was achieved in only 25 min compared to **2.5a**, which required 45 minutes (entries 1 and 2). In contrast, the introduction of electron-donating groups on the pyridine ligand slowed down the reaction. The introduction of a methyl substituent on the pyridine ligand in **2.13a** led to longer reaction times before complete conversion was achieved (entry 5). For the methoxy-substituted pyridine complex **2.11a**, the reaction was sluggish and conversion remained at a modest 77% even after 6 h (entry 3). Finally, the 4-DMAP complex **2.12a** with the most strongly electron-donating ligand was completely inactive in this reaction. These observations suggest that the electron-withdrawing substituents on the pyridine ligand enhance the Lewis acidity of the Ag(I) metal center, resulting in greater binding to the alkyne moiety, which activates it towards nucleophilic attack by the imidate nucleophile.

Next, counteranion effects in the catalytic system was investigated. A series of five additional Ag(I) *bis*(4-acetylpyridine) complexes, [Ag(Ac-Py)$_2$]Y, where Y = ClO$_4^-$ (**2.10b**), BF$_4^-$ (**2.10c**), PF$_6^-$ (**2.10d**), SbF$_6^-$ (**2.10e**) and CF$_3$CO$_2^-$ (**2.10f**), were prepared. The conversion of **2.1k** to **2.2k** in the presence of 1

mol% of these complexes in acetone-$d_6$ was monitored *in situ* by $^1$H NMR spectroscopy over 25 min at room temperature (23 °C), and the results are presented in Fig. 2.2.

As catalysts **2.10a**, **c** and **d**, each bearing TfO⁻, BF$_4^-$ and PF$_6^-$ counteranions respectively, exhibited similar rates, the catalytic loading was further reduced to 0.7 mol% for a better comparison. From Fig. 2.3 and 2.4, it is established that the reaction rate increases in the order: CF$_3$CO$_2^-$ < SbF$_6^-$ < ClO$_4^-$ < BF$_4^-$ ≈ TfO⁻ < PF$_6^-$. With the exception of SbF$_6^-$, the reaction rate correlates inversely with the basicity of the counteranion, *i.e.* weakly and non-coordinating counteranions generally perform well, while basic counteranions such as trifluoroacetate have a detrimental effect on the reaction rate.
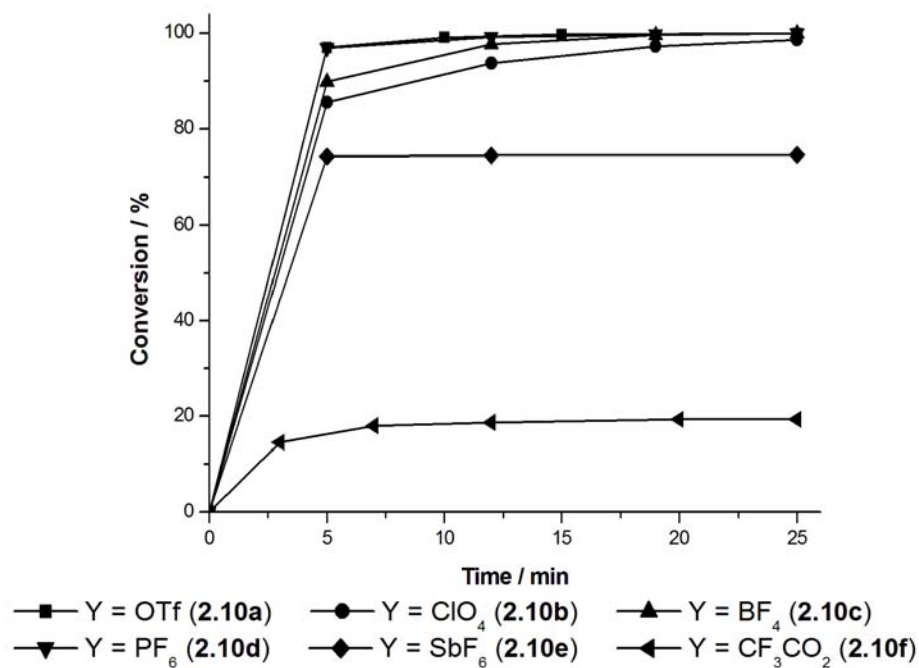


**Fig. 2.3.** Percentage conversion of **2.1k** vs. time in the presence of 1 mol% of *bis*(4-acetylpyridine) catalysts [Ag(Acpy)$_2$]Y
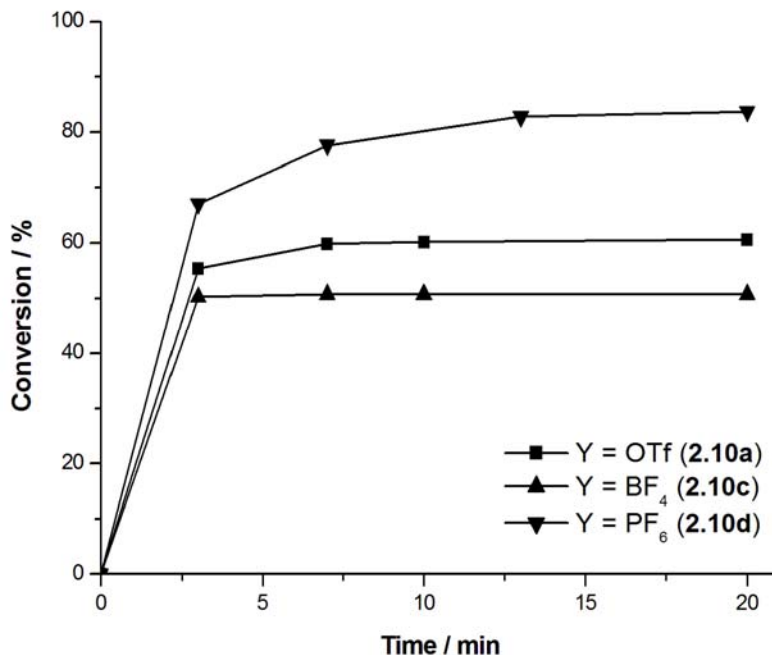
**Fig. 2.4.** Percentage Conversion of **2.1k** vs. time in the presence of 0.7 mol% of *bis*(4-acetylpyridine) catalysts [Ag(Acpy)$_2$]Y (Y = TfO$^-$, BF$_4^-$ and PF$_6^-$)

The general trends observed in the donating ability of the pyridine ligands and counteranion basicity were also similarly detected in the cyclization of substrate **2.9i** (Scheme 2.9, Figs. 2.5 and 2.6). Under optimized conditions (Scheme 2.10), **2.2k** and **2.9i** were isolated in excellent yields.
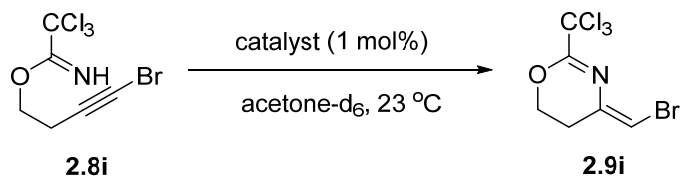


**Scheme 2.9.** Comparison of the catalytic activity of *bis*(pyridine) triflate complexes in the cyclization of substrate **2.8i** to **2.9i**

97
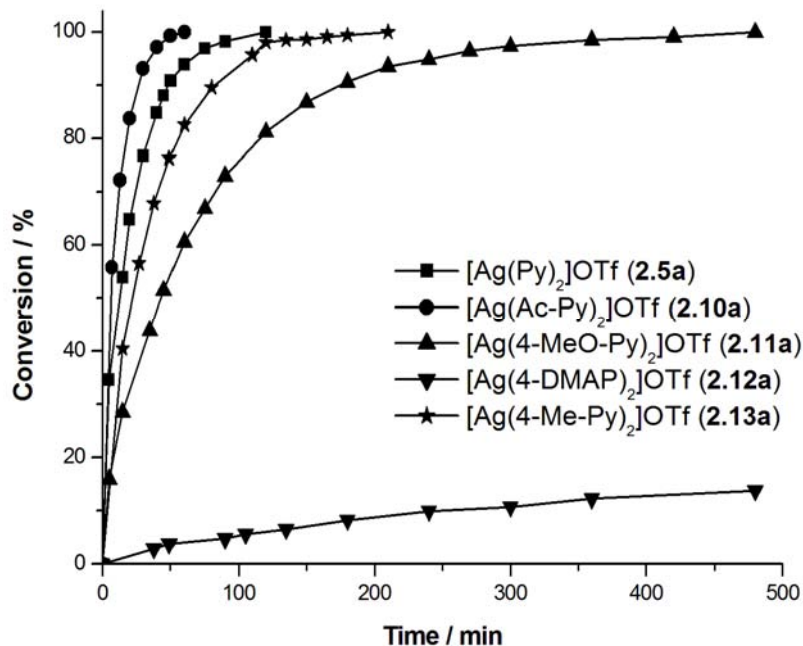
**Fig. 2.5.** Percentage Conversion of **2.8i** vs. time in the presence of 1 mol% of *bis*(pyridine) triflate complexes
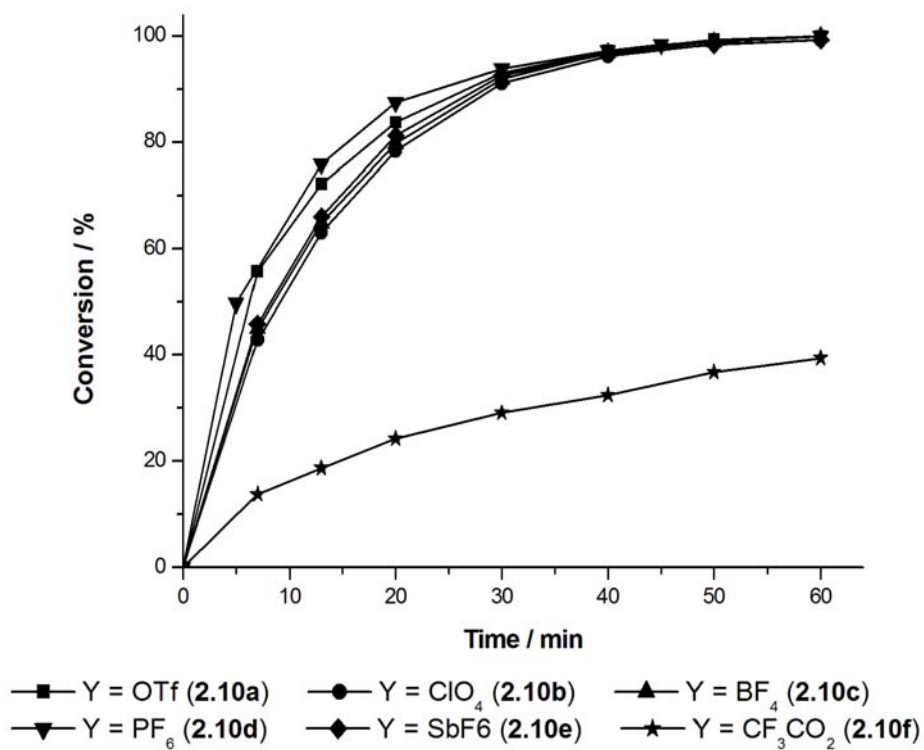


**Fig. 2.6.** Percentage Conversion of **2.8i** vs. time in the presence of 1 mol% of *bis*(4-acetylpyridine) catalysts [Ag(Acpy)₂]Y
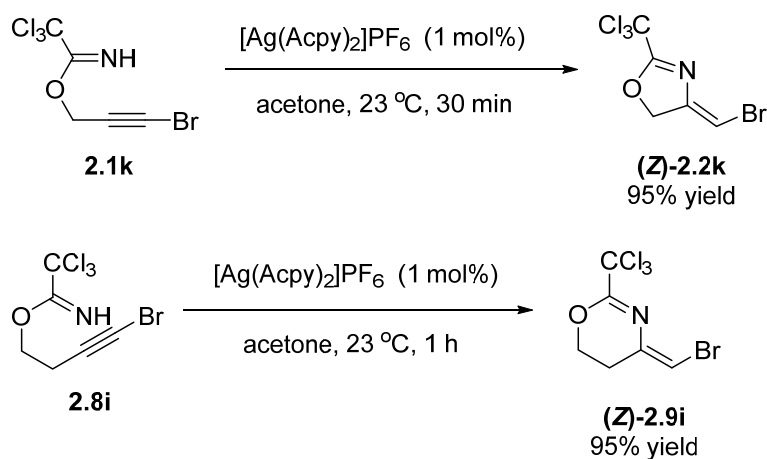
**Scheme 2.10.** Cyclization of **2.1k** and **2.8i** under optimized reaction conditions

## 2.5. Trapping of Organosilver Intermediates with Electrophiles
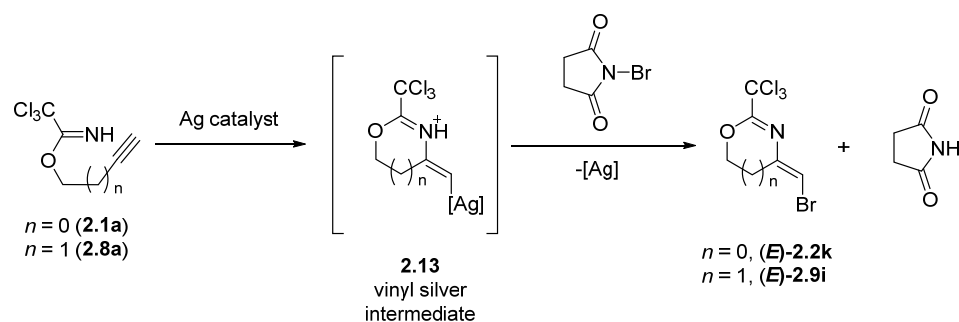


**Scheme 2.11.** Possible trapping of vinyl silver intermediates in the reaction with *N*-bromosuccinimide

Encouraged by the ability of our catalyst to deliver the (*Z*)-bromomethylene oxazoline **2.2k** and oxazine **2.9i** regioselectively, we envisaged that the intermediate organosilver species **2.13** may be trapped by an electrophilic halogen source such as *N*-bromosuccinimide (NBS), as shown in Scheme 2.11, to deliver the (*E*)-isomer. An experiment was carried out by conducting the cyclization of **2.1a** with 1.2 equivalents of NBS and 10 mol% of AgOTf in acetone. An initial exothermic reaction was observed, which was accompanied

by an immediate change in the color of the reaction mixture from colorless to brown. TLC indicated the complete consumption of **2.1a** after 6 h, and the formation of a new product which was isolated by column chromatography. Spectroscopic characterization confirmed the identity of this new product to be the expected (*E*)-bromomethylene oxazoline **2.2k**, which was obtained as a white crystalline solid in 63% yield. As **(*E*)-2.2k** was slightly thermally unstable and showed signs of decomposition when stored at room temperature overnight, it was postulated that the yield could be improved by avoiding the exothermic reaction that occurred during the initial stage of the reaction. To this end, the reaction mixture was repeated at 0 °C prior to the addition of AgOTf, which resulted in a cleaner reaction and an improved yield of 71% of **2.2k**. In comparison, the analogous reaction of the homopropylgylic **2.8a** with NBS resulted in a significantly lower yield of 25% of (*E*)-**2.9i**, due to the competitive formation of an equal amount of the unbrominated product **2.9a**.
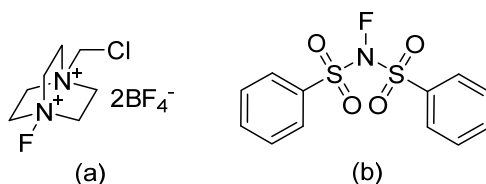


**Fig. 2.7** Electrophilic fluorinating reagents: (a) Selectfluor and (b) NFSI



AgOTf (10 mol%),
NXS (1.2 eq.)

acetone, 0 °C then r.t.,
6 h

*n* = 0 (**2.1a**)
*n* = 1 (**2.8a**)

*n* = 0, X = Br, (***E***)-**2.2k** (71%)
*n* = 1, X = Br, (***E***)-**2.9i** (25%)
*n* = 0, X = Cl, (***E***)-**2.2l** (34%)
*n* = 1, X = Cl, (***E***)-**2.9j** (11%)

100
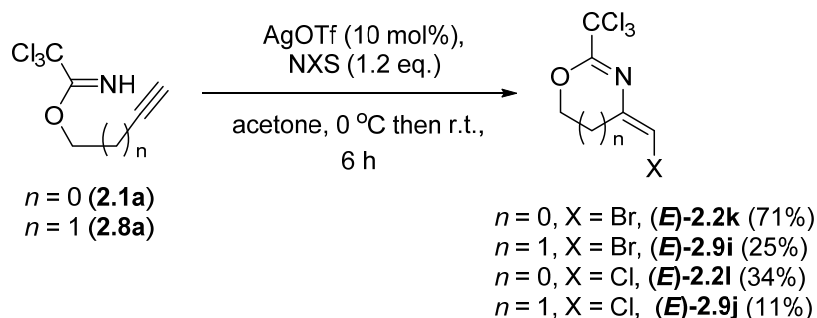
**Scheme 2.12.** Formation of halomethylene oxazolines from trichloroacetimidates

Attempts were made to extend the reaction to include electrophilic halogen sources such as *N*-chlorosuccinimide (NCS), Selectfluor and *N*-fluorobenzenesulfonimide (NFSI) (Fig. 2.7), and the results are summarized in Scheme 2.12. Lower yields were obtained with NCS compared to NBS, presumably due to its lower reactivity, as the major product was the unchlorinated product **2.9a**; and disappointingly, none of the expected fluoromethylene oxazolines and oxazines were formed using Selectfluor or NFSI as the trapping agent. Control experiments conducted under the same conditions in the absence of AgOTf showed no conversion in all cases, except in the reaction of NBS and **2.1a**, where a low yield of 7% of (*E*)-**2.2k** was obtained. The crystal structures of (*E*)-**2.9i** and (*E*)-**2.9j** were also obtained (Fig. 2.6), delivering unambiguous proof for geometry of the double bond.



(*E*)-**2.9i**          (*E*)-**2.9j**
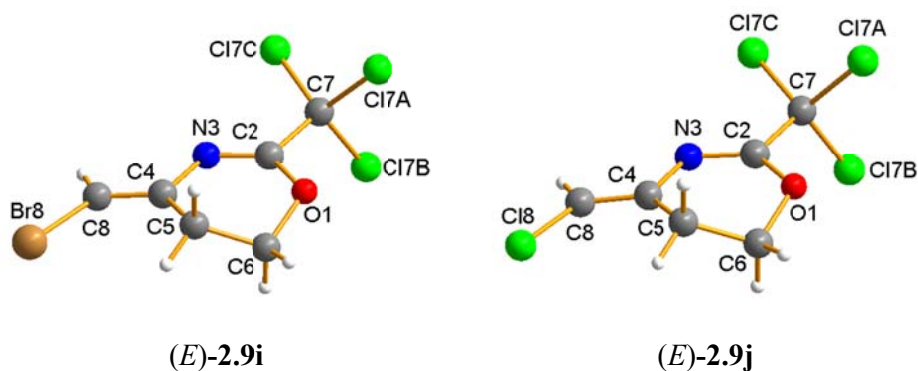
**Fig. 2.8.** Crystal structures of (*E*)-**2.9i** and (*E*)-**2.9j**.

## 2.6 Structural Analysis of Silver(I) *Bis*(pyridine) complexes



[Ag(Py)$_2$]PF$_6$ (**2.5d**)  [Ag(4-DMAP)$_2$]PF$_6$ (**2.12d**)

[Ag(Ac-Py)$_2$]PF$_6$ (**2.10d**)  [Ag(MeO-Py)$_2$]PF$_6$ (**2.11d**)
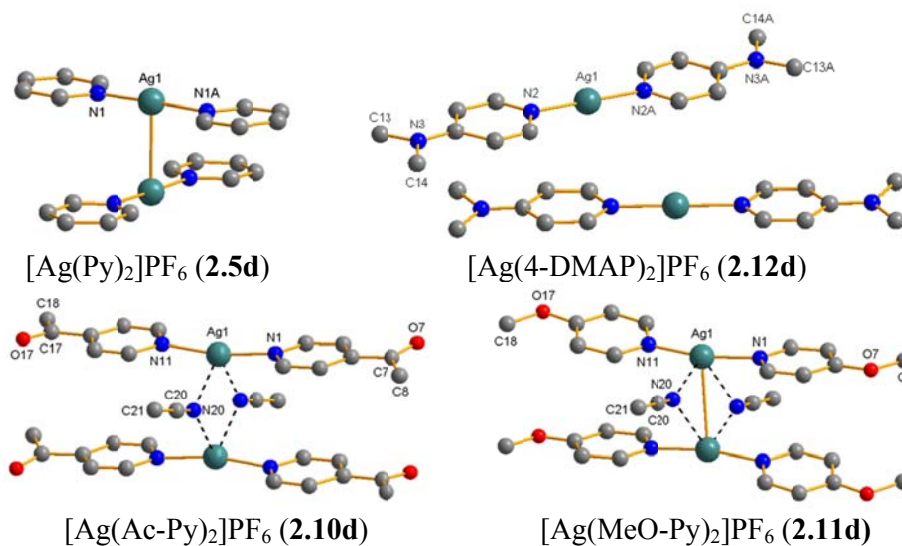
**Fig. 2.9.** Molecular structures of complexes **2.5d**, **2.10d, 2.11d and 2.12d**. Hydrogen atoms and PF$_6^-$ anions have been omitted for clarity.

The effect of *para*-substituents of the pyridine ligand has been found to exert a profound effect on the catalytic activity of these silver complexes (Section 2.4). In order to understand this effect, the solid state structures of four *bis*(pyridine)silver(I) complexes with the same (PF$_6^-$) counteranion, **2.5d**, **2.10d**, **2.11d** and **2.12d** were obtained and compared (Fig. 2.7). Complexes **2.10d** and **2.11d** are new, while the crystal structures of complexes **2.5d**[147] and **2.12d**[148] have previously been reported. The relevant bond distances and angles of the complexes are shown in Table 2.7.

A few prominent structural features of the solid-state structures of these can be noted. These include: 1) the coordination of two pyridine ligands to Ag(I) in a linear fashion in all four complexes; 2) the additional coordination of acetonitrile solvent molecules to Ag(I), as observed in the structures of complexes **2.10d** and **2.11d**, 3) the presence of unsupported argentophilic

interactions between two adjacent molecules present in complexes **2.5d** and **2.11d**, and 4) the different molecular packing in the solid state that could favor $\pi-\pi$ stacking interactions between the pyridine rings. The inclusion of solvent in the coordination sphere of Ag(I) in complexes **2.10d** and **2.11d** but not in **2.5d** and **2.12d** could have been brought about by the different solvents used for the crystallization of the complexes. Complexes **2.10d** and **2.11d** were crystallized from MeCN/Et$_2$O, while **2.5d** was crystallized by vapor diffusion of Et$_2$O into a CH$_2$Cl$_2$ solution of the complex. The crystallization solvent for **2.12d** was not stated. This additional coordination of MeCN in addition to two pyridyl ligands also results in a larger deviation of the N–Ag–N bond angle from 180°; **2.10d** and **2.11d** both have N–Ag–N bond angles of 169°, compared to 178° and 180° in **2.5d** and **2.12d** respectively.

Despite the similar coordination environment and geometry of Ag(I) in complexes **2.10d** and **2.11d**, a notable difference between them is the argentophilic interaction (Ag–Ag = 3.228 Å) that is present in **2.11d** but not in **2.10d**. Ag–Ag distances longer than the Ag–Ag separation in metallic silver (2.889 Å), but shorter than the sum of the van der Waals radii (3.44 Å) are usually an indication of such interactions.[149] However, the distance between two adjacent Ag centers in **2.10d** (4.513 Å) is too great for Ag⋯Ag interactions to occur. A plausible explanation for this is that the more basic 4-methoxypyridine ligands reduce the effective positive charge on the Ag metal center in **2.11d**, allowing two adjacent [AgL$_2$(NCMe)]$^+$ units to approach each other more closely and consequently to form Ag⋯Ag interactions. A slightly shorter and stronger Ag⋯Ag interaction (Ag–Ag = 2.964 Å) is present in **2.5d**

compared to **2.11d**. In **2.11d**, the Ag⋯Ag interaction is further complemented by face to face π–π stacking interactions between the pyridine moieties. In **2.5d**, however, such interactions are absent due to the staggered conformation of the two [Ag(Py)$_2$]$^+$ units relative to each other.

**Table 2.7** Selected bond lengths (Å) and angles (deg) for complexes **2.5a-d, 2.10d, 2.11d and 2.12d**

| Complex | Ag1–N1 | Ag1–N2 | N1–Ag1–N2 | Ag⋯Ag | Ref. |
|---|---|---|---|---|---|
| [Ag(Ac-py)$_2$]PF$_6$ (**2.10d**) | 2.170(3) | 2.173(3) | 169.3(1) | – | this work |
| [Ag(MeO-Py)$_2$]PF$_6$ (**2.11d**) | 2.133(2) | 2.134(2) | 169.22(9) | 3.2279(4) | this work |
| [Ag(4-DMAP)$_2$]PF$_6$ (**2.12d**) | 2.1087 | – | 180.0 | – | 148 |
| [Ag(Py)$_2$]PF$_6$ (**2.5d**) | 2.129(6) | – | 178.1(3) | 2.964(2) | 147 |
| [Ag(Py)$_2$]ClO$_4$ (**2.5b**) | 2.126(4) | 2.133(4) | 173.83(17) | 2.99917(10) | 147 |
| [Ag(Py)$_2$]BF$_4$ (**2.5c**) | 2.123(3) | 2.127(3) | 174.81(9) | 3.0001(5) | 147 |
| [Ag(Py)$_2$]OTf (**2.5a**) | 2.153(2) | 2.155(2) | 166.67(7) | 2.665(2) | 140 |

From Table 2.7, the most noticeable difference between the four complexes is that of the Ag–N bond length, which generally decreases with increasing basicity of the pyridine ligand. Complex **2.12d**, which has the most basic 4-dimethylaminopyridine ligand, also has the shortest Ag–N bond length of 2.109 Å, while complex **2.10d**, with the least basic 4-acetylpyridine ligand, has the longest Ag–N bond length of 2.172 Å. This is commensurate with a weaker binding of the least Lewis basic pyridyl ligand to the metal center. The additional coordination of the solvent to Ag in **2.10d** may also reflect its greater Lewis acidity.

[Ag(py)$_2$]PF$_6$ (**2.5d**)



[Ag(py)$_2$]ClO$_4$ (**2.5b**)



[Ag(py)$_2$]BF$_4$ (**2.5c**)



[Ag(py)$_2$]OTf (**2.5a**)
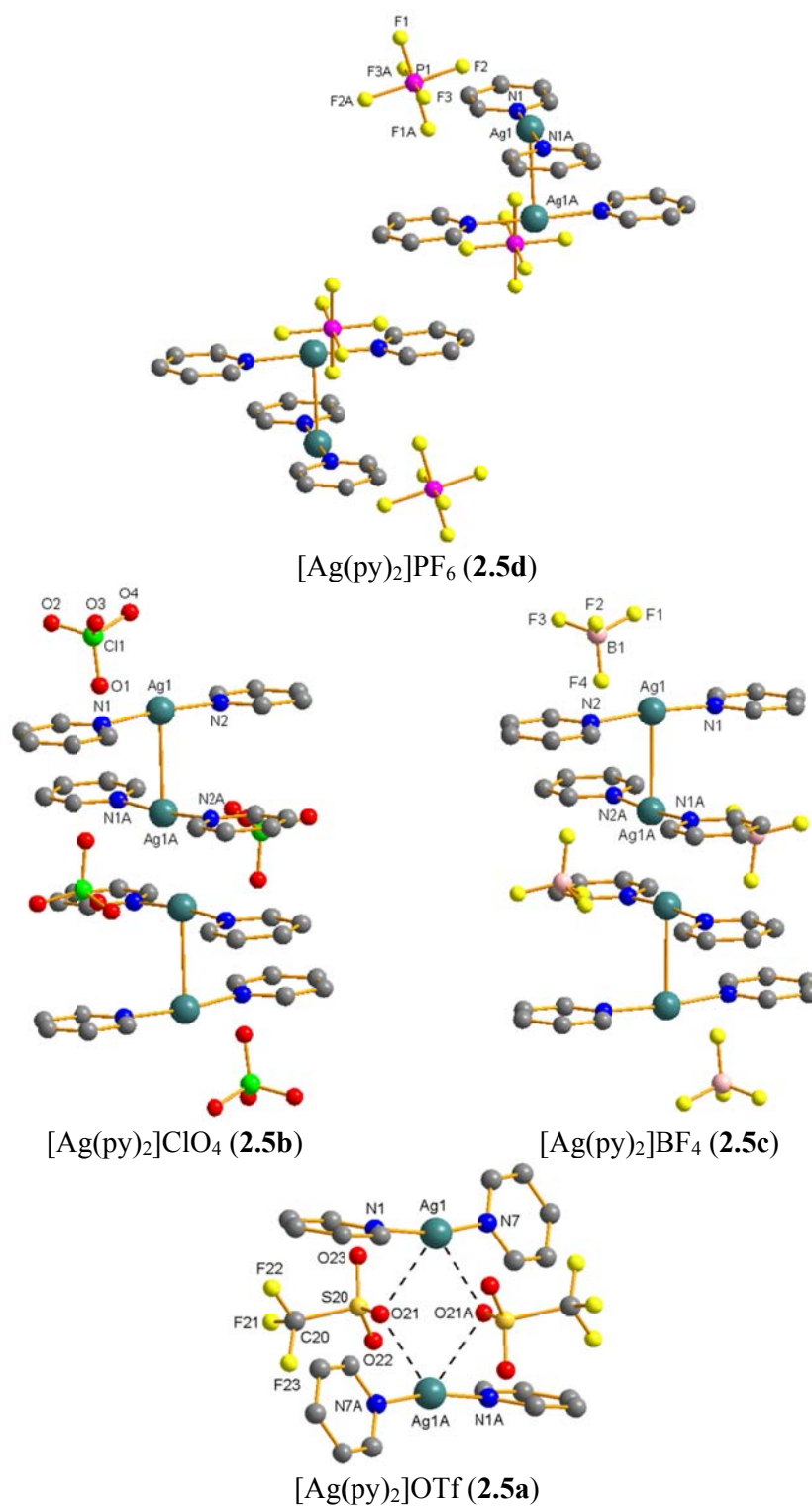
**Fig. 2.10.** Molecular structures of complexes **2.5a-d**. Hydrogen atoms have been omitted for clarity.

Similarly, a comparison of the solid state structures of four known *bis*(pyridine) complexes, [Ag(py)$_2$]X where py = pyridine, X = PF$_6^-$ (**2.5d**), ClO$_4^-$ (**2.5b**), BF$_4^-$ (**2.5c**) and, TfO$^-$ (**2.5a**), allows an investigation of the effect of the counteranion on the coordination geometry of these complexes. The ability of the counteranion to influence the resulting supramolecular structures of silver coordination polymers is well-known in existing literature,[150] and the same effect is expected to be observed in simple silver(I) pyridine complexes. The molecular structures of these complexes are shown in Fig. 2.10, and the bond distances and angles gathered from CIF files obtained from the Cambridge Structural Database (CSD), are tabulated in Table 2.7. The coordination environment around the silver atom in complexes **2.5b**, **2.5c** and **2.5d** which have ClO$_4^-$, BF$_4^-$, PF$_6^-$, counteranions, respectively, are largely similar. In each case, dimeric structures were observed, consisting of two monomeric [Ag(py)$_2$]$^+$ units held together by unsupported Ag···Ag interactions. Within each monomeric unit, the two pyridine ligands are coplanar, the Ag–N bond lengths of the complexes fall within the narrow range of 2.126(4)–2.129(6) Å, and the N−Ag−N bond lengths do not deviate significantly from 180°. The strength of the argentophilic interactions present in these complexes is evident from the Ag−Ag distances of 2.96–3.00 Å, which are just slightly longer than the Ag–Ag separation in metallic silver (2.889 Å).[150] The two [Ag(py)$_2$]$^+$ units are staggered with respect to each other with a N–Ag···Ag–N dihedral angle of ranging from 90.00° in **2.5b** to 94.13° in **2.5c**, which probably optimizes the Ag−Ag interaction energy at the expense of face to face π–π stacking interactions between the pyridine ligands within the dimer. Nevertheless, columns of adjacent dimeric units in **2.5b** and **2.5c** are oriented in a manner

that allows for 'head-to-head' $\pi-\pi$ stacking interactions to occur between pairs of dimers (centroid-centroid distance = 3.569 Å in **2.5b**, and 3.541 Å in **2.5c**). In **2.5d**, however, 'head to tail' $\pi-\pi$ stacking of the pyridine rings occurs, with a longer centroid–centroid distance of 3.734 Å.

In contrast, complex **2.5a**, which has a more coordinating TfO⁻ anion, exists as a dimer in the solid state, with two $[Ag(py)_2]^+$ units held together by two bridging TfO⁻ anions. As a result, the silver atom adopts a T-shaped geometry, and is coordinated to two nitrogen atoms of two distinct pyridine ligands and one oxygen atom from the TfO⁻ anion. The interaction of the Ag metal center with the TfO⁻ anion results in a greater deviation of the N−Ag−N bond angle from linearity (166.67°), which is accompanied by an increase in the Ag–N bond distance to 2.153 Å. The two pyridine ligands bonded to Ag are also not coplanar, which reflected by the dihedral angle of 63.97(6)°.

Although the structures of the complexes in solution might differ from their structures in the solid state, the above analysis of the structural characteristics has provided useful information regarding the relative strength of the Ag–N bond in the various pyridine complexes. A general decrease in Ag–N bond length was observed with increasing basicity of the pyridine ligands. Shorter and stronger Ag–N bonds reflect a greater donation of electron density from the pyridine ligands to Ag(I), which in turn affects its Lewis acidity and ability to coordinate to the substrate during the catalytic reaction. This is in agreement with experimental observations where Ag(I) complexes of the least basic 4-acetylpyridine ligand showed superior activities compared to

complexes of other more basic pyridine ligands. In addition, the ability of weakly coordinating anions such as triflate to bind to Ag(I) and perturb the original linear coordination geometry of Ag(I) to a significant extent supports experimental observations that the nature of counteranion of the catalyst can affect the outcome of the reaction, and that strongly coordinating anions are detrimental to the efficiency of the catalyst.

## 2.7 Mechanistic Considerations
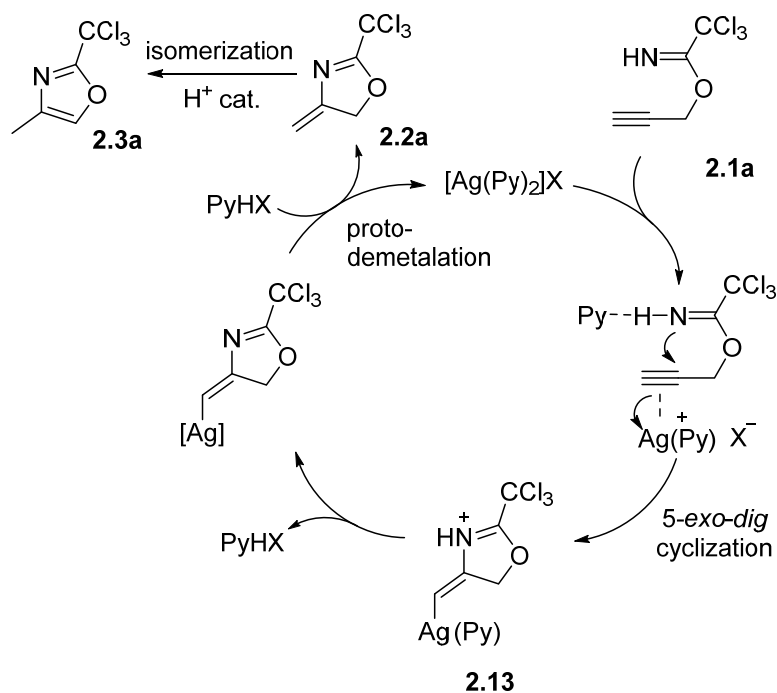


**Scheme 2.13.** Possible mechanism for the Ag(I)-catalyzed cyclization of **2.1a**

Based on experimental findings and by analogy with the proposed mechanism for the intramolecular hydroamination reactions catalyzed by gold, a mechanism for the formation cyclization of **2.1a** under silver catalysis is proposed (Scheme 2.13). In the first step, one of the pyridine ligands on Ag(I) dissociates, creating an electrophilic and coordinatively unsaturated Ag(I)

species that coordinates to the alkyne in substrate **2.1a**, activating it towards *5-exo*-dig attack by the imidate nitrogen. The ability of one of the pyridine ligands to dissociate appears to be crucial, as Ag(I) complexes with chelating ligands, such as [Ag(phen)₂]OTf, or strongly donating pyridine ligands, such as [Ag(4-DMAP)]OTf, were inactive towards the transformation. The *anti*-addition of the imidate nucleophile to the alkyne is supported by the stereochemistry of the cyclization products of internal alkyne substrates and the products of the trapping reactions of the vinyl silver intermediate **2.13** with electrophilic halogen sources. The zwitterionic vinyl silver intermediate **2.13** then undergoes protodemetallation to deliver the oxazoline product **2.2a**. The protodemetallation step may be assisted by the counteranion or free pyridine ligands. The free pyridine ligands can also act as acid scavengers, preventing the isomerization of **2.2a** to the oxazole **2.3a**.

## 2.8 Conclusion

In summary, silver salts have been found to be active catalysts for the intramolecular hydroamination addition of trichloroacetimidates to alkynes, where the nature of the counteranion and solvent affected both the yields and selectivity of the reaction. In the cyclization of the model substrate **2.1a**, the use of AgTFA in MeCN afforded the oxazoline product **2.2a**, while AgOTf in DCE resulted in the formation of the oxazole **2.3a** (Scheme 2.10). The formation of **2.3a** occurs via the Brønsted acid-catalyzed isomerization of **2.2a**, due to traces of TfOH produced *in situ* during the reaction.
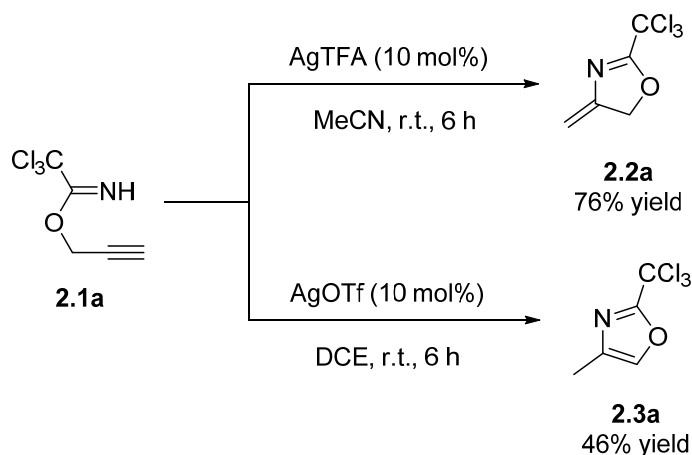
**Scheme 2.14.** Counteranion and solvent effects in the cyclization of model substrate **2.1a**

The silver(I) complexes of *N*-donor ligands such as 1,10-bipyridine and pyridine were also found to be active catalysts for the above transformation. Encouragingly, the *bis*(pyridine)silver(I) triflate complex, [Ag(py)₂]OTf, showed improved yields in the cyclization of the model substrate, and was also able to effect the cyclization of challenging internal alkyne substrates previously not possible with gold catalysts.

Further fine-tuning of the ligand electronic properties and counteranion of the silver(I) *bis*(pyridine) catalysts showed that electron-withdrawing substituents on the pyridine ligands, and the use of weakly coordinating counteranions led to an improvement in the efficiency of the catalyst. The silver(I) *bis*(4-acetylpyridine) hexafluorophosphate complex (**2.10d**) could promote the cyclization of propargylic and homopropargylic substrates with bromo-substitution at the alkyne to afford the corresponding (*Z*)-methylene bromooxazoline and oxazolines in quantitative yields and short reaction times

with catalytic loadings as low as 1 mol%, delivering a significant improvement to the process catalyzed by silver salts.

The trapping of vinylsilver intermediates in the reaction with NBS and NCS was demonstrated as a complementary approach that allows access to the opposite (*E*)-isomers of the halomethylene oxazolines and oxazines in moderate yields. It also lends support to the proposed mechanism, where *anti*-addition of the imidate nucleophile to the alkyne is believed to occur.

# Chapter 3 Cyclosiomerization of Propargyl Amides

In the previous chapter, the silver-catalyzed intramolecular addition of trichloroacetimidates to alkynes to give 4-methylene oxazolines (**2.2**) and oxazoles (**2.3**) was described (Scheme 3.1a). In this chapter, the cycloisomerization of propargyl amides (**3.1**), which could potentially afford the 5-alkylidene oxazolines (**3.2**), oxazoles (**3.3**) and also oxazines (**3.4**) (Scheme 3.1b), will be explored. The reaction involves a formal O–H addition to the alkyne, in contrast to the N–H addition described previously.
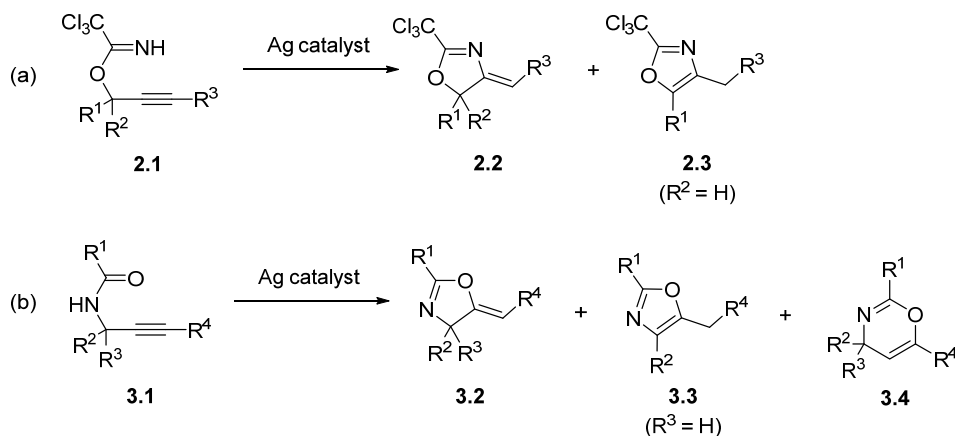


**Scheme 3.1.** (a) Intramolecular hydroamination of trichloroacetimidates with alkynes described in Chapter 2; (b) Cycloisomerization of propargyl amides described in this chapter.

The cycloisomerization of propargyl amides **3.1** was first reported to be catalyzed by strong bases such as sodium hydride to give the corresponding oxazoles **3.3**.[151] The use of transition metal catalysts, which initiate the transformation by activation of the alkyne, has allowed the reaction to proceed under milder conditions and with greater functional group tolerance. Gold and

palladium catalysts, in particular, have proven to be efficient and versatile catalysts for the transformation. With Pd(0) and Pd(II) catalysts,[152] the cycloisomerization step usually forms part of a tandem reaction sequence, preceding reactions that allow further elaboration of the oxazoline products; and an example of a Pd(II)-catalyzed cyclization-alkoxycarbonylation reaction of propargyl amides is shown in Scheme 3.2.
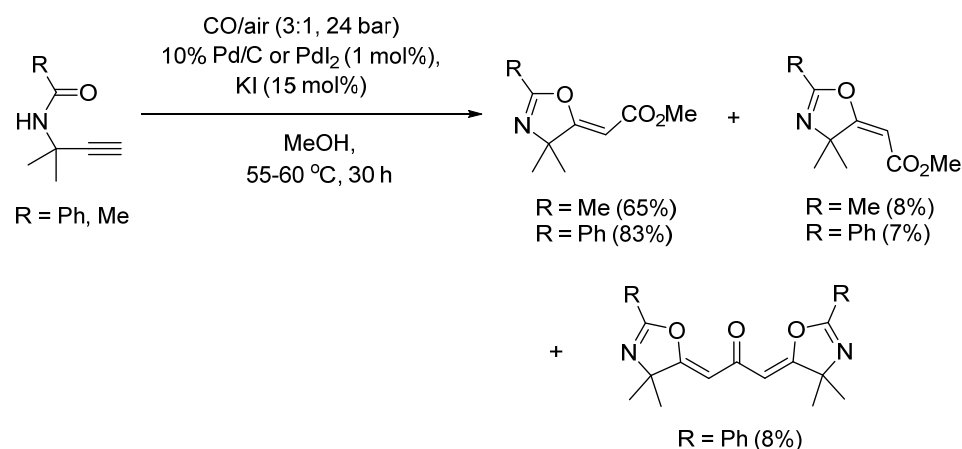


**Scheme 3.2.** An example of a Pd(II)-catalyzed cyclization-alkoxycarbonylation reaction of propargyl amides

**Table 3.1.** Comparison of the reactivity of several catalysts in the cycloisomerization of propargyl amides

|   | Cat. (Loading) | Reaction Cond. | $R^1$ | $R^2, R^3$ | $R^4$ | Prod. (Yield) | Ref |
|---|---|---|---|---|---|---|---|
| 1 | AuCl$_3$ (2.5-5 mol%) | CH$_2$Cl$_2$, 20 °C, 5 min - 48 h; or MeCN, 20-50 °C, 2 - 96 h | alkyl, aryl, heteroaryl | H, H | H | **3.3** (40% - quant.) | 153, 154 |
| 2 | [(Ph$_3$P)Au]X (1-5 mol%) (X = OTs or NTf$_2$) | CH$_2$Cl$_2$, r.t., 3 h - 6 days; | alkyl, aryl, heteroaryl | H, H | H | **3.2** (37-95%) | 154 |
| 3 | [(IPr)AuCl] | THF, r.t., | aryl, furyl, | H, H | alkyl | **3.2** | 155 |

113

| | | | | | | | |
|---|---|---|---|---|---|---|---|
| | (5 mol%), AgOTs (5 mol%) | 16 h | adamantyl | | | and/or **3.4** (28-78%) | |
| 4 | [(IPr)AuCl] (5 mol%), AgOTs (5 mol%) | THF, r.t.-40 °C, 12 h - 5 days | aryl, furyl, benzyl, *tert*-butyl | H, H | aryl, heteroaryl | **3.2** and/or **3.3** (14-94%) | 155 |
| 5 | W(CO)$_6$ (20 mol%), DABCO (1.0 eq.) | 1. toluene, r.t., 20 h, N$_2$, λ = 350 nm 2. TMAO, THF. | alkyl, aryl | H, H | H | **3.2** (80-91%) | 156 |
| 6 | W(CO)$_6$ (20 mol%), DABCO (1.0 eq.) | 1. toluene, r.t., 20 h, N$_2$, λ = 350 nm 2. TMAO, THF | alkyl, aryl | Me, H | H | **3.2** and **3.3** (20-73%) | 156 |
| 7 | Mo(CO)$_6$ or W(CO)$_6$ (20 mol%), DABCO (1.0 eq.) | 1. toluene, r.t., 20 h, N$_2$, λ =350 nm 2. TMAO, THF | alkyl, aryl | Me, Me | H | **3.2** and **3.4** (8-86%) | 156 |
| 8 | FeCl$_3$ (30-50 mol%) | DCE, 80 °C, 3 - 8 h, | alkyl, aryl, heteroaryl | H, H | H | **3.3** (65%-quant.) | 157 |
| 9 | ZnI$_2$ (50 mol%) | CH$_2$Cl$_2$, r.t., 18 min - 4 h | alkyl, aryl, indolyl | Me, Me; or -(CH$_2$)$_5$- | H | **3.2** (83-97%) | 157 |
| 10 | ZnI$_2$ (1.0 eq.) | CH$_2$Cl$_2$, r.t.-45 °C, 3 - 24 h | alkyl, aryl, heteroaryl | H, H | H | **3.2** (62-94%) | 157 |
| 11 | AgSbF$_6$ (1-5 mol%) | CH$_2$Cl$_2$, r.t., 5 - 10 min | alkyl, aryl | Me, Me; Et, Et; or -(CH$_2$)$_5$- | H | **3.2** (89-98%) | 62 |
| 12 | CuI (10 mol%) | DCE, 80 °C, overnight | aryl, heteroaryl | Me, Me; or -(CH$_2$)$_5$- | H | **3.2** (76-93%) | 158 |

When gold catalysts were employed, the product selectivity was found to be dependent upon the oxidation state and the ligand used (Table 3.1, entries 1-4). Au(III) chloride[153,154] afforded the aromatic oxazole products **3.3** exclusively *via* the methyleneoxazoline intermediate **3.2,** which was detected by *in situ*

NMR spectroscopy (entry 1), while Au(I) phosphine catalysts[155] gave the methylene oxazoline products **3.2** in good yields (entry 2). Notably, the reaction scope could also be extended to internal alkynes when a Au(I) *N*-heterocyclic carbene (NHC) catalyst was used.[155] In these cases, the selectivity towards the 5-membered oxazolines/oxazoles (**3.2** and **3.3**) and 6-membered oxazines (**3.4**) was highly substrate-dependent. With alkyl substituents at the alkyne, a mixture of both **3.2** and **3.4** was obtained (entry 3), with increasing selectivity towards **3.2** as the size of the alkyl substituent increases. In contrast, with aryl substituents at the alkyne, only the 5-membered oxazolines (**3.2**) and oxazoles (**3.3**) were obtained (entry 4); the formation of **3.3** was only observed with certain substrates where the long reaction times required resulted in the isomerization of **3.2** to **3.3**.

The only drawback associated with the use of Pd and Au catalysts is their high cost. As a result, other cheaper alternatives have also been explored. Molybdenum(0) and tungsten(0) hexacarbonyl complexes could also catalyze the reaction (entries 5-7);[156] however, higher catalytic loadings (20 mol%), the presence of 1 equivalent of a base (1,4-diazabicyclo[2.2.2]octane, DABCO), UV irradiation and an inert atmosphere were required. In addition, an oxidative work-up procedure involving trimethylamine *N*-oxide (TMAO), was required. It was also observed that the propargylic substituents ($R^2$ and $R^3$) had a large effect on the selectivity of the reaction.

The only other catalyst that can catalyze the selective formation of oxazoles **3.3** is iron(III) chloride (entry 8).[157] Despite the higher catalytic loading (30-

50 mol%) and harsher reaction conditions required compared to $AuCl_3$, good yields and a broad substrate scope was observed. There is also the added advantage of being able to obtain the oxazole products in a one-pot, sequential acylation-cyclization reaction starting from propargyl amine, without the need to isolate and purify the propargyl amide intermediate. Similarly, this one-pot synthetic approach could also be extended to the synthesis of oxazolines **3.2** using 50 mol% of zinc(II) iodide as a catalyst (entry 9). [157] However, it should be noted that the reaction ceases to be catalytic in $ZnI_2$ and harsher reaction conditions are required when geminal alkyl groups in the propargylic position are absent in the substrate (entry 10).

Similar to $ZnI_2$, the substrate scope of copper[158] and silver salts[62] is also limited to substrates with propargylic geminal dialkyl substitution. Nevertheless, good yields can be achieved with these substrates within 15 minutes in the presence of only 1-5 mol% of $AgSbF_6$ (entry 11). Copper(I) iodide, in comparison, is less efficient compared to $AgSbF_6$, as a higher catalyst loading of 10 mol% is required, in addition to higher temperatures and longer reaction times. The reaction is also not tolerant of alkyl groups at the position beside the carbonyl carbon ($R^1$).

## 3.1. Synthesis of Substrates
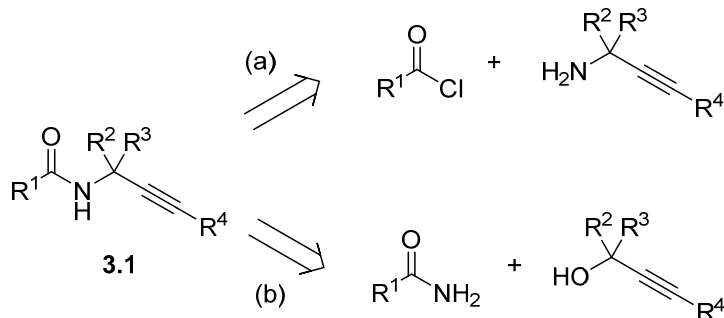


**Scheme 3.3.** Possible synthetic routes to propargyl amides **3.1**: (a) acylation of propargyl amines; (b) nucleophilic substitution of propargyl alcohols by primary amides

Two possible routes for the synthesis of the propargyl amide substrates **3.1** were envisioned. The first would involve the acylation of propargyl amines (Scheme 3.3, method a). Internal alkyne substrates with different $R^1$ substituents can be readily synthesized by this method, as a wide range of different acyl chlorides are commercially available. However, it is difficult to introduce substitution on both the propargylic ($R^2$ and $R^3$) and alkyne ($R^4$) positions using this method because of the limited number of primary propargyl amines that are commercially available and the lack of efficient methods for their preparation. For example, Hashmi *et al.* devised a three-step synthetic method (Scheme 3.4a) for the synthesis of internal alkyne substrates which began with the preparation of the appropriately substituted propargyl amine, followed by acylation of the amine as a final step. Though highly flexible, the method required the use of inert conditions, low temperatures and tedious workup procedures.[155]

(a)

1. $^n$BuLi, -78 °C to r.t., 1 h

2. [propargyl bromide], -20 °C, overnight

3. KH$_2$PO$_4$/Na$_2$HPO$_4$ buffer

TMS–N(H)–TMS → TMS–N(propargyl)–TMS

1. $^n$BuLi, -78 °C to r.t., 30 min
2. R$^1$X (R$^1$ = alkyl)

OR

R$^1$X (R$^1$ = aryl), Sonogashira coupling

TMS–N(CH$_2$C≡C–R$^1$)–TMS

TBAF (10 mol%), R$^2$COCl

CH$_2$Cl$_2$, r.t.

R$_2$C(O)–N(H)–CH$_2$C≡C–R$^1$

(b)

R$^1$–≡–H  +  R$^2$–C(O)–R$^3$

$^n$BuLi

-78 °C to r.t.,15 min

HO–C(R$^2$)(R$^3$)–C≡C–R$^1$

catalyst,

R$^4$–C(O)–NH$_2$

-H$_2$O

R$^4$–C(O)–N(H)–C(R$^2$)(R$^3$)–C≡C–R$^1$
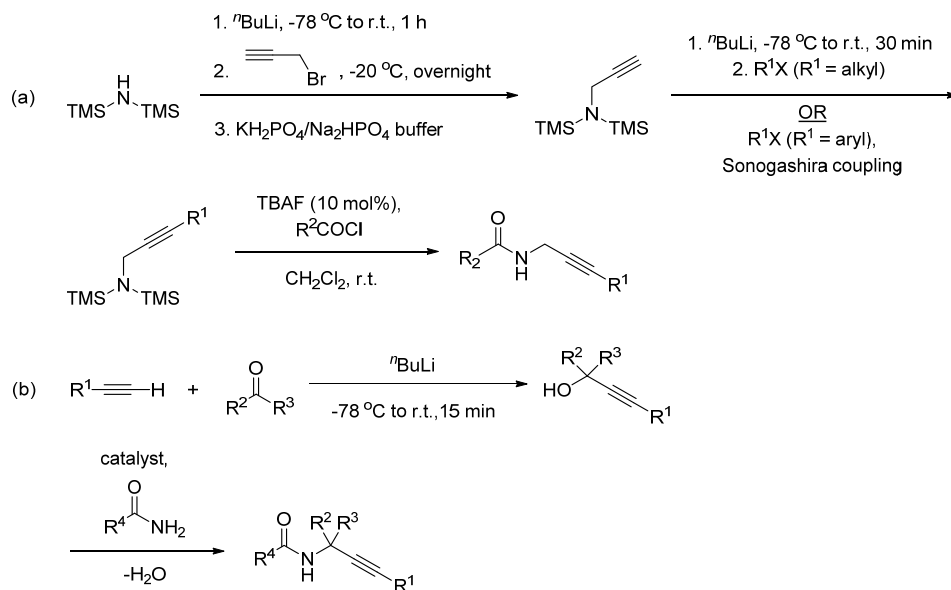
**Scheme 3.4.** Preparation of internal alkyne substrates via (a) the preparation of substituted propargyl amines, (b) the nucleophilic substitution reaction of propargyl alcohols with primary amides.

During this work, an alternative approach was envisaged (Scheme 3.3, method b), involving a nucleophilic substitution reaction of propargyl alcohols with primary amides. This might be a more efficient method as propargylic alcohols containing substituents at R$^2$, R$^3$ and R$^4$ can be easily prepared by addition of the appropriate acetylide nucleophile to aldehydes of ketones (Scheme 3.4b). As the only report on the cycloisomerization of non-terminal propargyl amides using Au(I) catalysts was focused on the effect of steric and electronic influences of R$^1$ and R$^4$ on product selectivity (Table 3.1, entries 3 and 4), it would be interesting to investigate the influence of substituents at R$^2$ and R$^3$ of internal alkyne substrates on the regioselectivity of the reaction.[155] The introduction of substituents at these positions could also potentially result in an electronic bias at the alkyne moiety, especially if R$^2$, R$^3$ and R$^4$ possess marked differences in electronic properties.

Numerous transition metal compounds and Lewis acids such as Ru(II) thiolate complexes, [159] iron(III) chloride, [160] molybdenum(V) chloride, [161] sodium tetrachloroaurate(III) dihydrate, [162] silver(I) triflimide, [163] bismuth(III) chloride, [164] bismuth(III) triflate, [165] aluminum(III) triflate [166] and tin(II) chloride [167] have been reported to promote the nucleophilic substitution reactions of propargylic alcohols with nitrogen nucleophiles such as aryl amides, carbamates and sulfonamides. However, these methods present drawbacks either in terms of cost, and/or relatively high catalytic loadings of 5-10 mol%.

In a recent report by Zheng *et al.*,[168] it was reported that the ion exchange resin Amberlite (IR-120H) can promote the propargyl substitution reaction with various carbon and heteroatom nucleophiles in excellent yields, including an example where an amide nucleophile was used. Prior to this work, there were no other reported literature examples of Brønsted-acid-catalyzed nucleophilic substitution reactions involving propargylic alcohols with less reactive nitrogen nucleophiles such as aryl amides, carbamates and sulfonamides. However, the possibility of using an aqueous solution of $HBF_4$ has been recently demonstrated in the Diez-Gonzalez group at Imperial College London to promote the propargyl substitution reactions with oxygen nucleophiles, carbamates and sulfonamides in good yields.[169] Hence the analogous reaction was explored in this work.

PMP = 4-methoxyphenyl
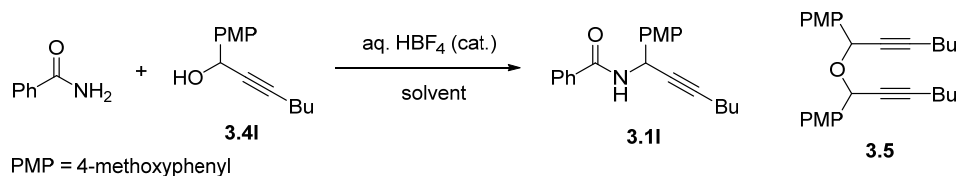
**Scheme 3.5.** Propargylic substitution reaction of 1-(4'-methoxyphenyl)-hept-2-yn-1-ol (**3.4l**) with benzamide catalyzed by 50 wt% aq. HBF$_4$.

**Table 3.2.** Optimization of reaction conditions for the HBF$_4$-catalyzed propargylic substitution reaction of **3.4l** with benzamide

| Entry | Cat. Loading (mol%) | Benzamide (Equiv.) | Solvent | Temp. (°C) | Time (h) | Yield[a] of 3.1l (%) | Yield[a] of 3.5 (%) |
|---|---|---|---|---|---|---|---|
| 1 | 2 | 2 | acetone | 23 | 6 | 94 | 0 |
| 2 | 2 | 2 | CH$_2$Cl$_2$ | 23 | 6 | 94 | 0 |
| 3 | 2 | 2 | MeCN | 80 | 1 | 75 | 0 |
| 4 | 2 | 1.5 | acetone | 23 | 6 | 20 | 35 |
| 5 | 5 | 2 | acetone | 23 | 4 | 92 | 0 |
| 6 | 1 | 2 | acetone | 23 | 24 | ND[b] | ND[b] |

[a] Isolated yields of product after purification by column chromatography on silica. [b] Isolated yields were not determined, as incomplete conversion of **3.4l** was observed by TLC.

The substitution reaction between **3.4l** and benzamide (2 equivalents) was initially conducted in acetone at ambient temperature, in the presence of 2 mol% of aqueous 50 wt% HBF$_4$ (Scheme 3.5). Pleasingly, the desired amide **3.1l** was obtained in an excellent yield of 94% after 6 h (Table 3.2, entry 1). Changing the solvent to CH$_2$Cl$_2$ resulted in an identical yield (entry 2); and while MeCN allowed the reaction temperature to be elevated to 80 °C, shortening the reaction time to 1 h, a diminished yield of 75% was obtained (entry 3). When the amount of benzamide nucleophile was reduced to 1.5 equivalents, the formation of an ether side product **3.5** was detected, as a result of dimerization of the propargyl alcohol **3.4l**. Increasing the amount of HBF$_4$ to 5 mol% decreased the reaction time to 4 h but failed to improve the yield, while decreasing the amount of HBF$_4$ to 1 mol% led to incomplete conversion

of **3.4l**. Therefore, a catalyst loading of 2 mol% and 2 equivalents of the amide

nucleophile was optimal.
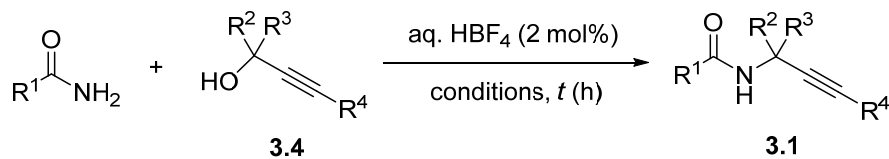


**Scheme 3.6.** Preparation of propargyl amide substrates via the HBF$_4$-catalyzed substitution of propargylic alcohols

**Table 3.3.** HBF$_4$-catalyzed propargylic substitution reaction of propargylic alcohols

| Entry | R$^1$ | R$^2$ | R$^3$ | R$^4$ | Conditions[a] | $t$ (h) | Product | Yield[b] (%) |
|-------|-------|-------|-------|-------|---------------|---------|---------|--------------|
| 1 | Ph | PMP | H | Bu | acetone, 23 °C | 6 | **3.1l** | 94 |
| 2 | Ph | PMP | H | TMS | acetone, 23 °C | 6 | **3.1m** | 68 |
| 3 | Ph | PMP | H | $\frac{\xi}{\xi}\!\triangleleft$ | acetone, 23 °C | 6 | **3.1n** | 89 |
| 4 | Ph | PMP | H | Ph | acetone, 23 °C | 6 | **3.1p** | 77 |
| 5 | Ph | PMP | H | cyclohexenyl | acetone, 23 °C | 1 | **3.1o** | 7 |
| 6 | Ph | PMP | H | cyclohexenyl | toluene, 111 °C | 1 | **3.1o** | 29 |
| 7 | Ph | PMP | H | H | acetone, 23 °C | 6 | **3.1q** | 15 |
| 8 | Ph | PMP | H | H | MeCN, 80 °C | 1 | **3.1q** | 66 |
| 9 | Cy | PMP | H | Bu | acetone, 23 °C | 24 | **3.1s** | – |
| 10 | Cy | PMP | H | Bu | MeCN, 80 °C | 12 | **3.1s** | 66 |
| 11 | Me | PMP | H | Bu | acetone, 23 °C | 24 | – | – |
| 12 | Me | PMP | H | Bu | MeCN, 80 °C | 24 | – | – |
| 13 | Ph | Ph | H | H | acetone, 23 °C | 24 | **3.1r** | – |
| 14 | Ph | Ph | H | H | MeCN, 80 °C | 12 | **3.1r** | 9 |

| | | | | | | | | |
|---|---|---|---|---|---|---|---|---|
| 15 | Ph | Me | Me | H | acetone, 23 °C | 24 | – | – |

With these optimal conditions in hand, the preparation of several propargyl amides with different substituents at the position beside the carbonyl group ($R^1$), the propargyl position ($R^2$, $R^3$) and alkyne ($R^4$) was attempted (Scheme 3.6 and Table 3.3). The reaction with propargylic alcohols, where $R^2$ = 4-methoxyphenyl and $R^4$ = alkyl, aromatic and trimethylsilyl substituents, all proceeded smoothly in good to excellent yields (entries 1-4), with the exception of the propargyl alcohol substrate where $R^4$ = cyclohexenyl (entry 5). In this case, heating in toluene at reflux afforded only a slight improvement in yield from 7% to 29% (entry 5 vs. 6). The π-conjugated system present in this system could have caused regioselectivity issues that led to the formation of undesired side products. Similarly, the reaction of the propargyl alcohol with a terminal alkyne group ($R^4$ = H) afforded the corresponding amide product in a poor yield of 15% when acetone was used as the reaction solvent (entry 7). However, the yield could be raised to 66% by changing the solvent to MeCN and shortening the reaction time by elevating the reaction temperature to 80 °C (entry 8).
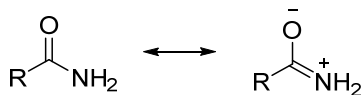


**Scheme 3.7.** Resonance forms of amides

The reaction was also extended to include alkyl amides such as cyclohexylamide (entries 9 and 10), although the reaction with acetamide was did not furnish any product (entries 11 and 12). This is attributed to greater interaction of the nitrogen lone pairs with the carbonyl group (Scheme 3.7) compared to cyclohexylamide and benzamide, resulting in a reduced nucleophilicity for this reactant.

The presence of an electron-rich aromatic ring at the propargyl position ($R^2$) seems to be necessary for the substitution reaction to take place. This is indicative of a $S_N1$ reaction that occurs *via* a propargylic cation intermediate. When the 4-methoxyphenyl substituent at $R^2$ was replaced with a phenyl substituent, none of the desired amide product was formed in acetone at room temperature (entry 1 vs. 13). Even under harsher reaction conditions of reflux in acetonitrile, the amide product was only obtained in 9% yield after 12 h (entry 14). In addition, no reaction occurred when the aromatic propargylic substituent was replaced by methyl groups (entry 15). In this case, nearly all of the starting materials could be recovered.

It was also noted that tandem propargylation and cycloisomerization reactions between propargyl alcohols and aryl amides to oxazoles can be achieved in 'one-pot' using certain dual catalyst combinations such as Ru(II,III)/Au(III)[170] and Ru(III)/Zn(III)[171], stoichiometric amounts of *p*-toluenesulfonic acid,[172] and ytterbium(III) triflate.[173] This is very attractive as it bypasses the need to isolate the acyclic amide substrate. With this in mind, the propargyl alcohol

**3.4l** was subjected to two equivalents of benzamide in the presence of 10 mol% of AgOTf or [Ag(Py)₂]OTf (**2.5a**) in toluene at 60 °C for 16 h (Scheme 3.8).
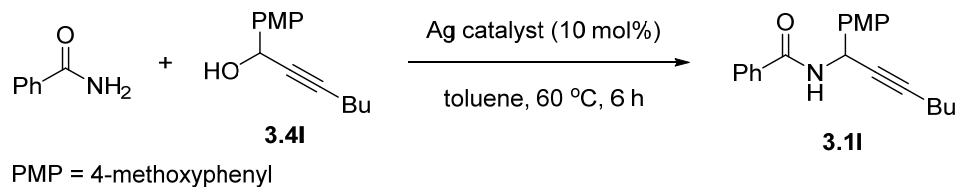


**Scheme 3.8.** Propargylic substitution reaction of 1-(4'-methoxyphenyl)-hept-2-yn-1-ol (**3.4l**) with benzamide in the presence of AgOTf and [Ag(py)₂]OTf (**2.5a**)

It was found that AgOTf promoted the complete conversion of the propargyl alcohol **3.4l** to the corresponding amide **3.1l**, but did not catalyze the cycloisomerization of **3.1l** to the corresponding oxazoline or oxazole. The *bis*(pyridine) complex **2.5a**, on the other hand, could not catalyze the propargylic substitution reaction, and most of **3.4l** remained largely unreacted.

## 3.2 Initial Screening of Silver(I) and Copper(I) Salts
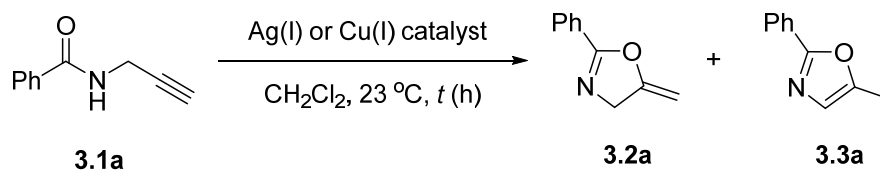


**Scheme 3.9.** Model reaction for the initial screening of Ag(I) and Cu(I) salts

*N*-Benzoyl propargyl amide **3.1a** was initially selected as the model substrate to assess the catalytic activity of several silver and copper salts and to determine the optimum reaction conditions for the cycloisomerization reaction (Scheme 3.9). **3.1a** was chosen as it lacks substituents at the propargylic

position, and the results will not be biased by the operation of the Thorpe-Ingold effect. In these experiments, a mixture of **3.1a** and 10 mol% of the silver or copper salt was stirred in $CH_2Cl_2$ at room temperature. After 6 h, the internal standard (1,3,5-methoxybenzene) was added, and the solvent was removed *in vacuo*. ^{1}H NMR analyses of the crude reaction mixtures in $CDCl_3$ showed the appearance of multiplet resonances at 4.82 and 4.36 ppm, which correspond to the diastereomeric alkene protons of **3.2a**. No other peaks were observed in the 1-3 ppm region, other than the triplet resonance at 2.28 ppm corresponding to the alkyne proton of **3.1a**, indicating that the oxazole product **3.3a** was not formed. The NMR yields of **3.2a** were calculated by comparing the integrals of the alkene protons of **3.2a** with the proton signal of 1,3,5-methoxybenzene, and the results are reported in Table 3.4.

**Table 3.4.** Initial screening of Ag(I) and Cu(I) salts in the cycloisomerization of **3.1a**[a]

| Entry | Catalyst | $pK_a$ of conjugate acid | $t$ (h) | Conversion[b] (%) | Yield[b] of 2.2a (%) |
|---|---|---|---|---|---|
| 1 | AgOAc | 4.8[131] | 6 | – | – |
| 2 | AgTFA | 0.2[131] | 6 | 72 | 60 |
| 3 | AgClO$_4$ | -1.6[174] | 6 | 94 | 15 |
| 4 | AgOTs | -2.8[133] | 6 | – | trace |
| 5 | AgBF$_4$ | -4.9[134] | 6 | – | trace |
| 6 | AgSbF$_6$ | -13[135] | 6 | 56 | 40 |
| 7[c] | AgSbF$_6$ | -13[135] | 10 min | – | 7 |
| 8[c] | AgSbF$_6$ | -13[135] | 24 h | – | 25 |
| 9 | AgOTf | -14[136] | 6 | 46 | 29 |
| 10 | AgPF$_6$ | -20[135] | 6 | 61 | 56 |
| 11 | [Cu(OTf)]$_2$·C$_6$H$_6$ | -14[136] | 24 h | – | – |
| 12 | [Cu(MeCN)$_4$]PF$_6$ | -20[135] | 24 h | 12 | 5 |
| 13 | TfOH | -14[136] | 6 h | – | – |

[a] Reaction conditions: substrate **3.1a** (0.4 mmol), catalyst (0.04 mmol, 10 mol%), 23 °C, $CH_2Cl_2$ (1 mL). [b] Determined by ^{1}H NMR spectroscopy, using 1,3,5-trimethoxybenzene as internal standard. [c] 5 mol% catalytic loading, $MeNO_2$ used as solvent.

Although the conversions and yields obtained were generally modest, only the unaromatized oxazoline product **3.2a** was obtained in all cases. A counteranion effect on catalytic activity was also observed, which again did not correlate with the $pK_a$ values of the conjugate acids. AgTFA gave the highest yield of **3.2a** in 60% yield after 6 h (entry 2), and the copper(I) *tetrakis*(acetonitrile) hexafluorophosphate complex, $[Cu(MeCN)_4]PF_6$, only resulted in a low level of conversion after 24 h (entry 12). A control experiment revealed that triflic acid could not catalyze the reaction (entry 13).

Harmata *et al.* have previously reported that **3.2a** was obtained in 91% yield within 10 min when 5 mol% of $AgSbF_6$ in $MeNO_2$ was used. However, in our hands, only 7% yield of **3.2a** was obtained under identical conditions (entry 7). Prolonging the reaction time to 24 h only resulted in 25% yield (entry 8). Indeed, further correspondence with Prof. Hamata revealed that the reported example is irreproducible, and an errata has subsequently been issued.[175]

## 3.3 Screening of Ag(I) *Bis*(pyridine) Complexes

Having established the performance of simple silver salts in the cycloisomerization of the model substrate **3.1a**, the effect of adding ligands was explored. To provide a direct comparison to the previous work described in Chapter 2, the *bis*(pyridine) Ag(I) triflate complexes **2.5a** and **2.10-2.13a**, were assessed for their catalytic activity towards the cycloisomerization of the model substrate **3.1a**. The results are summarized in Table 3.5.

**Table 3.5.** Screening of Ag(I) *bis*(pyridine) complexes in the cycloisomerization of **3.1a**[a]

| Entry | Catalyst | Solvent | *t* (h) | Conv[b] (%) | Yield[b] of 2.2a (%) |
|---|---|---|---|---|---|
| 1 | [Ag(py)₂]OTf (**2.5a**) | CH₂Cl₂ | 6 | 29 | 8 |
| 2 | [Ag(4-Ac-Py)₂]OTf (**2.10a**) | CH₂Cl₂ | 6 | 47 | 26 |
| 3 | [Ag(4-MeO-Py)₂]OTf (**2.11a**) | CH₂Cl₂ | 6 | 94 | 85 |
| 4 | [Ag(4-DMAP)₂]OTf (**2.12a**) | CH₂Cl₂ | 6 | 23 | 5 |
| 5 | [Ag(4-Me-Py)₂]OTf (**2.13a**) | CH₂Cl₂ | 6 | 75 | 59 |
| 6 | [Ag(4-MeO-Py)₂]ClO₄ (**2.11b**) | CH₂Cl₂ | 6 | 100 | 98 |
| 7 | [Ag(4-MeO-Py)₂]BF₄ (**2.11c**) | CH₂Cl₂ | 6 | 100 | >99 |
| 8 | [Ag(4-MeO-Py)₂]PF₆ (**2.11d**) | CH₂Cl₂ | 6 | 100 | >99 |
| 9 | [Ag(4-MeO-Py)₂]SbF₆ (**2.11e**) | CH₂Cl₂ | 6 | 100 | >99 |
| 10 | [Ag(4-MeO-Py)₂]CF₃CO₂ (**2.11f**) | CH₂Cl₂ | 6 | 49 | 31 |
| 11[c] | **2.11c** | CH₂Cl₂ | 24 | 100 | 93 |
| 12[c] | **2.11d** | CH₂Cl₂ | 24 | 98 | 96 |
| 13[c] | **2.11e** | CH₂Cl₂ | 24 | 100 | 95 |
| 14 | **2.11d** | acetone | 6 | 41 | 22 |
| 15 | **2.11d** | THF | 6 | 61 | 50 |
| 16 | **2.11d** | DCE | 6 | 100 | 99 |
| 17 | **2.11d** | MeCN | 6 | 39 | 20 |
| 18 | **2.11d** | MeOH | 6 | 24 | 8 |

[a] Reaction conditions: substrate **3.1a** (0.4 mmol), catalyst (0.04 mmol, 10 mol%), 23 °C, CH₂Cl₂ (1 mL). [b] Determined by $^1$H NMR spectroscopy, using 1,3,5-trimethoxybenzene as internal standard. [c] 5 mol% of catalyst used.

The parent *bis*(pyridine)silver(I) triflate complex, **2.5a**, only gave a disappointing yield of 8% after 6 h (entry 1), lower than that obtained with AgTFA as the catalyst (Table 3.4, entry 2). Screening of four other silver(I) complexes of different pyridyl ligands, **2.10-2.13a**, showed that the efficiency of the catalyst increased in the order: 4-DMAP < py < 4-Ac-py < 4-Me-py < 4-MeO-Py. With all five complexes, some catalyst deactivation was apparent

from the formation of insoluble white precipitates during the reaction. This deactivation occurred to varying extents depending on the pyridine ligand, being the most severe with the DMAP complex **2.10a**. With the exception of complexes **2.10a** and **2.12a**, bearing 4-acetylpyridine and 4-dimethylaminopyridine ligands respectively (entries 2 and 4), a general increase in catalyst efficiency was brought about by more electron-donating pyridine ligands. This result is highly significant, as the trend is opposite to that observed in the hydroamination reaction described in the previous Chapter (section 2.4). This implies that a different rate-limiting step operates in the O−H addition, compared to the N−H addition.

In the previous work on hydroamination reactions, the activation of the alkyne by $\pi$-coordination was proposed to be the rate-limiting step, on the basis that the reaction is accelerated by electron-poor pyridyl ligands (Section 2.4). For the cyclisation of **3.1a**, the opposite trend was observed. This led us to postulate that the protodemetallation to be the rate-limiting step (*vide infra*).

Having determined that the *bis*(4-methoxypyridine) Ag(I) triflate complex **2.11a** gave the highest conversions and yields among the series of silver(I) complexes, the effect of the counteranion on the catalytic activity was investigated. At 10 mol% catalytic loading, the *bis*(4-methoxypyridine) Ag(I) complexes with the non-coordinating counteranions $PF_6^-$, $BF_4^-$, $SbF_6^-$ and $ClO_4^-$ produced near quantitative yields (entries 6-9), while those of the slightly coordinating $TfO^-$ and $CF_3CO_2^-$ counteranions resulted in significantly lower yields (entries 3 and 10). A reduction of the catalytic loading to 5 mol%

revealed that the complex with the $PF_6^-$ counteranion (**2.11d**) was the best catalyst for the reaction (entries 11-13). A solvent screen (entries 8 and 14-18) showed that chlorinated solvents $CH_2Cl_2$ and DCE were the best solvents for the reaction. $CH_2Cl_2$ was used as the solvent for further investigation of the substrate scope, as it is less toxic and has a lower boiling point compared to DCE, facilitating its removal from the product.

## 3.4 Substrate Scope

The optimized reaction conditions were used to investigate the scope and limitations of the Ag(I) *bis*(4-methoxypyridine) hexafluorophosphate complex **2.11d** (Table 3.6). The propargyl amide substrates **3.1a-q** and **3.1s** were subjected to 10 mol% of **2.11d** in $CH_2Cl_2$ at room temperature, and NMR yields were obtained in a similar manner to that described in Section 3.2: by calculating the relative integral ratios of the alkene protons in the product relative to those of 1,3,5-trimethoxybenzene. With more reactive substrates such as **3.1i** and **3.1q**, the catalytic loading was reduced; while an increase in catalytic loading to 15 mol% was necessary with the internal alkyne substrates **3.1l, m** and **o** which showed low conversions at 10 mol% catalytic loading. For substrates that showed conversions to the desired products, the reaction was repeated on a 2.0 mmol preparative scale and the products were isolated and characterized after purification by column chromatography or preparative TLC. Due to the volatility of the products, only the NMR yields in $CD_2Cl_2$ were reported for substrates **3.1b** and **3.1c**.

With the exception of substrate **3.1m**, the reactions proceeded with complete regioselectivity towards the 5-membered methylene oxazline products. Substrates bearing alkyl and aryl substituents at the amide ($R^1$) were well tolerated, leading to the corresponding heterocycles in good to excellent yields (entries 1-3). The presence of a crotonyl group in substrate **3.1d** did not affect the yield (entry 4); however, the presence of a vinyl group resulted in decomposition of the catalyst (entry 5). In comparison, substrates with electron-withdrawing substituents at the amide position resulted in poorer yields (entries 7 and 8), presumably due to the reduced nucleophilicity of the carbonyl oxygen atom. The difficulty in promoting the cycloisomerization of such substrates was also observed using the Au(I) catalysts,[154] where higher catalytic loadings and prolonged reaction times up of to 2 days, were required. As expected, the introduction of *gem*-dimethyl or electron-donating substituents at the propargylic position ($R^2/R^3$) resulted in faster reaction times and satisfying yields of between 90-96% (entries 9 and 10).

Substrates **3.1j** and **3.1k** with two propargylic moieties delivered the double cycloisomerized products only in moderate yields (entries 10 and 11). Complete conversion of **3.1j** was obtained after 24 h, but the yield of **3.2j** was compromised by the formation of other unknown side products. This problem was not encountered with the Au(I) catalyst, [(Ph$_3$P)Au]OTs, where 5 mol% of catalyst under identical reaction conditions afforded **3.2j** in 80% isolated yield.[154]

Even more interestingly, substrates with alkyl and phenyl substituents at the alkyne ($R^4$) underwent cycloisomerization smoothly with good regioselectivity to give the corresponding five-membered alkylidene oxazoline products exclusively (entries 13-17). However, when the phenyl substituent at the amide position ($R^1$) was replaced with a cyclohexyl substituent, a complex mixture of products was obtained (entries 13 vs. 18), showing the greater sensitivity of internal alkyne substrates to substitution at this position compared to the terminal alkyne substrates.

It was mentioned in the beginning of this Chapter that the use of Au(I) catalysts furnished a mixture of both the five-membered and six-membered oxazoline and oxazines with substrates that possess alkyl substituents at the alkyne (refer to Table 3.1). This issue of 5-*exo*/6-*endo* regioselectivity, however, does not arise with our *bis*(pyridine) Ag(I) catalyst. However, both the *E*- and *Z*- isomers of the oxazoline products were obtained (entries 13-15). The selectivity towards the *Z*-isomer is greater when the alkyl substituent at the alkyne is large, possibly due to the greater instability of the *E*-isomer as a result of steric hindrance with the 4-methoxyphenyl substituent. These results contrast with those obtained in the previous Chapter, where *anti* addition of the imidate nucleophile to the alkyne occurs, resulting in complete diastereoselectivity towards the *Z*-isomer. This again highlights the differences in the mechanism brought about by a change in the nucleophile.

The only exception was with substrate **3.1p**, when the alkyne is substituted by a phenyl group. In this case, the reaction proceeded with complete

regioselectivity and diastereoselectivity towards the *Z*-isomer of the five-membered methylene oxazoline product (entry 16). This result was also obtained with the Au(I) catalyst, [(IPr)AuCl]/AgOTs.[154] The *Z*-configuration of the product, **3.2p**, was confirmed by its solid state structure (Fig. 3.1) and nOe observed by ^{1}H spectroscopy. A long-rage allylic [4]*J* coupling can be observed between the alkenyl and methine protons, which could be used to identify *Z*-isomers in the other product mixtures. With the exception of **3.2p** and the *Z*-isomer of **3.2o**, the cycloisomerization products of the internal alkyne substrates decomposed during purification by column chromatography. For this reason, only their NMR yields are reported in Table 3.6.
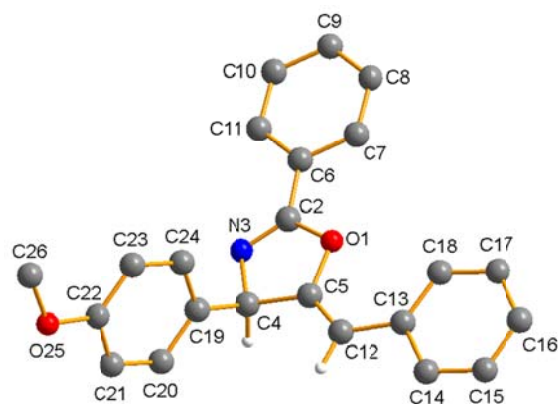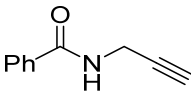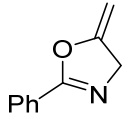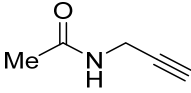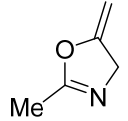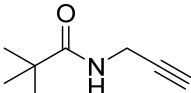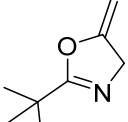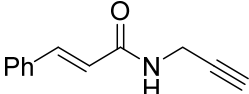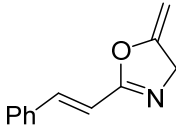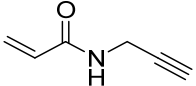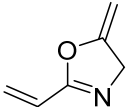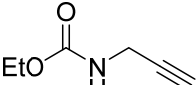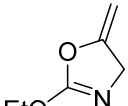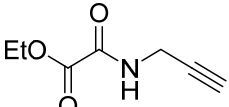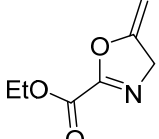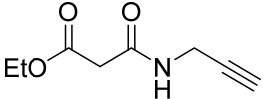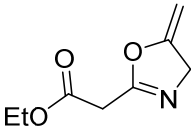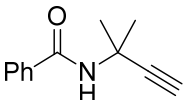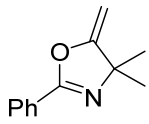


**Fig. 3.1.** Structural confirmation of (*Z*)-**3.2p**

The most surprising result was obtained with substrate **3.1m**, bearing a trimethylsilyl (TMS) substituent at the terminal position of the alkyne. In this particular case, two products **3.2q** and **3.4m** were obtained in a 1:3.8 ratio (entry 17). The former arises from the desilylation of the either the substrate prior to cycloisomerization, or the product; and the latter was obtained from the 6-*endo-dig* cyclization. The switch in regioselectivity can be attributed to

the electronic influence of the TMS substituent, which withdraws electron density from the alkyne π-bond via interaction of the alkyne pπ orbital with the Si-C σ* orbital. Being closer to the TMS substituent, the carbon atom of the alkyne closest to the TMS substituent is more electrophilic, and was preferentially attacked by the *O*-nucleophile, resulting in the observed oxazine product.

**Table 3.6.** Substrate Scope[a]

| Entry | Substrate | Cat. Loading | Time | Product | Yield[b] |
|-------|-----------|--------------|------|---------|----------|
| 1 | 3.1a | 10 mol% | 24 h | 3.2a | >99 (94) |
| 2[c] | 3.1b | 10 mol% | 24 h | 3.2b | 74 |
| 3[c] | 3.1c | 10 mol% | 24 h | 3.2c | 90 |
| 4 | 3.1d | 10 mol% | 24 h | 3.2d | 91 (84) |

| 5 |  3.1e | 10 mol% | 24 h |  3.2e | – |
| 6 |  3.1f | 10 mol% | 24 h |  3.2f | – |
| 7 |  3.1g | 10 mol% | 24 h |  3.2g | – |
| 8 |  3.1h | 10 mol% | 24 h |  3.2h | 10 |
| 9 |  3.1i | 1 mol% | 1 h |  3.2i | >99 (96) |

| 10 | **3.1q** | 5 mol% | 30 min | **3.2q** | 97 (90) |
| 11 | **3.1j** | 10 mol% | 24 h | **3.2j** | 34 (28) |
| 12 | **3.1k** | 10 mol% | 24 h | **3.2k** | 45 (42) |

| 13 | 
3.1l | 15 mol% | 24 h | 
3.2l | 74 (E:Z = 1:2.7) |
| 14 | 
3.1n | 10 mol% | 10 h | 
3.2n | 86 (E:Z = 1:1.1) |
| 15 | 
3.1o | 15 mol% | 24 h | 
3.2o | 95 (49) (E:Z = 1:2.8) |
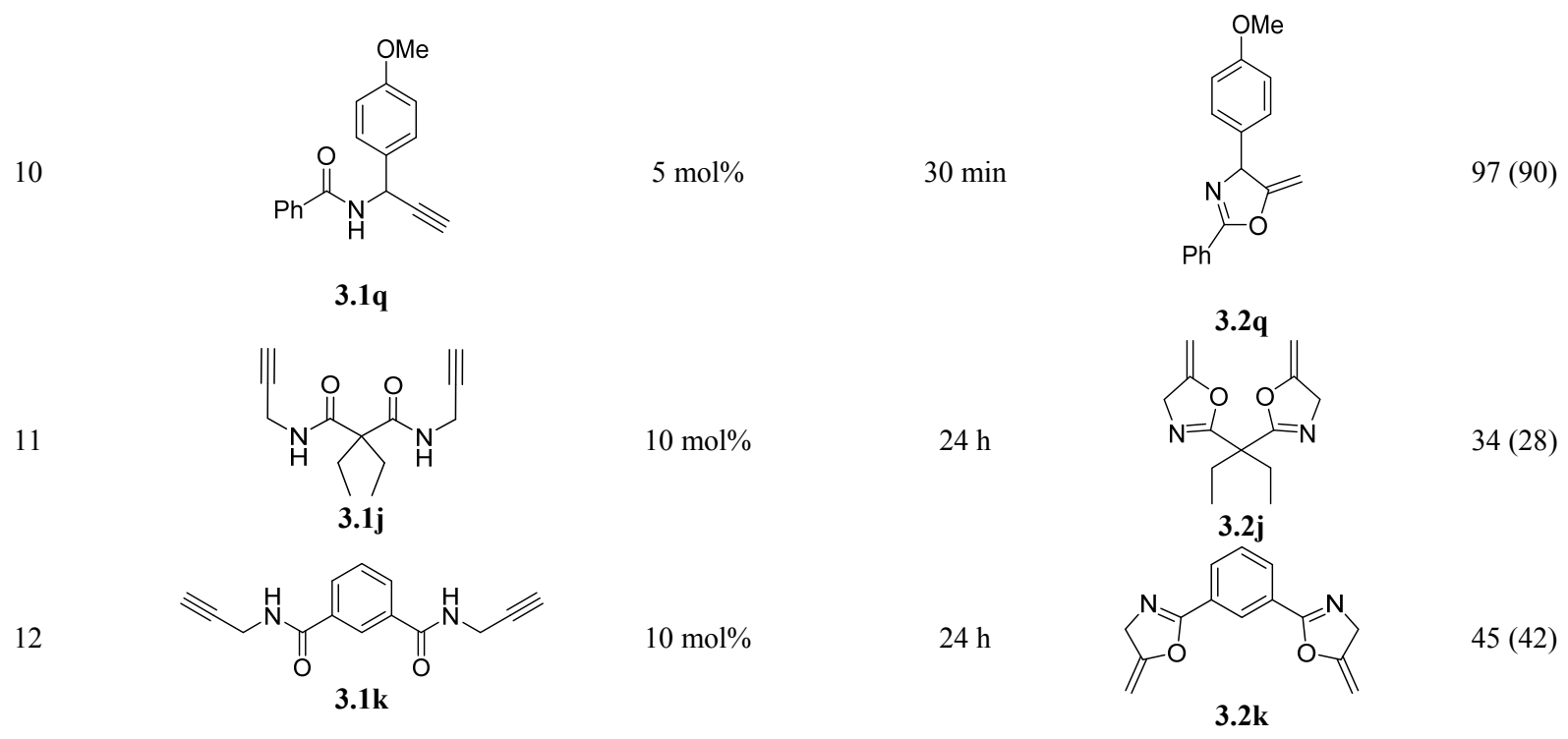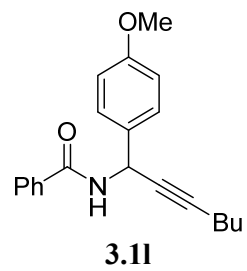
137

| 16 |  | 10 mol% | 10 h |  | 96 (82) |

**3.1p**

**3.2p**
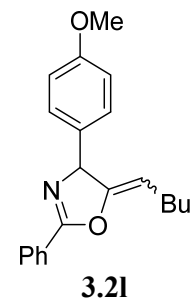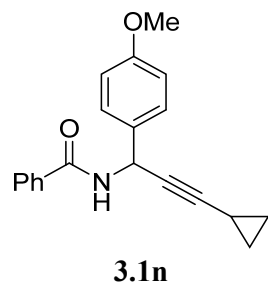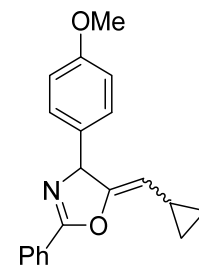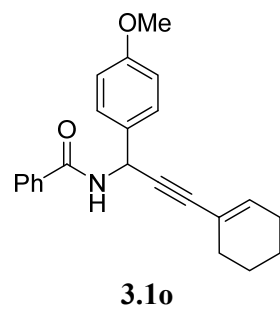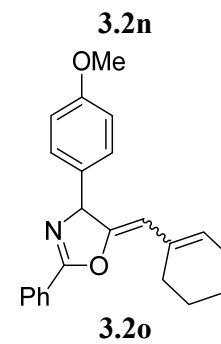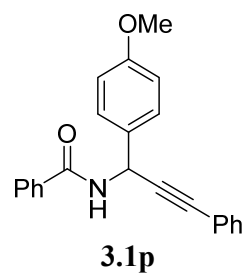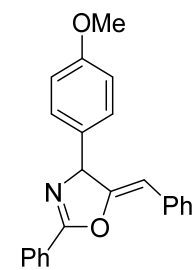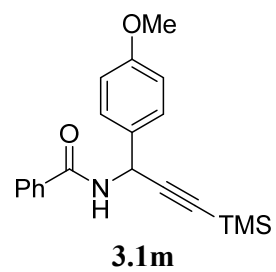
| 17 |  | 15 mol% | 24 h |  | **3.4m**: 76 |
| | | | | | **3.2q**: 21 |

**3.1m**

**3.4m**

and

18

3.1s

10 mol%

24 h

3.2q

3.2s

–
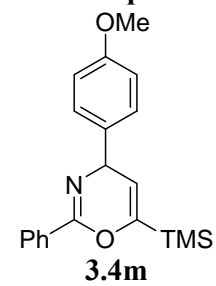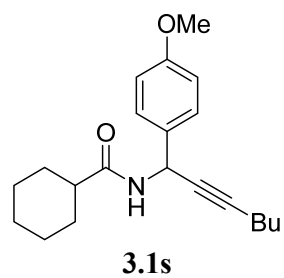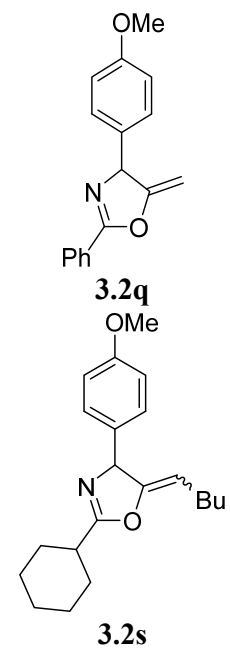
[a] Reaction conditions: substrate **3.1** (0.4 mmol), catalyst **2.11d** (1-15 mol%), CH$_2$Cl$_2$ (1 mL), 23 °C.
[b] Determined by $^1$H NMR spectroscopy, using 1,3,5-trimethoxybenzene as internal standard. Isolated yields after purification by column chromatography or preparative TLC are indicated in parentheses.
[c] Reaction carried out in CD$_2$Cl$_2$.

# 3.5. Trapping of Organosilver(I) Intermediates with Electrophiles
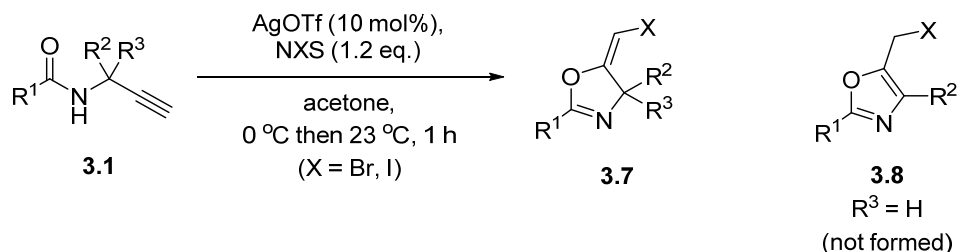


**Scheme 3.10.** Trapping of organosilver intermediates with *N*-halosuccinimides

**Table 3.7.** Synthesis of halomethyleneoxazolines **3.7** by trapping of organosilver intermediates

| Entry | Substrate | R$^1$ | R$^2$ | R$^3$ | NXS | Product | Yield of 3.7 |
|-------|-----------|-------|-------|-------|-----|---------|--------------|
| 1 | | | | | NBS | **3.7a** | 84 |
| 2 | **3.1a** | Ph | H | H | NBS[a] | **3.7a** | 8 |
| 3 | | | | | NIS | **3.7b** | 56 |
| 4 | | | | | NIS[a] | **3.7b** | 28 |
| 5 | **3.1c** | $^t$Bu | H | H | NBS | **3.7c** | 64 |
| 6 | | | | | NBS[a] | **3.7c** | –[b] |
| 7 | **3.1d** | ⤳Ph | H | H | NBS | **3.7d** | 61 |
| 8 | | | | | NBS[a] | **3.7d** | –[b] |
| 9 | | | | | NBS | **3.7e** | 98 |
| 10 | **3.1i** | Ph | Me | Me | NBS[a] | **3.7e** | 90 |
| 11 | | | | | NIS[a] | **3.7f** | 96 |
| 12 | **3.1q** | Ph | PMP | H | NBS | **3.7g** | 98 |
| 13 | | | | | NBS[a] | **3.7g** | 25 |

[a] Reaction carried out in the absence of AgOTf catalyst. [b] Degradation products observed.

In a similar manner to that previously described in Chapter 2, the cyclization of five propargyl amide substrates were performed in the presence of 1.2 equivalents of the *N*-halosuccinimides (NBS, NIS or NCS) and 10 mol% of AgOTf in acetone (Scheme 3.10, Table 3.7). Where reactions were observed, only the unaromatized oxazolines **3.7** were obtained regiospecifically; good to

excellent yields of the desired (*E*)-bromomethyleneoxazoline products were obtained with NBS, while the (*E*)-iodomethyleneoxazoline products could only be obtained with substrates **3.1a** and **3.1i**, resulting in decomposition of the substrate in other cases. The solid state structure of **3.7d** was also obtained (Fig. 3.2), providing unambiguous evidence for the *E*-geometry about the double bond. NCS was not an effective electrophile in this reaction with all the substrates tested.
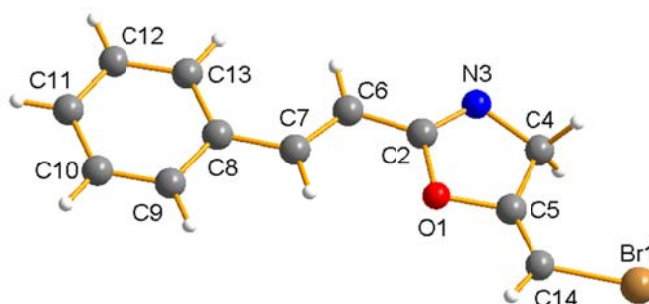


**Fig. 3.2.** Solid-state structure of **3.7d** (50% thermal ellipsoids), showing the *E*-geometry.

In the absence of AgOTf, only low yields of the halomethyleneoxazoline products were obtained. The only exception was substrate **3.1i**, whereby NBS and NIS alone could promote the electrophilic cyclization as a result of the presence of a prominent Thorpe-Ingold effect.

These results are significant, as previous attempts to intercept the vinylgold(I) catalytic intermediates with *N*-halosuccinimides in the analogous gold(I) catalyzed reactions have not been successful.[154] Instead of the expected halomethyleneoxazolines **3.7**, only the halomethyloxazoles **3.8** were obtained in low yields *via* the reaction of the methyleneoxazolines with

halosuccinimide. Moreover, these observations provide interesting clues to the reaction mechanism, which will be discussed in the next section.

## 3.6 Mechanistic Considerations
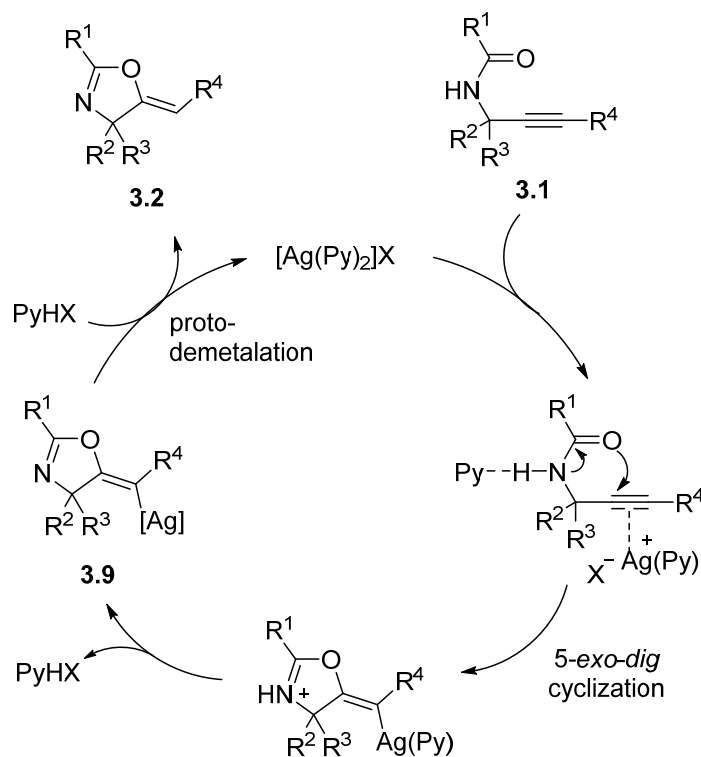


**Scheme 3.11.** Proposed mechanism

On the basis of our experimental findings, a general mechanism for the cycloisomerization reaction is proposed in Scheme 3.11. The stereospecific addition of the oxygen nucleophile to the alkyne in the proposed mechanism is supported by the sole formation of the *Z*-halomethylene oxazolines as described in the previous section, which also implies that the mixture of *E*- and *Z*-isomers observed with internal alkyne substrates (Table 3.6, entries 13-15) could be due to competitive processes occurring in subsequent steps.

The fact that AgOTf performed poorly as a catalyst in the cycloisomerization reaction of **3.1a** (Table 3.4, entry 9) but resulted in 84% yield of the bromomethylene oxazoline product **3.7a** within 1 hour in the presence of NBS (Table 3.7, entry 1) provides support for the hypothesis that the rate-determining step in the silver-catalyzed cycloisomerization reaction may be the final protodemetallation step. This final step involves the breaking of the Ag–C bond in the putative vinylsilver intermediate **3.9** in the presence of a proton, and is crucial for achieving catalytic turnover. NBS could have supplied a high concentration of electrophilic $Br^+$ ions that assisted the demetallation process, resulting in a significant increase in reaction rate. The profound effect exerted by substituents on the pyridine ligand in the *bis*(pyridine) silver(I) complexes on catalytic activity has led us to propose the involvement of the pyridine ligands in proton transfer steps of the catalytic cycle. It might be possible that strongly basic pyridine ligands such as DMAP hamper the protodemetallation step; while weakly basic pyridine ligands such as 4-acetylpyridine are ineffective proton transfer agents.

At this point, however, we cannot rule out two possible alternative mechanisms that can also explain the mixture of *E*- and *Z*-isomers observed with internal alkyne substrates (Scheme 3.12): 1) the stereoselective *syn* addition of the carbonyl oxygen nucleophile across the alkyne, to give (*E*)-**3.2**, which then isomerizes slowly to the thermodynamically more stable (*Z*)-isomer as the reaction proceeds (Scheme 3.12a), and; 2) the silver- and base assisted isomerization of the propargyl amide to an allenic intermediate, which then undergoes 5-*endo-dig* cyclization to affords both the *E*- and *Z*-isomers of

the methyleneoxazoline **3.2.** This latter pathway is through to be less likely due to the observed Thorpe-Ingold effect observed earlier in the study of substrate scope.
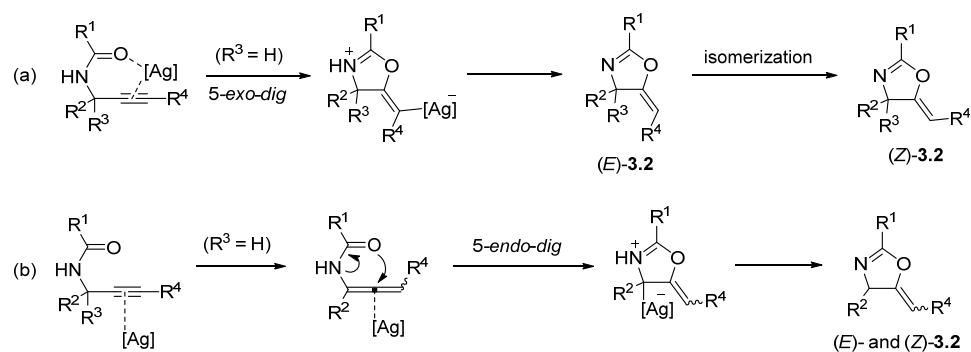


**Scheme 3.12.** Alternative mechanistic pathways that explain the formation of of *E*- and *Z*-methylene oxazolines **3.2**

## 3.7 Conclusion

Two synthetic procedures were used to prepare the propargyl amide substrates for the cycloisomerization reactions. The first and most commonly used method involves the reaction of acyl chlorides with propargyl amines. This method is convenient for the synthesis of substrates with different substituents at the position beside the carbonyl group. The second method involves a newly-developed HBF$_4$-catalyzed nucleophilic substitution of propargyl alcohols with primary amides, which is advantageous if substituents are to be introduced at the propargylic position or at the alkyne.

Initial catalyst screening was performed using **3.1** as the model substrate. The use of silver salts in the cycloisomerization reaction generally gave poor yields. The best result was obtained with the use of 10 mol% of AgTFA in CH$_2$Cl$_2$ that gave the highest yield of 60% after 6 h at room temperature. *Bis*(pyridine)

144

complexes could also catalyze the reaction; however, the nature of the ligand and the counteranion had a considerable influence on the catalytic activity. A general increase in efficiency of the catalyst was observed in the presence of more electron-donating pyridine ligands and non-coordinating counteranions. The Ag(I) *bis*(4-methoxypyridine) hexafluorophosphate complex showed a broad tolerance towards substituents at several positions including the amide ($R^1$), propargylic ($R^2/R^3$) and at the alkyne ($R^4$). Despite the higher catalytic loading of 10 mol%, comparable yields to those obtained with cationic Au(I) catalysts could be obtained in certain cases. Significant differences in stereoselectivity were revealed between the gold and silver catalysts in the cycloisomerization of internal alkyne substrates, suggesting that the Ag(I)-catalyzed reaction might proceed via a different mechanism from that of previously reported Au(I)-catalyzed reactions.

In addition, the trapping of vinylsilver intermediates in the reaction with electrophilic halogen sources such as NBS and NIS has also been successful, affording the (*E*)-bromo- and iodo-substituted oxazolines in good yield and regioselectivity. This allows for future possibility of the further functionalization of the oxazoline products, for the construction of more complex and synthetically useful compounds.

# Chapter 4 Silver(I) *N*-Heterocyclic Carbene Carboxylate Complexes: Synthesis, Structure and Catalysis

## 4.1 General Introduction on Silver(I) *N*-Heterocyclic Carbene Carboxylate Complexes

The silver(I) ion is known for its coordinative flexibility,[176] affinity for both hard and soft donor atoms,[177,178] ability to form short Ag···Ag contacts[179] and ligand-unsupported Ag···Ag interactions.[180] Concurrently, due to their various coordination modes to metal ions and their ability to act as both hydrogen-bonding acceptors and donors,[181] carboxylate ligands have frequently been employed in the design and construction of supramolecular architectures, which find applications in new functional materials for ion and molecular recognition, ion-exchange, and catalysis.[182] Hence, the combination of silver(I) with carboxylate ligands[183,184] or polydentate ligands containing carboxylate and other functionalities[185] for the formation of coordination polymers and metal-organic frameworks constitutes an active area of research.

Silver(I) acetate compounds containing *N*-heterocyclic carbene (NHC) ligands have found applications in medicinal chemistry,[186,187,188] electrochromic materials,[189] and as synthons that allow access to other Ag(I) NHC complexes of the type [(NHC)AgX] (where X = halide, $N_3$, SPh, SePh) by reaction with silylated nucleophiles $SiMe_3X$.[190,191,192]

The first silver(I) NHC carboxylate complex **4.2** (Fig. 4.3, *vide infra*) was reported as a CVD- and spin-on glass (SOM) precursor in 2002 by Chung.[193] Later, in 2006, Young reported the synthesis of the silver(I) acetate complex containing an NHC ligand derived from caffeine (complex **4.1a**, Fig. 4.1) which showed good antimicrobial activity against numerous resistant respiratory pathogens from the lungs of cystic fibrosis patients.[194] Later, the anticancer activity of silver(I) acetate complexes containing NHC ligands derived from 4,5-dichloro-1*H*-imidazole (complexes **4.13**, **4.14** and **4.15**, Fig. 4.3) was also discovered.[195] Subsequent reports on the synthesis of silver(I) NHC acetate complexes have largely been focused on exploring their biological capabilities and improving their efficacy through fine-tuning of the substituent pattern on the NHC ligand. The syntheses, structures and applications of silver(I) NHC complexes containing halides as either coordinating or non-coordinating counteranions have been covered extensively in several reviews.[196] In contrast, no systematic analysis of the structural and spectroscopic features of silver(I) NHC acetate complexes has been undertaken. Furthermore, with the only exception of the benzoate complex **4.2** (shown in Fig. 4.10), all the reported complexes contain only acetate as a carboxylate ligands, and the catalytic activity of such complexes has been largely unexplored: To date, there is only one example of silver(I) NHC carboxylate complexes being employed as catalysts.[197]

This chapter will begin with the structural analysis and spectroscopic properties of silver(I) NHC carboxylate complexes reported in the literature, followed by a discussion on the methods to prepare these complexes. Notable

structural features of this class of complexes and trends in bonding and structure will be highlighted, which will allow a better understanding of our approach in developing catalytically active NHC silver(I) complexes for heterocyclization reactions of alkynes. Finally, the synthesis and characterization of new silver(I) NHC carboxylate complexes and their catalytic application towards the cycloisomerization of propargyl amides will be discussed.

## 4.1.1 Solid State Structures

All Ag(I) NHC carboxylate complexes published to date contain monodentate NHC ligands, and all but one (complex **4.20**) contain acetate as the anionic ligand. The discussion of their structures in the solid state will be divided into three parts based on the type of heterocycle the NHC ligand is derived from: 1) xanthine, 2) imidazole and 3) benzimidazole. Within each family of NHC ligands, the complexes differ by the nature of substituents on the heterocyclic backbone, and the substituents in the N atoms. The effect of this change in substitution on the $Ag-C_{carbene}$ and $Ag-O_{carboxylate}$ bond lengths, and the geometry around Ag(I) will be described. In addition, general trends and comparisons with the cationic *bis*(NHC) complexes and (NHC)AgX (X = halide) complexes will be discussed.

148

### 4.1.1.1 Xanthine-derived NHCs
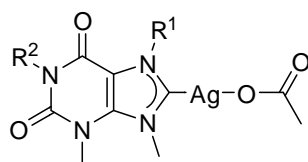


**4.1a**   $R^1$ = Me, $R^2$ = Me
**4.1b**   $R^1$ = Me, $R^2$ = $CH_2CH_2OH$
**4.1c**   $R^1$ = $CH_2CH(OH)CH_2OH$, $R^2$ = Me
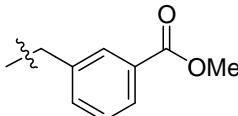
**4.1d**   $R^1$ = Me, $R^2$ =

**Fig. 4.1.** Ag(I) NHC carboxylate complexes with xanthine-derived NHCs.



**4.1a**

**4.1b**

**4.1c**

**4.1d**
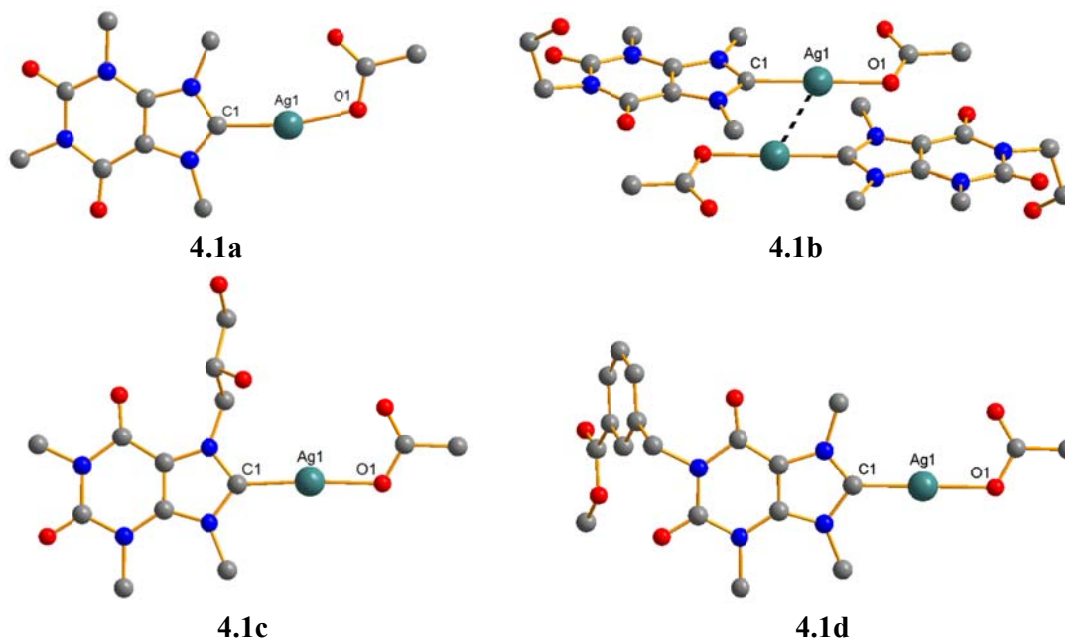
**Fig. 4.2**. Molecular structure of complexes **4.1a-d**. Hydrogen atoms have been omitted for clarity.

**Table 4.1.** Selected bond lengths (Å) and angles (deg) for complexes **4.1a-d**

| Complex | Ag1-C1 | Ag1-O1 | C1-Ag1-O1 | Ag···Ag | Ref |
|---------|--------|--------|-----------|---------|-----|
| **4.1a** | 2.067(3) | 2.1198(19) | 168.19(9) | – | 194 |
| **4.1b** | 2.072(4) | 2.118(3) | 175.9(1) | 3.199 | 198 |
| **4.1c** | 2.068(2) | 2.112(2) | 174.78(9) | – | 199 |
| **4.1d** | 2.022(7) | 2.064(5) | 178.2(2) | – | 200 |

There are 4 reported examples of silver acetate complexes containing xanthine-derived NHC ligands (Fig. 4.1). All complexes are mononuclear, with a two-coordinate silver atom bound to the NHC and a monodentate acetate ligand. Selected bond lengths and angles are given in Table 4.1, and their molecular structures are shown in Fig. 4.2. Complexes **4.1b** and **4.1c** incorporate hydrophilic hydroxyl groups tethered to the xanthine ring to improve their solubility in water, while complex **4.1d** contains a methyl benzoate group in order to improve its ability to bind to certain targeting groups that might aid in the delivery of the compound to bacteria cells *in vivo*. The C1-Ag-O1 angle of 168.19(9)° in complex **4.1a** deviates significantly from linearity due a weak interaction of 2.949 Å between the carbonyl of the acetate ligand and the metal center, as shown in Fig. 4.2. Complex **4.1d**, on the other hand, shows a C1-Ag-O1 angle close to linearity of 178.2(2)°. It also has the shortest Ag1-C1 and Ag1-O1 bond lengths in the series of 2.022(7) Å and 2.064(5) Å respectively.

Xanthine-derived NHCs are known to have good π-accepting ability,[201] and this property is expected to be enhanced in the NHC ligand of complex **4.1d** due to the presence of the electron-withdrawing methyl benzoate substituent. This results in the observed stronger and shorter Ag1-C1 bond. However, the expected lengthening of the *trans* Ag1-O1 bond was not observed. Instead, the Ag1-O1 bond was shortened, possibly due to the π-donating acetate ligand which interacts synergistically with the backbonding of the Ag to the NHC ligand in a "push-pull" effect. The Ag1-O1 bond length and C1-Ag1-O1 angle

in complexes **4.1b** and **4.1c** are similar, although **4.1b** possesses a longer Ag-C

bond and a short Ag···Ag contact of 3.199 Å.

## 4.1.1.2 Imidazole-derived NHCs



|       |       |
|-------|-------|
| **4.5a** | R = H |
| **4.5b** | R = OMe |
| **4.5c** | R = CN |
| **4.5d** | R = CO$_2$Me |
| **4.5e** | R = NO$_2$ |

|       |       |
|-------|-------|
| **4.6a** | R = H |
| **4.6b** | R = Me |
| **4.6c** | R = CO$_2$Me |

|       | R$^1$ |   | R$^2$ |
|-------|-------|---|-------|
| **4.7** | H | **a** | Ph |
| **4.8** | Me | **b** | Me |
| **4.9** | $^i$Pr | **c** | OMe |
| **4.10** | OMe | **d** | CN |
| **4.11** | Cl | **e** | CO$_2$Me |

|       |       |
|-------|-------|
| **4.12a** | R = H |
| **4.12b** | R = CN |
| **4.12c** | R = CO$_2$Me |
| **4.12d** | R = NO$_2$ |

**Fig. 4.3.** Ag(I) NHC carboxylate complexes with imidazole-derived NHCs.

**4.13a**  R = Me

**4.13b**  R = (2-naphthylmethyl)

**4.14a**  R = H
**4.14b**  R = OMe
**4.14c**  R = CN
**4.14d**  R = CO$_2$Me
**4.14e**  R = NO$_2$

**4.15a**  R = H
**4.15b**  R = CN
**4.15c**  R = CO$_2$Me
**4.15d**  R = NO$_2$

**4.16**

**4.17**

**4.18**

**Fig. 4.3. cont'd** Ag(I) NHC carboxylate complexes with imidazole-derived NHCs.

**4.19**      **4.20**

**Fig. 4.3. cont'd** Ag(I) NHC carboxylate complexes with imidazole-derived NHCs.

Perhaps unsurprisingly, silver(I) complexes of imidazole-derived NHC ligands constitute the largest class in this series, exhibiting the greatest diversity in their coordination chemistry. There are a total of 57 reported examples, which can be broadly divided into three main structural variations (Fig. 4.3). A compilation of all relevant bond distances and angles for these structures is given in Table A1 of Appendix 1. The first and most common variation involves the *N*-substituents on the NHC ligand, with most complexes bearing *para*-substituted benzyl groups, which were chosen to improve the lipophilicity of the resulting complexes and their ability to penetrate the cell membrane of microorganisms.



**4.5a**      **4.5d**

153

**4.5c**
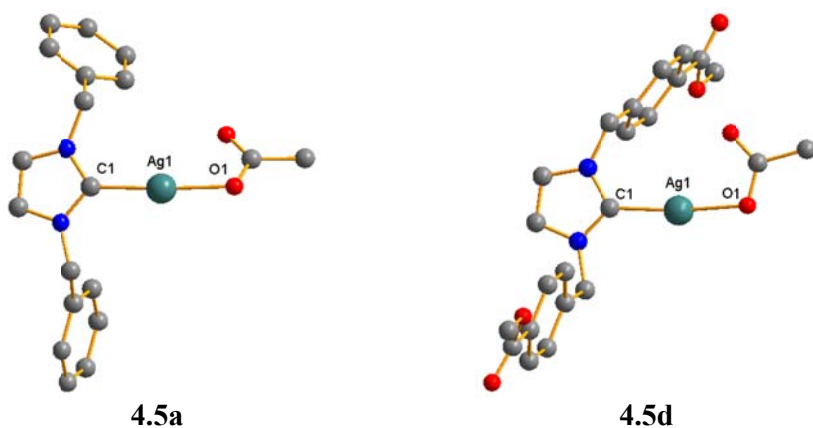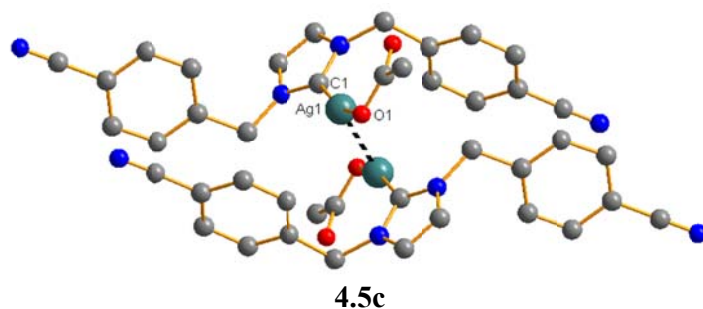
**Fig. 4.4.** Effect of *N*-substituents: molecular structures of **4.5a**, **c** and **d**. Hydrogen atoms have been omitted for clarity.

The first comparisons are made with the series of substituted complexes **4.5a-e**. When the methyl substituents on complex **4.3** were replaced by benzyl groups in **4.5a**, only small changes were observed in the Ag1-C1 and Ag1-O1 bond lengths. The benzyl ring substituents in **4.5a** are not co-planar with the imidazole rings, but approximately perpendicular in their arrangement. They are also disposed *syn* to each other. However, when the hydrogen atoms in the 4-position of the benzyl rings are replaced with electron-withdrawing cyano and ester groups in **4.5c** and **4.5d** respectively, the benzyl substituents are orientated away from each other, one above the plane of the imidazole ring and the other below in an *anti* arrangement (See Fig. 4.4). In addition, an increase in the Ag1-C1 and Ag1-O1 bond lengths was also observed, due to the reduced σ-donating ability of the carbene carbon in the presence of more electron-withdrawing substituents on the nitrogen atoms. Complex **4.5c** also displays short Ag···Ag contacts of 3.0050(5) Å, resulting in a C1-Ag1-O1 angle of 163.4(1)° which deviates significantly from linearity. In **4.5d**, the coordination mode of the acetate ligand also changes from monodentate to an asymmetric bidentate mode.
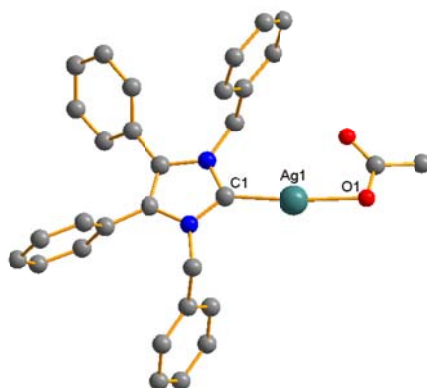
**Fig. 4.5.** Molecular structure of complex **4.7a**, chosen as a lead compound for biological studies. Hydrogen atoms have been omitted for clarity.

A series of complexes (**4.7-4.11**) were prepared by Tacke and co-workers,[202,204,205] and the effects of varying the substituents in the 4-position of the phenyl rings on the NHC backbone and on the benzyl substituents on nitrogen was studied. Of these, complex **4.7a** (Fig. 4.5) was chosen as a lead compound for further optimization to enhance the antibacterial and cytotoxic activity of the resulting silver complexes.[202] Notably, complex **4.7a** has the longest Ag1-C1 bond length, and the Ag1-O1 bond length is at the upper limit for the range of Ag1-O1 bond lengths for monodentate acetate ligands in this series [2.101(1)-2.164(1) Å]. A short Ag···Ag distance of 2.9107(2) Å was also observed, together with a significant deviation from linear geometry of 163.40(6) Å around the silver atom. Comparing complexes **4.7a**, **d**, and **e**, which differ in the *para*-substituent of the benzyl groups on nitrogen, the Ag1-C1 bond length was found to decrease in the presence of electron-withdrawing substituents, which is opposite to the trend observed for complexes **4.5a**, **c** and **d** mentioned above.

155
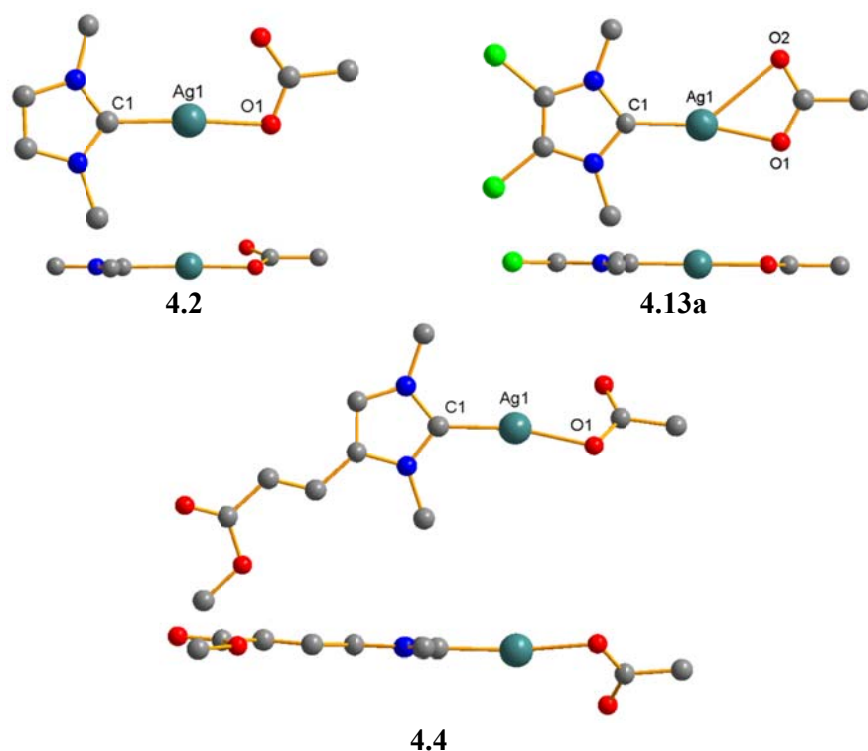
**Fig. 4.6.** Effect of substitution on C4/C5: molecular structures of **4.2**, **4.4** and **4.13a** showing their spatial arrangement and view from the side. Hydrogen atoms have been omitted for clarity.

**Table 4.2.** Comparison of bond lengths (Å) and bond angles (deg) of complexes **4.2**, **4.4** and **4.13a**.

|            | **4.2**   | **4.4**   | **4.13a**  |
|------------|-----------|-----------|------------|
| Ag1-C1     | 2.064(5)  | 2.030(8)  | 2.061(6)   |
| Ag1-O1     | 2.117(3)  | 2.154(5)  | 2.129(5)   |
| C1-Ag1-O1  | 176.0(2)  | 168.9(3)  | 167.3(2)   |
| Ref.       | 203       | 203       | 203, 195   |

The substituents on the backbone (C4 and C5 carbons) of the NHC can also be varied, and these include *para*-substituted phenyl substituents and chlorine substituents. The chloro-substituted complex **4.13a** was found to have greater stability in water and NaCl solution compared to **4.2** and **4.4,** which was attributed to the σ-electron inductive effect and π-donating ability of Cl atoms, leading to a reduction of the σ-donor capability and electron density of the

carbene carbon, making it less susceptible to protonolysis in an aqueous environment. The conjugated methyl ester group in **4.4**, which is both σ-withdrawing and π-withdrawing, however, did not contribute to stability of the complex. This could be due to free rotation of the methyl ester in solution which breaks the conjugation with the electronic framework of the imidazole ring.[203] A closer examination of the solid state structures of the three complexes reveals that in the presence of electron-withdrawing substituents on the NHC backbone, the Ag1-C1 bond shortens, Ag1-O1 bond lengthens and the acetate ligand tends towards a bidentate coordination mode. In complex **4.4**, the weak interaction (2.945 Å) between the carbonyl of the acetate ligand and silver results in a bent C1-Ag2-O1 angle of 167.3(2)°, which is similar to that in **4.13a**. Another interesting difference between the three complexes is the twist of the acetate ligand relative to the plane of the NHC ring, apparent from their side view (Fig. 4.6). Complex **4.13a** is completely planar, while only a slight twist is observed in **4.2** and in **4.4** (approximately 45°).
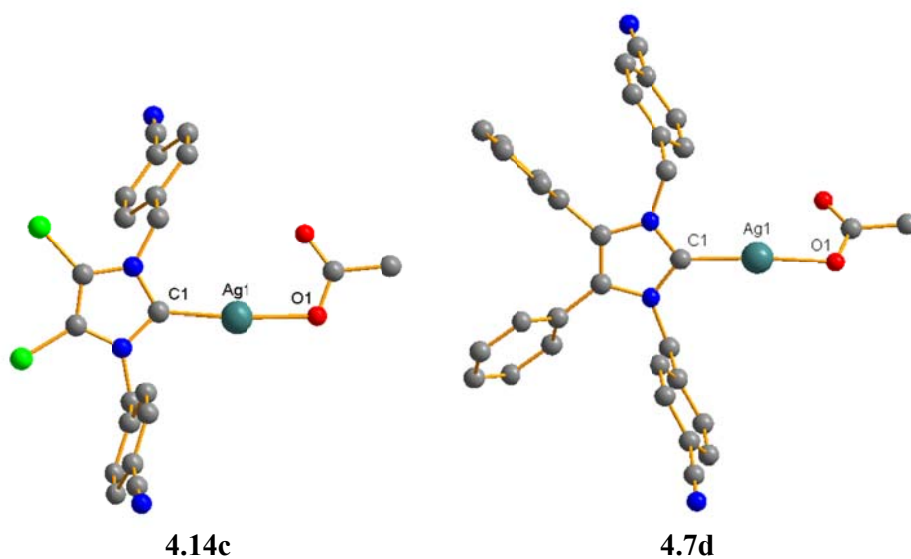


**4.14c**                                    **4.7d**

**Fig. 4.7**. Effect of substitution on C4/C5: molecular structures of **4.14c** and **4.7d**. Hydrogen atoms have been omitted for clarity.

**Table 4.3.** Comparison of bond lengths (Å) and bond angles (deg) of complexes **4.5c**, **4.7d** and **4.14c**.

|  | **4.5c** | **4.7d** | **4.14c** |
|---|---|---|---|
| Ag-C1 | 2.077(5) | 2.060(2) | 2.062(2) |
| Ag-O1 | 2.165(3) | 2.101(1) | 2.118(2) |
| C1-Ag-O1 | 163.4(1) | 178.76(8) | 174.89(7) |
| Ref. | 204 | 205 | 203 |

Next, the molecular structures of complexes **4.5c**, **4.7d** and **4.14c,** containing the same *N*-substituents but with hydrogen, chlorine, and phenyl groups on the 4- and 5- positions of the imidazole ring respectively, are compared (Fig. 4.4 and 4.7). It appears that the π-withdrawing 4,5-bisphenyl substitution in complex **4.7d** has the largest effect on the Ag-C bond length, even more pronounced than that of the σ-withdrawing 4,5-dichloro substitution in **4.14c**. The a shorter and stronger Ag1-C1 bond compared to **4.5c** could be suggestive of π-backbonding interactions between Ag(I) and the carbene *p*-orbital, a feature that is greatly enhanced by π-acidic substituents on the NHC.[206]

In an attempt to understand how modifications of the phenyl rings on the backbone of complex **4.7d** could affect the structure and bonding, complexes **4.7d**, **4.8d** and **4.9d** were compared. However, no direct correlation between bond length and the π-withdrawing ability could be established, possibly due to the fact that the phenyl substituents on the backbone are twisted relative to the plane of the imidazole ring, prohibiting π-overlap and resulting in the substituents on the phenyl ring, imposing little electronic effect on the NHC ligand. The crystal structure of **4.8d** was also disordered, with two species

differing in the coordination mode of acetate to silver, further hampering attempts to draw conclusions based on structure and π-backbonding ability of the NHC ligands.

Complex **4.18**, with *bis*(bithiophene) groups in the NHC backbone,[189] displayed the longest Ag-O bond length of 2.196(5) Å. The Ag-C bond length of 2.084(6) Å was also longer than most complexes in this class. As expected from the relatively weak Ag-C and Ag-O bonds, complex **4.18** is unstable in solution, decomposing over the course of a few days.

Another structural variation is the introduction of unsymmetrical NHC ligands (uNHCs) as ligands in metal-catalyzed reactions. Although they show similar structural parameters to symmetrical NHCs, further fine tuning of the reactivity and selectivity of their corresponding metal complexes can be achieved.[207] Likewise, in anticipation that replacing one benzyl substitutent on the lead compound **4.7a** with a methyl group would increase its solubility in DMSO and increase the viable dose of the complex *in vitro*, the unsymmetrical complexes **4.12a-d** were prepared. Modifications to the NHC backbone (see complexes **4.15** and **4.17**) and the incorporation of various combinations of different *N*-substituents (see complexes **4.6** and **4.16**) were also investigated. Unsurprisingly, only small differences in the structural parameters were observed compared to the corresponding symmetrical complexes.

At this point it will be useful to quantify differences in the size of the NHC ligands in the symmetrical and unsymmetrical complexes. The percent buried volume (%$V_{bur}$),[208,209] defined as the percentage of the total volume of a sphere centered upon the metal atom that is occupied by the ligand, was used to evaluate this. Using the Samb$V$ca[210] application, the %$V_{bur}$ was calculated using the exact Ag-C bond lengths from the X-ray data of complexes **4.5d**, **4.12c**, **4.15b** and **4.14c**. These values, together with their respective bond lengths and angles are shown in Table 4.4, and their molecular structures are shown in Fig. 4.8. As expected, only small differences in the %$V_{bur}$ were observed between the symmetrical and unsymmetrical complexes, showing that the difference in steric bulk of a benzyl substituent on nitrogen is similar to that of a methyl substituent, and the influence of the substituents on nitrogen on the %$V_{bur}$ value is only limited to a close area around the nitrogen.



**4.12c**

**4.5d**
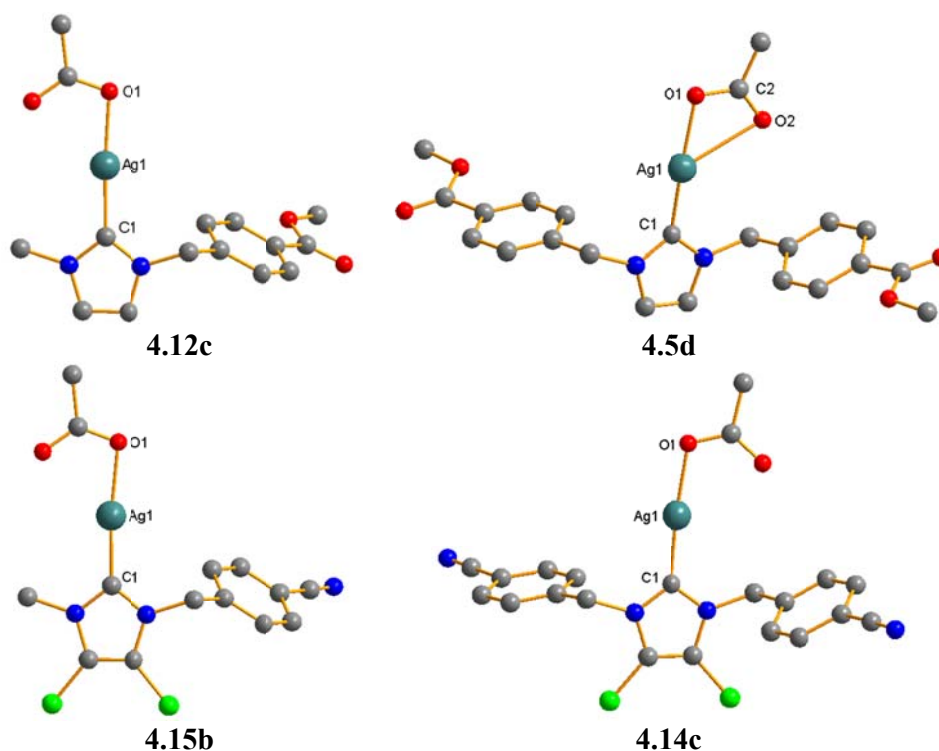
**4.15b**

**4.14c**

**Fig. 4.8.** Comparing symmetrical and unsymmetrical complexes: molecular structures of **4.5d**, **4.12c**, **4.15b** and **4.14c**. Hydrogen atoms have been omitted for clarity.

**Table 4.4.** Comparison of bond lengths (Å), bond angles (deg) and %$V_{bur}$ of complexes **4.5d**, **4.12c**, **4.15b** and **4.14c**.

|           | **4.12c**  | **4.5d**   | **4.15b**   | **4.14c**  |
|-----------|-----------|-----------|------------|-----------|
| Ag1-C1    | 2.067(3)  | 2.067(2)  | 2.069(4)   | 2.062(2)  |
| Ag1-O1    | 2.137(2)  | 2.156(1)  | 2.140(3)   | 2.118(2)  |
| C1-Ag1-O1 | 176.10(9) | 171.80(7) | 173.86(14) | 174.89(7) |
| %$V_{bur}$ | 28.0     | 29.5      | 28.5       | 28.5      |
| Ref.      | 203       | 211       | 202        | 204       |

The acetate ligand mostly adopts the monodentate coordination mode for this class of complexes, although the symmetric and asymmetric bidentate modes were observed in a few complexes, namely **4.5e**, **4.13a**, **4.14a**, **4.15d** and **4.16**, and their solid-state structures are shown in Fig. 4.9. One common feature of all these complexes is the presence of electron-withdrawing groups either on the NHC backbone or wingtip substituents. Complex **4.5e**, the only complex with a symmetric chelating acetate ligand, has an unexceptional Ag1-C1 bond length of 2.065 Å. The Ag1-O1 bond length, however, is significantly longer than that in complexes with monodentate acetate ligands (which have Ag1-O1 bond lengths in the range of 2.101(1)-2.196(5) Å). According to the theory by Hocking and Hambley,[212,213] a carboxylate C2-O1 bond length larger than 1.2505 Å indicates a high covalent character of the metal oxygen bond in the complex, while a C2-O1 bond shorter than 1.2505 Å indicates a largely ionic interaction. An analysis of the C2-O1 bond lengths of the complexes in Table 4.5 reveal a high covalent character in the Ag1-O1 bond, with the exception of complex **4.14a**. This is consistent with the observed Ag-O1 bond length of

2.278(4) Å in **4.14a**, the longest among the complexes with asymmetric chelating acetate ligands.



**4.5e**

**4.13a**

**4.14a**

**4.16**
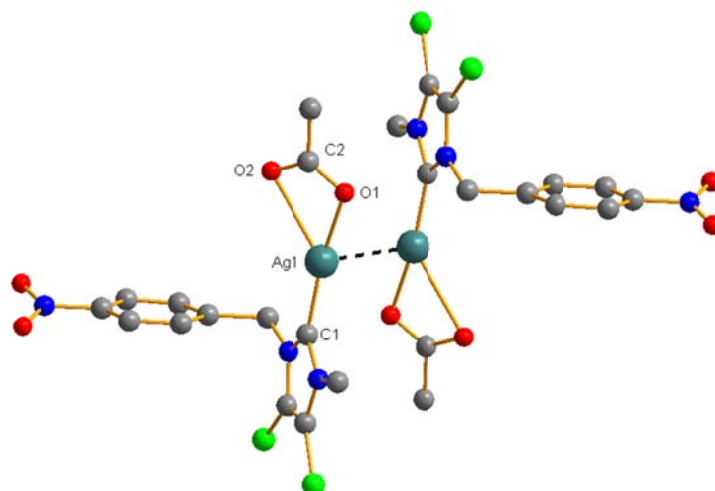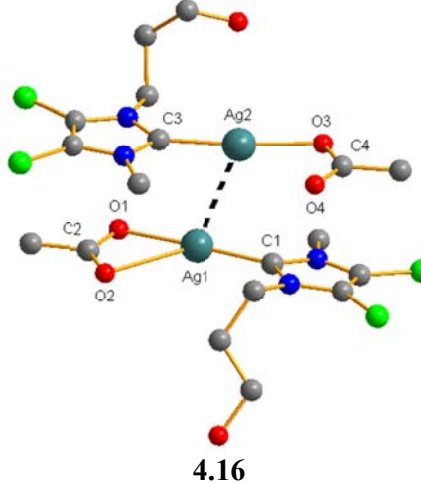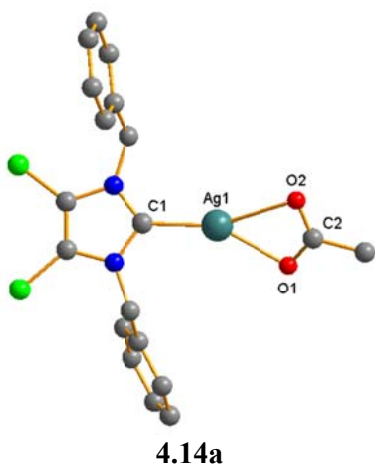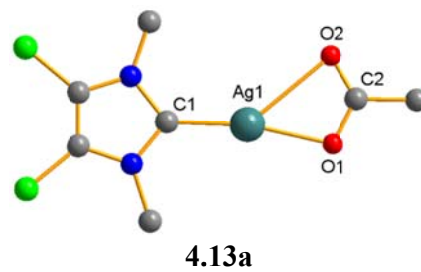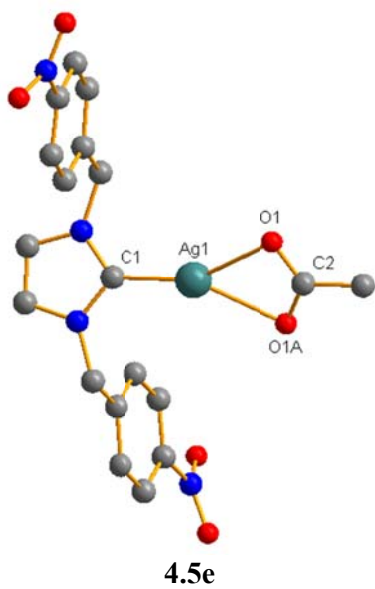
**Fig. 4.9.** Complexes with bidentate acetate ligands: molecular structures of **4.5e**, **4.13a**, **4.14a**, **4.15d** and **4.16**. Hydrogen atoms have been omitted for clarity.

**Table 4.5.** Comparison of bond lengths (Å) and bond angles (deg) of complexes **4.5e**, **4.13a**, **4.14a**, **4.15d** and **4.16**.

| Symmetric bidentate mode | | Asymmetric bidentate mode | | | |
|---|---|---|---|---|---|
| | **4.5e** | | **4.13a** | **4.14a** | **4.15d** | **4.16** |
| Ag1-C1 | 2.065 | Ag1-C1 | 2.030(8) | 2.064(4) | 2.040(9) | 2.053(8) |
| Ag1-O1 | 2.438 | Ag1-O1 | 2.154(5) | 2.278(4) | 2.173(6) | 2.138(5) |
| | | Ag1-O2 | 2.715(5) | 2.503(5) | 2.687(8) | 2.713(7) |
| C2-O1 | 1.257 | C2-O1 | 1.274(9) | 1.238(7) | 1.27(1) | 1.27(1) |
| | | C2-O2 | 1.24(1) | 1.225(7) | 1.25(1) | 1.255(7) |
| O1-Ag-O2 | 53.7 | O1-Ag-O2 | 52.1(2) | 53.4(1) | 53.2(3) | 52.8(2) |
| | | Ag···Ag | - | - | 3.1412 | 3.2267 |
| Ref. | 214 | Ref. | 195, 203 | 215 | 214 | 199 |

**4.1.1.3 Benzimidazole-derived NHCs**



**4.21**

**4.22**

**4.23a**  R = H
**4.23b**  R = CN
**4.23c**  R = CO$_2$Me
**4.23d**  R = NO$_2$
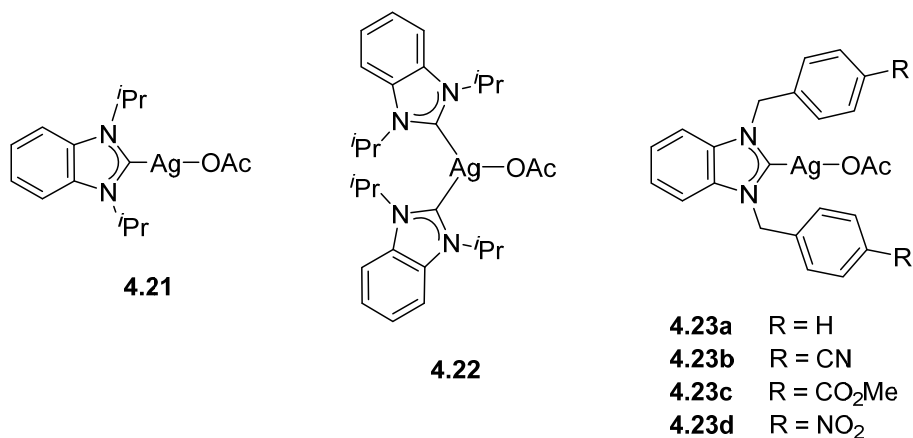
**Fig. 4.10.** Ag(I) NHC carboxylate complexes with benzimidazole-derived NHCs.

**4.24**



| **4.25a** | R = H |
| **4.25b** | R = Me |
| **4.25c** | R = OMe |
| **4.25d** | R = CO₂Me |

| **4.26a** | R = H |
| **4.26b** | R = CO₂Me |
| **4.26c** | R = NO₂ |
| **4.26d** | R = CN |

| **4.27a** | R = H |
| **4.27b** | R = CN |

| **4.28a** | R = Me |
| **4.28b** | R = -CH₂CH₂OH |
| **4.28c** | R = |
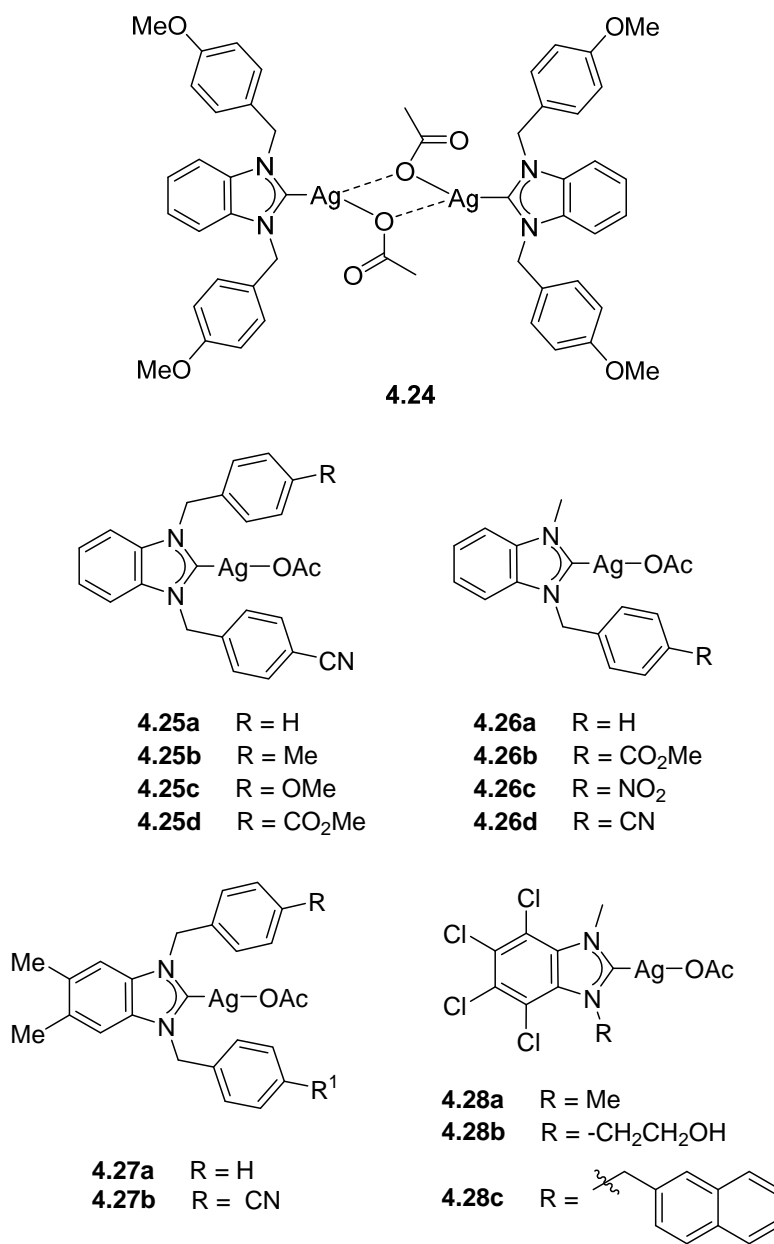
**Fig. 4.10. cont'd** Ag(I) NHC carboxylate complexes with benzimidazole-derived NHCs.

The annelation of a benzene ring to imidazole results in a new class of benzimidazole NHC ligands, which possess stronger π-acidity and a greater propensity for π-backbonding upon coordination to a metal. The silver(I) carboxylate complexes of this class of ligand are depicted in Fig. 4.10, and selected bond lengths and angles are given in Table A1 of Appendix 1. As a

consequence of the synergistic bonding between π-acceptor NHCs and the metal, more robust metal-NHC bonds may result – a desirable feature in numerous applications of these metal complexes. The additional benzene ring also allows for further functionalization and tuning of electronic properties by substitution with methyl groups or electron-withdrawing chlorine atoms, for instance, in complexes **4.27** and **4.28**.

An inspection of the solid state structures of **4.23a-d** and **4.27a-b** appears to highlight the presence of a *trans* effect, where an elongation of the Ag-O bond is observed with the shortening of the Ag-C bond – a phenomenon not observed in the previously discussed xanthine and imidazole-type NHCs. The presence of electron-withdrawing groups on the wingtip substituents of the NHC decreases the Ag-C bond length, and this was accompanied by an increase in Ag-O bond length. A comparison of complexes **4.23a** and **4.27a**, which differ in the substitution of two hydrogen atoms on the benzene ring by electron-donating methyl groups, result in a change in the coordination mode of the acetate ligand from bidentate to monodentate, and an increase in Ag-C bond length. The effect of the addition of two methyl groups on the benzene ring of the NHC is also evident from the observed decrease in Ag-C bond length from 2.072(6) to 2.052(3) Å and the corresponding increase in Ag-O bond length from 2.085(5) to 2.113(2) Å when comparing complexes **4.23b** and **4.27b**. This is commensurate with an increased π-accepting ability of the NHC ligand in **4.27b**, leading to a stronger Ag-C bond.
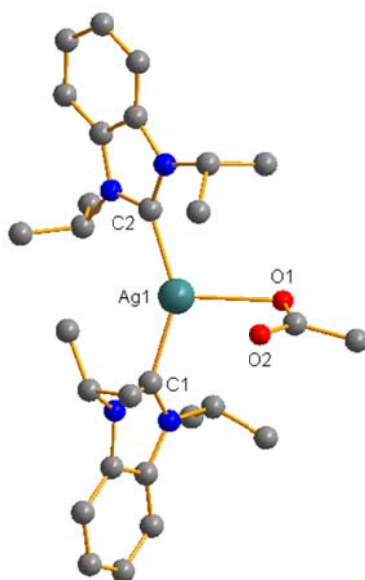
**Fig. 4.11.** Molecular structure of complex **4.22** featuring a three-coordinate silver atom. Hydrogen atoms have been omitted for clarity.

Complex **4.22** has a unique structure with a three-coordinate silver atom (see Fig. 4.11), binding to two NHC ligands and one monodentate acetate ligand in a trigonal planar geometry. Only small deviations away from ideal trigonal planar geometry that result from the steric requirements of the $^i$Pr substituents are observed. The planes of the NHC rings are twisted with respect to the coordination plane of silver, and the C-Ag-C angle is 146.3°. In comparison to complex **4.21**, the Ag-O bond length in **4.22** is markedly longer (2.568(2) Å vs. 2.120(7) Å).
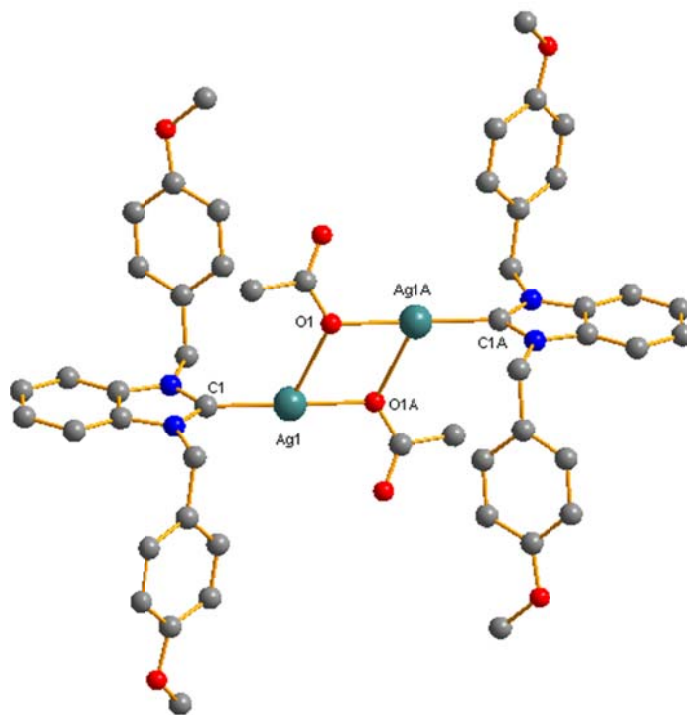
**Fig. 4.12.** Molecular structure of complex **4.24** showing the unsymmetrical bridging mode of the acetate ligand. Hydrogen atoms have been omitted for clarity.

An unsymmetrical bridging mode of the acetate ligand is observed in complex **4.24** (See Fig. 4.12), which exists as a dimer in the solid state. One oxygen atom of the acetate ligand connects strongly to one silver (2.1206 Å) and weakly (2.612(2) Å) to another, resulting in a binuclear species around an inversion center (Fig. 11). The Ag−Ag distance is 3.814 Å and the C1-Ag1-O1A angle is 170.1°.

## 4.1.2 ^{13}C NMR Spectroscopy

The most diagnostic feature of ^{13}C NMR spectrum of the silver(I) NHC carboxylate complexes is the downfield resonance signal of the carbene donor atom, which appears in the range from 150.4 to 207.8 ppm. The chemical shifts and coupling constants for this carbene carbon reported for all the

complexes are given in Table A1 of Appendix 1. Downfield shifts of the carbene carbon signal are generally observed in the presence of electron-withdrawing substituents on the both the nitrogen atoms and backbone of the NHC. A change from an unsaturated to saturated backbone of the NHC (compare complexes **4.19** and **4.20**) results in a downfield shift of the carbene signal. Notably, only complexes **4.19** and **4.20** display a pair of doublets for the carbene carbon signal that arises from coupling to $^{107}$Ag and $^{109}$Ag (which are magnetically active with spin ½ and a relative abundance of 52% and 48% respectively).[216]
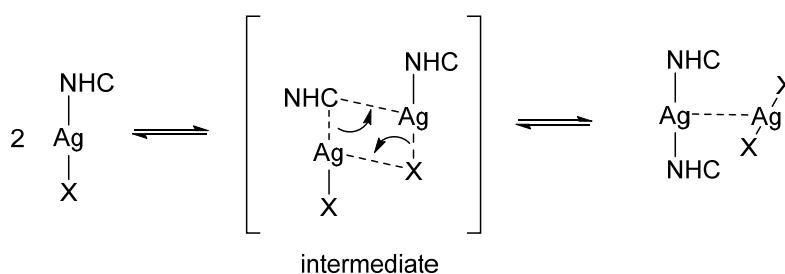


**Scheme 4.1.** Fluxional behavior of silver NHC complexes.

This coupling to silver is an indication of relatively strong Ag-C bonds, which can only be observed in cases where there is none or only a slow exchange of the carbene moiety between silver atoms on the NMR timescale. The absence of coupling to silver is due to the fluxional behavior. A plausible mechanism for the exchange has been proposed by Lin[217] (Scheme 4.1), and factors affecting this dynamic behavior, such as the steric bulk of the ligand, type of halide ion present and solvent polarity have been studied.[218,219] Complexes **4.18** and **4.22** showed the lack of an observable resonance for the carbene

carbon, suggesting the presence of dynamic behavior or the poor relaxation of the quaternary carbene carbon.[196c]

## 4.1.3 Comparison with Analogous Cationic *bis*(NHC) Complexes and (NHC)AgX (X = halide) Complexes
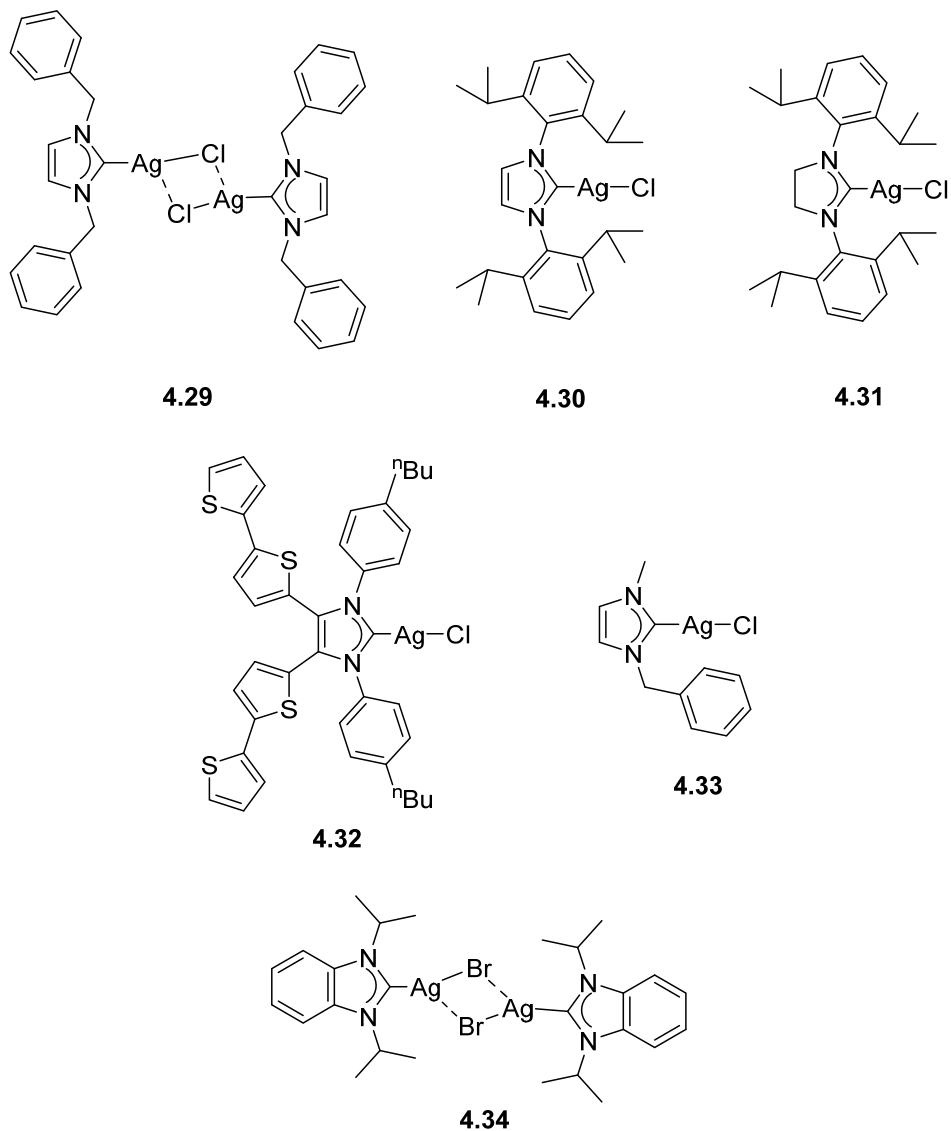


**Fig. 4.13.** (NHC)AgX (X = Cl or Br) complexes **4.29-4.34**.
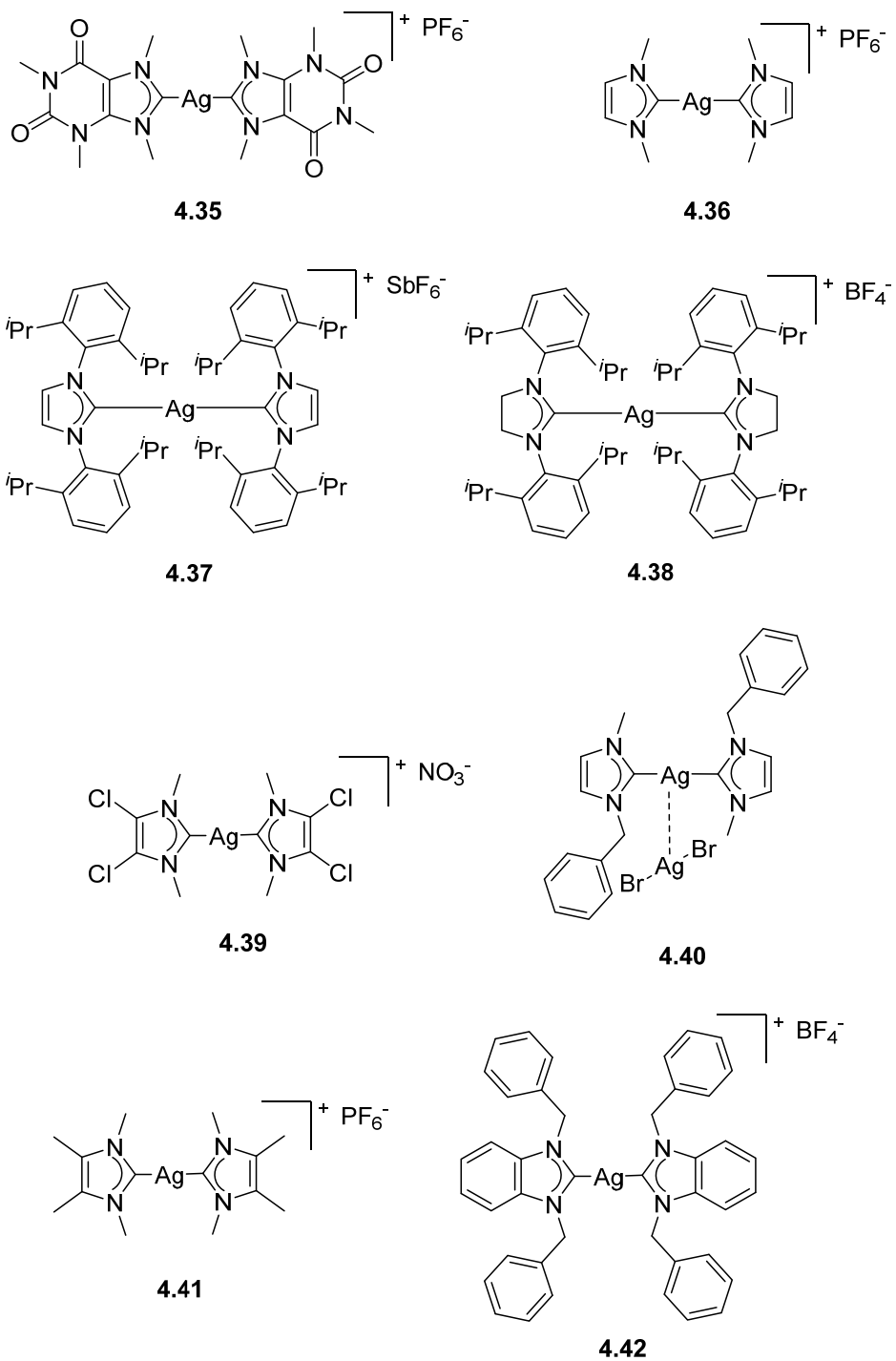
**Fig. 4.14.** Cationic *bis*(NHC) complexes **4.35**-**4.42**.

Given that the carbene carbon resonance is shifted upfield with increasing Lewis acidity of the metal center,[220,221] it might be possible to estimate the relative donor strengths of carboxylate, halide and NHC ligands towards Ag(I)

by comparing the carbene carbon chemical shift value of silver(I) NHC acetate complexes with their halide and cationic *bis*(NHC) congeners. The structures of these analogous complexes are depicted in Fig. 4.13 and 4.14, and their relevant spectroscopic and structural data obtained from literature references, are compiled in Table A2 of Appendix 1. More strongly donating co-ligands will enhance the electron density on the silver atom, reduce its Lewis acidity and shift the carbene carbon resonance downfield. From Table 4.6, it can be seen that the carbene carbon resonance of the acetate complexes generally appear upfield compared to their corresponding halide and *bis*(NHC) analogues. This implies that carboxylate ligands are weaker donors to silver compared to halides and NHC ligands, which is unsurprising, as silver is known to have good affinity towards halide ions.

**Table 4.6.** Comparison of $^{13}$C $\delta C_{carbene}$ of (NHC)Ag(O$_2$CR), (NHC)AgX (X = Cl or Br) and *bis*(NHC) complexes

| (NHC)Ag(O$_2$CR) complex[d] | $\delta C_{carbene}$ | (NHC)AgX complex[d] | $\delta C_{carbene}$ | *bis*(NHC) complex[d] | $\delta C_{carbene}$ |
|---|---|---|---|---|---|
| 4.1a | 186.2[b] | – | – | 4.35 | 186.7[b] |
| 4.3 | 178.6[b] | – | – | 4.36 | 181.0[b] |
| 4.5a | 177.0[a] | 4.29 | 151.2[a] | – | – |
| 4.19 | 184.3[a] | 4.30 | 184.6[a] | 4.37 | 183.6[a] |
| 4.20 | 207.8[a] | 4.31 | 207.7[a] | 4.38 | 205.8[c] |
| 4.13a | 176.1[b] | – | – | 4.39 | 181.3[b] |
| 4.12a | 179.9[a] | 4.33 | 180.7[a] | 4.40 | 179.9[b] |
| 4.2 | 173.0[c] | – | – | 4.41 | 177.6[b] |
| 4.21 | 179.4[a] | 4.34 | 185.4[a] | – | – |

[a] CDCl$_3$. [b] DMSO-d$_6$. [c] CD$_2$Cl$_2$. [d] See Table A2 in Appendix 1 for references.

**Table 4.7.** Comparison of Ag-C bond lengths (Å) of (NHC)Ag(O$_2$CR), (NHC)AgX (X = Cl or Br) and *bis*(NHC) complexes

| (NHC)Ag(O$_2$CR) complex[b] | Ag-C | (NHC)AgX complex[b] | Ag-C | *bis*(NHC) complex[b] | Ag-C |
|---|---|---|---|---|---|
| 4.1a | 2.067(3) | – | – | 4.35 | 2.068 |
| 4.3 | 2.064(5) | – | – | 4.36 | 2.086 |
| 4.5a | 2.065(1) | 4.29 | 2.091(2) | – | – |

| | | | | | |
|---|---|---|---|---|---|
| [a]**4.19** | 2.064(5) | **4.30** | 2.056(7) | **4.37** | 2.129 |
| [a]**4.20** | 2.059(7) | **4.31** | 2.081(9) | – | – |
| **4.18** | 2.084(6) | **4.32** | 2.087(4) | – | – |
| **4.13a** | 2.030(8) | – | – | **4.39** | 2.082 |
| **4.21** | 2.070(6) | **4.34** | 2.094(3) | – | – |
| **4.23a** | 2.059(3) | – | – | **4.42** | 2.089(3) |

[a] Ag-C bond lengths are obtained from complexes synthesized in this work. As more than one molecule is present in the asymmetric unit, the averaged bond length is used. [b] See Table A2 in Appendix 1 for references.

Table 4.7 provides a comparison of the Ag-C bond lengths of silver(I) NHC acetate complexes with their halide and cationic *bis*(NHC) congeners. The Ag-C bond lengths for the carboxylate complexes are shorter than those of the corresponding halide and cationic *bis*(NHC) complexes.

### 4.1.4 General Trends

As silver adopts a two-coordinate linear geometry in majority of the complexes with the carboxylate ligand binding in a monodentate manner, it is apparent that this coordination mode is highly preferred for complexes of this type. However, it is worth noting that electron-withdrawing groups on the NHC results in an increased tendency for the carboxylate ligand to bind in a chelating mode (see section 4.1.1.2). Large deviations from linear geometry around the metal center can result from weak interactions of the silver atom with the carbonyl oxygen atom of the carboxylate ligand (as observed in complex **4.1a** in Fig. 4.2), or with the carbonyl oxygen atom of the carboxylate ligand in the adjacent complex in the crystal structure (complex **4.24** in Fig. 4.12). As can be seen from Table A1 in Appendix 1, the presence of argentophilic interactions arising from closed shell $d^{10}$-$d^{10}$ interactions[222] in the solid state also tend to result in large deviations from linear geometry. This

has also been observed in cationic *bis*(NHC) complexes of 1,3-dialkylimidazol-2-ylidene ligands.[223]

It is evident from the discussion above, that the Ag-C bond length is not a good indicator of the strength of the Ag-C bond, which is the result of an interplay between the electron-donating and π-acceptor ability of the NHC ligand bonded to silver. Indeed, π-backbonding from NHC ligands to group 11 metals can contribute to as much as 30% of the overall orbital interaction energy based on experimental observations[224] and DFT calculations.[225] Other factors affecting the Ag-C bond length are the co-ligand *trans* to the NHC, and the presence of argentophilic interactions in the solid state.

When σ- and π-electron-withdrawing groups are present on the NHC ligand, it is difficult to deconvolute their σ-withdrawing and π-backbonding effects. This is because NHCs are stabilized by a push-pull effect (Fig. 4.15), as a result of: 1) the electron-withdrawing nitrogen atoms inductively stabilizing the σ-nonbonding orbital of the carbene by increasing its s-character; and 2) the donation of electron density from the nitrogen lone pairs into the vacant carbene pπ-orbital, increasing its energy. These two effects increases the σ-pπ gap and stabilizes the singlet carbene over the more reactive triplet state.[226] Electron-withdrawing substituents can therefore reduce the σ-donating ability of the NHC, but increase its π-accepting ability, both of which have opposite effects on Ag-C bond length. The absence of a *trans* effect in most of the complexes also does not allow comparisons of the electron donating abilities of the NHC.
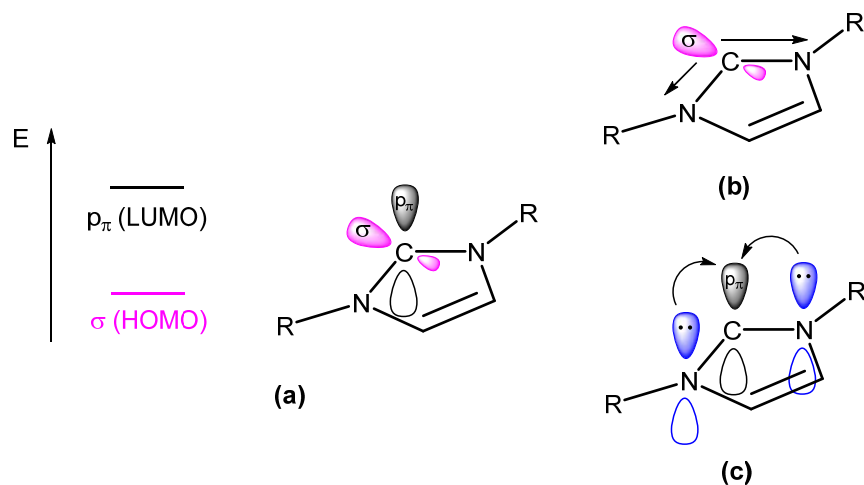
**Fig. 4.15 (a)** Frontier orbitals of the NHC; **(b)** electron-withdrawing nitrogen atoms stabilizing the σ-nonbonding orbital of the NHC; **(c)** the donation of electron density from the nitrogen into the carbene pπ-orbital.

The chemical shift values of the carbene carbon in the ^{13}C NMR also did not allow the unambiguous determination of the different donor abilities of NHCs in the complexes. The generally accepted rule is that a more strongly donating NHC would result in a more downfield shifted resonance peak of the carbene carbon. The fact that only complexes **4.19** and **4.20** with bulky 2,6-diisopropylphenyl substituents on the NHC displayed coupling to silver indicates that the rate of ligand exchange processes is slowed down by steric hindrance in the NHC. This was also observed for the chloride analogues of these complexes.[227] Generally, such fluxional complexes are undesirable as catalysts, as they may rapidly decompose. Thus, steric parameters of the NHC ligand were an important consideration in the design of our catalyst.

## 4.1.5 Synthetic Routes to Ag(I) NHC Carboxylate Complexes

Two methods have been used to prepare Ag(I) NHC carboxylate complexes: 1) the reaction of the free NHC with silver carboxylate and 2) *in situ* deprotonation of imidazolium salts with silver carboxylate (Scheme 4.2). In this work, complexes **4.2** (Fig. 4.3), **4.21** and **4.22** (Fig. 4.10) were prepared using the first method. The reaction took place at room temperature in solvents such as THF and toluene, and reaction times were short (1-3 h).

(a) $\text{NHC·HX} \xrightarrow{\text{base}} \text{NHC} \xrightarrow{\text{Ag(O}_2\text{CR)}} \text{[(NHC)Ag(O}_2\text{CR)]}$

(b) $\text{NHC·HX} + 2\text{Ag(O}_2\text{CR)} \longrightarrow \text{[(NHC)Ag(O}_2\text{CR)]} + \text{RCO}_2\text{H} + \text{AgX}$
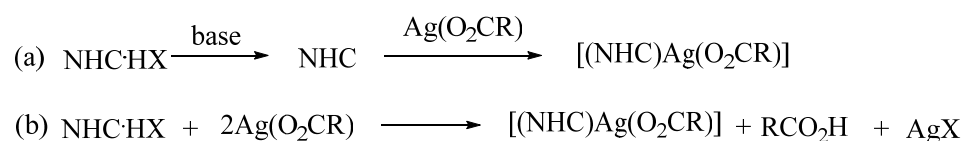
**Scheme 4.2.** Synthetic routes to Ag(I) NHC carboxylate complexes: (a) Free NHC route; (b) Deprotonation with silver carboxylate.

The second method involves the reaction of silver carboxylate with the imidazolium salt in solvents such as dichloromethane, methanol and ethanol, depending on the solubility of the imidazolium salt used. Reaction times can range from 30 min to 4 days at room temperature, depending on the acidity of the imidazolium salt. The reaction mixture can also be refluxed to speed up the reaction. Imidazolium salts with electron-withdrawing substituents, especially on the backbone, give faster reaction rates. A major disadvantage of this method  is the waste associated with using an added equivalent of silver carboxylate. This method is also not applicable for the synthesis of less basic carboxylate salts.

As the first method requires dry solvents, inert conditions and strong bases for the generation of the free carbene species, the second method is generally

preferred and is also the more widely used method for the preparation of Ag-NHC complexes.

## 4.2 Results and Discussion

As observed in the previous chapter, more electron-donating pyridine ligands promote the silver-catalyzed cycloisomerization of propargyl amides more efficiently. This encouraged us to explore the use of strong σ-donating NHC ligands with the aim of achieving even greater catalytic activity.

We began by preparing the chloride and the cationic *bis*(NHC) complexes of the commercially available *N,N'*-*bis*(2,6-diisopropylphenyl)imidazol-2-ylidine (IPr) ligand, [(IPr)AgCl][228] and [Ag(IPr)$_2$]PF$_6$,[229] and carried out a preliminary screening of their catalytic activity towards the cyclization of our model substrate (see section 4.3). Disappointingly, neither of these complexes exhibited any catalytic activity. This was attributed to the kinetic stability of these complexes, which disfavors the dissociation of either the neutral or anionic ligand to allow the coordination and activation of the alkyne. In light of this, the chloride complex of the slightly less hindered *N,N'*-*bis*(2,4,6-trimethylphenyl)imidazol-2-ylidine (SIMes), [(SIMes)AgCl][43] was prepared. This was also found to be catalytically inactive, which was attributed to the poor Lewis acidity of the metal center in the presence of strongly electron donating ligands. This led us to consider silver-NHC complexes containing more labile anionic ligands. Carboxylate ligands were attractive as they are known to bind less strongly to d$^{10}$ metals[191] and a number of silver NHC acetate complexes have been successfully prepared.[186,187,188] In the next

section, the synthesis of these complexes using previously reported methods and a newly developed method using a mild base will be described.

## 4.2.1 Synthesis of New Ag(I) NHC Carboxylate Complexes

### 4.2.1.1 *In situ* deprotonation of imidazolium salts with silver(I) acetate

[(IPr)AgOAc] (**4.19**) was successfully prepared according to a literature procedure,[190] which involves the reaction of the imidazolium chloride salt IPr·HCl with two equivalents of silver(I) acetate in $CH_2Cl_2$ at room temperature for 2 hours. However, attempts to prepare the SIMes complex by the same method failed, yielding mainly the cationic *bis*(NHC) product, $[Ag(SIMes)_2]X$ (X = Cl or OAc) and only small amounts of the desired [(SIMes)AgOAc]. Increasing the reaction time led to the formation of more $[Ag(SIMes)_2]X$, implying that [(SIMes)AgOAc] could be formed initially, but slowly converted to the thermodynamically more stable *bis*(NHC) complex under the reaction conditions. This is not surprising, given that Ag-O bonds are weaker than Ag-C bonds. This problem was, however, not encountered with the more sterically hindered IPr ligand, as the coordination of two bulky IPr ligands on silver is kinetically disfavoured.

**4.2.1.2 Reaction of free NHCs with silver(I) acetate and silver(I) trifluoroacetate**

$$\text{SIMes·HCl} \xrightarrow[\text{THF, r.t., 4 h}]{\text{KO}^t\text{Bu}} \underset{(in\ situ)}{\text{SIMes}}$$

with AgOAc → no reaction

with Ag(CF$_3$CO$_2$) → Ag$_4$(SIMes)$_2$(CF$_3$CO$_2$)$_4$ (**4.43**)
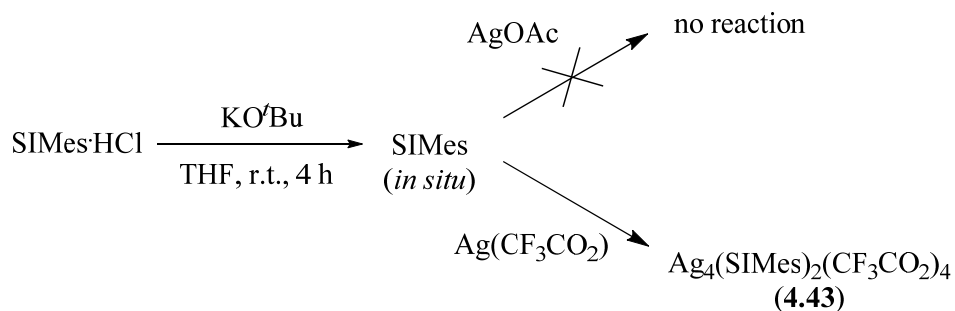
**Scheme 4.3.** Synthesis of **4.43**.

Attempts were made to prepare [(SIMes)AgOAc] by the reaction of free SIMes generated *in situ* with a suspension of silver acetate in THF. However, none of the desired complex was formed despite stirring the mixture overnight, and silver acetate remained largely unreacted. Suspecting this might arise from the poor solubility of silver acetate, the reaction was attempted with the more soluble silver trifluoroacetate (Scheme 4.3). Upon stirring overnight, a brown solution was obtained. The solvents were removed *in vacuo* and the resulting oily residue triturated with hexane to give an off-white solid. A $^1$H NMR of the product in CDCl$_3$ showed the absence of the imidazolium proton peak at 9.40 ppm, and the peaks observed in the $^{13}$C NMR spectrum were slightly different from those the imidazolium salt, although the signal of the carbene carbon was not observed. X-ray quality single crystals of the compound were obtained by cooling a saturated MeOH:Et$_2$O (1:1) solution of the compound at -20 °C overnight. The resolved structure shows that the resulting complex is an unexpected tetramer, formulated as Ag$_4$(SIMes)$_2$(CF$_3$CO$_2$)$_4$ (**4.43**). The structure of this complex will be discussed in greater detail in section 4.2.2.

### 4.2.1.3 Mild base method

Due to the shortage of literature methods for the preparation of silver(I) NHC carboxylate complexes, the development of a general and operationally simple method for the synthesis of such complexes would be highly desirable. Earlier work by Nolan[230,231] and Gimeno[232] have shown that NHC complexes of group 11 metals of the type [(NHC)MX] (X = halide) can be prepared efficiently by employing a mild base such as $K_2CO_3$ to deprotonate the imidazolium salt in the presence of a suitable metal source. It was envisaged that silver(I) carboxylate complexes could also be accessible if an imidazolium salt with a weakly coordinating anion such as $BF_4^-$ was used in the presence of the desired silver carboxylate. Initially, a mixture of the IPr·HBF$_4$ salt with silver acetate was stirred in $CH_2Cl_2$ at room temperature for 15 min, followed by the addition of 10 equivalents of $K_2CO_3$. This led to the formation of the expected [(IPr)AgOAc] complex and concomitant formation of the homoleptic bis(NHC) complex [Ag(IPr)$_2$][X] (X = BF$_4$ or RCO$_2$) after 1 h. The base was increased to 20 equivalents in an attempt to reduce the competitive deprotonation of IPr·HBF$_4$ by AgOAc or [(IPr)AgOAc] to give the bis(NHC) complex. Gratifyingly, this was effective in suppressing the formation of the bis(NHC) complex, and the method was subsequently extended to the preparation of other Ag(I) NHC acetate complexes of SIPr, IAd and IPent (Fig. 4.16), as well as benzoate complexes as shown in Scheme 4.4. After recrystallization, the complexes were obtained as air- and moisture-stable white crystalline solids in moderate to good yields (45-70%). Notably, none of the homoleptic complex was formed where IAd and IPent were used. In

comparison, IPr and SIPr Ag(I) complexes of the 4-substituted benzoate ligands were always obtained as a mixture of the neutral [(L)AgX] complex and the cationic *bis*(NHC) complex. Attempted purification of these complexes by recrystallization was unsuccessful, due to the greater solubility of the desired acetate complex compared to the *bis*(NHC) complex in most organic solvents.
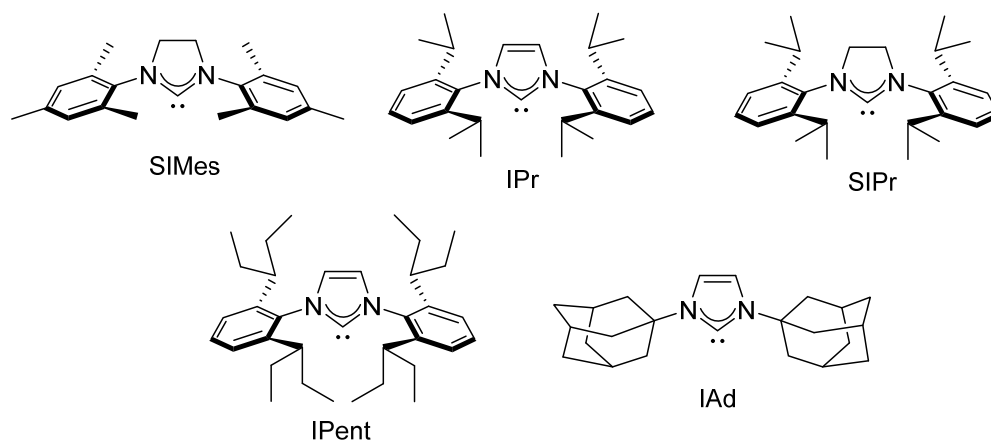


**Fig. 4.16.** Abbreviations of NHC ligands used in this study



| | |
|---|---|
| **4.19** (NHC = IPr) | **a** ($R^2$ = Me) |
| **4.20** (NHC = SIPr) | **b** ($R^2$ = Ph) |
| **4.44** (NHC = IPent) | **c** ($R^2$ = 4-MeC$_6$H$_4$) |
| **4.45** (NHC = IAd) | **d** ($R^2$ = 4-ClC$_6$H$_4$) |
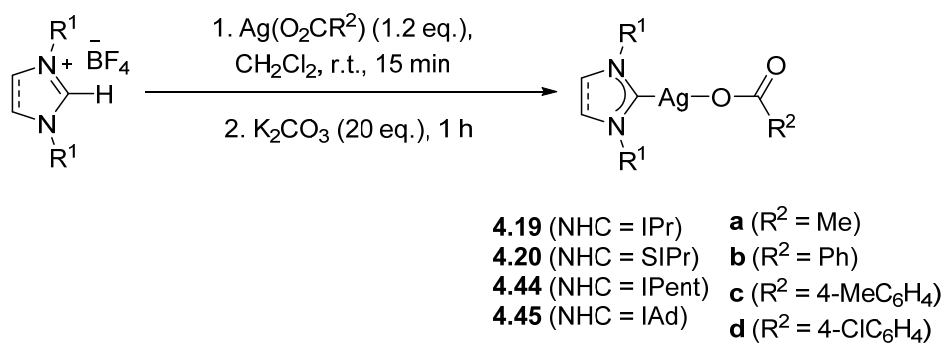
**Scheme 4.4.** Synthesis of [(NHC)Ag(RCO$_2$)] complexes

## 4.2.2 Spectral Characteristics

The $^1$H NMR spectra of complexes **4.19**, **4.20**, **4.44** and **4.45** show the absence of the low-field resonance around 9-10 ppm, indicating the removal of the C2

imidazolium proton. At the same time, the ^{13}C signal for the carbenic carbon of complexes **4.19**, **4.20** and **4.44** appear as two distinct doublets shifted downfield from that of the parent imidazolium salt, ranging between 173.5 to 207.9 ppm, consistent with coupling to [107]Ag and [109]Ag (Table 4.8).[233] The observed coupling indicates relatively strong Ag-C bonds, as a result of no or slow exchange of the carbene ligand between silver atoms on the NMR timescale.[234] The values of $^1J(^{109}\text{Ag-}^{13}\text{C})$ and $^1J(^{107}\text{Ag-}^{13}\text{C})$ are consistent with the gyromagnetic ratio $\gamma(^{109}\text{Ag})/\gamma(^{107}\text{Ag}) = 1.15$. However, the IAd complexes **4.45a** and **4.45b** are relatively unstable in solution and their decomposition is evident from the appearance of additional peaks in the ^{13}C spectra that increase in intensity over time. Thus no ^{13}C NMR of pure **4.45a** and **4.45b** could be obtained.

**Table 4.8.** [13]C chemical shifts (ppm) of the carbenic carbon $\delta$(C2) of complexes **4.19**, **4.20**, **4.44** and **4.45**, recorded in CDCl$_3$

| Complex | $\delta$(C2) | $^1J(^{107,109}\text{Ag-C})$ |
|---|---|---|
| [(IPr)AgOAc] (**4.19a**) | 184.5 | 249, 288 |
| [(IPr)AgOBz] (**4.19b**) | 184.4 | 251, 290 |
| [(IPr)Ag(4-MeC$_6$H$_4$CO$_2$)] (**4.19c**) | 184.5 | 250, 289 |
| [(IPr)Ag(4-ClC$_6$H$_4$CO$_2$)] (**4.19d**) | 184.1 | 252, 291 |
| [(IPr)AgCl][228] | 184.6 | 253, 271 |
| [(SIPr)AgOAc] (**4.20a**) | 207.9 | 234, 271 |
| [(SIPr)AgOBz] (**4.20b**) | 207.9 | 235, 271 |
| [(SIPr)Ag(4-MeC$_6$H$_4$CO$_2$)] (**4.20c**) | 207.9 | 235, 271 |
| [(SIPr)Ag(4-ClC$_6$H$_4$CO$_2$)] (**4.20d**) | 207.6 | 236, 273 |
| [(SIPr)AgCl][228] | 207.7[a] | 219, 253 |
| [(IPent)AgOAc] (**4.44a**) | 184.3 | 250, 288 |
| [(IPent)AgOBz] (**4.44b**) | 184.2 | 250, 289 |
| [(IPent)Ag(4-ClC$_6$H$_4$CO$_2$)] (**4.44d**) | 183.9 | 252, 291 |
| [(IAd)AgOAc] (**4.45a**) | 173.7 | 251, 289 |
| [(IAd)AgOBz] (**4.45b**) | 173.5 | 256, 290 |
| [(IAd)AgCl][228] | 173.8[a] | − (broad singlet) |

[a] NMR spectrum was obtained in CD$_2$Cl$_2$.

Interestingly, the chemical shifts of the carbenic carbon of complexes are scarcely influenced by the nature of the carboxylate co-ligand, although there is a slight increase in the coupling constant with decreasing basicity of the carboxylate ligand. Overall, the chemical shift values of the carbenic carbon, and hence the electron-donating ability of the NHC ligands decrease in the order: SIPr > IPr > IPent > IAd. The same trend was also observed in the analogous chloride complexes.[228]

ESI-MS analysis of the IPr, SIPr and IPent complexes **4.19**, **4.20** and **4.44** afforded the $[Ag(NHC)(MeCN)]^+$ fragment as the major peak when MeCN was used as the carrier solvent, highlighting the stability of this cationic species in solution. The $[Ag(NHC)_2]^+$ fragment, often observed in other reports as a result of ligand scrambling,[198c] was not observed in all cases, which supports the non-fluxional behavior of these complexes, as suggested by NMR. The IAd complexes **4.45a** and **4.45b**, however, displayed only the $[NHC+H]^+$ peak, commensurate with previous observations of their instability in solution.

**Table 4.9.** Carboxyl stretching vibrations and $\Delta v$ values ($cm^{-1}$) of complexes **4.19**, **4.20**, **4.44** and **4.45**, compared with unligated silver carboxylate salts

| Complex | $v_{asym}(COO)$ | $v_{sym}(COO)$ | $\Delta v$ |
|---|---|---|---|
| **4.19a** | 1588.3 | 1326.1 | 262.2 |
| **4.19b** | 1611.7 | 1346.2 | 265.5 |
| **4.19c** | 1602.7 | 1359.2 | 243.5 |
| **4.19d** | 1605.9 | 1364.6 | 241.3 |
| **4.20a** | 1587.2 | 1326.1 | 261.1 |
| **4.20b** | 1613.8 | 1346.8 | 267.0 |
| **4.20c** | 1603.6 | 1360.2 | 243.4 |
| **4.20d** | 1606.6 | 1365.9 | 240.7 |
| **4.44a** | 1599.9 | 1375.8 | 224.1 |
| **4.44b** | 1606.7 | 1364.5 | 242.2 |

| | | | |
|---|---|---|---|
| **4.44d** | 1607.5 | 1369.6 | 237.9 |
| **4.45a** | 1595.0 | 1372.2 | 222.8 |
| **4.45b** | 1597.8 | 1368.3 | 229.5 |
| AgOAc | 1509.1 | 1380.3 | 128.8 |
| AgOBz | 1512.8 | 1379.3 | 133.5 |
| $Ag(4\text{-}MeC_6H_4CO_2)$ | 1510.3 | 1379.3 | 131.0 |
| $Ag(4\text{-}ClC_6H_4CO_2)$ | 1508.8 | 1371.5 | 137.3 |

The solid-state IR frequencies for the asymmetric stretch, $v_{asym}(COO)$, the symmetric stretch, $v_{sym}(COO)$, and the $\Delta v$ value[235] ($\Delta v = v_{asym}(COO) - v_{sym}(COO)$) of the carboxylate group of complexes **4.19**, **4.20**, **4.44** and **4.45** are shown in Table 4.9. The $v(COO)$ bands were identified by comparisons with spectra of the NHC imidazolium salt precursor and other closely related compounds such as [(NHC)AgCl]. The calculated $\Delta v$ values $\Delta v = v_{asym}(COO) - v_{sym}(COO)$ of all the complexes are greater than 200 cm$^{-1}$, and are characteristic of a monodentate[236,237] or asymmetric bidentate[238] mode of carboxylate coordination, in line with their solid state structures (*vide infra*). The $\Delta v$ values of the complexes are also significantly larger than the corresponding silver carboxylates as a result of an increase in $v_{asym}(COO)$ and decrease in $v_{sym}(COO)$ on coordination of the NHC ligand, which led to an overall increase in $\Delta v$. Although $\Delta v$ was inversely correlated with the basicity of the carboxylate ligand for the silver carboxylates, no clear correlation was observed in complexes **4.19**, **4.20**, **4.44** and **4.45**. Instead, $\Delta v$ increases in the order: $RCO_2 = 4\text{-}ClC_6H_4CO_2 < 4\text{-}MeC_6H_4CO_2 < MeCO_2 < PhCO_2$.

## 4.2.3 Solid-State Structures

### 4.2.3.1 Solid-state structure of complex 4.43

Complex **4.43** crystallizes as a tetranuclear silver complex of the formula $Ag_4(SIMes)_2(O_2CCF_3)_4$. The complex may be viewed as an aggregated 2:1 adduct of $[(SIMes)Ag(O_2CCF_3)]$ and $[Ag_2(\mu_2\text{-}O,O'\text{-}CF_3CO_2)_2]$, held together by bridging bidentate trifluoroacetate ligands and Ag···Ag interactions. The asymmetric unit of complex **4.43** contains 12 silver atoms, 12 trifluoroacetate units, and 6 SIMes ligands. Considered in this fashion, the asymmetric unit contains three independent clusters. However, two of the clusters are complete, while the third cluster comprises of two distinct half clusters situated across centers of symmetry. Fig. 4.17 shows the complete clusters 4.43A and 4.43B, while Fig. 4.18 shows the $C_i$-symmetric clusters 4.43C and 4.43D. The four clusters differ slightly in the distance between the silver atoms of the $[(SIMes)Ag(O_2CCF_3)]$ and $[Ag_2(\mu_2\text{-}O,O'\text{-}CF_3CO_2)_2]$ core.
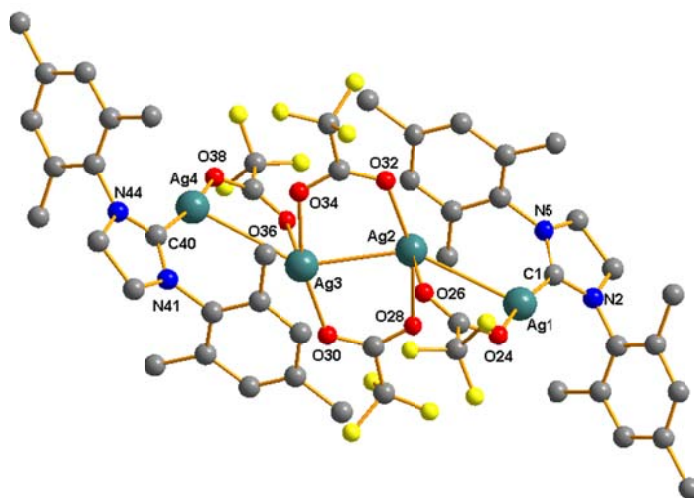


**4.43A**
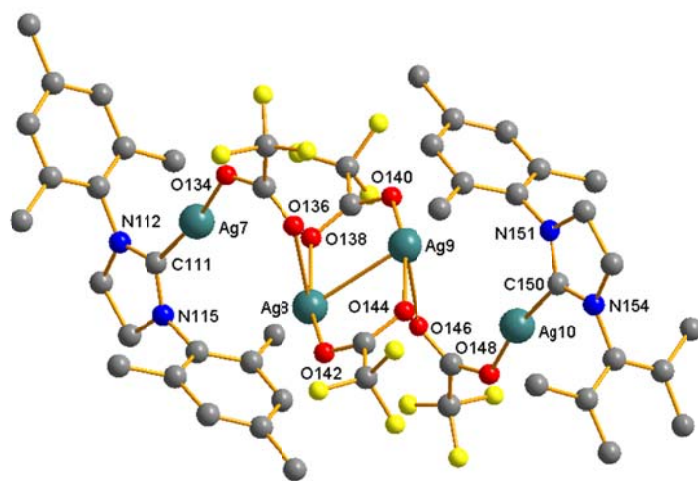
**4.43B**

**Fig. 4.17.** Complete Ag$_4$(SIMes)$_2$(O$_2$CCF$_3$)$_4$ clusters **4.43A** and **4.43B** in the asymmetric unit of complex **4.43**.
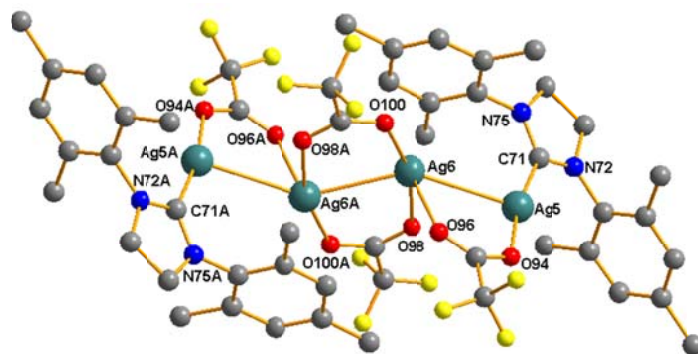


**4.43C**
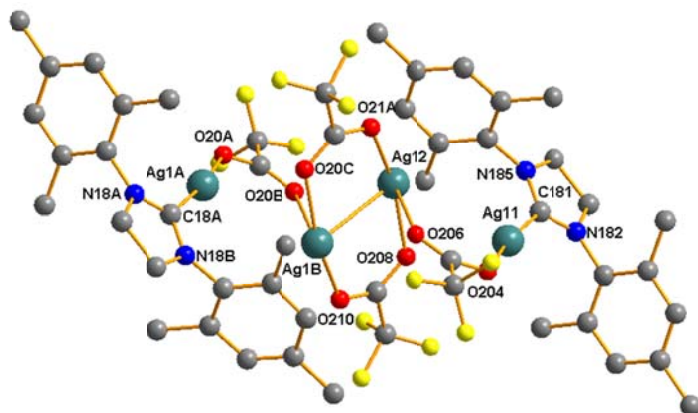


**4.43D**

**Fig. 4.18.** C$_i$-symmetric Ag$_4$(SIMes)$_2$(O$_2$CCF$_3$)$_4$ clusters **4.43C** and **4.43D** in the asymmetric unit of complex **4.43**.

Clusters 4.43A and 4.43C consisting of a zig-zag $Ag_4$ chain, where four silver atoms are held together by short Ag⋯Ag contacts. The distances between the terminal silver atoms and those of the $[Ag_2(\mu_2\text{-}O,O'\text{-}CF_3CO_2)_2]$ core are in the range 3.114 - 3.168 Å, shorter than that in clusters 4.44B and 4.44D (3.411 - 3.531 Å). The distances between the two atoms within the $[Ag_2(\mu_2\text{-}O,O'\text{-}CF_3CO_2)_2]$ core are also much shorter, ranging from 2.865 to 2.915 Å.

The terminal Ag atoms in all four clusters are coordinated to one SIMes NHC ligand and one oxygen atom of the trifluoroacetate ligand in a linear fashion, with C-Ag-O angles between 168.88° and 170.63°. The Ag-C bond distances are rather short (2.050 - 2.066 Å) compared to those of Ag-NHC complexes in the literature.[198c] The Ag-O bond distances between the terminal Ag atoms and the oxygen atoms of the trifluoroacetate ligands (2.085 - 2.107 Å) are also shorter than those in the $[Ag_2(\mu_2\text{-}O,O'\text{-}CF_3CO_2)_2]$ core (2.207 - 2.244 Å).

**4.2.3.2 Solid state structures of complexes 4.19, 4.20, 4.44 and 4.45**

Suitable X-ray diffraction quality crystals of complexes **4.19, 4.20, 4.44** and **4.45** were grown from $CH_2Cl_2$/hexane at 0 °C, and their molecular structures are shown in Figures 4.19, 4.20 and 4.21. The crystallographic details are summarized in Appendix 2, and selected bond lengths and angles are listed in Tables 4.10, 4.11 and 4.12. With the exception of the IAd complexes **4.45a** and **4.45b**, the Ag-C and Ag-O bond lengths of all the complexes are in the range of previously reported silver(I) NHC carboxylate complexes. No argentophilic interactions were observed in all the complexes.
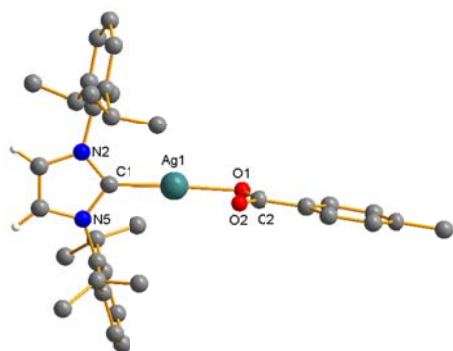
**4.19c**
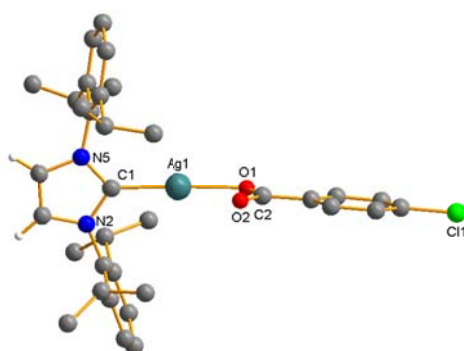
**4.19d**
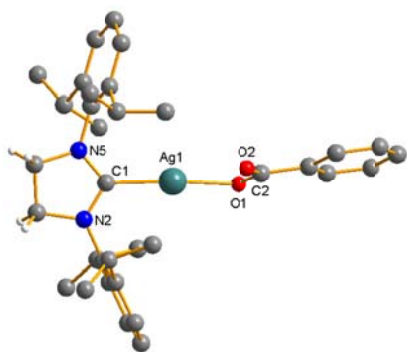
**4.20b**
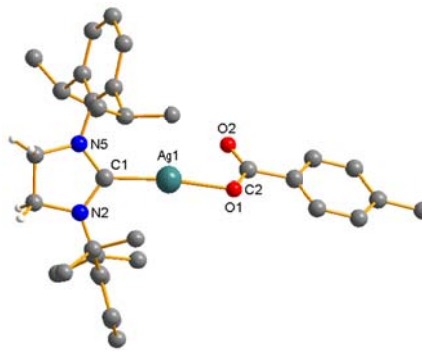
**4.20c**
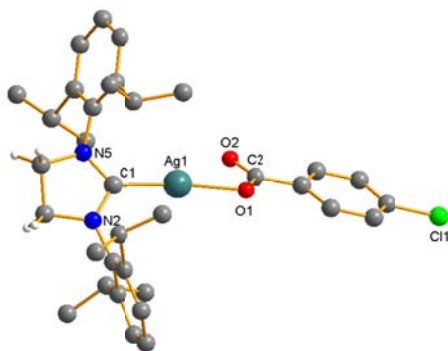
**4.20d**

**4.44a**

**4.44d**

**4.45a**

**4.45b**
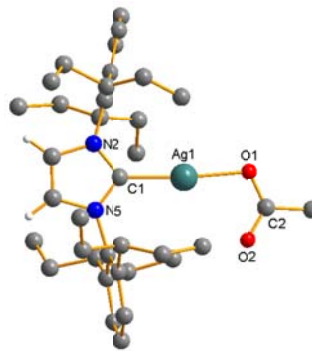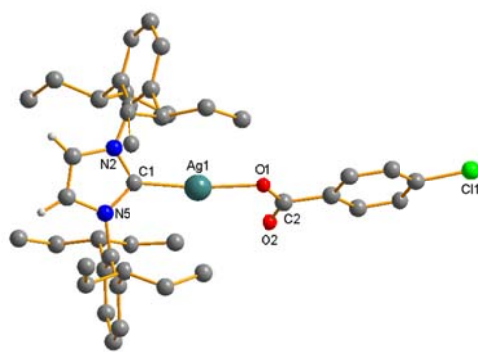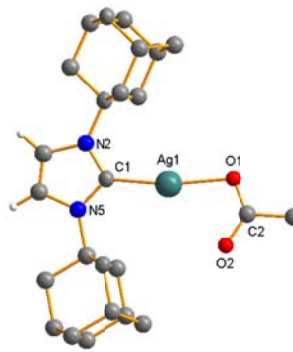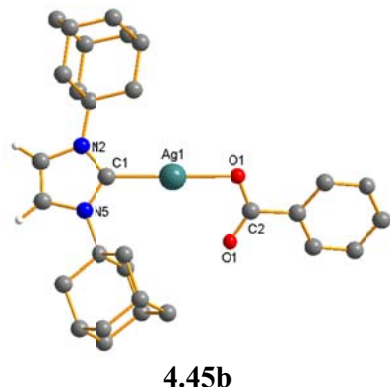
**Fig. 4.19.** Molecular structure of complexes **4.19c,d**, **4.20b-d**, **4.44a,d** and **4.45a,b**. Non-essential hydrogen atoms are omitted for clarity.

**Table 4.10.** Selected bond lengths (Å) and angles (deg) of complexes **4.19c,d**, **4.20b-d**, **4.44a,d** and **4.45a,b**

|        | Ag1-C1    | Ag1-O1    | C1-Ag1-O1  | C2-O1     | C2-O2     | % covalent character[a] |
|--------|-----------|-----------|------------|-----------|-----------|-------------------------|
| **4.19c** | 2.063(3)  | 2.114(2)  | 175.51(8)  | 1.268(3)  | 1.225(4)  | 22 |
| **4.19d** | 2.059(3)  | 2.121(2)  | 175.26(9)  | 1.263(3)  | 1.229(4)  | 16 |
| **4.20b** | 2.069(3)  | 2.131(2)  | 170.2(1)   | 1.277(5)  | 1.234(5)  | 32 |
| **4.20c** | 2.060(3)  | 2.101(2)  | 171.83(9)  | 1.253(3)  | 1.222(3)  | 4 |
| **4.20d** | 2.059(2)  | 2.101(2)  | 171.85(9)  | 1.267(3)  | 1.227(3)  | 21 |
| **4.44a** | 2.067(3)  | 2.111(2)  | 174.5(1)   | 1.269(4)  | 1.217(5)  | 23 |
| **4.44d** | 2.064(3)  | 2.100(2)  | 165.7(1)   | 1.255(4)  | 1.223(4)  | 7 |
| **4.45a** | 2.075(4)  | 2.117(2)  | 170.1(1)   | 1.254(4)  | 1.234(4)  | 5 |
| **4.45b** | 2.103(3)  | 2.123(2)  | 175.2(1)   | 1.269(4)  | 1.231(4)  | 23 |

[a]Calculated using the formula: $\{640(C2\text{-}O1) - 800\}/\{2.4(C2\text{-}O1) - 2.5264\}$

Differences in Ag-C bond lengths are observable between complexes bearing the same carboxylate ligand but different NHC ligands. The Ag-C bond length generally increases in the order: SIPr < IPr < IPent < IAd, and the differences are most prominent when comparing acetate complexes **4.19a**, **4.20a**, **4.44a** and **4.45a**. In this case the Ag-C bond length appears to reflect the strength of the Ag-C bond and hence the electron-donating ability of the NHC, thus allowing us to infer that the donating abilities of the NHC ligands decrease in

the order: SIPr > IPr > IPent > IAd, which is in agreement with that previously deduced from $^{13}$C NMR data.

The Ag-O bond lengths do not correlate with the basicity of the carboxylate ligands and the steric size of the NHC ligand. The differences in Ag-O bond lengths between the complexes do not appear to reflect the *trans* influence of the NHC ligands. Nevertheless, the length of Ag-C and Ag-O bonds can provide clues about the stability of these complexes. The Ag-C and Ag-O bond lengths of the IAd complexes **4.45a** and **4.45b** are significantly longer than those the other complexes, further corroborating their instability in solution. Complex **4.18** (see Fig. 4.3) which also has relatively long Ag-C and Ag-O bond lengths of 2.084(6) Å and 2.196(5) Å respectively, exhibits the same instability in solution.[189]

The percentage covalent character of the Ag-O bond was estimated on the basis of the theory by Hocking and Hambley.[212, 213] However, contrary to our expectations, the covalency of the Ag-O bond was found to correlate poorly to the Ag-O bond length, suggesting that other factors, such as crystal packing effects or the different steric parameters of the NHC ligands might affect the Ag-O bond length.
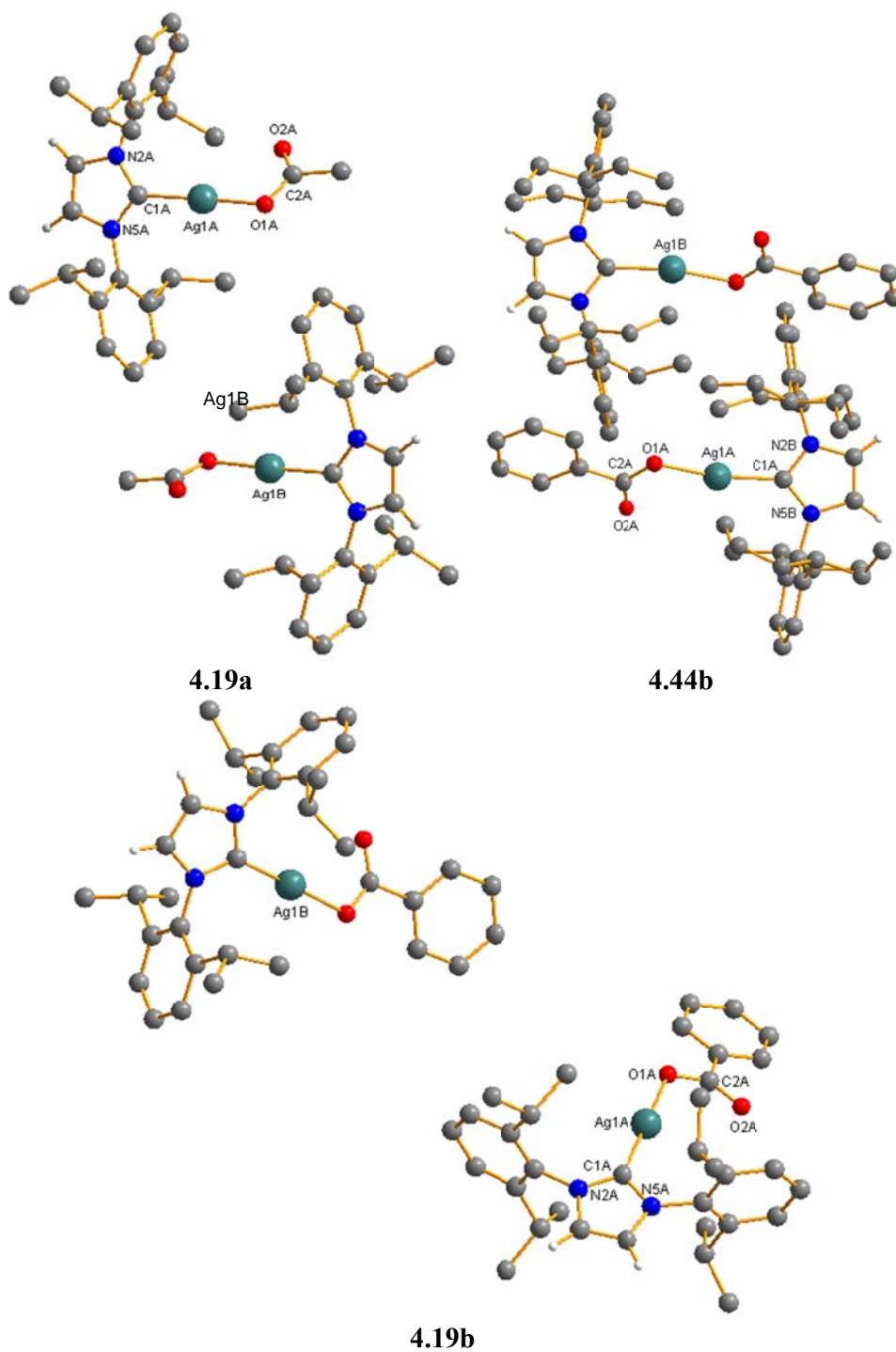
**4.19a**                                        **4.44b**



**4.19b**

**Fig. 4.20.** Molecular structures of complexes **4.19a**, **4.19b** and **4.44b**, showing two molecules in the asymmetric unit. Non-essential hydrogen atoms have been omitted for clarity.

**Table 4.11.** Selected bond lengths (Å) and angles (deg) of complexes **4.19a**, **4.19b** and **4.44b**, which have two molecules in the asymmetric unit.

|                                  | 4.19a     | 4.19b      | 4.44b    |
| -------------------------------- | --------- | ---------- | -------- |
| Ag(1A)-C(1A)                     | 2.064(4)  | 2.071(2)   | 2.059(3) |
| Ag(1A)-O(1A)                     | 2.112(3)  | 2.098(2)   | 2.100(3) |
| O(1A)-Ag(1A)-O(2A)               | 176.8(1)  | 174.85(7)  | 164.0(1) |
| C(2A)-O(1A)                      | 1.257(6)  | 1.273(3)   | 1.243(6) |
| C(2A)-O(2A)                      | 1.230(7)  | 1.233(2)   | 1.209(5) |
| Ag(1B)-C(1B)                     | 2.064(5)  | 2.059(2)   | 2.069(3) |
| Ag(1B)-O(1B)                     | 2.113(3)  | 2.094(2)   | 2.089(3) |
| O(1B)-Ag(1B)-O(2B)               | 177.6(2)  | 177.80(7)  | 166.2(1) |
| C(2B)-O(1B)                      | 1.253(6)  | 1.252(3)   | 1.264(6) |
| C(2B)-O(2B)                      | 1.227(7)  | 1.226(2)   | 1.219(4) |
| % covalent character[a]          | 7         | 16         | 4        |

[a]Calculated using the formula: $\{640(C2\text{-}O1) - 800\}/\{2.4(C2\text{-}O1) - 2.5264\}$, and averaged for the two molecules in the asymmetric unit.
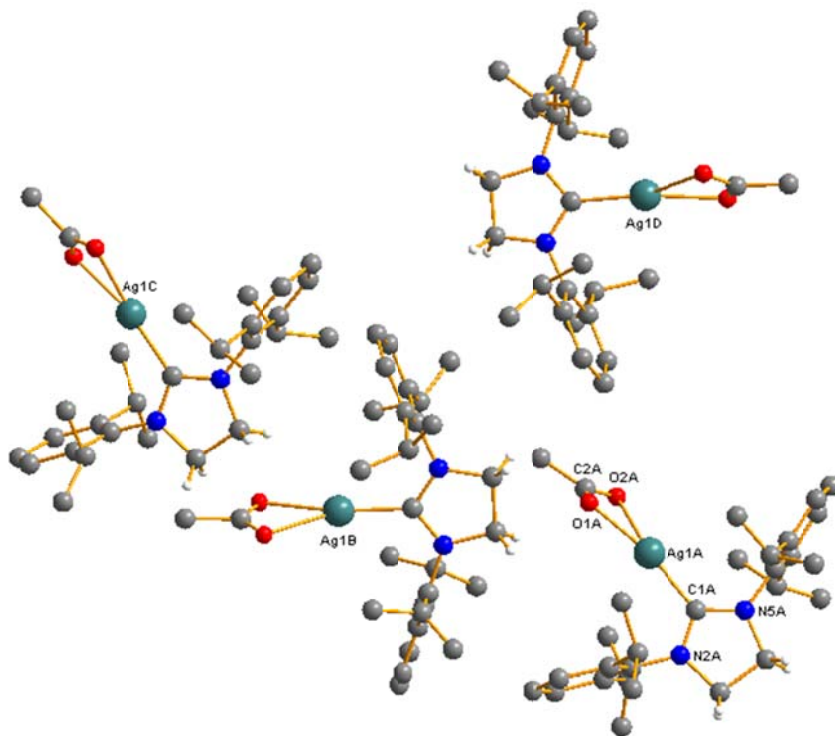


**Fig. 4.21.** Solid state structure of $(SIPr)Ag(O_2CCH_3)$ (**4.20a**) showing four molecules in the asymmetric unit. Non-essential hydrogen atoms have been omitted for clarity.

Complex **4.20a** is unique as it is the only complex where the carboxylate ligand exhibits an asymmetric chelating mode. It consists of 4 distinct molecules in the asymmetric unit (Fig. 4.21) that show only slight differences in their bond lengths and angles (Table 4.12). The Ag1-C1 bond lengths fall

191

within the range of previously reported isostructural complexes (see Table A1 of Appendix 1). However, unlike the previously reported complexes, the difference between the Ag1-O1 and Ag1-O2 bond lengths is smaller and the C2-O1 bond lengths are also smaller than 1.2505 Å, indicating a largely ionic interaction between the carboxylate ligand and Ag(I) in the complex.[212, 213] It is also worthy of note that the Ag-O distances in **4.20a** are the longest in our series of synthesized complexes.

**Table 4.12.** Selected bond lengths (Å) and angles (deg) of complex **4.20a**

| Ag(1A)-C(1A) | 2.059(7) | Ag(1C)-C(1C) | 2.058(7) |
|---|---|---|---|
| Ag(1A)-O(1A) | 2.151(6) | Ag(1C)-O(1C) | 2.326(7) |
| Ag(1A)-O(2A) | 2.590(8) | Ag(1C)-O(2C) | 2.420(7) |
| C(2A)-O(1A) | 1.18(1) | C(2C)-O(1C) | 1.22(1) |
| C(2A)-O(2A) | 1.24(1) | C(2C)-O(2C) | 1.18(1) |
| O(1A)-Ag(1A)-O(2A) | 52.4(3) | O(1C)-Ag(1C)-O(2C) | 52.5(3) |
| Ag(1B)-C(1B) | 2.060(7) | Ag(1D)-C(1D) | 2.059(7) |
| Ag(1B)-O(1B) | 2.338(7) | Ag(1D)-O(1D) | 2.300(7) |
| Ag(1B)-O(2B) | 2.415(8) | Ag(1D)-O(2D) | 2.445(6) |
| C(2B)-O(1B) | 1.24(1) | C(2D)-O(1D) | 1.25(1) |
| C(2B)-O(2B) | 1.23(1) | C(2D)-O(2D) | 1.24(1) |
| O(1B)-Ag(1B)-O(2B) | 54.1(3) | O(1D)-Ag(1D)-O(2D) | 54.6(2) |

**Table 4.13.** Steric Parameter (%$V_{bur}$) Calculated for NHCs of complexes **4.19**, **4.20**, **4.44** and **4.45**

| Complex | %$V_{bur}$[a] | %$V_{bur}$[b] |
|---|---|---|
| [(IPr)AgOAc] (**4.19a**)[c] | 43.0, 45.8 | 41.7, 44.6 |
| [(IPr)AgOBz] (**4.19b**)[c] | 45.0, 47.2 | 43.6, 46.1 |
| [(IPr)Ag(4-MeC$_6$H$_4$CO$_2$)] (**4.19c**) | 42.7 | 41.5 |
| [(IPr)Ag(4-ClC$_6$H$_4$CO$_2$)] (**4.19d**) | 42.6 | 41.5 |
| [(IPr)AgCl] | 46.5 | – |
| [(SIPr)AgOAc] (**4.20a**)[c] | 46.0 – 47.5 | 45.1 – 46.3 |
| [(SIPr)AgOBz] (**4.20b**) | 47.2 | 45.9 |
| [(SIPr)Ag(4-MeC$_6$H$_4$CO$_2$)] (**4.20c**) | 44.6 | 43.4 |
| [(SIPr)Ag(4-ClC$_6$H$_4$CO$_2$)] (**4.20d**) | 44.5 | 43.4 |
| [(SIPr)AgCl] | 45.5 | – |
| [(IPent)AgOAc] (**4.44a**) | 49.6 | 48.5 |
| [(IPent)AgOBz] (**4.44b**)[c] | 50.3, 53.0 | 49.1, 52.1 |
| [(IPent)Ag(4-ClC$_6$H$_4$CO$_2$)] (**4.44d**) | 54.6 | 53.6 |
| [(IAd)AgOAc] (**4.45a**) | 40.5 | 39.3 |

| | | |
|---|---|---|
| [(IAd)AgOBz] (**4.45b**) | 38.5 | 37.0 |
| [(IAd)AgCl] | 40.2 | – |

To evaluate the steric environment of the NHC ligands around the metal center, the percentage buried volume (%$V_{bur}$) of the complexes was calculated using Samb*V*ca.[210] Using Ag-C bond lengths obtained from crystallographic data, the calculated %$V_{bur}$ of the complexes range from 37.0 to 53.6% (Table 4.13). IPent is the bulkiest ligand in the series, followed by SIPr, IPr and IAd. However, in the analogous silver(I) chloride complexes, IPr is only marginally larger than SIPr.[208] The trend could be reversed in this case because of the torsion and greater rigidity in the saturated NHC backbone of SIPr, which increases the proximity of the aromatic rings to silver. The fact that the %$V_{bur}$ values of the IPr complexes fall within a larger range (41.5 - 46.1) compared to SIPr (43.4 - 46.3) supports this.

Only small differences between %$V_{bur}$ values of complexes with the same NHC ligand but different carboxylate ligands are observed. This is because alkyl and aryl substituents on the carboxylate ligands reside away from the immediate coordination environment of silver, and hence can be considered to exhibit a similar steric profile. The differences in %$V_{bur}$ values can be attributed to differences in Ag-C bond length, or simply, to crystal packing effects in the solid state. It is also important to note that the %$V_{bur}$ values are calculated from solid state structures and might not be an accurate representation of the coordination environment of the Ag atom in solution.

Nonetheless, the range of $\%V_{bur}$ values observed reflect the ability of these ligands to adapt to the ancillary ligand environment by rearrangement of the *N*-aryl substituents. The bulkiest ligand in the series, IPent, seems particularly apt at this, as the range of $\%V_{bur}$ values observed for its complexes span 5.1 units, from 48.5 to 53.6. This bulky yet flexible property of the IPent ligand has implications in the catalytic activity of the resulting silver complexes, which will be discussed in the following section.


## 4.3 Catalysis

The catalytic properties of complexes **4.19a,b**, **4.20a-c**, **4.44a,d** and **4.45a,b** for the cycloisomerization of propargyl amides was investigated. Hashmi *et al.* have previously reported the application of cationic Au(I) NHC complexes,[155] [(NHC)Au]OTs, in the cycloisomerization of non-terminal propargyl amides. Varying the substituents on both the N atoms and backbone of the NHC did not affect the efficiency of the resulting catalyst, which was instead greatly affected by the solvent of the reaction. Quantitative conversions could be obtained in THF in most cases. In contrast, the Au(I) triphenylphosphine complex, [(Ph$_3$P)Au]OTs resulted in a lower conversion of 92% under identical reaction conditions.


The conversion of the model substrate **3.1a** to the oxazoline **3.2a** was monitored *in situ* by $^1$H NMR spectroscopy over 10 h in the presence of 10 mol% of the Ag(I) NHC carboxylate complexes at room temperature (23 °C). The results are shown in Scheme 4.5. The conversions recorded after 24 h are

shown in Table 4.14, where the results obtained with other silver complexes

are also produced for comparison.

**Scheme 4.5.** Comparison of the catalytic activity of complexes **4.19a,b**, **4.20a-c**, **4.44a,d** and **4.45a,b** for the cycloisomerization of **3.1a**
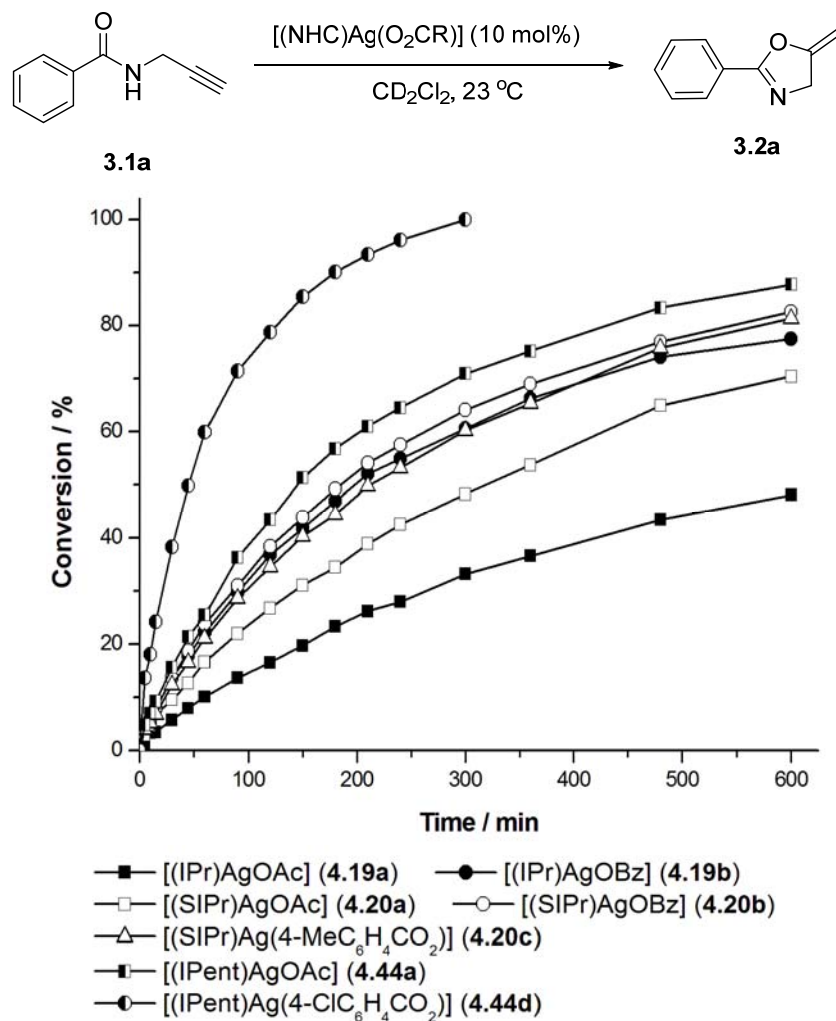


Effective catalysis was only observed with complexes containing both NHC

and carboxylate ligands (entries 1-5 vs 11-14). The efficiency of the catalyst is

clearly affected by both the NHC ligand and the carboxylate co-ligand. The

reaction rate increased in the order IPr < SIPr < IPent, which is most evident

when comparing acetate complexes **4.19a**, **4.20a** and **4.44a**. There also

appears to be a correlation of the reaction rate with the basicity of the carboxylate ligands. Carboxylate ligands with lower basicity display a faster reaction rate, as shown by the increase in reaction rate as the carboxylate ligand is varied from acetate to 4-methylbenzoate to benzoate in the SIPr complexes **4.20a-c**. The dramatic increase in reaction rate observed with complex **4.44d**, which has an IPent ligand and the least basic 4-chlorobenzoate co-ligand, also supports this. In this particular case, complete conversion of substrate **3.1a** to the product was observed within 6 h. In contrast, the IAd complexes **4.45a** and **4.45b** did not give any conversions due to catalyst decomposition. The corresponding SIMes and IPr chloride and cationic *bis*(NHC) complexes as well as the silver carboxylate salts were also inactive, emphasizing the importance of both the NHC and carboxylate ligands for catalytic activity.

**Table 4.14.** Catalyst screening for the cycloisomerization of **3.1a**

| Entry | Catalyst | Time | Conversion |
|---|---|---|---|
| 1 | [(IPr)AgOAc] (**4.19a**) | 24 h | 75 |
| 2 | [(IPr)AgOBz] (**4.19b**) | 24 h | 91 |
| 3 | [(SIPr)AgOAc] (**4.20a**) | 24 h | 85 |
| 4 | [(SIPr)AgOBz] (**4.20b**) | 24 h | 83 |
| 5 | [(SIPr)Ag(4-MeC$_6$H$_4$CO$_2$)] (**4.20c**) | 24 h | 93 |
| 6 | [(IPent)AgOAc] (**4.44a**) | 24 h | 93 |
| 7 | [(IPent)Ag(4-ClC$_6$H$_4$CO$_2$)] (**4.44d**) | 6 h | 100 |
| 8 | [(IAd)AgOAc] (**4.45a**) | 24 h | – |
| 9 | [(IAd)AgOBz] (**4.45b**) | 24 h | – |
| 10 | [(IPr)AgCl] | 24 h | – |
| 11 | [Ag(IPr)$_2$]PF$_6$ | 24 h | – |
| 12 | [(SIMes)AgCl] | 24 h | – |
| 13 | AgOAc | 24 h | – |
| 14 | Ag(4-ClC$_6$H$_4$CO$_2$) | 24 h | – |

Considering that the electronic properties of IPr, SIPr and IPent are very similar, the differences activity of the catalysts can be largely attributed to the steric properties of the NHC ligand. IPent[239,240] may be regarded as a member of the family of bulky NHCs with "flexible sterics". Due to the ability of such ligands to adjust their steric bulk to incoming substrates while enabling the stabilization of low-valent active catalytic intermediates, metal complexes containing these ligands have shown excellent catalytic activity.[241,242,243,244] The superior activity of complex **4.44d** could thus be either due to the ability of IPent to provide steric shielding of the reactive metal center, hence slowing or preventing catalyst decomposition. In fact, in the case of the IPr complexes **4.19a** and **4.19b**, the formation of the *bis*(NHC) complex $[Ag(IPr)_2]X$ as a result of ligand scrambling reactions was identified as one of the routes of catalyst deactivation. The steric bulk on IPent, however, makes this route of catalyst deactivation highly unfavourable.

The correlation of the basicity of the carboxylic acids with the reaction rate could also suggest the dissociation of the carboxylate ligand and an formation of an active cationic $[Ag(NHC)]^+$ catalytic species either by a dissociative or associative ligand exchange with the substrate. These ligand exchange process with the substrate would be more facile in the presence of carboxylate ligands with lower basicity, as they would form weaker bonds with silver. Once dissociated, these anions also afford stronger conjugate acids, which can facilitate the protodemetallation step. This, coupled with the steric pressure exerted by the *trans* IPent ligand, could account for excellent activity of complex **4.44d**.
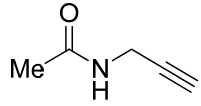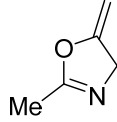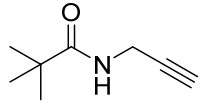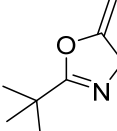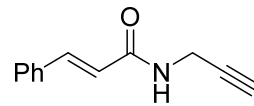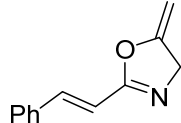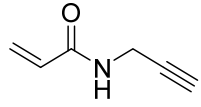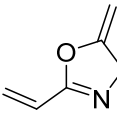
**Table 4.15.** Optimization of reaction conditions for catalyst **4.44d**
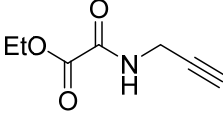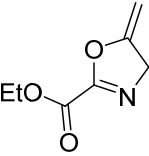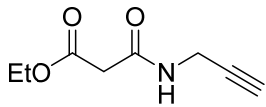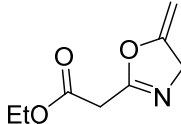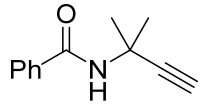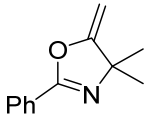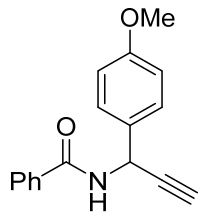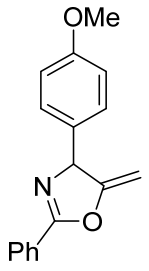
| Entry | Cat. loading | Solvent | Time | Conversion | Yield[a] |
|-------|-------------|---------|------|-----------|----------|
| 1 | 10 mol% | $CH_2Cl_2$ | 6 h | 100 | 95 |
| 2 | 5 mol% | $CH_2Cl_2$ | 18 h | 100 | 95 |
| 2 | 5 mol% | chloroform | 18 h | 100 | 93 |
| 3 | 5 mol% | THF | 18 h | 88 | 80 |
| 4 | 5 mol% | acetone | 18 h | 80 | 75 |
| 5 | 5 mol% | MeCN | 18 h | 89 | 81 |
| 6 | 5 mol% | $MeNO_2$ | 18 h | 100 | 82 |
| 7 | 5 mol% | MeOH | 18 h | 100 | 89 |

[a] Determined by $^1H$ NMR spectroscopy, using 1,3,5-trimethoxybenzene as internal standard.

Based on the preliminary results, complex **4.44d** was chosen as the best catalyst and the catalyst loading, solvent and reaction time were subsequently optimized. Complete conversion of substrate was also obtained on reduction of the catalyst loading from 10 mol% to 5mol%, albeit with a three-fold increase in reaction time form 6 h to 18 h. Moderate yields were obtained in both protic and aprotic solvents, although chlorinated solvents such as $CH_2Cl_2$ and chloroform were superior. Thus, $CH_2Cl_2$ was chosen as the solvent due to its lower boiling point and toxicity.

**Table 4.16.** Substrate Scope[a]

| Entry | Substrate | Cat. Loading | Time | Product | Conv. | Yield[b] |
|-------|-----------|--------------|------|---------|-------|----------|
| 1 | **3.1b** | 5 mol% | 18 h | **3.2b** | 100 | 90 |
| 2 | **3.1c** | 5 mol% | 18 h | **3.2c** | 100 | 99 |
| 3 | **3.1d** | 5 mol% | 18 h | **3.2d** | 100 | 80 |
| 4 | **3.1e** | 5 mol% | 18 h | **3.2e** | 100 | 71 |

| 5 | **3.1g** | 5 mol% | 18 h | **3.2g** | 48 | 37 |
| 6 | **3.1h** | 5 mol% | 18 h | **3.2h** | 100 | 92 |
| 7 | **3.1i** | 1 mol% | 15 min | **3.2i** | 100 | >99 |
| 8 | **3.1q** | 5 mol% | 24 h | **3.2q** | 83 | 26 |

| | | | | | | |
|---|---|---|---|---|---|---|
| 9 |  **3.1n** | 5 mol% | 24 h |  **3.2n** | 39 | 14 (E:Z = 1:2.5) |
| 10 |  **3.1j** | 5 mol% | 24 h |  **3.2j** | 67 | 65 |
| 11 |  **3.1k** | 5 mol% | 24 h |  **3.2k** | 100 | >99 |
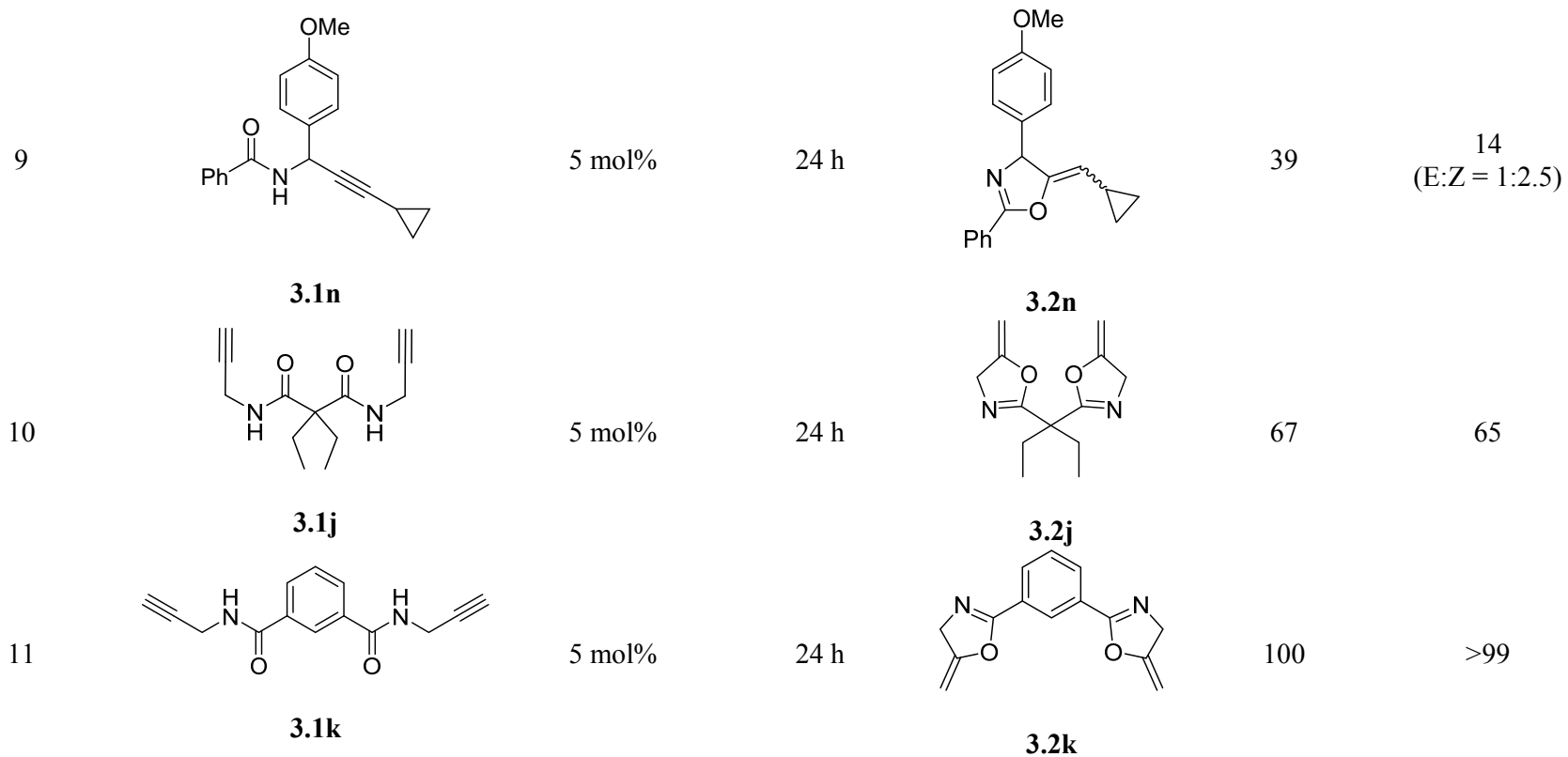
[a] Reaction conditions: substrate **3.1** (0.4 mmol), catalyst **4.45d** (1-5 mol%), CD$_2$Cl$_2$ (1 mL), 23 °C.
[b] Determined by ^{1}H NMR spectroscopy, using 1,3,5-trimethoxybenzene as internal standard.

With the optimized reaction conditions in hand, the cycloisomerization of several other propargyl amide substrates were carried out (Table 4.16). The results showed that complex **4.44d** is highly complementary to the substrate scope of [Ag(MeO-Py)$_2$]PF$_6$ (**2.11d**) described in the previous Chapter. At 5 mol% catalytic loading, a wider range of substituents were tolerated at the amide. For example, the double cyclization of substrate **3.1k** proceeded smoothly to afford the double cycloisomerized product **3.2k** in quantitative yield (entry 11). In contrast, only 45% yield was obtained with 10 mol% of [Ag(MeO-Py)$_2$]PF$_6$ as catalyst. Substrates **3.1e** and **3.1g**, which only resulted in catalyst decomposition when [Ag(MeO-Py)$_2$]PF$_6$ was employed, could be successfully transformed into the corresponding products in 71% and 37% yields respectively using **4.44d** as catalyst (entries 3 and 5). However, with substrate **3.1k**, which also has two propargyl amide groups linked by a one carbon atom spacer, gave an incomplete conversion (entry 10), possibly due to its ability to form a chelate with the catalyst via the two carbonyl oxygen atoms, thus deactivating it. Notably, only small substituents at the propargylic position are tolerated, as substrate **3.1i** cyclized quickly compared to substrates **3.1q** and **3.1n**. The larger *p*-methoxybenzyl substituent in these substrates could hinder the approach of the catalyst (bearing the large IPent ligand) to the alkyne, resulting in slower reaction rates. For the non-terminal alkyne substrate **3.1n**, a mixture of *E/Z*-double bond isomers was obtained.

In light of experimental observations, a plausible mechanism shown in Scheme 4.6 is proposed. The active cationic silver species [(NHC)Ag]$^+$ is first generated either by associative or dissociative ligand exchange with the

substrate. Activation of the alkyne substrate upon coordination to silver occurs, followed by nucleophilic attack by the carbonyl oxygen atom of the amide. Protodemetallation of the resulting vinyl silver intermediate affords the oxazoline product and regenerates the catalyst. The *anti*-addition of the oxygen nucleophile to the π-coordinated alkyne, followed by a stereospecific protodemetallation step proposed in our mechanism would only result in the formation of the *Z*-alkene product with non-terminal alkyne substrates ($R^4 \neq$ H). However, a mixture of *E* and *Z* isomers were obtained with substrate **3.1n**. Further investigations are needed to determine if this is the result of isomerization of the vinyl silver intermediate or the final oxazoline product.
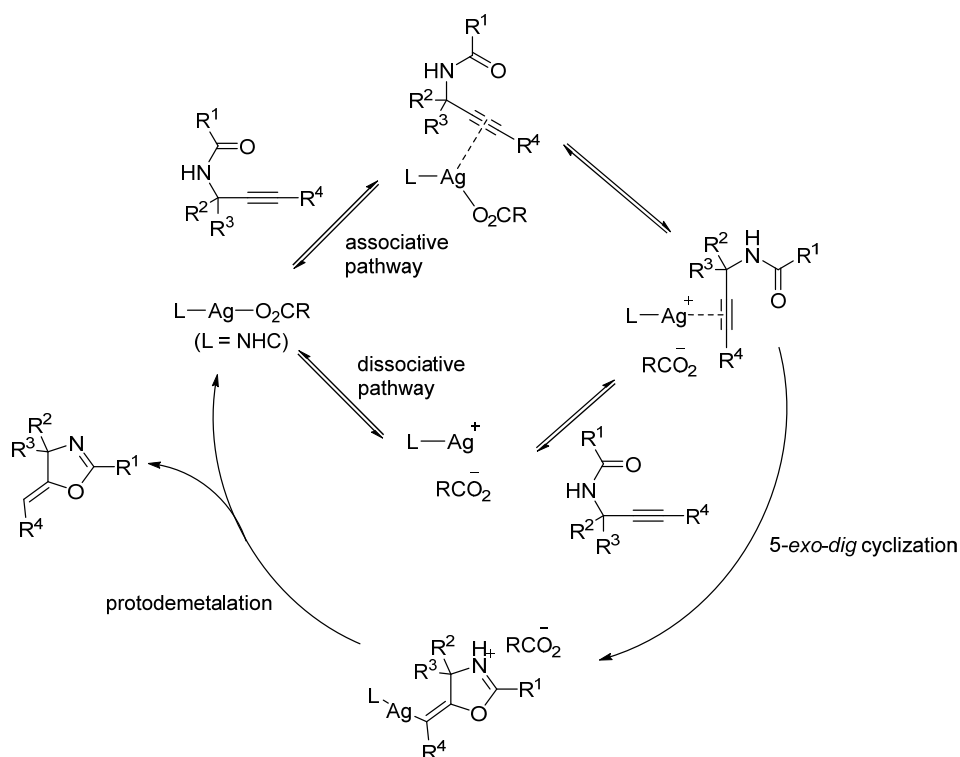


**Scheme 4.6.** Proposed Mechanism

## 4.5 Conclusion

The review of the structural features and $^{13}$C NMR spectroscopic properties of silver(I) NHC carboxylate complexes in the beginning of this chapter shows that there is a strong preference for two-coordinate linear geometry, although electron-withdrawing groups on the NHC can increase the tendency for the carboxylate to bind in a bidentate manner. Argentophilic interactions also cause deviations from the ideal linear geometry in the solid state. A comparison of the carbene $^{13}$C NMR resonance of the analogous halide complexes confirmed our hypothesis that carboxylate ligands are weaker donors compared to halides. All the complexes except those with NHCs that have large substituents on nitrogen show a lack of coupling of the carbene carbon with $^{107,109}$Ag in their $^{13}$C NMR spectra, an indication of their fluxional behavior in solution. Lastly, no direct correlation of Ag-C bond length and $^{13}$C NMR chemical shift values of the carbene carbon with electronic differences between the NHC ligands was observed.

We have also reported the synthesis and structural characterization of a series of silver(I) carboxylate complexes supported by NHC ligands by a new route involving the deprotonation of the HBF$_4$ salt of the NHC precursors with K$_2$CO$_3$ in the presence of silver carboxylates. The complexes proved to be highly active in the cycloisomerization of propargyl amides, with a substrate scope complementary to that of the *bis*(4-methoxypyridine) silver(I) hexafluorophosphate complex (**2.11d**) described in the previous chapter. Large but flexible NHC ligands such as IPent, and carboxylate co-ligands on silver(I) with lower basicity improve catalyst efficiency. A plausible mechanism for the

reaction is also proposed, but further investigation is needed to confirm the

identity of the active catalytic species and the rate-limiting step of the reaction.

# Chapter 5 Conclusion and Future Work

## 5.1 Conclusion

This thesis describes the development of Ag(I) catalysts for intramolecular N−H and (formal) O−H addition to alkynes, allowing the preparation of *N,O*-heterocycles. Two examples of such reactions, namely, the hydroamination of trichloroacetimidates, and the cycloisomerization of propargyl amides were explored (Scheme 5.1).
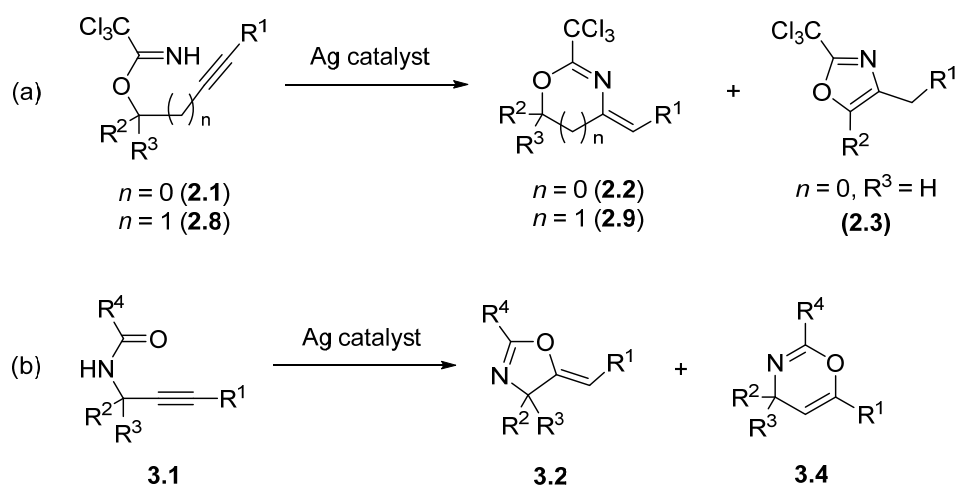


**Scheme 5.1.** (a) Hydroamination of trichloroacetimidates (b) Cycloisomerization of propargyl amides.

Initial experiments using silver salts showed that they were active catalysts for these reactions, although only moderate yields could be obtained. The reactivity was also highly dependent on the counteranion and solvent employed (Table 5.1, entries 1 and 2). The use of AgTFA in MeCN at room temperature afforded the methylene oxazoline product **2.2a** exclusively, while changing the counteranion to triflate and the solvent to DCE resulted in a

selectivity switch towards the oxazole product **2.3a**. In the cycloisomerization of the propargyl amide substrate **3.1a**, AgTFA again proved to be the best catalyst, furnishing the methylene oxazoline product **3.2a** as the sole product in 60% yield (entry 3).

Further studies on ligand effects revealed that *bis*(pyridine) silver(I) complexes showed enhanced catalytic activities with a broad substrate scope. In the case of the cyclization of the (homo)propargyl trichloroacetimidates **2.1** and **2.8**, excellent yields of the methylene oxazoline and oxazine products, **2.2** and **2.9** respectively, were obtained when $R^1$ = H (entries 4 and 5). The internal alkyne substrates ($R^1$ = Ph, TMS) also cyclized smoothly, albeit under harsher reaction conditions and an increase in catalytic loading (entries 6 and 7). Similarly, the cyclization of the propargyl amide substrates **3.1** proceeded with complete regioselectivity towards the methylene oxazoline product **3.2** when $R^1$ = H (entry 8). With the internal alkyne substrates where $R^1$ = alkyl, however, a mixture of both the *E*- and *Z*- isomers of **3.2** were obtained; and when $R^1$ = TMS, a change in regioselectivity towards the oxazine **3.4** was observed (entry 9).

The success of the *bis*(pyridine) silver(I) complexes is evident from the fact that they form the first examples of Ag-catalysts that can achieve comparable yields to that achieved with gold catalysts in these reactions. They also present an added economic advantage as they can be prepared easily in good yields from silver salts and pyridine ligands, which are cheaper than gold salts.

**Table 5.1.** Comparison of the reactivity of silver catalysts in the cycloisomerization of propargyl amides

| | Cat. (Loading) | Reaction Conditions | Substrate | R$^1$ | R$^2$ | R$^3$ | R$^4$ | Product (Yield)[a] |
|---|---|---|---|---|---|---|---|---|
| 1 | AgTFA (10 mol%) | MeCN, 23 °C, 6 h | **2.1a** | H | H | H | – | **2.2a** (76%) |
| 2 | AgOTf (10 mol%) | DCE, 23 °C, 6 h | **2.1a** | H | H | H | – | **2.3a** (46%) |
| 3 | AgTFA (10 mol%) | CH$_2$Cl$_2$, 23 °C, 6 h | **3.1a** | H | H | H | Ph | **3.2a** (60%) |
| 4 | [Ag(Py)$_2$]OTf (**2.5a**) (10 mol%) | acetone, 23 °C, 6 h | **2.1** | H | alkyl | H | – | **2.2** (67-86%[b]) |
| 5 | [Ag(Py)$_2$]OTf (**2.5a**) (10 mol%) | acetone, 23 °C, 6 h | **2.8** | H | alkyl, aryl | H | – | **2.9** (70-93%[b]) |
| 6 | [Ag(Py)$_2$]OTf (**2.5a**) (10 mol%) | MeCN, 60 °C, 7 h | **2.1** | Ph, TMS | H | H | – | **2.2** (R$^1$ = Ph, 29%; R$^1$ = TMS, 72%[b]) |
| 7 | [Ag(Py)$_2$]OTf (**2.5a**) (10-20 mol%) | acetone, reflux, 7 - 8 h | **2.8** | Ph, TMS | H | H | – | **2.9** (R$^1$ = Ph, 31%; R$^1$ = TMS, 71%[b]) |
| 8 | [Ag(MeO-Py)$_2$]PF$_6$ (**2.11d**) (1-10 mol%) | CH$_2$Cl$_2$, 23 °C, 30 min - 24 h | **3.1** | H | Me, PMP | H | alkyl, aryl | **3.2** (10%-quant.) |
| 9 | [Ag(MeO-Py)$_2$]PF$_6$ (**2.11d**) (10-15 mol%) | CH$_2$Cl$_2$, 23 °C, 10-24 h | **3.1** | H | PMP | H | alkyl, Ph, TMS | **3.2** (R$^1$ = alkyl, Ph, 74-96%) **3.4** (R$^1$ = TMS, 76%) |
| 10 | [(IPent)Ag(4-ClC$_6$H$_4$CO$_2$) (**4.44d**) (5 mol%) | CD$_2$Cl$_2$, 23 °C, 18 h | **3.1** | H | H | H | alkyl, aryl | **3.2** (37% to quant.) |

[a] NMR yields, calculated using 1,3,5-trimethoxybenzene as internal standard, unless otherwise stated. [b] Isolated yields.

Encouraged by the positive ligand effects on the catalytic activity, the catalytic activity of silver(I) *N*-heterocyclic carbene (NHC) carboxylate complexes towards the cyclization of the propargyl amide substrates **3.1** was also investigated (entry 10). Interestingly, complementary reactivity was observed compared to the *bis*(pyridine) Ag(I) catalyst. Substrates that reacted poorly with the *bis*(pyridine) Ag(I) catalyst, such as those with electron-poor $R^4$ substituents, underwent smooth cyclization with the Ag(I) NHC catalyst in good yields. In contrast, substrates with propargyl substituents ($R^2$ and $R^3$) that cyclized easily with the *bis*(pyridine) Ag(I) catalyst reacted sluggishly in the presence of the Ag(I) NHC catalyst.
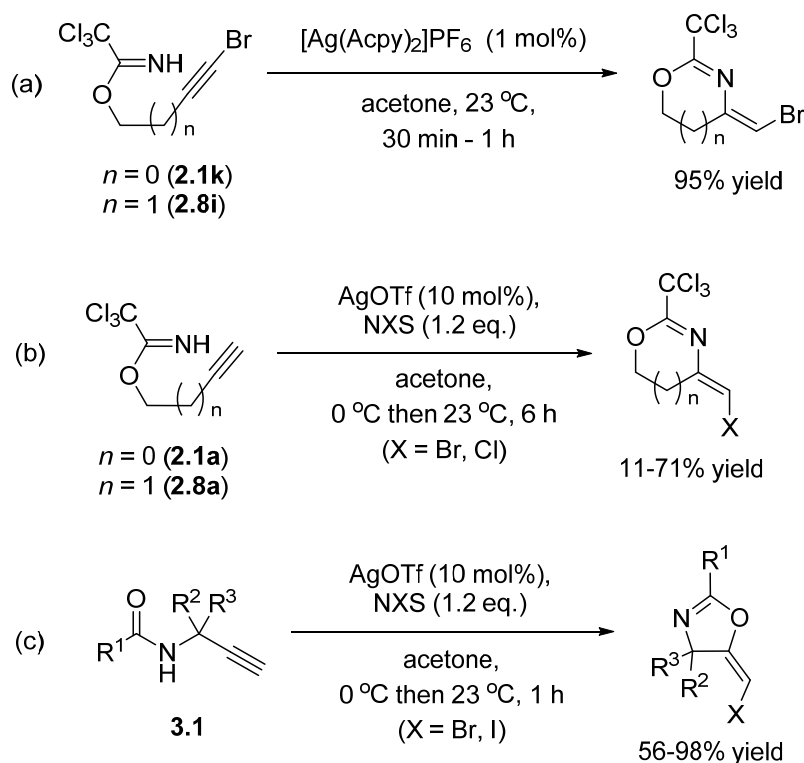


**Scheme 5.2.** Synthesis of halomethylene oxazolines

The scope of these reactions has also been extended to the synthesis of halomethylene oxazolines. These reactions occur in a highly stereospecific manner, yielding either the *Z*-isomer (Scheme 5.2a) or the *E*-isomer (Scheme 5.2b and c) exclusively.

## 5.2 Future Work

Future work will include exploring the potential of the *bis*(pyridine) Ag(I) complexes and Ag(I) NHC carboxylate complexes developed in this work in more challenging transformations, such as in intermolecular hydroamination of alkenes. The ability of AgOTf to catalyze the hydroamination of alkenes with sulfonamides and *p*-nitroaniline has been reported,[245] albeit in lower yields and a limited substrate scope compared to gold catalysts. It would be thus interesting to explore if possibility that the addition of suitable ligands to Ag would allow an improvement in the efficiency of the Ag catalyst.

Experiments to provide evidence for the proposed mechanisms for the N-H and O-H addition examined in this work should be performed, which will provide a better understanding of the role of the pyridine ligands in the mechanism, and the observed regioselectivity and diastereoselectivity of the reaction. This will also offer fundamental insight to the unique catalytic activity of silver compared to gold, as well the complementary activity observed between pyridyl and NHC ligands.
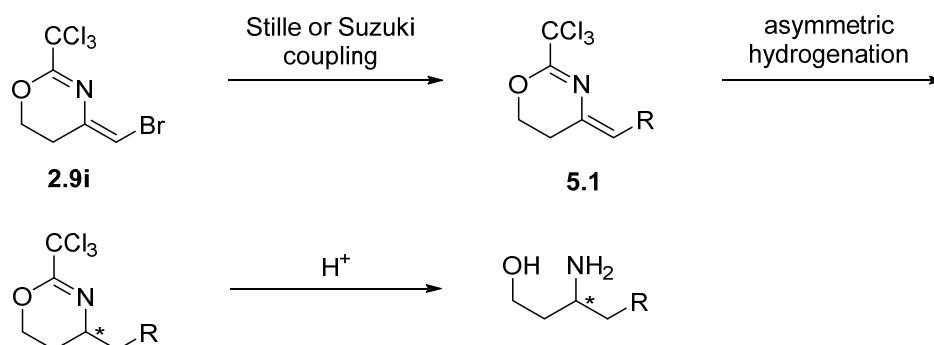
**Scheme 5.3.** Proposed synthetic route to 1,3-diamino alcohols from the 4-bromomethylene oxazine **2.9i**

Lastly, further functionalization of the bromo and iodomethylene oxazoline products shown in Scheme 5.3 can be carried out. For instance, cross-coupling reactions of the vinyl halide moiety in compound **2.9i** via Suzuki and Stille reactions can be explored. This provides an alternative synthetic route to 4-benzylidene oxazines (R = aryl) (**5.1**), as the cyclization of the phenyl substituted internal alkyne substrate in the presence of the *bis*(pyridiyl) Ag(I) catalyst only afforded low yields. Asymmetric hydrogenation of the alkene in **5.1**, followed by the hydrolysis of the trichloroactimidate moiety may then provide chiral 1,3-amino alcohols, which are not only commonly found in natural products and pharmaceuticals[246] but also are useful synthons for organic syntheses.[247]

# Chapter 6 Experimental

Materials were obtained from commercial suppliers and used without purification. We are grateful to Prof. Steven P. Nolan (University of St Andrews) for the gift of the imidazolium salts, IAd·HBF$_4$ and IPent·HBF$_4$. Unless otherwise stated, all reactions were carried out in air and using technical solvents. Solvents were dried by passing through the columns of molecular sieves in a solvent purification system (Innovative Technology Inc.). All reactions involving air-sensitive reagents were performed using standard Schlenk techniques and oven dried glassware. All reactions involving silver compounds were performed in the dark by covering the reaction vessels with aluminum foil. Catalytic reactions were carried out in Radley tubes in a Radley's 12-place reaction carousel, or in screw-cap vials. Column chromatography was performed on silica gel (Kieselgel 60) or neutral alumina**.** Preparative TLC was performed on 20cm × 20 cm glass plates with a 1.5 mm thick layer of silica gel 60 F$_{254}$ (Analtech).

Unless otherwise stated, $^1$H, $^{13}$C, $^{31}$P and $^{19}$F spectra were recorded at 25 °C on Bruker Avance™ spectrometers operating at 400 MHz, 101 MHz, 162 MHz and 376 MHz respectively. Residual protic solvents were used as an internal standard and $^{13}$C resonances were referenced to the deuterated carbon. Chemical shifts (δ) are reported in ppm, and $J$ values in Hz. Multiplicity is abbreviated to s (singlet), br s (broad singlet), d (doublet), t (triplet), q (quartet), sept (septet), and multiplet (m). Where required, 2D NMR (COSY, DEPT, NOESY and HMQC) experiments were used to distinguish and assign
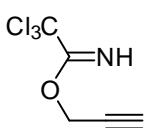
$^{1}$H and $^{13}$C peaks. Infrared spectra were recorded using a Perkin Elmer 100 series FT-IR spectrometer, equipped with an ATR accessory. Melting points were recorded using an Electrothermal Gallenhamp apparatus, and were uncorrected. Single crystal X-ray diffraction was performed by Dr. Andrew J. P. White (Imperial College London) using an Agilent Xcalibur diffractometer. Mass spectra (MS) were recorded by the Mass Spectrometry Service (Dr. Lisa Haigh) at Imperial College London on Micromass Autospec Premier, Micromass LCT Premier, or VG Platform II spectrometers using EI, CI or ESI techniques. Elemental analyses were performed by the Analytical Services at London Metropolitan University.

## 6.1 Compounds used in Chapter 2

**General procedure for the synthesis of the propargylic trichloroacetimidates (2.1a-j) (Procedure A):**
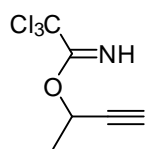
A solution of propargylic alcohol (1.0 eq.) and trichloroacetonitrile (1.2 eq.) in $CH_2Cl_2$ (2.5 mL per mmol of propargylic alcohol) was cooled to 0 °C in an ice bath and DBU (0.1 eq.) was added dropwise. The reaction mixture was allowed to stir at 0 °C (for $t_1$ min), then warmed to room temperature and stirred (for another $t_2$ min). The solvent was removed *in vacuo*, and the residue was purified by column chromatography on silica gel.

**Prop-2-ynyl 2,2,2-trichloroacetimidate (2.1a).**[129]

$t_1 = 60$, $t_2 = 30$. Prepared from propargyl alcohol (1.16 mL, 20 mmol) by procedure A, obtained as a colorless oil after purification by column chromatography (petroleum ether/ethyl acetate, 8:1).

Yield: 3.11 g (78%). $^1$H NMR (CDCl$_3$): δ = 8.50 (br s, 1H, N$H$), 4.91 (d, $J$ = 2.4, 2H, C$H_2$), 2.55 (t, $J$ = 2.4, 1H, ≡C$H$). $^{13}$C NMR (CDCl$_3$): δ = 161.8 ($C$=NH), 90.7 ($C$Cl$_3$), 77.1 ($C$≡CH), 75.1 (C≡$C$H), 56.6 ($C$H$_2$). MS [CI]: $m/z$ (%) = 198 (100) [M-H]$^+$.

### 1-Methylprop-2-ynyl 2,2,2-trichloroacetimidate (2.1b).[129]

$t_1$ = 60, $t_2$ = 60. Prepared from 3-butyn-2-ol (1.57 mL, 20 mmol) by procedure A, obtained as a colorless oil after purification by column chromatography (petroleum ether/ethyl acetate, 10:1).

Yield: 3.43 g (80%). $^1$H NMR (CDCl$_3$): δ = 8.48 (br s, 1H, N$H$), 5.54 (dq, $J$ = 6.7, 2.1, 1H, OC$H$), 2.52 (d, $J$ = 2.1, 1H, ≡C$H$), 1.64 (d, $J$ = 6.7, 3H, C$H_3$). $^{13}$C NMR (CDCl$_3$): δ = 161.4 ($C$=NH), 91.1 ($C$Cl$_3$), 81.4 ($C$≡CH), 73.6 (C≡$C$H), 64.9 (O$C$H), 20.8 ($C$H$_3$). MS [CI]: $m/z$ (%) = 214 (100) [M+H]$^+$.

### 1-Ethylprop-2-ynyl 2,2,2-trichloroacetimidate (2.1c).

$t_1$ = 60, $t_2$ = 120. Prepared from 1.00 g (11.9 mmol) of 1-pentyn-3-ol by procedure A, obtained as a colorless oil after purification by column chromatography (petroleum ether/ethyl acetate, 8:1).

Yield: 1.42 g (52%). $^1$H NMR (CDCl$_3$): δ = 8.46 (br s, 1H, N$H$), 5.39 (td, $J$ = 6.4, 2.2, 1H, OC$H$), 2.52 (d, $J$ = 2.2, 1H, ≡C$H$), 2.00 – 1.93 (m, 2H, C$H_2$CH$_3$), 1.10 (t, $J$ = 7.4, 3H, C$H_3$). $^{13}$C NMR (CDCl$_3$): δ = 161.6 ($C$=NH), 91.2 ($C$Cl$_3$), 80.3 ($C$≡CH), 74.1 (C≡$C$H), 69.8 (O$C$H), 27.8 ($C$H$_2$CH$_3$), 9.3 (CH$_2$$C$H$_3$). MS [CI]: $m/z$ (%) = 228 (100) [M+H]$^+$.

## Synthesis of 1-Methyl-4-pentyn-3-ol.[248]
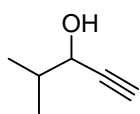
A solution of isobutyraldehyde (0.91 mL, 10 mmol, 1.0 eq.) in dry THF (25 mL) and added to a solution of ethynylmagnesium bromide in THF (0.5 M in THF, 30 mL, 15 mmol) at 0 °C, with stirring. After 3 h, the reaction mixture was quenched by addition of saturated aq. $NH_4Cl$ solution (50 mL) at 0 °C. Volatiles were removed under reduced pressure, and $Et_2O$ (50 mL) was added. The organic layer was separated, washed with brine (50 mL) and dried over $Na_2SO_4$. The solvent was removed *in vacuo*, to furnish 1-methyl-4-pentyn-3-ol as an orange oil, which was used in the next step without further purification. $^1H$ NMR ($CDCl_3$): δ = 4.20 (dd, $J$ = 5.8, 2.1, 1H, C*H*OH), 2.48 (d, $J$ = 2.1, 1H, ≡C*H*), 1.96 − 1.86 (m, 1H, C*H*(CH_3)_2), 1.80 (br s, 1H, O*H*), 1.04 (dd, $J$ = 7.8, 6.8, 6H, C*H*_3).

## 1-(1-Methylethyl)-prop-2-ynyl 2,2,2-trichloroacetimidate (2.1d).

$t_1$ = 60, $t_2$ = 120. Prepared from 0.60 g (6.11 mmol) of 1-methyl-4-pentyn-3-ol by procedure A, obtained as a light yellow oil after purification by column chromatography (petroleum ether/ethyl acetate, 8:1). Yield: 0.75 g (50%). $^1H$ NMR ($CDCl_3$): δ = 8.45 (s, 1H, N*H*), 5.26 (dd, $J$ = 5.6, 2.2, 1H, OC*H*), 2.50 (d, $J$ = 2.2, 1H, ≡C*H*), 2.25 − 2.13 (m, 1H, C*H*(CH_3)_2), 1.10 (dd, $J$ = 9.3, 6.7, 6H, C*H*_3). $^{13}C$ NMR ($CDCl_3$): δ = 161.7 (*C*=NH), 91.3 (*C*Cl_3), 79.2 (*C*≡CH), 74.7 (C≡*C*H), 73.6 (O*C*H), 32.4 (*C*H(CH_3)_2), 17.9 (*C*H_3), 17.7 (*C*H_3). MS [CI]: *m/z* (%) = 242 (28) [M+H]$^+$.

**1-Phenylprop-2-ynyl 2,2,2-trichloroacetimidate (2.1e).**[129]
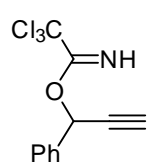
$t_1 = 60$, $t_2 = 300$. Prepared from 1-phenyl-2-propyn-1-ol (2.43 mL, 20 mmol) by procedure A, obtained as a white solid after purification by column chromatography (petroleum ether/ethyl acetate, 10:1). Yield: 1.45 g (26%). $^1$H NMR (CDCl$_3$): $\delta$ = 8.62 (br s, 1H, N$H$), 7.69 − 7.61 (m, 2H, C$H$-aromatic), 7.49 − 7.41 (m, 3H, C$H$-aromatic), 6.58 (d, $J$ = 2.2, 1H, OC$H$), 2.76 (d, $J$ = 2.3, 1H, ≡C$H$). $^{13}$C NMR (CDCl$_3$): $\delta$ = 161.3 ($C$=NH), 135.0 ($C$H-aromatic), 129.2 ($C$H-aromatic), 128.7 ($C$H-aromatic), 127.5 ($C$H-aromatic), 91.0 ($C$Cl$_3$), 79.6 ($C$≡CH), 76.2 (C≡$C$H), 69.9 (O$C$H). MS [CI]: $m/z$ (%) = 133 (100), 116 (85), 264 (23).

**1,1-Dimethylprop-2-ynyl 2,2,2-trichloroacetimidate (2.1f).**[129]
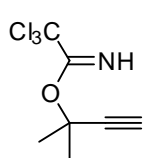
$t_1 = 60$, $t_2 = 300$. Prepared from 2-methyl-3-butyn-2-ol (1.94 mL, 20 mmol) by procedure A, obtained as a colorless oil after purification by column chromatography (petroleum ether/ethyl acetate, 10:1). Yield: 1.22 g (27%). $^1$H NMR (CDCl$_3$): $\delta$ = 8.56 (br s, 1H, N$H$), 2.61 (s, 1H, ≡C$H$), 1.81 (s, 6H, C$H_3$). $^{13}$C NMR (CDCl$_3$): $\delta$ = 159.8 ($C$=NH), 91.9 ($C$Cl$_3$), 83.9 ($C$≡CH), 75.3 (C≡$C$H), 73.3 ($C$(CH$_3$)$_2$), 28.6 ($C$H$_3$). MS [CI]: $m/z$ (%) = 228 (100) [M+H]$^+$.

**But-2-ynyl 2,2,2-Trichloroacetimidate (2.1g).**
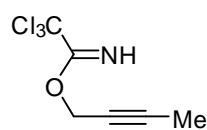
$t_1 = 60$, $t_2 = 30$. Prepared from 2-butyn-1-ol (1.50 mL, 20 mmol) by procedure A, obtained as a colorless oil after purification by column chromatography (petroleum ether/ethyl acetate, 10:1). Yield: 3.20 g (75%). $^1$H NMR (CDCl$_3$): $\delta$ = 8.44 (br s, 1H, N$H$), 4.90 (q, $J$ =

2.3, 2H, OC$H_2$), 1.91 (t, $J$ = 2.3, 3H, C$H_3$). $^{13}$C NMR (CDCl$_3$): δ = 162.06

($C$=NH), 90.99 ($C$Cl$_3$), 84.08 ($C$≡CCH$_3$), 72.56 (C≡$C$CH$_3$), 57.59 (O$C$H$_2$),

3.81 ($C$H$_3$). MS [CI]: $m/z$ (%) = 214 (100) [M+H]$^+$.


### 3-Phenylprop-2-ynyl 2,2,2-Trichloroacetimidate (2.1h).
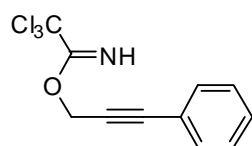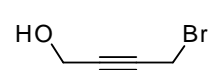


$t_1$ = 60, $t_2$ = 90. Prepared from 3-phenyl-2-propyn-1-ol (1.0 mL, 8.0 mmol) by procedure A, obtained as a colorless oil after purification by column chromatography (petroleum ether/ethyl acetate, 8:1). Yield: 1.72g (78%). $^1$H NMR (CDCl$_3$): δ = 8.51 (br s, 1H, N$H$), 7.49 (dd, $J$ = 7.5, 2.2, 2H, C$H$-aromatic), 7.37 – 7.29 (m, 3H, C$H$-aromatic), 5.15 (s, 2H, OC$H_2$). $^{13}$C NMR (CDCl$_3$): δ = 161.98 ($C$=NH), 131.98 ($C$H-aromatic), 128.87 ($C$H-aromatic), 128.33 ($C$H-aromatic), 122.10 ($C$H-aromatic), 90.95 ($C$Cl$_3$), 87.23 ($C$≡CC$_6$H$_5$), 82.29 (C≡$C$C$_6$H$_5$), 57.58 (O$C$H$_2$). MS [CI]: $m/z$ (%) = 229 (100), 133 (86), 246 (62). (M$^+$ not observed)


### 4-Tosyloxy-2-butyn-1-ol.
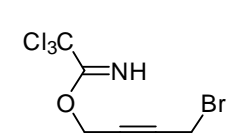


This compound was prepared by a modified method of a previously published procedure.[249] A mixture of triethylamine (2.0 mL, 14.4 mmol, 1.6 eq.), trimethylamine hydrochloride (0.086 g, 0.9 mmol, 0.1 eq.) and $p$-toluenesulfonyl chloride (1.72 g, 9.0 mmol, 1.0 eq.) in MeCN (20 mL) was added dropwise over 1 h to a solution of 2-butyne-1,4-diol (3.87 g, 45 mmol, 5 eq.) in MeCN (30 mL) at 0 °C. The reaction mixture was warmed to room temperature and quenched with water (75 mL) and ethyl acetate (75 mL). The aqueous layer was extracted with another 50 mL of ethyl acetate. The

combined organic layers were washed with saturated aqueous $NH_4Cl$ solution (40 mL) and brine (40 mL), and dried over $Na_2SO_4$. The solvent was removed *in vacuo*, leaving behind a dark brown oil. The crude product was purified by column chromatography on silica, using petroleum ether/ethyl acetate, 3:7 then 1:1 as eluting solvent. 1.14 g (53%) of 4-tosyloxy-2-butyn-1-ol was obtained as an orange oil. ^{1}H NMR ($CDCl_3$): $\delta$ = 7.84 (d, $J$ = 8.3, 2H, C*H*-aromatic), 7.39 (d, $J$ = 8.3, 2H, C*H*-aromatic), 4.76 (t, $J$ = 1.7, 2H, TsOC*H_2*), 4.19 (t, $J$ = 1.7, 2H, C*H_2*OH), 2.48 (s, 3H, C*H_3*), 2.07 (s, 1H, $CH_2$O*H*).

**1-Bromo-2-butyn-4-ol.**[249]
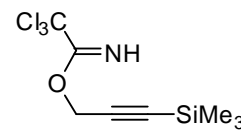
To a stirred solution of 4-tosyloxy-2-butyn-1-ol (1.14 g, 4.74 mmol, 1.0 eq.) in acetone (8.0 mL) was added LiBr (0.82 g, 9.49 mmol, 2.0 eq.) which caused a minor exotherm in the mixture. Stirring was continued at room temperature for 1 h and then diluted with $Et_2O$ (35 mL) and $H_2O$ (17 mL). The organic layer was washed with brine (5 mL) and dried over $MgSO_4$. The solvent was removed *in vacuo*, and the resulting brown oil (0.63 g, 89%) was used without further purification. ^{1}H NMR ($CDCl_3$): $\delta$ = 4.35 (t, $J$ = 2.0, 2H, C*H_2*OH), 3.97 (t, $J$ = 2.0, 2H, C*H_2*Br), 2.20 (s, 1H, $CH_2$O*H*). ^{13}C NMR ($CDCl_3$): $\delta$ = 85.0 ($\equiv$*C*CH_2OH), 80.8 ($\equiv$*C*CH_2Br), 51.1 (*C*H_2OH), 14.3 (*C*H_2Br).

**Synthesis of 4-Bromo-but-2-ynyl 2,2,2-trichloroacetimidate (2.1i).**
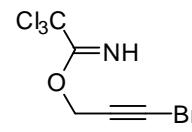
$t_1$ = 60, $t_2$ = 120. Prepared from 1-bromo-2-butyn-4-ol (0.87 g, 5.84 mmol) by procedure A, obtained as a colorless oil after purification by column chromatography (petroleum

ether/ethyl acetate, 5:1). Yield: 1.14 g (67%). $^{1}$H NMR (CDCl$_3$): δ = 8.51 (br s, 1H, N$H$), 5.00 (t, $J$ = 2.1, 2H, OC$H_2$), 3.99 (t, $J$ = 2.1, 2H, C$H_2$Br). $^{13}$C NMR (CDCl$_3$): δ = 161.8 ($C$=NH), 90.7 ($C$Cl$_3$), 82.4 ($C$≡CCH$_2$Br), 80.0 (C≡$C$CH$_2$Br), 56.8 (O$C$H$_2$), 13.8 ($C$H$_2$Br). MS [CI]: $m/z$ (%) = 294 (100) [M+H]$^{+}$.

**3-(Trimethylsilyl)prop-2-ynyl 2,2,2-trichloroacetimidate (2.1j).**



$t_1$ = 60, $t_2$ = 60. Prepared from 3-(trimethylsilyl)propargyl alcohol (1.00 g, 7.8 mmol) by procedure A, obtained as a colorless oil after purification by column chromatography (petroleum ether/ethyl acetate, 8:1). Yield: 1.97 g (93%). $^{1}$H NMR (CDCl$_3$): δ = 8.45 (br s, 1H, N$H$), 4.91 (s, 2H, OC$H_2$), 0.19 (s, 9H, C$H_3$). $^{13}$C NMR (CDCl$_3$): δ = 161.9 ($C$=NH), 98.2 ($C$Cl$_3$), 93.0 ($C$≡CSi), 90.9 (C≡$C$Si), 54.7 (O$C$H$_2$), -0.3 (Si($C$H$_3$)$_3$). MS [CI]: $m/z$ (%) = 272 (100) [M+H]$^{+}$.

**Synthesis of 3-Bromoprop-2-ynyl 2,2,2-trichloroacetimidate (2.1k).**



A mixture of propargyl alcohol (1.16 mL, 20 mmol, 1.0 eq.), $N$-bromosuccinimide (3.92 g, 22 mmol, 1.1 eq.) and silver nitrate (0.34 g, 2.0 mmol, 0.1 eq.) in acetone (50 mL) was stirred at room temperature for 2 h. The solvent was removed *in vacuo* and the residue dissolved in water (50 mL). The resulting solution was extracted with Et$_2$O (2 × 50 mL), and the combined organic extracts washed with brine (20 mL), dried over Na$_2$SO$_4$, filtered and concentrated to afford the bromopropargylic alcohol as a colorless oil. CH$_2$Cl$_2$ (50 mL) and

trichloroacetonitrile (2.4 mL, 24 mmol, 1.2 eq.) were added, and the solution was cooled to 0 °C in an ice bath. DBU (0.3 mL, 2.0 mmol, 0.1 eq.) was then added dropwise. The reaction mixture was allowed to stir at 0 °C for 1 h, then warmed to room temperature and stirred for another 3 h. The solvent was removed *in vacuo*, and the resulting brown oil chromatographed on silica using petroleum ether/ethyl acetate (8:1) as eluting solvent, to furnish **2.1k** as a light yellow oil. Yield: 3.34 g (60%). $^1$H NMR (CDCl$_3$): δ = 8.49 (br s, 1H, N*H*), 4.93 (s, 2H, OC*H*$_2$). $^{13}$C NMR (CDCl$_3$): δ = 161.8 (*C*=NH), 90.7 (*C*Cl$_3$), 73.5 (*C*≡CBr), 57.5 (C≡*C*Br), 48.2 (O*C*H$_2$). MS [CI]: *m/z* (%) = 280 (83) [M+H]$^+$.

**General procedure for the preparation of homopropargyl trichloroacetimidates (2.8a-c) (Procedure B):**

A solution of the appropriate homopropargyl alcohol (20 mmol, 1.0 eq.) and trichloroacetonitrile (24 mmol, 1.2 eq.) in CH$_2$Cl$_2$ (50 mL) was cooled to 0 °C in an ice bath and DBU (2 mmol, 0.1 eq.) was added dropwise. The reaction mixture was allowed to stir at 0 °C (for t$_1$ min), then warmed to room temperature and stirred (for another t$_2$ min). The solvent was removed *in vacuo*, and the residue chromatographed on silica.

**But-3-ynyl 2,2,2-trichloroacetimidate (2.8a).**
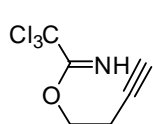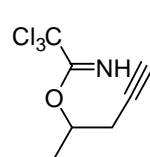
This compound was previously reported[129] but no experimental details and spectroscopic data were given. t$_1$ = 60, t$_2$ = 60. Prepared from 3-butyn-1-ol (1.51 mL, 20 mmol) by procedure B, obtained as a colorless oil after purification by column chromatography (petroleum
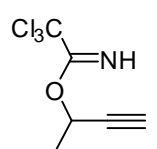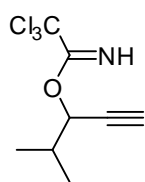
ether/ethyl acetate, 10:1). Yield: 3.28 g (76%). $^1$H NMR (CDCl$_3$): δ = 8.35 (br

s, 1H, N*H*), 4.40 (t, *J* = 7.0, 2H, OC*H*$_2$), 2.68 (td, *J* = 7.0, 2.7, 2H, C*H*$_2$C≡),

2.01 (t, *J* = 2.7, 1H, ≡C*H*). $^{13}$C NMR (CDCl$_3$): δ = 162.5 (*C*=NH), 91.2 (*C*Cl$_3$),

79.6 (*C*≡CH), 70.1 (C≡*C*H), 66.8 (O*C*H$_2$), 18.5 (*C*H$_2$C≡C). MS [CI]: *m/z* (%)

= 214 (100) [M+H]$^+$.


**1-Methyl-but-3-ynyl 2,2,2-trichloroacetimidate (2.8b).**

t$_1$ = 60, t$_2$ = 360. Prepared from 4-pentyn-2-ol (1.90 mL, 20 mmol) by procedure B, obtained as a colorless oil after purification by column chromatography (petroleum ether/ethyl

acetate, 5:1). Yield: 3.71 g (81%). $^1$H NMR (CDCl$_3$): δ = 8.31 (br s, 1H, N*H*),

5.17 − 5.09 (m, 1H, OC*H*), 2.68 − 2.54 (m, 2H, C*H*$_2$C≡), 2.02 (t, *J* = 2.7, 1H,

≡C*H*), 1.47 (d, *J* = 6.3, 3H, C*H*$_3$). $^{13}$C NMR (CDCl$_3$): δ = 161.9 (*C*=NH), 91.6

(*C*Cl$_3$), 79.5 (*C*≡CH), 73.6 (C≡*C*H), 70.6 (O*C*H), 24.9 (*C*H$_2$C≡C), 18.3 (*C*H$_3$).

MS [CI]: *m/z* (%) = 228 (100) [M+H]$^+$.


**1-Ethyl-but-3-ynyl 2,2,2-trichloroacetimidate (2.8c).**

t$_1$ = 60, t$_2$ = 60. Prepared from 5-hexyn-3-ol (1.00 g, 10.2 mmol) by procedure B, obtained as a colorless oil after purification by column chromatography (petroleum ether/ethyl acetate, 5:1).

Yield: 2.37 g (96%). $^1$H NMR (CDCl$_3$): δ = 8.32 (br s, 1H, N*H*), 5.02 − 4.96

(m, 1H, OC*H*), 2.64 − 2.62 (m, 2H, C*H*$_2$C≡), 2.00 (t, *J* = 2.7, 1H, ≡C*H*), 1.91 −

1.86 (m, 2H, C*H*$_2$CH$_3$), 1.01 (t, *J* = 7.5, 3H, CH$_2$C*H*$_3$). $^{13}$C NMR (CDCl$_3$): δ =

162.3 (*C*=NH), 91.7 (*C*Cl$_3$), 79.5 (*C*≡CH), 78.0 (C≡*C*H), 70.5 (O*C*H), 25.7

($CH_2C{\equiv}C$), 22.5 ($CH_2CH_3$), 9.4 ($CH_2CH_3$). MS [CI]: $m/z$ (%) = 242 (100) [M+H]$^+$.

**General procedure for the preparation of homopropargyl alcohols (Procedure C):**

Propargylmagnesium bromide was prepared by a modified literature procedure:[250] A mixture of Mg turnings (1.94 g, 80 mmol) and $HgCl_2$ (75 mg) was suspended in dry $Et_2O$ (20 mL) and stirred at room temperature for 30 min. 1.0 mL of propargyl bromide solution (80% in toluene, 6.72 mmol) was added in one portion to initiate the reaction (indicated by a slight exotherm). The reaction mixture was cooled to 0 °C in an ice bath, and another 5.0 mL of propargyl bromide solution (80% in toluene, 33.6 mmol) was added dropwise over 30 min. Stirring was continued for another 45 min at 0 °C, after which the solution was decanted into a solution of the corresponding aldehyde (20 mmol) in $Et_2O$ (15 mL) at 0 °C. The ice bath was removed, and reaction mixture stirred overnight at room temperature. The reaction was quenched by the addition of 40 mL of saturated aq. $NH_4Cl$ at 0 °C. The aqueous layer was extracted with 3 × 40 mL of $Et_2O$, and the combined organic extracts washed with brine (75 mL), dried over $Na_2SO_4$, filtered and concentrated *in vacuo*. The crude homopropargyl alcohols were obtained as orange oils, which were used in the next steps without further purification.

**General procedure for the synthesis of the homopropargyl trichloroacetimidates (2.8d-f) (Procedure D):**

A solution of the requisite homopropargyl alcohol (either obtained from commercial sources or prepared by procedure C) (10 mmol, 1.0 eq.) and trichloroacetonitrile (12 mmol, 1.2 eq.) in $CH_2Cl_2$ (25 mL) was cooled to 0 °C in an ice bath and DBU (1 mmol, 0.1 eq.) was added dropwise. The reaction mixture was allowed to stir at 0 °C for 15 min, then warmed to room temperature and stirred for further 4 h. The solvent was removed *in vacuo*, and the residue chromatographed on silica.

**1-Phenyl-but-3-ynyl 2,2,2-trichloroacetimidate (2.8d).**
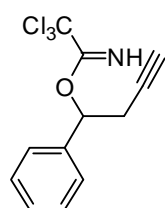
Prepared by procedure D. After purification by column chromatography (petroleum ether/ethyl acetate, 6:1), 1.88 g (65%) of **2.8d** was obtained as a white crystalline solid. ^{1}H NMR (CDCl$_3$): δ = 8.39 (br s, 1H, N*H*), 7.49 − 7.46 (m, 2H, C*H*-aromatic), 7.41 − 7.32 (m, 3H, C*H*-aromatic), 5.99 (t, *J* = 6.6, 1H, OC*H*), 2.97 − 2.79 (m, 2H, C*H*$_2$C≡), 2.00 (t, *J* = 2.7, 1H, ≡C*H*). ^{13}C NMR (CDCl$_3$): δ = 161.4 (*C*=NH), 138.5 (*C*H-aromatic), 128.5 (*C*H-aromatic), 126.3 (*C*H-aromatic), 91.4 (*C*H-aromatic), 79.2 (*C*≡CH), 78.3 (C≡*C*H), 70.9 (O*C*H), 26.6 (*C*H$_2$C≡C). (*C*Cl$_3$ was too broad to be detected). MS [CI]: *m/z* (%) = 257 (100), 274 (94), 145 (86) (M$^+$ not observed).

**1-(4-Chlorophenyl)-but-3-ynyl 2,2,2-trichloroacetimidate (2.8e).**
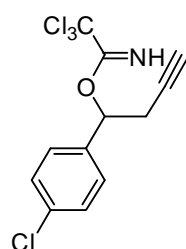
Prepared by procedure D. After purification by column chromatography (petroleum ether/ethyl acetate, 10:1), 1.36 g (42%) of **2.8e** was obtained as an orange oil. This compound

was previously reported[129] but no experimental details and spectroscopic data were given. $^1$H NMR (CDCl$_3$): δ = 8.40 (br s, 1H, N*H*), 7.42 − 7.34 (m, 4H, C*H*-aromatic), 5.94 (t, *J* = 6.6, 1H, OC*H*), 3.94 − 2.77 (m, 2H, C*H*$_2$C≡), 2.00 (t, *J* = 2.6, 1H, ≡C*H*). $^{13}$C NMR (CDCl$_3$): δ = 161.3 (*C*=NH), 136.9 (*C*H-aromatic), 134.4 (*C*H-aromatic), 128.7 (*C*H-aromatic), 127.9 (*C*H-aromatic), 91.2 (*C*≡CH), 78.8 (C≡*C*H), 71.2 (O*C*H), 26.4 (*C*H$_2$C≡C). (*C*Cl$_3$ was too broad to be detected). MS [CI]: *m/z* (%) = 181 (100), 164 (31), 364 (26) (M$^+$ not observed).

**1-(4-Trifluoromethylphenyl)-but-3-ynyl 2,2,2-trichloroacetimidate (2.8f).**
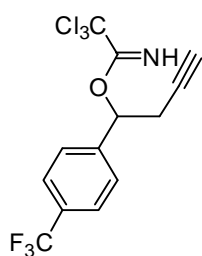
Prepared by procedure D. After purification by column chromatography (petroleum ether/ethyl acetate, 10:1), 1.56 g (44%) of **2.8f** was obtained as an orange oil. $^1$H NMR (CDCl$_3$): δ = 8.43 (br s, 1H, N*H*), 7.66 − 7.58 (m, 4H, C*H*-aromatic), 6.01 (t, *J* = 6.4, 1H, OC*H*), 2.97 − 2.80 (m, 2H, C*H*$_2$C≡), 2.01 (t, *J* = 2.7, 1H, ≡C*H*). $^{13}$C NMR (CDCl$_3$): δ = 161.2 (*C*=NH), 142.3 (*C*H-aromatic), 130.6 (q, *J* = 32.4, *C*F$_3$), 126.7 (*C*H-aromatic), 125.5 (*C*H-aromatic), 125.5 (*C*H-aromatic), 122.6 (*C*Cl$_3$), 91.1 (*C*≡CH), 78.5 (C≡*C*H), 71.5 (O*C*H), 26.4 (*C*H$_2$C≡C). MS [CI]: *m/z* (%) = 371 (100), 215 (34). (M$^+$ not observed)
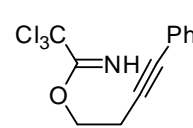
**Synthesis of 4-Phenyl-3-butyn-1-ol.[251]**
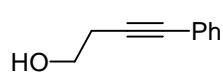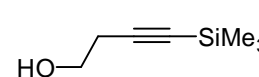
A mixture of *bis*(triphenylphosphine)palladium(II) dichloride (0.15 g, 0.2 mmol, 0.02 eq.), copper(I) iodide (19 mg, 0.01 mmol, 0.01 eq.), iodobenzene (1.1 mL, 10 mmol, 1.0 eq.) and 3-butyn-1-ol (0.9 mL, 12 mmol, 1.2 eq.) was dissolved in dry Et$_3$N (60 mL) and

refluxed for 2.5 h. The resultant dark brown solution was quenched with 22.5 mL of an ethyl acetate/water mixture (1:1.25). The aqueous and organic phases were separated, and the organic layer was washed with water (50 mL) and then brine (50 mL), dried over anhydrous $Na_2SO_4$, filtered and concentrated *in vacuo*. The resulting orange oil was and purified by column chromatography (petroleum ether/ethyl acetate, 1:2) on silica gel to afford 0.86 g (59%) of 4-phenyl-3-butyn-1-ol as a light yellow oil. $^1$H NMR (CDCl$_3$):

δ = 7.48 − 7.40 (m, 2H, C*H*-aromatic), 7.36 − 7.27 (m, 3H, C*H*-aromatic), 3.84 (t, *J* = 6.3, 2H, C*H*$_2$OH), 2.72 (t, *J* = 6.3, 2H, ≡CC*H*$_2$), 1.82 (br s, 1H, O*H*).

**Synthesis of 4-Phenyl-but-3-ynyl 2,2,2-trichloroacetimidate (2.8g).**
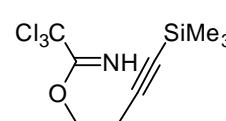
Prepared on a 5.88 mmol scale by procedure D. After purification by column chromatography (petroleum ether/ethyl acetate, 6:1), 1.59 g (93%) of **2.8g** was obtained as a light yellow crystalline solid. $^1$H NMR (CDCl$_3$): δ = 8.37 (br s, 1H, N*H*), 7.41 − 7.37 (m, 3H, C*H*-aromatic), 7.30 − 7.28 (m, 2H, C*H*-aromatic), 4.49 (t, *J* = 7.0, 2H, OC*H*$_2$), 2.92 (t, *J* = 7.0, 2H, C*H*$_2$C≡). $^{13}$C NMR (CDCl$_3$): δ = 162.6 (*C*=NH), 131.6 (*C*H-aromatic), 128.0 (*C*H-aromatic), 123.4 (*C*H-aromatic), 91.3 (*C*H-aromatic), 85.0 (*C*≡C*C*$_6$H$_5$), 82.2 (C≡*C*C$_6$H$_5$), 67.1 (O*C*H$_2$), 19.5 (*C*H$_2$C≡C). (CCl$_3$ was too broad to be detected). MS [CI]: *m/z* (%) = 290 (33) [M+H]$^+$.

**Synthesis of 4-(Trimethylsilyl)but-3-yn-1-ol.**[251, 252]

*n*-BuLi (1.6 M in hexane, 27.5 mL, 44 mmol, 2.2 eq.)

was added dropwise to a solution of 3-butyn-1-ol (1.5 mL, 20 mmol, 1.0 eq.) in dry THF (25 mL) at -78 °C. After stirring for 1 h, the yellow suspension was allowed to warm to room temperature, before cooling down again to -78 °C, whereupon trimethylchlorosilane (5.6 mL, 44 mmol, 2.2 eq.) was added dropwise. The cooling bath was removed, and the reaction mixture was stirred overnight at room temperature. The reaction was quenched by the dropwise addition of 5M $H_2SO_4$ (10 mL) at 0 °C, stirring for 1 h to ensure complete hydrolysis of the TMS-ether. The aqueous layer was then separated and extracted with $Et_2O$ (2 × 10 mL). The combined organic layers was washed with water (10 mL) and brine (10 mL), dried over $MgSO_4$, filtrated and concentrated under reduced pressure to give 1.89 g (66%) of 4-(trimethylsilyl)but-3-yn-1-ol as a light yellow oil, which was used for the next step without further purification. $^1$H NMR (CDCl$_3$): δ = 3.71 (t, $J$ = 6.3, 2H, C$H_2$OH), 2.50 (t, $J$ = 6.3, 2H, ≡C$H_2$), 1.74 (s, 1H, O$H$), 0.16 (s, 9H, Si(C$H_3$)$_3$).

**4-(Trimethylsilyl)but-3-ynyl 2,2,2-trichloroacetimidate (2.8h).**

Prepared on a 12.4 mmol scale by procedure D. After purification by column chromatography (petroleum ether/ethyl acetate, 8:1), 2.90 g (81%) of **2.8h** was obtained as a white crystalline solid. $^1$H NMR (CDCl$_3$): δ = 8.33 (br s, 1H, N$H$), 4.38 (t, $J$ = 7.0, 2H, OC$H_2$), 2.71 (t, $J$ = 7.0, 2H, C$H_2$C≡), 0.13 (s, 9H, C$H_3$). $^{13}$C NMR (CDCl$_3$): δ = 162.6 ($C$=NH), 101.8 ($C$Cl$_3$), 91.3 ($C$≡CSi), 86.8 (C≡$C$Si), 66.9 (OC$H_2$), 19.9 (CH$_2$C≡C), -0.02 (Si(CH$_3$)$_3$). MS [CI]: $m/z$ (%) = 286 (100) [M+H]$^+$.

**4-Bromobut-3-ynyl 2,2,2-trichloroacetimidate (2.8i).**
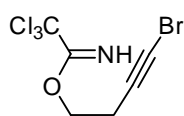
A mixture of 3-butyn-1-ol (0.34 mL, 4.5 mmol, 1.0 eq.), *N*-bromosuccinimide (0.88 g, 4.95 mmol, 1.1 eq.) and silver nitrate (76.4 mg, 0.45 mmol, 0.1 eq.) in acetone (10 mL) was stirred at room temperature for 2 h. The solvent was removed *in vacuo* and the residue dissolved in water (10 mL). The resulting solution was extracted with $Et_2O$ (2 × 10 mL), and the combined organic extracts washed with brine (10 mL), dried over $Na_2SO_4$, filtered and concentrated to afford 4-bromo-but-3-yn-1-ol as a colorless oil. $CH_2Cl_2$ (10 mL) and trichloroacetonitrile (0.54 mL, 5.4 mmol, 1.2 eq.) were added, and the solution was cooled to 0 °C in an ice bath. DBU (67.3 μL, 0.45 mmol, 0.1 eq.) was then added dropwise. The reaction mixture was allowed to stir at 0 °C for 1 h, then warmed to room temperature and stirred for another 3 h. The solvent was removed *in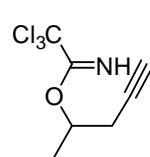 vacuo*, and the resulting brown oil chromatographed on silica using petroleum ether/ethyl acetate (5:1) as eluting solvent, to furnish 0.83 g (63%) of **2.8i** as a colorless oil. $^1$H NMR ($CDCl_3$): δ = 8.35 (br s, 1H, N*H*), 4.38 (t, *J* = 6.9, 2H, OC*H$_2$*), 2.70 (t, *J* = 6.9, 2H, C*H$_2$*C≡). $^{13}$C NMR ($CDCl_3$): δ = 162.4 (*C*=NH), 91.1 (*C*Cl$_3$), 75.5 (*C*≡CBr), 66.4 (C≡*C*Br), 40.4 (O*C*H$_2$), 19.6 (*C*H$_2$C≡C). HRMS (ESI) calcd for $C_6H_5BrCl_3NO$ [M+H]$^+$: 291.8698; found 291.8706.

**General procedure for the synthesis of Ag(I) *bis*(pyridine) complexes (Procedure E):**[139]

The silver salt AgX (0.5 mmol, 1.0 eq.) and the appropriate pyridine ligand (1.0 mmol, 1.0 eq.) were mixed in MeCN (5 mL) and stirred at room temperature overnight. The reaction mixture was filtered through Celite, and

the solvent removed from the filtrate *in vacuo*. The resulting residue was washed with diethyl ether to afford the desired complexes as colorless, air- and moisture-stable solids.

**Bis(pyridine)silver(I) trifluoromethanesulfonate [Ag(Py)₂]OTf (2.5a).[139]**

Prepared by procedure E. Yield: 0.14 g (69%). $^1$H NMR (CDCl$_3$): δ = 8.74 − 8.72 (m, 4 H), 7.84 − 7.82 (m, 2 H), 7.42 − 7.41 (m, 4H). $^{13}$C NMR (CDCl$_3$): δ = 152.0, 138.9, 125.3. Anal. Calc. for C$_{11}$H$_{10}$AgF$_3$N$_2$O$_3$S: C, 31.83; H, 2.43; N, 6.75%. Found: C, 31.83; H, 2.37; N, 6.68%.

**Bis(4-acetylpyridine)silver(I) trifluoromethanesulfonate [Ag(Ac-Py)₂]OTf (2.10a).**

Prepared by procedure E. Yield: 0.22 g (90%). $^1$H NMR (DMSO-d$_6$): δ = 8.82 − 8.81 (m, 4H), 7.86 − 7.84 (m, 4H), 2.63 (s, 6H). $^{13}$C NMR (DMSO-d$_6$): δ = 198.5, 151.6, 143.3, 122.0, 27.4. Anal. Calc. for C$_{15}$H$_{14}$AgF$_3$N$_2$O$_5$S: C, 36.09; H, 2.83; N, 5.61%. Found: C, 36.13; H, 2.75; N, 5.69%.

**Bis(4-acetylpyridine)silver(I) perchlorate [Ag(Ac-Py)₂]ClO₄ (2.10b).**

Prepared by procedure E. Yield: 0.18 g (80%). $^1$H NMR (DMSO-d$_6$): δ = 8.82 − 8.80 (m, 4H), 7.83 − 7.82 (m, 4H), 2.63 (s, 6H). $^{13}$C NMR (DMSO-d$_6$): δ = 197.9, 151.3, 142.9, 121.7, 26.9. Anal. Calc. for C$_{14}$H$_{14}$AgClN$_2$O$_6$: C, 37.40; H, 3.14; N, 6.23%. Found: C, 37.54; H, 3.06; N, 6.35%.

**Bis(4-acetylpyridine)silver(I) tetrafluoroborate [Ag(Ac-Py)₂]BF₄ (2.10c).**

Prepared by procedure E. Yield: 0.17 g (78%). $^1$H NMR (DMSO-d$_6$): δ = 8.82 − 8.81 (m, 4H), 7.84 − 7.82 (m, 4H), 2.63 (s, 6H). $^{13}$C NMR (DMSO-d$_6$): δ = 197.9, 151.3, 142.9, 121.7, 26.9. Anal. Calc. for $C_{14}H_{14}AgBF_4N_2O_2$: C, 38.48; H, 3.23; N, 6.41%. Found: C, 38.60; H, 3.17; N, 6.49%.

**Bis(4-acetylpyridine)silver(I) hexafluorophosphate [Ag(Ac-Py)₂]PF₆ (2.10d).**

Prepared by procedure E. Yield: 0.19 g (77%). $^1$H NMR (DMSO-d$_6$): δ = 8.82 − 8.81 (m, 4H), 7.85 − 7.82 (m, 4H), 2.63 (s, 6H). $^{13}$C NMR (DMSO-d$_6$): δ = 198.0, 151.1, 142.8, 121.6, 26.9. Anal. Calc. for $C_{14}H_{14}AgF_6N_2O_2P$: C, 33.96; H, 2.85; N, 5.66%. Found: C, 34.03; H, 2.67; N, 5.70%.

**Bis(4-acetylpyridine)silver(I) hexafluoroantimonate [Ag(Ac-Py)₂]SbF₆ (2.10e).**

Prepared by procedure E. Yield: 0.26 g (89%). $^1$H NMR (DMSO-d$_6$): δ = 8.82 − 8.81 (m, 4H), 7.86 − 7.83 (m, 4H), 2.63 (s, 6H). $^{13}$C NMR (DMSO-d$_6$): δ = 197.9, 151.2, 143.0, 121.8, 26.9. Anal. Calc. for $C_{14}H_{14}AgF_6N_2O_2Sb$: C, 28.70; H, 2.41; N, 4.78%. Found: C, 28.88; H, 2.47; N, 4.82%.

**Bis(4-acetylpyridine)silver(I) trifluoroacetate [Ag(Ac-Py)₂]CF₃CO₂ (2.10f).**

Prepared by procedure E. Yield: 0.20 g (86%). $^1$H NMR (CDCl$_3$): δ = 8.81 − 8.79 (m, 4H), 7.81 − 7.77 (m, 4H), 2.64 (s, 6H). $^{13}$C NMR (CDCl$_3$): δ = 196.4, 152.2, 143.6, 122.2, 26.6. Anal. Calc. for $C_{16}H_{14}AgF_3N_2O_4$: C, 41.49; H, 3.05; N, 6.05%. Found: C, 41.60; H, 2.98; N, 6.04%.

**Bis(4-methoxypyridine)silver(I) trifluoromethanesulfonate [Ag(MeO-Py)₂]OTf (2.11a).**

Prepared by procedure E. Yield: 0.21 g (88%). ^{1}H NMR (CDCl₃): δ = 8.54 − 8.51 (m, 4H), 6.88 − 6.83 (m, 4H), 3.87 (s, 6H). ^{13}C NMR (CDCl₃): δ = 166.9, 153.3, 111.0, 55.7. Anal. Calc. for $C_{13}H_{14}AgF_3N_2O_5S$: C, 32.86; H, 2.97; N, 5.90%. Found: C, 32.77; H, 2.97; N, 5.90%.

**Bis(4-dimethylaminopyridine)silver(I) trifluoromethanesulfonate [Ag(4-DMAP)₂]OTf (2.12).**

Yield: 0.24 g (96%). ^{1}H NMR (CDCl₃): δ = 8.21 − 8.20 (m, 4H), 6.54 − 6.52 (m, 4H), 3.04 (s, 12H). ^{13}C NMR (CDCl₃): δ = 154.8, 150.9, 107.0, 39.1. Anal. Calc. for $C_{15}H_{20}AgF_3N_4O_3S$: C, 35.94; H, 4.02; N, 11.18%. Found: C, 36.04; H, 3.97; N, 11.08%.

**Bis(4-methylpyridine)silver(I) trifluoromethanesulfonate [Ag(Me-Py)₂]OTf (2.13).**

Yield: 0.14 g (65%). ^{1}H NMR (CDCl₃): δ = 8.55 − 8.54 (m, 4H), 7.26 − 7.20 (m, 4H), 2.38 (s, 6H). ^{13}C NMR (CDCl₃): δ = 151.4, 150.8, 125.9, 21.3. Anal. Calc. for $C_{13}H_{14}AgF_3N_2O_3S$: C, 35.23; H, 3.18; N, 6.32%. Found: C, 35.16; H, 3.19; N, 6.21%.

**(Triphenylphosphine)silver(I) trifluoromethanesulfonate [(Ph₃P)Ag(OTf)] (2.4).**[139]

Silver(I) trifluoromethanesulfonate (0.26 g, 1.0 mmol, 1.0 eq.) and triphenylphosphine (0.26 g, 1.0 mmol. 1.0 eq.). and $CH_2Cl_2$ (10 mL) were

added to a 25 mL round-bottomed flask and the reaction mixture stirred for 12 h at room temperature. The clear solution was concentrated to half of its original volume under reduced pressure and *ca.* 4 mL of pentane was added. The solution was cooled to -20°C to yield 0.38 g (73%) of **2.4** as a white, crystalline solid. $^1$H NMR (CDCl$_3$): δ = 7.49 – 7.39 (m, 15H). $^{13}$C NMR (CDCl$_3$): δ = 133.9, 133.8, 131.2, 129.2, 129.1. $^{31}$P NMR (CDCl$_3$): δ = 16.31. Anal. Calc. for C$_{19}$H$_{15}$AgF$_3$O$_3$PS: C, 43.95; H, 2.91%. Found: C, 43.96; H, 2.93%.

### Synthesis of [Ag(bpy)$_2$]OTf (2.6).

Silver(I) trifluoromethanesulfonate (0.13 g, 0.5 mmol, 1.0 eq.) was added to a solution of 2,2'-bipyridine (0.16 g, 1.0 mmol, 2.0 eq.) in MeCN (5 mL). The reaction mixture was stirred at room temperature overnight, and the solvent was removed *in vacuo* to give a light yellow crystalline solid. X-ray diffraction quality single crystals were obtained by recrystallization from CH$_2$Cl$_2$/*n*-hexane at room temperature overnight. Yield: 0.17 g (60%). Light yellow solid. $^1$H NMR (CDCl$_3$): δ = 8.61 – 8.59 (m, 2H), 8.38 – 8.30 (m, 2H), 8.09 (td, *J* = 7.9, 1.8, 2H), 7.59 – 7.55 (m, 2H). $^{13}$C NMR (CDCl$_3$): δ = 151.8, 150.8, 139.4, 125.8, 122.9. Anal. Calc. for C$_{21}$H$_{16}$AgF$_3$N$_4$O$_3$S: C, 44.30; H, 2.83; N, 9.84%. Found: C, 44.37; H, 2.82; N, 9.98%.

### Synthesis of [Ag(phen)]OTf (2.7).[69]
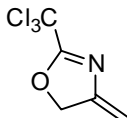
A solution of silver(I) trifluoromethanesulfonate (0.29 g, 1.11 mmol, 1.0 eq.) in 7 mL of water was added a solution of 1,10-phenanthroline (0.20 g, 1.11 mmol, 1.0 eq.) in 7 mL of methanol. The reaction mixture was stirred for 15

min. The pale yellow precipitate was filtered off, washed with methanol and dried *in vacuo*. Yield: 0.28 g (58%). $^1$H NMR (DMSO-$d_6$): δ = 9.17 – 9.14 (m, 2H), 8.79 – 8.75 (m, 2H), 8.21 (d, *J* = 5.4, 2H), 8.02 – 7.98 (m, 2H). $^{13}$C NMR (DMSO-$d_6$): δ = 151.9, 142.4, 138.9, 129.5, 127.7, 125.4.

**General catalytic procedure for the Ag(I)-catalyzed conversion of 2.1 to 2.2 or 2.8 to 2.9 (Procedure F):**

Substrate **2.1 or 2.8** (4.0 mmol, 1.0 eq.) was dissolved in acetone (2.5 mL per mmol of substrate) at room temperature and [Ag(Py)$_2$]OTf (166.0 mg, 0.4 mmol, 0.1 eq.) was added. After 6 h, the reaction mixture was filtered, and the filtrate concentrated *in vacuo*. The residue was purified by column chromatography on silica.

**4-Methylene-2-(trichloromethyl)-4,5-dihydrooxazole (2.2a).**[129, 130]

Prepared from **2.1a** (0.80 g) by procedure F, isolated as a yellow oil after purification by column chromatography (petroleum ether/ethyl acetate, 8:1). Yield: 0.54 g (67%). $^1$H NMR (CDCl$_3$): δ = 5.39 (td, *J* = 3.3, 1.6, 1H, =C*H*), 5.23 (t, *J* = 3.1, 2H, OC*H*$_2$), 4.87 (td, *J* = 3.3, 1.6, 1H, =C*H*). $^{13}$C NMR (CDCl$_3$): δ = 168.6 (N*C*O), 153.3 (*C*=CH$_2$), 102.1 (C=*C*H$_2$), 74.4 (O*C*H$_2$). (CCl$_3$ was too broad to be detected). HRMS (ESI) calcd for C$_5$H$_4$Cl$_3$NO [M+H]$^+$: 199.9437; found 199.9447.

### 5-Methyl-4-methylene-2-(trichloromethyl)-4,5-dihydrooxazole (2.2b).[129]
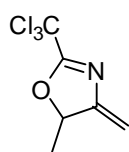
Prepared from **2.1b** (0.86 g) by procedure F, Isolated as a yellow oil after purification by column chromatography (petroleum ether/ethyl acetate, 8:1). Yield: 0.63 g (74%). $^1$H NMR (CDCl$_3$): δ = 5.46 (qt, $J$ = 6.4, 3.0, 1H, =C$H$), 5.35 (dd, $J$ = 3.4, 1.5, 1H, OC$H$), 4.77 − 4.76 (m, 1H, =C$H$), 1.57 (d, $J$ = 6.5, 3H, C$H_3$). $^{13}$C NMR (CDCl$_3$): δ = 166.9 (N$C$O), 158.5 ($C$=CH$_2$), 101.8 (C=$C$H$_2$), 83.4 (O$C$H), 21.4 ($C$H$_3$). (CCl$_3$ was too broad to be detected). HRMS (ESI) calcd for C$_6$H$_6$Cl$_3$NO [M+H]$^+$: 213.9593; found 213.9580.

### 5-Ethyl-4-methylene-2-(trichloromethyl)-4,5-dihydrooxazole (2.2c).
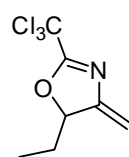
Prepared from **2.1c** (0.91 g) by procedure F, isolated as a yellow oil after purification by column chromatography (petroleum ether/ethyl acetate, 5:1). Yield: 0.79 g (86%). $^1$H NMR (CDCl$_3$): δ = 5.42 − 5.39 (m, 2H, =C$H_2$), 4.76 (t, $J$ = 2.0, 1H, OC$H$), 2.05 − 1.95 (m, 1H, C$H_2$CH$_3$), 1.81 − 1.71 (m, 1H, CH$_2$C$H_3$), 1.01 (t, $J$ = 7.4, 3H, C$H_3$). $^{13}$C NMR (CDCl$_3$): δ = 167.3 (N$C$O), 156.7 ($C$=CH$_2$), 102.1 (C=$C$H$_2$), 87.8 (O$C$H), 28.5 ($C$H$_2$CH$_3$), 7.6 (CH$_2$$C$H$_3$). (CCl$_3$ was too broad to be detected). MS [CI]: $m/z$ (%) = 228 (100) [M+H]$^+$.

### 5-(1-Methylethyl)-4-methylene-2-(trichloromethyl)-4,5-dihydrooxazole (2.2d).[129]

Prepared from **2.1d** (0.97 g) by procedure F, isolated as a yellow oil after purification by column chromatography (petroleum

ether/ethyl acetate, 10:1). Yield: 0.80 g (82%). $^1$H NMR (CDCl$_3$): δ = 5.42 (dd, $J$ = 3.0, 1.4, 1H, =C$H$), 5.26 (dd, $J$ = 5.8, 3.0, 1H, =C$H$), 4.78 − 4.77 (m, 1H, OC$H$), 2.09 − 1.98 (m, 1H, C$H$(CH$_3$)$_2$), 1.11 (d, $J$ = 6.9, 3H, C$H_3$), 0.95 (d, $J$ = 6.9, 3H, C$H_3$). $^{13}$C NMR (CDCl$_3$): δ = 167.4 (N$C$O), 155.9 ($C$=CH$_2$), 102.6 (C=$C$H$_2$), 91.4 (O$C$H), 33.8 ($C$H(CH$_3$)$_2$), 18.1 ($C$H$_3$), 14.8 ($C$H$_3$). (CCl$_3$ was too broad to be detected). HRMS (ESI) calcd for C$_8$H$_{10}$Cl$_3$NO [M+H]$^+$: 241.9906; found 241.9911.

**5,5-Dimethyl-4-methylene-2-(trichloromethyl)-4,5-dihydrooxazole (2.2f).**

Prepared from **2.1f** (0.91 g) by procedure F, isolated as a yellow oil after purification by column chromatography (petroleum ether/ethyl acetate, 8:1). Yield: 0.72 g (79%). $^1$H NMR (CDCl$_3$): δ = 5.31 (d, $J$ = 1.5, 1H, =C$H$), 4.71 (d, $J$ = 1.5, 1H, =C$H$), 1.59 (s, 6H, C$H_3$). $^{13}$C NMR (CDCl$_3$): δ = 165.3 (N$C$O), 162.0 ($C$=CH$_2$), 100.9 (C=$C$H$_2$), 91.8 ($C$(CH$_3$)$_2$), 27.7 (C($C$H$_3$)$_2$). (CCl$_3$ was too broad to be detected). HRMS (ESI) calcd for C$_7$H$_8$Cl$_3$NO [M+H]$^+$: 229.9720; found 229.9730.

**(Z)-4-Trimethylsilylmethylene-2-(trichloromethyl)-4,5-dihydrooxazole (Z)-2.2j.**

Prepared by procedure F from **2.1j** (1.09 g), but with [Ag(Py)$_2$]OTf (166.0 mg, 0.4 mmol, 0.2 eq.) in MeCN at 60 °C for 7 h. Isolated as a yellow oil after purification by column chromatography (petroleum ether/ethyl acetate, 10:1). Yield: 0.79 g (74%). $^1$H NMR (CDCl$_3$): δ = 5.28 (t, $J$ = 2.6, 1H, =C$H$), 5.14 (d, $J$ = 2.6, 2H, C$H_2$), 0.18 (s, 9H, Si(C$H_3$)$_3$). $^{13}$C NMR (CDCl$_3$): δ = 168.5 (N$C$O), 159.2

($C$=CSi), 116.2 (C=$C$Si), 75.7 (O$CH_2$), -0.2 (Si($CH_3$)$_3$). ($CCl_3$ was too broad to be detected). HRMS (ESI) calcd for $C_8H_{12}Cl_3NOSi$ [M]$^+$: 272.9724; found 272.9844.

**(Z)-4-Bromomethylene-2-(trichloromethyl)-4,5-dihydrooxazole (Z)-2.2k.**

Prepared by procedure F from **2.1k** (1.12 g), but with and [Ag(Ac-Py)$_2$]PF$_6$ (19.8 mg, 0.04 mmol, 0.01 eq.) as catalyst and a reaction time of 30 min. Isolated as a white crystalline solid after purification by column chromatography (petroleum ether/ethyl acetate, 8:1). Yield: 1.06 g (95 %). $^1$H NMR (CDCl$_3$): δ = 5.92 (t, $J$ = 2.8, 1H, =C$H$), 5.24 (d, $J$ = 2.8, 2H, C$H_2$). $^{13}$C NMR (CDCl$_3$): δ = 169.7 (N$C$O), 149.8 ($C$=CBr), 92.4 (C=$C$Br), 74.8 (O$CH_2$). ($CCl_3$ was too broad to be detected). HRMS (ESI) calcd for $C_5H_3BrCl_3NO$ [M+H]$^+$: 279.8521; found 279.8533.

**2-(Trichloromethyl)-4-methylene-5,6-dihydro-4$H$-1,3-oxazine (2.9a).**[129]

Prepared by procedure F from **2.8a** (0.86 g), isolated as a light yellow oil after purification by column chromatography (petroleum ether/ethyl acetate, 5:1). Yield: 0.65 g (76%). $^1$H NMR (CDCl$_3$): δ = 5.29 (s, 1H, =C$H$), 4.86 (s, 1H, =C$H$), 4.47 − 4.44 (m, 2H, O$CH_2$), 2.64 − 2.61 (m, 2H, C$H_2$C=). $^{13}$C NMR (CDCl$_3$): δ = 153.74 (N$C$O), 140.99 (N$C$=C), 111.47 (NC=$C$), 67.40 (O$CH_2$), 26.21 ($C$H$_2$C=). ($CCl_3$ was too broad to be detected). HRMS (ESI) calcd for $C_6H_6Cl_3NO$ [M+H]$^+$: 215.9564; found 215.9571.

**2-(Trichloromethyl)-4-methylene-6-methyl-5,6-dihydro-1,3-oxazine (2.9b).**

Prepared by procedure F from **2.8b** (0.91 g), Isolated as a yellow oil after purification by column chromatography (petroleum ether/ethyl acetate, 5:1). Yield: 0.85 g (93%). $^{1}$H NMR (CDCl$_3$):

δ = 5.31 (s, 1H =C*H*), 4.85 (s, 1H, =C*H*), 4.59 − 4.51 (m, 1H, OC*H*), 2.68 − 2.63 (m, 1H, C*H$_2$*C=), 2.35 − 2.29 (m, 1H, C*H$_2$*C=), 1.42 (d, $J$ = 6.4, 3H, C*H$_3$*). $^{13}$C NMR (CDCl$_3$): δ = 153.9 (N*C*O), 141.2 (N*C*=C), 111.8 (NC=*C*), 74.4 (O*C*H), 33.0 (*C*H$_2$), 20.0 (*C*H$_3$). (CCl$_3$ was too broad to be detected). HRMS (ESI) calcd for C$_7$H$_8$Cl$_3$NO [M+H]$^+$: 227.9750; found 227.9752.

**2-(Trichloromethyl)-4-methylene-6-ethyl-5,6-dihydro-1,3-oxazine (2.9c).**

Prepared by procedure F from **2.8c** (0.97 g), isolated as a light yellow oil after purification by column chromatography (petroleum ether/ethyl acetate, 5:1). Yield: 0.88 g (91%). $^{1}$H NMR (CDCl$_3$): δ = 5.28 (s, 1H, =C*H*), 4.84 (s, 1H, =C*H*), 4.34 − 4.30 (m, 1H), 2.64 − 2.60 (m, 1H, OC*H*), 2.38 −2.32 (m, 1H, C*H$_2$*C=), 1.79 − 1.67 (m, 2H, C*H$_2$*CH$_3$), 1.04 (t, $J$ = 7.5, 3H, CH$_2$C*H$_3$*). $^{13}$C NMR (CDCl$_3$): δ = 154.0 (N*C*O), 141.4 (N*C*=C), 111.6 (NC=*C*), 79.3 (O*C*H), 31.0 (*C*H$_2$C=), 27.2 (*C*H$_2$CH$_3$), 9.1 (CH$_2$*C*H$_3$). (CCl$_3$ was too broad to be detected). HRMS (ESI) calcd for C$_8$H$_{10}$Cl$_3$NO [M+H]$^+$: 243.9877; found 243.9888.

## 2-(Trichloromethyl)-4-methylene-6-phenyl-5,6-dihydro-1,3-oxazine (2.9d).[129]

Prepared by procedure F from **2.8d** (1.16 g), isolated as a light yellow solid after purification by column chromatography (petroleum ether/ethyl acetate, 5:1). Yield: 1.05 g (90%). $^1$H NMR (CDCl$_3$): δ = 7.45 − 7.37 (m, 5H, C*H*-aromatic), 5.38 − 5.34 (m, 2H, =C*H$_2$*), 4.92 (d, *J* = 1.7, 1H, OC*H*), 2.90 − 2.85 (m, 1H, C*H$_2$*C=), 2.67 − 2.60 (m, 1H, C*H$_2$*C=). $^{13}$C NMR (CDCl$_3$): δ = 154.2 (N*C*O), 141.4 (*C*H-aromatic), 138.2 (*C*H-aromatic), 128.9 (*C*H-aromatic), 125.7 (*C*H-aromatic), 112.0 (N*C*=C), 92.0 (NC=*C*), 79.2 (O*C*H), 34.1 (*C*H$_2$C=). (*C*Cl$_3$ was too broad to be detected). HRMS (ESI) calcd for C$_{12}$H$_{10}$Cl$_3$NO [M+H]$^+$: 289.9906; found 289.9894.

## 2-(Trichloromethyl)-4-methylene-6-(4-chlorophenyl)-5,6-dihydro-1,3-oxazine (2.9e).[129]

Prepared by procedure F from **2.8e** (1.30 g), isolated as an orange oil after purification by column chromatography (petroleum ether/ethyl acetate, 8:1). Yield: 1.13 g (87%). $^1$H NMR (CDCl$_3$): δ = 7.41 − 7.39 (m, 2H, C*H*-aromatic), 7.38 − 7.30 (m, 2H, C*H*-aromatic), 5.39 (d, *J* = 1.6, 1H, =C*H*), 5.33 (dd, *J* = 10.4, 3.6, 1H, =C*H*), 4.93 (d, *J* = 1.6, 1H, OC*H*), 2.89 − 2.84 (m, 1H, C*H$_2$*C=), 2.59 (m, 1H, C*H$_2$*C=). $^{13}$C NMR (CDCl$_3$): δ = 153.9 (N*C*O), 141.0 (*C*H-aromatic), 136.7 (*C*H-aromatic), 134.8 (*C*H-aromatic), 129.1 (*C*H-aromatic), 127.2 (N*C*=C), 112.4 (NC=*C*), 91.9 (*C*Cl$_3$), 78.4 (O*C*H), 33.9 (*C*H$_2$C=). HRMS (ESI) calcd for C$_{12}$H$_9$Cl$_4$NO [M+H]$^+$: 325.9487; found 325.9491.

## 2-(Trichloromethyl)-4-methylene-6-(4-trifluoromethylphenyl)-5,6-dihydro-1,3-oxazine (2.9f).

Prepared by procedure F from **2.8f** (1.43 g), isolated as a yellow oil after purification by column chromatography (petroleum ether/ethyl acetate, 8:1). Yield: 1.00 g (70%). $^1$H NMR (CDCl$_3$): $\delta$ = 7.69 (d, $J$ = 8.2, 2H, C$H$-aromatic), 7.51 (d, $J$ = 8.2, 2H, C$H$-aromatic), 5.44 – 5.41 (m, 2H, =CH$_2$), 4.95 (d, $J$ = 1.7, 1H, OC$H$), 2.91 (dd, $J$ = 15.2, 3.7, 1H, C$H_2$C=), 2.65 – 6.57 (m, 1H, C$H_2$C=). $^{13}$C NMR (CDCl$_3$): $\delta$ = 153.7 (N$C$O), 142.1 ($C$H-aromatic), 140.6 ($C$H-aromatic), 131.0 (q, $J$ = 33.0, $C$F$_3$), 126.0 ($C$H-aromatic), 125.9 ($C$H-aromatic), 122.5 (N$C$=C), 112.7 (NC=$C$), 91.8 ($C$Cl$_3$), 78.3 (O$C$H), 33.9 ($C$H$_2$C=). HRMS (ESI) calcd for C$_{13}$H$_9$Cl$_3$F$_3$NO [M+H]$^+$: 357.9780; found 357.9776.

## (Z)-2-(Trichloromethyl)-4-(trimethylsilyl)methylene-5,6-dihydro-1,3-oxazine (Z)-2.9h.

Prepared by procedure F from **2.8h** (1.15 g), but with [Ag(Py)$_2$]OTf (0.33 g, 0.8 mmol, 0.2 eq.) in acetone at reflux for 8 h. Isolated as a light yellow oil after purification by column chromatography (petroleum ether/ethyl acetate, 8:1). Yield: 0.81 g (71%). $^1$H NMR (CDCl$_3$): $\delta$ = 5.30 (t, $J$ = 1.1, 1H, =CH), 4.44 (t, $J$ = 6.1, 2H, OC$H_2$), 2.61 (td, $J$ = 6.1, 1.1, 2H, C$H_2$C=), 0.17 (s, 9H, Si(C$H_3$)$_3$). $^{13}$C NMR (CDCl$_3$): $\delta$ = 152.3 (N$C$O), 146.9 ($C$=CSi), 127.1 (C=$C$Si), 92.4 ($C$Cl$_3$), 67.6

(OCH$_2$), 28.8 (CH$_2$C=), -0.1 (Si(CH$_3$)$_3$). HRMS (ESI) calcd for C$_9$H$_{14}$Cl$_3$NOSi [M+H]$^+$: 285.9988; found 285.9994.

**(Z)-2-(Trichloromethyl)-4-bromomethylene-5,6-dihydro-1,3-oxazine (Z)-2.9i.**

Prepared by procedure F from **2.8i** (1.17 g), but with [Ag(Ac-Py)$_2$]PF$_6$ (19.8 mg, 0.04 mmol, 0.01 eq.) as catalyst and a reaction time of 1 h. Isolated as a white solid after purification by column chromatography (petroleum ether/ethyl acetate, 8:1). Yield: 1.11 g (95%). $^1$H NMR (CDCl$_3$): δ 6.00 (t, $J$ = 1.2, 1H, =CH), 4.45 (t, $J$ = 6.1, 2H, OCH$_2$), 2.63 (td, $J$ = 6.1, 1.2, 2H, CH$_2$C=). $^{13}$C NMR (CDCl$_3$): δ = 155.3 (NCO), 136.9 (C=CBr), 102.5 (C=CBr), 91.7 (CCl$_3$), 67.1 (OCH$_2$), 26.4 (CH$_2$C=). HRMS (ESI) calcd for C$_6$H$_5$BrCl$_3$NO [M+H]$^+$: 291.8698; found 291.8706.

**General procedure for trapping of organosilver(I) intermediates with electrophiles (Procedure G):**

To a solution of **2.1a** (0.80 g, 4.0 mmol, 1.0 eq.) or **2.8a** (0.86 g, 4.0 mmol, 1.0 eq.) in acetone (10 mL) was added N-bromosuccinimide (0.85 g, 4.8 mmol, 1.2 eq.) or N-chlorosuccinimide (0.64 g, 4.8 mmol, 1.2 eq.). The resulting mixture was cooled to 0 °C before the addition of silver(I) trifluoromethanesulfonate (102.7 mg, 0.4 mmol, 10 mol%). The reaction mixture was allowed to rise to room temperature, and stirred for another 6 h. The solvent was removed *in vacuo*, and the residue extracted with 20 mL of petroleum ether/ethyl acetate (8:1). The resulting solution was concentrated *in*

*vacuo* and purified by column chromatography on silica, using petroleum ether/ethyl acetate (8:1) as eluting solvent.

**(*E*)-4-Bromomethylene-2-(trichloromethyl)-4,5-dihydrooxazole  (*E*)-2.2k.**

Prepared by procedure G. Yield: 0.79 g (71%). White solid. mp 60 – 65 °C. $^1$H NMR (CDCl$_3$): δ = 6.56 (t, $J$ = 3.5, 1H, =C*H*), 5.21 (d, $J$ = 3.5, 2H, OC*H$_2$*). $^{13}$C NMR (CDCl$_3$): δ = 169.2 (N*C*O), 151.7 (N*C*=C), 97.5 (NC=*C*), 75.8 (*C*H$_2$). (CCl$_3$ was too broad to be detected). MS [CI]: m/z (%) = 312 (100), 192 (38), 329 (19). (M$^+$ not observed)

**(*E*)-4-Chloromethylene-2-(trichloromethyl)-4,5-dihydrooxazole  (*E*)-2.2l.**

Prepared by procedure G. Yield: 0.32 g (34%). White solid. mp 59 – 60 °C. $^1$H NMR (CDCl$_3$): δ = 6.52 (t, $J$ = 3.5, 1H, =C*H*), 5.34 (d, $J$ = 3.5, 2H, OC*H$_2$*). $^{13}$C NMR (CDCl$_3$): δ = 168.7 (N*C*O), 149.8 (N*C*=C), 109.5 (NC=*C*), 74.4 (*C*H$_2$). (CCl$_3$ was too broad to be detected). MS [CI]: m/z (%) = 236 (100), 179 (11).

**(*E*)-2-(Trichloromethyl)-4-bromomethylene-5,6-dihydro-1,3-oxazine  (*E*)-2.9i.**

Prepared by procedure G. Yield: 0.29 g (25%). White solid. Single crystals suitable for X-ray diffraction studies were obtained from a saturated solution of **(*E*)-2.9i** in petroleum ether/ethyl acetate (8:1) at -20 °C. mp 98 – 101 °C. $^1$H NMR (CDCl$_3$): δ = 6.64 (d, $J$ = 1.4, 1H, =C*H*Br), 4.45 (t, $J$ = 6.1, 2H, OC*H$_2$*), 2.77 (td, $J$ = 6.1, 1.4, 2H, C*H$_2$*C=). $^{13}$C NMR (CDCl$_3$): δ = 153.2 (N*C*O), 139.0 (*C*=CBr), 107.5

(C=*C*Br), 91.5 (*C*Cl$_3$), 66.3 (O*C*H$_2$), 23.5 (*C*H$_2$C=). MS [CI]: m/z (%) = 294

(100), 236 (12).

**(*E*)-2-(Trichloromethyl)-4-chloromethylene-5,6-dihydro-1,3-oxazine (*E*)-2.9j.**

Prepared by procedure G. Yield: 0.11 g (11%). White solid. Single crystals suitable for X-ray diffraction studies were obtained from a saturated solution of **(*E*)-2.9j** in petroleum ether/ethyl acetate (8:1) at -20 °C. mp 80 – 83 °C. ^{1}H NMR (CDCl$_3$): δ = 6.50 (d, *J* = 1.8, 1H, =C*H*Cl), 4.44 (t, *J* = 6.1, 2H, OC*H*$_2$), 2.78 (td, *J* = 6.1, 1.8, 2H, C*H*$_2$C=). ^{13}C NMR (CDCl$_3$): δ = 153.2 (N*C*O), 137.2 (*C*=CHCl), 117.7 (C=*C*HCl), 91.6 (*C*Cl$_3$), 66.0 (O*C*H$_2$), 21.7 (*C*H$_2$C=). MS [CI]: m/z (%) = 250 (100), 214 (9), 193 (8).

## 6.2 Compounds used in Chapter 3

**Ethyl-2-chloro-2-oxoacetate.**[253]

To oxalyl chloride (1.72 mL, 20 mmol, 2.0 eq.) at 0 °C was added ethanol (10 0.58 mL, 10 mmol, 1.0 eq.) dropwise with a syringe pump over 1 h. Upon completion of addition, the mixture was allowed to warm to room temperature over 2 h. The crude material was distilled (lit. [254] 132 – 135 °C at 760 Torr) under N$_2$ to give the desired product as a colorless oil, which was used immediately in the reaction with propargylamine. Yield: 0.29 g (11%).

**Ethyl potassium malonate.**[255]

To a 100 mL round bottomed flask was added diethyl malonate (3.0 mL, 20 mmol, 1.0 eq.) and 13 mL of ethanol. A solution of potassium hydroxide (1.12 g, 20 mmol, 1.0 eq.) in 13 mL of ethanol was added dropwise with stirring. A large amount of white precipitate was formed. The suspension was stirred for 2 h at room temperature, and allowed to stand overnight. The resulting mixture was refluxed for another 1 h, and was filtered hot. The filtrate obtained was cooled to 0 °C in the freezer overnight, and the resulting colorless crystals were filtered off, washed with diethyl ether and dried *in vacuo*. Yield: 2.40 g (71%). $^1$H NMR (D$_2$O): δ = 4.18 (q, $J$ = 7.2, 2H, C$H_2$), 3.29 (s, 2H, C$H_2$CH$_3$), 1.26 (t, $J$ = 7.1, 3H, CH$_2$C$H_3$). $^{13}$C NMR (D$_2$O): δ = 174.3 (*C*=O), 171.5 (*C*=O), 62.06 (*C*H$_2$), 44.67 (*C*H$_2$CH$_3$), 13.21 (CH$_2$*C*H$_3$).

**2-Ethoxycarbonylacetyl chloride.**

Prepared by a modified literature procedure.[256] Ethyl potassium malonate (1.70 g, 10 mmol, 1.0 eq.) was suspended in CH$_2$Cl$_2$ (20 mL) at 0 °C under a positive pressure of N$_2$. Oxalyl chloride (1.0 mL, 12 mmol, 1.2 eq.) was then added dropwise over 5 min followed by DMF (3-5 drops). The resulting solution was stirred for 1 h at 0 °C then at room temperature for 1 h. The resulting mixture was filtered, and the solvent removed from the filtrate to give a red oil, which was distilled under reduced pressure (b.p. 70 °C at 16 Torr)[257] to give a colorless oil, which was used immediately in the reaction with propargylamine. Yield: 0.62 g (41%).

**General procedure for the synthesis of substrates 3.1a-I (Procedure H):**

To a solution of propargylic amine (10 mmol, 1.0 eq.) in $CH_2Cl_2$, triethylamine (1.4 mL, 10 mmol, 1.0 eq.) and 4-dimethylaminopyridine (24.4 mg, 0.2 mmol, 0.02 eq.) were added. The resulting mixture was cooled to 0 °C, and the acid chloride (10 mmol, 1.0 eq.) was added. The mixture was stirred for 30 min at 0 °C and 3 h at room temperature. $H_2O$ (15 mL) was added, and the aqueous layer extracted with another 3 × 15 mL of $CH_2Cl_2$. The combined organic extracts were washed with saturated $NaHCO_3$, $H_2O$ and brine, dried over $Na_2SO_4$ and concentrated *in vacuo*. The crude product was purified by column chromatography on silica.

*N*-(Prop-2-ynyl)benzamide (3.1a).[258]

Prepared by procedure H from benzoyl chloride (1.2 mL) and propargylamine (0.64 mL), isolated as a white crystalline solid after purification by column chromatography (petroleum ether/ethyl acetate, 1:1). Yield: 1.51 g (95%). $^1$H NMR (CDCl$_3$): δ = 7.80 − 7.77 (m, 2H, C*H*-aromatic), 7.56 − 7.47 (m, 1H, C*H*-aromatic), 7.49 − 7.40 (m, 2H, C*H*-aromatic), 6.29 (br s, 1H, N*H*), 4.26 (dd, *J* = 5.1, 2.5, 2H, C*H*$_2$≡CH), 2.29 (t, *J* = 2.5, 1H, CH$_2$≡C*H*). $^{13}$C NMR (CDCl$_3$): δ = 167.8 (*C*=O), 133.9 (*C*H-aromatic), 132.0 (*C*H-aromatic), 128.8 (*C*H-aromatic), 127.5 (*C*H-aromatic), 79.9 (*C*≡CH), 71.8 (C≡*C*H), 29.9 (*C*H$_2$C≡CH). ν$_{max}$/cm$^{-1}$: 3289 (N−H), 1638 (C=O).

***N*-(Prop-2-ynyl)acetamide (3.1b).**[153]

Prepared by procedure H from acetyl chloride (0.71 mL) and propargylamine (0.64 mL), isolated as a white solid after purification by column chromatography ($CH_2Cl_2$/ethyl acetate, 1:1). Yield: 0.16 g (16%). ^{1}H NMR ($CDCl_3$): δ = 5.87 (br s, 1H, N*H*), 4.04 (dd, *J* = 5.1, 2.5, 2H, C*H*$_2$≡CH), 2.23 (t, *J* = 2.5, 1H, CH$_2$≡C*H*), 2.01 (s, 3H, C*H*$_3$). ^{13}C NMR ($CDCl_3$): δ = 169.8 (*C*=O), 79.4 (*C*≡CH), 71.6 (C≡*C*H), 29.2 (*C*H$_2$C≡CH), 23.0 (*C*H$_3$). $\nu_{max}$/cm$^{-1}$: 3226 (N−H), 1632 (C=O).

***N*-(Prop-2-ynyl)pivalamide (3.1c).**[259]

Prepared by procedure H from trimethylacetyl chloride (1.2 mL) and propargylamine (0.64 mL), isolated as a white solid after purification by column chromatography ($CH_2Cl_2$/ethyl acetate, 9:1). Yield: 1.14 g (82%). ^{1}H NMR ($CDCl_3$): δ = 5.86 (br s, 1H, N*H*), 4.02 (dd, *J* = 5.0, 2.6, 2H, C*H*$_2$≡CH), 2.22 (t, *J* = 2.6, 1H, CH$_2$≡C*H*), 1.19 (s, 9H, C(C*H*$_3$)$_3$). ^{13}C NMR ($CDCl_3$): δ = 178.0 (*C*=O), 79.8 (*C*≡CH), 71.5 (C≡*C*H), 38.6 (*C*(CH$_3$)$_3$), 29.3 (*C*H$_2$C≡CH), 27.4 (C(*C*H$_3$)$_3$). $\nu_{max}$/cm$^{-1}$: 3263 (N−H), 1634 (C=O).

***N*-(Prop-2-ynyl)cinnamamide (3.1d).**[260]

Prepared by procedure H from cinnamoyl chloride (1.67 g) and propargylamine (0.64 mL), isolated as a white solid after purification by column chromatography (petroleum ether/ethyl acetate, 1:1). Yield: 1.02 g (55%). ^{1}H NMR ($CDCl_3$): δ = 7.67 (d, *J* = 15.7, 1H, C*H*CO), 7.49 − 7.47 (m, 2H, C*H*-aromatic), 7.39 −7.28 (m, 3H,

C*H*-aromatic), 6.48 (d, *J* = 15.7, 1H, C*H*=CHCO), 6.44 (br s, 1H, N*H*), 4.20

(dd, *J* = 5.3, 2.5, 2H, C*H₂*C≡), 2.25 (t, *J* = 2.5, 1H, C≡C*H*). $^{13}$C NMR (CDCl₃):

δ = 165.7 (*C*=O), 141.7 (*C*HCO), 134.6 (*C*H-aromatic), 129.8 (*C*H-aromatic),

128.8 (*C*H-aromatic), 127.8 (*C*H-aromatic), 119.9 (*C*H=CHCO), 79.5 (*C*≡CH),

71.7 (C≡*C*H), 29.4 (*C*H₂C≡CH). $\nu_{max}$/cm$^{-1}$: 3216 (N–H), 1609 (C=O).


*N*-(Prop-2-ynyl)acrylamide (3.1e).[261]

Prepared by procedure H from cinnamoyl chloride (0.81 mL) and propargylamine (0.64 mL), isolated as a white

solid after purification by column chromatography (CH₂Cl₂/ethyl acetate, 1:1).

Yield: 0.55 g (50%). $^{1}$H NMR (CDCl₃): δ = 6.32 (dd, *J* = 17.0, 1.3, 1H,

C*H₂*=CH), 6.11 (dd, *J* = 17.0, 10.3, 1H, C*H₂*=CH), 5.91 (br s, 1H, N*H*), 5.69

(dd, *J* = 10.3, 1.3, 1H, CH₂=C*H*), 4.13 (dd, *J* = 5.2, 2.6, 2H, C*H₂*C≡CH), 2.25

(t, *J* = 2.6, 1H, C≡C*H*). $^{13}$C NMR (CDCl₃): δ = 165.1 (*C*=O), 130.0 (*C*H₂=CH),

127.4 (*C*H₂=CH), 79.2 (*C*≡CH), 71.8 (C≡*C*H), 29.3 (*C*H₂C≡CH). $\nu_{max}$/cm$^{-1}$:

3251 (N–H), 1620 (C=O).


**Prop-2-ynylcarbamic acid ethyl ester (3.1f).**[259]

Prepared by procedure H from ethyl chloroformate (0.96 mL) and propargylamine (0.64 mL), isolated as a light

yellow oil after purification by column chromatography (petroleum ether/ethyl

acetate, 7:3). Yield: 0.72 g (57%). $^{1}$H NMR (CDCl₃): δ = 5.06 (br s, 1H, N*H*),

4.11 (q, *J* = 7.1, 2H, C*H₂*CH₃), 3.94 (dd, *J* = 5.7, 2.5, 2H, C*H₂*≡CH), 2.22 (t, *J*

= 2.5, 1H, CH₂≡C*H*), 1.21 (t, *J* = 7.1, 3H, CH₂C*H₃*). $^{13}$C NMR (CDCl₃): δ =

156.1 ($C$=O), 79.8 ($C$≡CH), 71.3 (C≡$C$H), 61.2 ($C$H$_2$CH$_3$), 30.6 ($C$H$_2$C≡CH), 14.5 (CH$_2$$C$H$_3$). $v_{max}$/cm$^{-1}$: 3296 (N−H), 1694 (C=O).
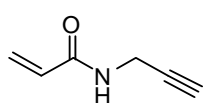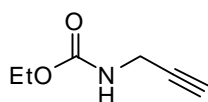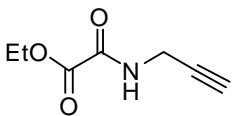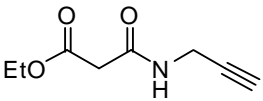
**Ethyl oxo(prop-2-yn-ylamino)acetate (3.1g).**[153]

Prepared by procedure H from 2-ethoxycarbonylacetyl chloride (1.51 g) and propargylamine (0.64 mL), isolated as a white solid after purification by column chromatography (CH$_2$Cl$_2$/methanol, 95:5) and trituration with diethyl ether. Yield: 0.67 g (43%). $^1$H NMR (CDCl$_3$): δ = 7.29 (br s, 1H, N$H$), 4.35 (q, $J$ = 7.2, 2H, C$H_2$CH$_3$), 4.13 (dd, $J$ = 5.7, 2.6, 2H, C$H_2$≡CH), 2.29 (t, $J$ = 2.6, 1H, CH$_2$≡C$H$), 1.38 (t, $J$ = 7.2, 3H, CH$_2$C$H_3$). $^{13}$C NMR (CDCl$_3$): δ = 160.0 ($C$=O), 156.1 ($C$=O), 77.9 ($C$≡CH), 72.5 (C≡$C$H), 63.4 ($C$H$_2$CH$_3$), 29.6 ($C$H$_2$C≡CH), 13.9 (CH$_2$$C$H$_3$). $v_{max}$/cm$^{-1}$: 3276 (N−H), 1736 (C=O), 1679 (C=O).

**Ethyl 3-oxo-3-(prop-2-yn-1-ylamino)propanoate (3.1h).**[154]

Prepared by procedure H from 2-ethoxycarbonylacetyl chloride (1.51 g) and propargylamine (0.64 mL), isolated as an off-white solid after purification by column chromatography (CH$_2$Cl$_2$/ethyl acetate, 7:3). Yield: 1.05 g (62%). $^1$H NMR (CDCl$_3$): δ = 7.46 (br s, 1H, N$H$), 4.21 (q, $J$ = 7.1, 2H, C$H_2$CH$_3$), 4.09 (dd, $J$ = 5.2, 2.6, 2H, C$H_2$C≡C), 3.33 (s, 2H, COC$H_2$), 2.24 (t, $J$ = 2.5, 1H, C≡C$H$), 1.29 (t, $J$ = 7.1, 3H, CH$_2$C$H_3$). $^{13}$C NMR (CDCl$_3$): δ = 169.4 ($C$O), 164.7 ($C$O), 79.1 ($C$≡CH), 71.6 (C≡$C$H), 61.7 ($C$H$_2$CH$_3$), 40.7 (CO$C$H$_2$CO), 29.1 ($C$H$_2$C≡CH), 14.0 (CH$_2$$C$H$_3$). $v_{max}$/cm$^{-1}$: 3282 (N−H), 1732 (C=O), 1643 (C=O).

**_N_-(α,α-Dimethylpropargyl)-1-benzenecarboxamide (3.1i).**[156]
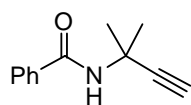
Prepared by procedure H from benzoyl chloride (1.2 mL) and 2-methyl-3-butyn-2-amine (1.1 mL), isolated as a white solid after purification by column chromatography (CH$_2$Cl$_2$/ethyl acetate, 9:1). Yield: 1.60 g (85%). $^1$H NMR (CDCl$_3$): δ = 7.79 – 7.71 (m, 2H, C_H_-aromatic), 7.53 – 7.45 (m, 1H, C_H_-aromatic), 7.42 – 7.38 (m, 2H, C_H_-aromatic), 6.26 (br s, 1H N_H_), 2.38 (s, 1H, C≡C_H_), 1.76 (s, 6H, C(C_H_$_3$)$_2$). $^{13}$C NMR (CDCl$_3$): δ = 166.4 (_C_O), 134.8 (_C_H-aromatic), 131.4 (_C_H-aromatic), 128.5 (_C_H-aromatic), 126.8 (_C_H-aromatic), 87.1 (_C_≡CH), 69.3 (C≡_C_H), 48.0 (_C_(CH$_3$)$_2$), 29.0 (C(_C_H$_3$)$_2$). ν$_{max}$/cm$^{-1}$: 3286 (N−H), 1639 (C=O).

**5,5-Diethyl-1,3-di(prop-2-yn-1-yl)pyrimidin-2,4,6-(1_H_,3_H_,5_H_)-trione.**[154]
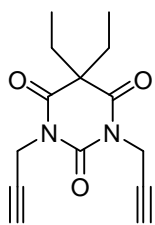
Propargyl bromide (80 wt% solution in toluene, 7.6 mL, 44 mmol, 2.2 eq.) and sodium hydroxide (0.88 g, 22 mmol, 1.1 eq.) were added to a solution of sodium barbital (4.12 g, 20 mmol, 1.0 eq.) in 40 mL of ethanol/water (1:1). The resulting mixture was stirred at room temperature for 48 h, before all the volatile components were removed _in vacuo_. The residue was extracted with CH$_2$Cl$_2$ (3 × 50 mL). The combined organic layers were dried over MgSO$_4$, and the solvent was removed _in vacuo_ to afford a brown oil. 15 mL of ethanol was added, and the resulting mixture cooled to 0 °C overnight. The colorless crystals that were obtained were filtered off and dried _in vacuo_. Yield: 3.05 g (59%). Colorless crystals. $^1$H NMR (CDCl$_3$): δ = 4.70 (d, _J_ = 2.5, 4H, C_H_$_2$C≡CH), 2.22 (t, _J_ = 2.5, 2H, C≡C_H_), 2.08 (q, _J_ = 7.4, 4H, C_H_$_2$CH$_3$), 0.81 (t, _J_ = 7.4, 6H, CH$_2$C_H_$_3$).

$^{13}$C NMR (CDCl$_3$): δ = 170.8 (C=O), 149.3 (C=O), 77.3 (C≡CH), 71.5 (C≡CH), 58.4 (C(CH$_2$CH$_3$)$_2$), 33.5 (CH$_2$C≡CH), 31.2 (CH$_2$CH$_3$), 9.4 (CH$_2$CH$_3$).

**2,2-Diethyl-*N,N'*-di(prop-2-yn-1-yl)malonamide (3.1j).**
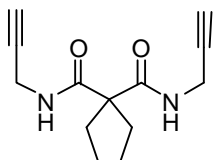
Prepared by a modified literature procedure.[154] 5,5-Diethyl-1,3-di(prop-2-yn-1-yl)pyrimidin-2,4,6-(1*H*,3*H*,5*H*)-trione (1.30 g, 5.0 mmol, 1.0 eq.) was suspended in ethanol (10 mL) and as solution of potassium hydroxide (0.56 g, 10 mmol, 2.0 eq.) in ethanol (20 mL) was added. The resulting mixture was stirred for 1 h at room temperature, and the solvent removed *in vacuo* to give a yellow oil. The resulting oil was dissolved in 25 mL of 0.5 M HCl, and extracted with CH$_2$Cl$_2$ (3 × 25 mL). The combined organic layers were dried over MgSO$_4$, and the solvent removed *in vacuo*. The crude product was purified by column chromatography on silica (petroleum ether/ethyl acetate, 7:3 then 1:1) to afford the desired product as a white solid. Yield: 0.78 g (67%). $^1$H NMR (CDCl$_3$): δ = 7.48 (s, 2H, N*H*), 4.07 (dd, *J* = 5.3, 2.6, 4H, C*H*$_2$C≡CH), 2.22 (t, *J* = 2.5, 2H, C≡C*H*), 1.90 (q, *J* = 7.4, 4H, C*H*$_2$CH$_3$), 0.85 (t, *J* = 7.4, 6H, CH$_2$C*H*$_3$). $^{13}$C NMR (CDCl$_3$): δ = 172.5 (C=O), 79.0 (C≡CH), 71.1 (C≡CH), 57.8 (C(CH$_2$CH$_3$)$_2$), 30.5 (CH$_2$C≡CH), 28.9 (CH$_2$CH$_3$), 9.0 (CH$_2$CH$_3$). ν$_{max}$/cm$^{-1}$: 3290 (N–H), 1660 (C=O), 1622 (C=O).

**N1,N3-Di(prop-2-ynyl)isophthalamide (3.1k).**
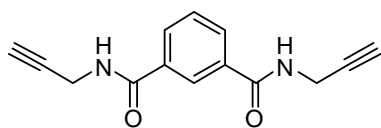
Prepared by a modified literature procedure. [262] A mixture of isophthaloyl chloride (2.03 g, 10 mmol, 1.0 eq.), triethylamine (3.0 mL, 22 mmol, 2.2 eq.) and propargylamine (1.4 mL, 22 mmol, 2.2 eq.) in 90 mL of $CH_2Cl_2$ was stirred for 3 days at room temperature. The white precipitate that appeared was filtered off and dried *in vacuo*. The filtrate was diluted with 30 mL of 1.0 M HCl solution and extracted with $2 \times 75$ mL of $CH_2Cl_2$. The combined organic extracts were dried over $MgSO_4$ and the solvent removed *in vacuo* to afford a light gray solid, which was combined with the white solid obtained earlier. Purification by column chromatography on silica ($CH_2Cl_2$/methanol, 95:5) afforded the desired product as white needles. Yield: 2.00 g (83%). $^1$H NMR (DMSO-$d_6$): δ = 9.05 (t, $J$ = 5.5, 2H, C$H$-aromatic), 8.33 (t, $J$ = 1.7, 1H, C$H$-aromatic), 7.99 (dd, $J$ = 7.6, 1.7, 2H, N$H$), 7.58 (t, $J$ = 7.7, 1H, C$H$-aromatic), 4.07 (dd, $J$ = 5.5, 2.4, 4H, C$H_2$C≡CH), 3.14 (t, $J$ = 2.4, 2H, C≡C$H$). NMR (DMSO-$d_6$): δ = 165.5 (*C*H-aromatic), 134.1 (*C*H-aromatic), 130.1 (*C*H-aromatic), 128.6 (*C*H-aromatic), 126.4 (*C*H-aromatic), 81.2 (*C*≡CH), 73.0 (C≡*C*H), 28.6 (*C*H$_2$C≡CH). $\nu_{max}$/cm$^{-1}$: 3290 (N–H), 1660 (C=O), 1622 (C=O). $\nu_{max}$/cm$^{-1}$: 3302 (N–H), 3237 (N–H), 1642 (C=O).

**General procedure for the synthesis of propargyl alcohols (Procedure I):**

To a solution of alkyne (11 mmol, 1.1 eq.) in anhydrous THF (35 mL) at -78 °C under $N_2$ was added $^n$BuLi (1.6 M solution in hexanes, 6.6 mL, 10.5 mmol, 1.05 eq.). After stirring at -78 °C for 15 min, aldehyde (10 mmol, 1.0 eq.) was added. The reaction mixture was allowed to warm to room temperature and

stirred for another 1 h, and quenched with 30 mL of saturated aq. NH₄Cl solution. The resulting mixture was extracted with $CH_2Cl_2$ (3 × 30 mL). The combined organic phases were dried over $MgSO_4$, concentrated *in vacuo*, and the residue purified by column chromatography on silica.

### 1-(4'-Methoxyphenyl)-hept-2-yn-1-ol.[163]
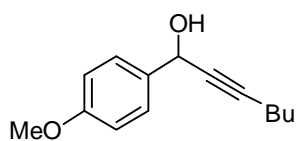


Prepared by procedure I from 1-hexyne (1.3 mL) and *p*-anisaldehyde (1.2 mL), isolated as a yellow oil after purification by column chromatography (petroleum ether/ethyl acetate, 4:1). Yield: 1.73g (79%). ¹H NMR (CDCl₃): δ = 7.47 (d, *J* = 8.7, 2H, C*H*-aromatic), 6.90 (d, *J* = 8.7, 2H, C*H*-aromatic), 5.40 (d, *J* = 6.0, 1H, O*H*), 3.81 (s, 3H, OC*H₃*), 2.47 (d, *J* = 6.0, 1H, C*H*OH), 2.28 (td, *J* = 7.1, 2.0, 2H, C≡CC*H₂*), 1.58 – 1.48 (m, 2H, C*H₂*), 1.48 – 1.37 (m, 2H, C*H₂*), 0.92 (t, *J* = 7.2, 3H, CH₂C*H₃*). ¹³C NMR (CDCl₃): δ = 159.5 (*C*H-aromatic), 133.6 (*C*H-aromatic), 128.0 (*C*H-aromatic), 113.7 (*C*H-aromatic), 87.4 (*C*≡CCH₂), 80.0 (C≡*C*CH₂), 64.4 (*C*HOH), 55.3 (O*C*H₃), 30.7 (C≡C*C*H₂), 22.0 (*C*H₂), 18.5 (*C*H₂), 13.6 (CH₂*C*H₃). HRMS (ESI) calcd for C₁₄H₁₈O₂ [M-OH]⁺: 201.12794; found 201.1277.

### 1-(4'-Methoxyphenyl)-3-(trimethylsilyl)prop-2-yn-1-ol.[263]
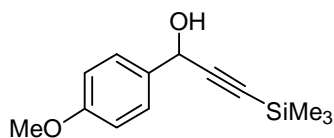


Prepared by procedure I from trimethylsilylacetylene (1.6 mL) and *p*-anisaldehyde (1.2 mL), isolated as a colorless oil after purification by column chromatography (petroleum ether/ethyl acetate, 8:1). ¹H NMR (CDCl₃): δ = 7.47 (d, *J* = 8.7, 2H, C*H*-aromatic), 7.41 (d, *J* =

8.7, 2H, C*H*-aromatic), 5.41 (d, *J* = 5.5, 1H, O*H*), 3.82 (s, 3H, OC*H*₃), 2.11 (d, *J* = 5.5, 1H, C*H*OH), 0.20 (s, 9H, Si(C*H*₃)₃). ¹³C NMR (CDCl₃): δ = 159.7 (*C*H-aromatic), 132.6 (*C*H-aromatic), 128.2 (*C*H-aromatic), 113.8 (*C*H-aromatic), 105.1 (CH*C*≡C), 91.3 (CHC≡*C*), 64.6 (*C*HOH), 55.3 (O*C*H₃), -0.18 (Si(*C*H₃)₃). HRMS (ESI) calcd for C₁₃H₁₈O₂Si [M-OH]⁺: 217.1048; found 217.1058.

### 1-(4'-Methoxyphenyl)-3-cyclopropyl-prop-2-yn-1-ol.
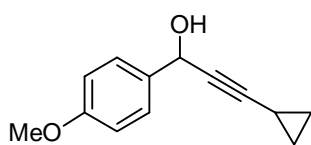


Prepared by procedure I from cyclopropylacetylene (0.93 mL) and *p*-anisaldehyde (1.2 mL), isolated as a white solid after purification by column chromatography (petroleum ether/ethyl acetate, 3:1) and recrystallization from toluene at -20 °C overnight. Yield: 1.74 g (86%). mp 43 – 45 °C. ¹H NMR (CDCl₃): δ = 7.44 (d, *J* = 8.7, 2H, C*H*-aromatic), 6.89 (d, *J* = 8.7, 2H, C*H*-aromatic), 5.37 (d, *J* = 5.7, 1H, O*H*), 3.81 (s, 3H, OC*H*₃), 2.11 (d, *J* = 5.7, 1H, C*H*OH), 1.32 – 1.29 (m, 1H, cyclopropyl C*H*), 0.82 – 0.76 (m, 2H, cyclopropyl C*H*₂) 0.74 – 0.70 (m, 2H, cyclopropyl C*H*₂). ¹³C NMR (CDCl₃): δ = 159.5 (*C*H-aromatic), 133.5 (*C*H-aromatic), 128.0 (*C*H-aromatic), 113.8 (*C*H-aromatic), 90.4 (CH*C*≡C), 75.3 (CHC≡*C*), 64.4 (*C*HOH), 55.3 (O*C*H₃), 8.5 (cyclopropyl *C*H), -0.15 (cyclopropyl *C*H₂). IR (neat): 2199, 1489, 1028, 961, 758, 694 cm⁻¹. HRMS (ESI) calcd for C₁₃H₁₄O₂ [M-OH]⁺: 185.0966; found 185.0956. Anal. Calc. for C₁₃H₁₄O₂: C, 77.20; H, 6.98%. Found: C, 77.29; H, 6.90%.

### 1-(4'-Methoxyphenyl)-3-(1-cyclohexenyl)-prop-2-yn-1-ol.
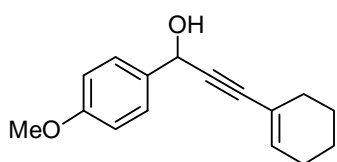
Prepared from 1-ethynylcyclohexene (1.3 mL) and *p*-anisaldehyde (1.2 mL), isolated as a white solid after purification by column chromatography (petroleum ether/ethyl acetate, 3:1) and washing of the resulting oily solid with cold diethyl ether. Yield: 1.87 g (77%). mp 102 − 108 °C. $^1$H NMR (CDCl$_3$): δ = 7.47 (d, $J$ = 8.7, 2H, C*H*-aromatic), 6.90 (d, $J$ = 8.7, 2H, C*H*-aromatic), 6.17 − 6.15 (m, 1H, C*H*OH), 5.52 (d, $J$ = 5.6, 1H, O*H*), 3.81 (s, 3H, OC*H*$_3$), 2.17 − 2.08 (m, 5H, cyclohexenyl C*H*$_2$), 1.65 − 1.58 (m, 4H, cyclohexenyl C*H*$_2$). $^{13}$C NMR (CDCl$_3$): δ =159.6 (*C*H-aromatic), 135.6 (*C*H-aromatic), 133.3 (*C*H-aromatic), 128.1 (*C*H-aromatic), 120.0 (cyclohexenyl *C*), 113.9 (cyclohexenyl *C*), 88.4 (CH*C*≡C), 86.2 (CHC≡*C*), 64.6 (*C*HOH), 55.3 (O*C*H$_3$), 29.1 (cyclohexenyl *C*H$_2$), 25.6 (cyclohexenyl *C*H$_2$), 22.2 (cyclohexenyl *C*H$_2$), 21.4 (cyclohexenyl *C*H$_2$). HRMS (ESI) calcd for C$_{16}$H$_{18}$O$_2$ [M-OH]$^+$: 225.1279; found 225.1282. Anal. Calc. for C$_{16}$H$_{18}$O$_2$: C, 79.31; H, 7.49%. Found: C, 79.42; H, 7.43%.

### 1-(4'-Methoxyphenyl)-3-phenylprop-2-yn-1-ol.[264]
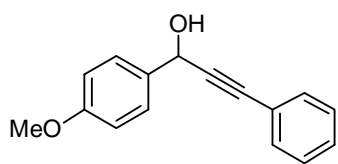
Prepared from phenylacetylene (1.2 mL) and *p*-anisaldehyde (1.2 mL), isolated as a white solid after purification by column chromatography (petroleum ether/ethyl acetate, 3:1). Yield: 2.07 g (87%). $^1$H NMR (CDCl$_3$): δ = 7.55 (d, $J$ = 6.4, 2H), 7.49 − 7.47 (m, 2H, C*H*-aromatic), 7.33 (m, 3H, C*H*-aromatic), 6.98 − 6.89 (d, $J$ = 6.4, 2H, C*H*-aromatic), 5.65 (d, $J$ = 6.0, 1H, CHO*H*), 3.83 (s, 3H, OC*H*$_3$), 2.30 (d, $J$ = 6.0, 1H, C*H*OH). $^{13}$C NMR (CDCl$_3$):

$\delta$ = 159.7 (*C*H-aromatic), 133.0 (*C*H-aromatic), 131.7 (*C*H-aromatic), 128.5 (*C*H-aromatic), 128.3 (*C*H-aromatic), 128.2 (*C*H-aromatic), 122.5 (*C*H-aromatic), 114.0 (*C*H-aromatic), 88.9 (CH*C*≡C), 86.5 (CHC≡*C*), 64.7 (*C*HOH), 55.3 (O*C*H$_3$). HRMS (ESI) calcd for C$_{16}$H$_{14}$O$_2$ [M-OH]$^+$: 221.0966; found 221.0976.

### 1-(4-Methoxyphenyl)-2-propyn-1-ol.[265]
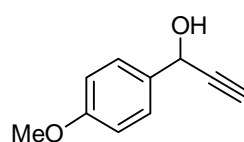


Ethynylmagnesium bromide (0.5 M in THF, 24.0 mL, 12 mmol, 1.2 eq.) was added to a solution of *p*-anisaldehyde (1.2 mL, 10 mmol, 1.0 eq.) in dry THF (20 mL) at 0 °C under N$_2$. The reaction mixture was stirred for 1 h at room temperature, then quenched with water (50 mL) and extracted with 50 mL of CH$_2$Cl$_2$. The organic layer was dried over Na$_2$SO$_4$, and the solvent was removed *in vacuo*. Purification by column chromatography on silica (petroleum ether/ethyl acetate, 3:1) afforded the desired product as a white solid. Yield: 1.15 g (71%). $^1$H NMR (CDCl$_3$): $\delta$ = 7.46 (d, *J* = 8.8, 2H, C*H*-aromatic), 6.90 (d, *J* = 8.8, 2H, C*H*-aromatic), 5.39 (dd, *J* = 6.4, 2.3, 1H, O*H*), 3.80 (s, 3H, OC*H*$_3$), 2.66 (d, *J* = 2.3, 1H, C*H*OH). $^{13}$C NMR (CDCl$_3$): $\delta$ = 159.7 (*C*H-aromatic), 132.4 (*C*H-aromatic), 128.0 (*C*H-aromatic), 114.0 (*C*H-aromatic), 83.7 (*C*≡CH), 74.6 (C≡*C*H), 63.9 (NH*C*H), 55.3 (O*C*H$_3$). HRMS (ESI) calcd for C$_{10}$H$_{10}$O$_2$ [M-OH]$^+$: 145.0653; found 145.0645.

### General procedure for the synthesis of substrates 3.1l-n, p (Procedure J):

The propargyl alcohol (5.0 mmol, 1.0 eq.) was dissolved in 5.0 mL of acetone. Benzamide (1.21g, 10.0 mmol, 2.0 eq.) and HBF$_4$ (50 wt% aqueous solution,

17.6 µL, 0.1 mmol, 0.02 eq.) were successively added, and the resulting mixture was stirred at room temperature for 6 h. The solvent was removed *in vacuo* and the residue purified by column chromatography on silica.

### *N*-[1-(4-Methoxyphenyl)hept-2-ynyl]benzamide (3.1l).
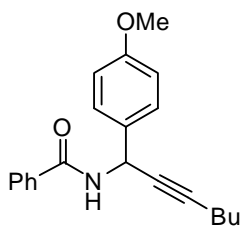


Prepared from 1-(4'-methoxyphenyl)-hept-2-yn-1-ol (1.09 g) by procedure J, isolated as a white solid after purification by column chromatography (petroleum ether/ethyl acetate, 3:1). Yield: 1.51 g (94%). mp 98 – 100 °C. $^{1}$H NMR (CDCl$_3$): δ = 7.81 – 7.74 (m, 2H, C*H*-aromatic), 7.55 – 7.46 (m, 3H, C*H*-aromatic), 7.46 – 7.39 (m, 2H, C*H*-aromatic), 6.94 – 6.85 (m, 2H, C*H*-aromatic), 6.52 (d, *J* = 8.4, 1H, N*H*), 6.15 (dt, *J* = 8.4, 2.2, 1H, C*H*C≡C), 3.80 (s, 3H, OC*H*$_3$), 2.27 (td, *J* = 7.1, 2.2, 2H, C≡CC*H*$_2$), 1.59 – 1.49 (m, 2H, C*H*$_2$), 1.48 – 1.38 (m, 2H, C*H*$_2$), 0.92 (t, *J* = 7.2, 3H, CH$_2$C*H*$_3$). $^{13}$C NMR (CDCl$_3$): δ = 166.0 (*C*O), 159.3 (*C*H-aromatic), 134.0 (*C*H-aromatic), 131.9 (*C*H-aromatic), 131.6 (*C*H-aromatic), 128.5 (*C*H-aromatic), 128.4 (*C*H-aromatic), 127.0 (*C*H-aromatic), 113.9 (*C*H-aromatic), 85.6 (*C*≡CCH$_2$), 78.0 (C≡*C*CH$_2$), 55.3 (O*C*H$_3$), 44.8 (*C*HC≡C), 30.7 (C≡C*C*H$_2$), 22.0 (*C*H$_2$), 18.5 (*C*H$_2$), 13.6 (CH$_2$*C*H$_3$). HRMS (ESI) calcd for C$_{21}$H$_{23}$NO$_2$ [M+H]$^+$: 322.1807; found 322.1782. ν$_{max}$/cm$^{-1}$: 3290 (N–H), 1632 (C=O). Anal. Calc. for C$_{21}$H$_{23}$NO$_2$: C, 78.47; H, 7.21; N, 4.36%. Found: C, 78.36; H, 7.13; N, 4.41%.

### N-[1-(4-Methoxyphenyl)- 3-(trimethylsilyl)prop-2-ynyl]benzamide (3.1m).
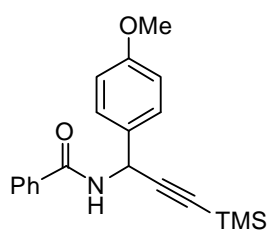
Prepared from 1-(4'-methoxyphenyl)-3-(trimethylsilyl)prop-2-yn-1-ol (1.17 g) by procedure J, isolated as a white solid after purification by column chromatography (petroleum ether/ethyl acetate, 4:1).

Yield: 1.15 g (68%). mp 167 – 169 °C. $^1$H NMR (CDCl$_3$): δ = 7.81 – 7.76 (m, 2H, C*H*-aromatic), 7.54 – 7.47 (m, 3H, C*H*-aromatic), 7.47 – 7.40 (m, 2H, C*H*-aromatic), 6.93 – 6.86 (m, 2H, C*H*-aromatic), 6.52 (d, $J$ = 8.5, 1H, N*H*), 6.21 (d, $J$ = 8.5, 1H, C*H*C≡C), 3.81 (s, 3H, OC*H*$_3$), 0.21 (s, 9H, Si(C*H*$_3$)$_3$). $^{13}$C NMR (CDCl$_3$): δ = 166.0 (*C*O), 159.4 (*C*H-aromatic), 133.9 (*C*H-aromatic), 131.8 (*C*H-aromatic), 131.0 (*C*H-aromatic), 128.6 (*C*H-aromatic), 128.4 (*C*H-aromatic), 127.1 (*C*H-aromatic), 114.0 (*C*H-aromatic), 103.3 (*C*≡CCH$_2$), 89.8 (C≡*C*CH$_2$), 55.3 (O*C*H$_3$), 45.1 (*C*HC≡C), -0.12 (Si(*C*H$_3$)$_3$). HRMS (ESI) calcd for C$_{20}$H$_{23}$NO$_2$Si [M+H]$^+$: 338.1576; found 338.1558. ν$_{max}$/cm$^{-1}$: 3262 (N−H), 1628 (C=O). Anal. Calc. for C$_{20}$H$_{23}$NO$_2$Si: C, 71.18; H, 6.87; N, 4.15%. Found: C, 70.92; H, 6.79; N, 4.22%.

### N-[1-(4-Methoxyphenyl)-3-cyclopropyl-prop-2-ynyl]benzamide (3.1n).
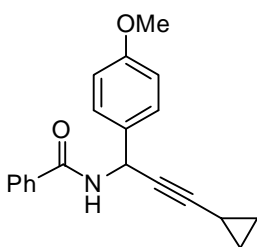
Prepared from 1-(4'-methoxyphenyl)-3-cyclopropyl-prop-2-yn-1-ol (1.01 g) by procedure J, isolated as a white solid after purification by column chromatography (petroleum ether/ethyl acetate, 2:1).

Yield: 1.36 g (89%). mp 119 – 123 °C. $^1$H NMR (CDCl$_3$): δ = 7.81 – 7.74 (m, 2H, C*H*-aromatic), 7.55 – 7.45 (m, 3H, C*H*-aromatic), 7.45 – 7.38 (m, 2H, C*H*-aromatic), 6.91 – 6.85 (m, 2H, C*H*-aromatic), 6.52 (d, $J$ = 8.4, 1H, N*H*),

6.12 (dd, $J$ = 8.4, 1.8, 1H, C$H$C≡C), 3.80 (s, 3H, OC$H_3$), 1.33 − 1.28 (m, 1H, cyclopropyl C$H$), 0.87 − 0.68 (m, 4H, cyclopropyl C$H_2$). $^{13}$C NMR (CDCl$_3$): δ = 165.9 ($C$O), 159.3 ($C$H-aromatic), 134.0 ($C$H-aromatic), 131.8 ($C$H-aromatic), 131.6 ($C$H-aromatic), 128.5 ($C$H-aromatic), 128.3 ($C$H-aromatic), 127.0 ($C$H-aromatic), 113.9 ($C$H-aromatic), 88.5 (CH$C$≡C), 73.3 (CHC≡$C$), 55.3 (O$C$H$_3$), 44.7 ($C$HC≡C), 8.2 (cyclopropyl $C$H), -0.5 (cyclopropyl $C$H$_2$). HRMS (ESI) calcd for C$_{20}$H$_{19}$NO$_2$ [M+H]$^+$: 306.1494; found 306.1505. ν$_{max}$/cm$^{-1}$: 3235 (N–H), 1625 (C=O). Anal. Calc. for C$_{20}$H$_{19}$NO$_2$: C, 78.66; H, 6.27; N, 4.59%. Found: C, 78.49; H, 6.16; N, 4.71%.

**$N$-[1-(4-Methoxyphenyl)-3-phenyl-prop-2-ynyl]benzamide (3.1p).**
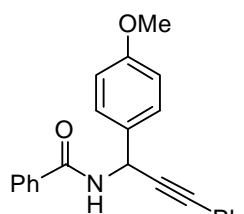
Prepared from 1-(4'-methoxyphenyl)-3-phenyl-prop-2-yn-1-ol (1.19 g) by procedure J, isolated as a white solid after purification by column chromatography (CH$_2$Cl$_2$/ethyl acetate, 20:1). Yield: 1.30 g (77%). mp 165 − 168 °C. $^1$H NMR (CDCl$_3$): δ = 7.84 − 7.77 (m, 2H, C$H$-aromatic), 7.63 − 7.56 (m, 2H, C$H$-aromatic), 7.55 − 7.47 (m, 3H, C$H$-aromatic), 7.48 − 7.40 (m, 2H, C$H$-aromatic), 7.34 − 7.31 (m, 3H, C$H$-aromatic), 6.97 − 6.89 (m, 2H, C$H$-aromatic), 6.64 (d, $J$ = 8.4, 1H, N$H$), 6.42 (d, $J$ = 8.4, 1H, C$H$C≡C), 3.82 (s, 3H, OC$H_3$). $^{13}$C NMR (CDCl$_3$): δ = 166.1 ($C$O), 159.5 ($C$H-aromatic), 133.8 ($C$H-aromatic), 131.8 ($C$H-aromatic), 131.8 ($C$H-aromatic), 131.2 ($C$H-aromatic), 128.6 ($C$H-aromatic), 128.6 ($C$H-aromatic), 128.5 ($C$H-aromatic), 128.3 ($C$H-aromatic), 127.1 ($C$H-aromatic), 122.5 ($C$H-aromatic), 114.1 ($C$H-aromatic), 87.2 (CH$C$≡C), 84.9 (CHC≡$C$), 55.3 (O$C$H$_3$), 45.1 ($C$HC≡C). HRMS (ESI) calcd for C$_{23}$H$_{19}$NO$_2$ [M+H]$^+$: 221.0966; found 221.0976.

$\nu_{max}$/cm$^{-1}$: 3255 (N–H), 1631 (C=O). Anal. Calc. for $C_{23}H_{19}NO_2$: C, 80.92; H, 5.61; N, 4.10%. Found: C, 80.81; H, 5.53; N, 4.18%.

**General procedure for the synthesis of substrates 3.1q-s (Procedure K):**

The propargyl alcohol (5.0 mmol, 1.0 eq.) was dissolved in 5.0 mL of MeCN. The corresponding amide (10.0 mmol, 2.0 eq.) and HBF$_4$ (50 wt% aqueous solution, 17.6 µL, 0.1 mmol, 0.02 eq.) were successively added, and the resulting mixture was heated at 80 °C for the specified time. After cooling to room temperature, the solvent was removed *in vacuo* and the residue purified by column chromatography on silica.

***N*-[1-(4-Methoxyphenyl)-prop-2-ynyl]benzamide (3.1q).**
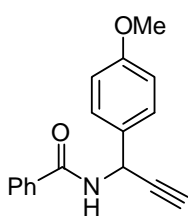
Prepared from 1-(4-methoxyphenyl)-2-propyn-1-ol (0.81 g) and benzamide (1.21 g) by procedure K. Reaction time = 1 h. Isolated as a white solid after purification by column chromatography (petroleum ether/ethyl acetate, 3:1). Yield: 0.87 g (66%). mp 159 – 163 °C. $^1$H NMR (CDCl$_3$): δ = 7.83 – 7.75 (m, 2H, C*H*-aromatic), 7.55 – 7.47 (m, 3H, C*H*-aromatic), 7.47 – 7.39 (m, 2H, C*H*-aromatic), 6.94 – 6.86 (m, 2H, C*H*-aromatic), 6.55 (d, *J* = 8.2, 1H, N*H*), 6.18 (dd, *J* = 8.2, 2.4, 1H, NHC*H*), 3.81 (s, 3H, OC*H*$_3$), 2.53 (d, *J* = 2.4, 1H, C≡C*H*). $^{13}$C NMR (CDCl$_3$): δ = 166.1 (*C*O), 159.6 (*C*H-aromatic), 133.7 (*C*H-aromatic), 131.8 (*C*H-aromatic), 130.4 (*C*H-aromatic), 128.6 (*C*H-aromatic), 128.4 (*C*H-aromatic), 127.1 (*C*H-aromatic), 114.1 (*C*H-aromatic), 81.9 (*C*≡CH), 73.1 (C≡*C*H), 55.3 (O*C*H$_3$), 44.5 (NH*C*H). HRMS (ESI) calcd for $C_{17}H_{15}NO_2$ [M+H]$^+$: 266.1181; found 266.1170. $\nu_{max}$/cm$^{-1}$: 3280 (N–H), 3255

($\equiv$CH), 1633 (C=O). Anal. Calc. for $C_{17}H_{15}NO_2$: C, 76.96; H, 5.70; N, 5.28%. Found: C, 76.99; H, 5.72, N, 5.26%.

### *N*-Benzoyl-1-phenyl-2-propynylamine (3.1r).[160]
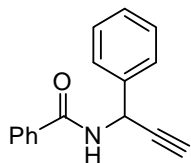
Prepared from 1-phenyl-2-propyn-1-ol (0.66 g) and benzamide (1.21 g) by procedure K. Reaction time = 12 h. Isolated as a white solid after purification by column chromatography (petroleum ether/ethyl acetate, 3:1). Yield: 0.11 g (9%). mp 130 – 133 °C. $^1$H NMR (CDCl$_3$): δ = 7.80 (dd, *J* = 7.3, 1.7, 2H, C*H*-aromatic), 7.64 – 7.49 (m, 3H, C*H*-aromatic), 7.47 – 7.31 (m, 5H, C*H*-aromatic), 6.57 (d, *J* = 8.5, 1H, N*H*), 6.25 (dd, *J* = 8.5, 2.4, 1H, NHC*H*), 2.55 (d, *J* = 2.4, 1H, C$\equiv$C*H*). $^{13}$C NMR (CDCl$_3$): δ = 146.2 (*C*O), 138.2 (*C*H-aromatic), 133.6 (*C*H-aromatic), 132.0 (*C*H-aromatic), 128.8 (*C*H-aromatic), 128.6 (*C*H-aromatic), 128.3 (*C*H-aromatic), 127.1 (*C*H-aromatic), 81.6 (*C*$\equiv$CH), 73.3 (C$\equiv$*C*H), 45.0 (NH*C*H). HRMS (ESI) calcd for $C_{16}H_{13}NO$ [M+H]$^+$: 236.1075; found 236.1083. ν$_{max}$/cm$^{-1}$: 3280 (N–H), 3255 ($\equiv$CH), 1633 (C=O).

### *N*-[1-(4-Methoxyphenyl)hept-2-ynyl]cyclohexane carboxamide (3.1s).
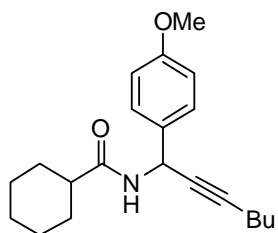
Prepared from 1-(4'-methoxyphenyl)-3-phenyl-prop-2-yn-1-ol (1.19 g) and cyclohexane carboxamide (1.27 g) by procedure K. Reaction time = 12 h. Isolated as a white solid after purification by column chromatography (petroleum ether/ethyl acetate, 4:1). Yield: 1.08 g (66%). mp 109 – 111 °C. $^1$H NMR (CDCl$_3$): δ = 7.43 – 7.37 (m, 2H, C*H*-aromatic), 6.89 – 6.83 (m, 2H, C*H*-aromatic), 5.94 (dd, *J* = 8.6, 2.3, 1H, C*H*C$\equiv$C), 5.83 (d, *J* =

8.6, 1H, N*H*), 3.79 (s, 3H, OC*H*₃), 2.24 (td, *J* = 7.0, 2.3, 2H, C≡CC*H*₂), 2.06 (tt, *J* = 11.8, 3.5, 1H, cyclohexyl C*H*), 1.94 – 1.72 (m, 4H, cyclohexyl C*H*₂), 1.66 (m, 1H, cyclohexyl C*H*), 1.57 – 1.35 (m, 6H, cyclohexyl C*H*₂, C*H*₂C*H*₂CH₃), 1.23 (m, 3H, cyclohexyl C*H*₂), 0.91 (t, *J* = 7.2, 3H, CH₂C*H*₃). ¹³C NMR (CDCl₃): δ = 174.5 (*C*O), 159.1 (*C*H-aromatic), 132.2 (*C*H-aromatic), 128.2 (*C*H-aromatic), 113.8 (*C*H-aromatic), 85.2 (CH*C*≡C), 78.2 (CH*C*≡*C*), 55.3 (O*C*H₃), 45.3 (*C*HC≡C), 43.9 (cyclohexyl *C*H), 30.7 (C≡C*C*H₂), 29.6 (cyclohexyl *C*H₂), 29.4 (cyclohexyl *C*H₂), 25.7 (cyclohexyl *C*H₂), 22.0 (CH₂*C*H₂CH₃), 18.4 (*C*H₂CH₂CH₃), 13.6 (CH₂*C*H₃). HRMS (ESI) calcd for C₂₁H₂₉NO₂ [M+H]⁺: 328.2277; found 328.2285. ν*max*/cm⁻¹: 3280 (N−H), 3278 (≡CH), 1634 (C=O). Anal. Calc. for C₂₁H₂₉NO₂: C, 77.02; H, 8.93; N, 4.28%. Found: C, 76.89; H, 8.99; N, 4.25%.

**N-[1-(4-Methoxyphenyl)-3-(cyclohex-1-enyl)-prop-2-ynyl]benzamide (3.1o).**
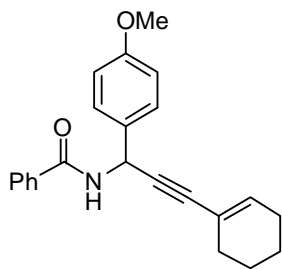


1-(4'-methoxyphenyl)-3-(1-cyclohexenyl)-prop-2-yn-1-ol (1.21 g, 5.0 mmol, 1.0 eq.) was dissolved in 5.0 mL of toluene. Benzamide (1.21 g, 10.0 mmol, 2.0 eq.) and HBF₄ (50 wt% aqueous solution, 17.6 μL, 0.1 mmol, 0.02 eq.) were successively added, and the resulting mixture was refluxed for 1 h. After cooling to room temperature, the solvent was removed *in vacuo* and the residue purified by column chromatography on silica (petroleum ether/ethyl acetate, 4:1). Yield: 0.50 g (29%). mp 146 – 151 °C. ¹H NMR (CDCl₃): δ = 7.79 – 7.77 (m, 2H), 7.57 – 7.47 (m, 3H), 7.47 – 7.38 (m, 2H), 6.93 – 6.85 (m, 2H), 6.54 (d, *J* = 8.5,

1H, N*H*), 6.30 (d, *J* = 8.5, 1H, C*H*C≡C), 6.18 (tt, *J* = 3.8, 1.8, 1H, cyclohexenyl C*H*), 3.80 (s, 3H, OC*H*$_3$), 2.23 − 2.04 (m, 4H, cyclohexenyl C*H*$_2$), 1.71 − 1.53 (m, 4H, cyclohexenyl C*H*$_2$). $^{13}$C NMR (CDCl$_3$): δ = 166.0 (*C*O), 159.3 (*C*H-aromatic), 135.7 (*C*H-aromatic), 134.0 (*C*H-aromatic), 131.7 (*C*H-aromatic), 131.6 (*C*H-aromatic), 128.6 (*C*H-aromatic), 128.4 (*C*H-aromatic), 127.1 (*C*H-aromatic), 120.1 (cyclohexenyl *C*), 114.0 (cyclohexenyl *C*H), 87.0 (CH*C*≡C), 84.3 (CHC≡*C*), 55.3 (O*C*H$_3$), 45.0 (*C*HC≡C), 29.2 (cyclohexenyl *C*H$_2$), 25.6 (cyclohexenyl *C*H$_2$), 22.2 (cyclohexenyl *C*H$_2$), 21.4 (cyclohexenyl *C*H$_2$). HRMS (ESI) calcd for C$_{23}$H$_{23}$NO$_2$ [M+H]$^+$: 225.1279; found 225.1282. ν$_{max}$/cm$^{-1}$: 3306 (N–H), 1633 (C=O). Anal. Calc. for C$_{21}$H$_{29}$NO$_2$: C, 79.97; H, 6.71; N, 4.05%. Found: C, 80.03; H, 6.74; N, 4.01%.

*Bis*(4-methoxypyridine)silver(I) perchlorate [Ag(MeO-Py)$_2$]ClO$_4$ (2.11b).

Prepared by procedure E. Yield: 0.21 g (78%). $^1$H NMR (DMSO-d$_6$): δ = 8.48 − 8.46 (m, 4H), 7.16 − 7.14 (m, 4H), 3.88 (m, 6H). $^{13}$C NMR (DMSO-d$_6$): δ = 166.2, 152.4, 111.0, 55.7. Anal. Calc. for C$_{12}$H$_{14}$AgClN$_2$O$_6$: C, 33.87; H, 3.32; N, 6.58%. Found: C, 33.92; H, 3.29; N, 6.64%.

*Bis*(4-methoxypyridine)silver(I) tetrafluoroborate [Ag(MeO-Py)$_2$]BF$_4$ (2.11c).

Prepared by procedure E. Yield: 0.19 g (93%). $^1$H NMR (DMSO-d$_6$): δ = 8.48 − 8.47 (m, 4H), 7.16 − 7.14 (m, 4H), 3.88 (m, 6H). $^{13}$C NMR (DMSO-d$_6$): δ = 166.2, 152.4, 111.0, 55.7. Anal. Calc. for C$_{12}$H$_{14}$AgBF$_4$N$_2$O$_2$: C, 34.90; H, 3.42; N, 6.78%. Found: C, 34.70; H, 3.47; N, 6.75%.

**Bis(4-methoxypyridine)silver(I) hexafluorophosphate [Ag(MeO-Py)₂]PF₆ (2.11d).**

Prepared by procedure E. Yield: 0.21 g (87%). X-ray diffraction quality single crystals were grown from MeCN/Et$_2$O at -20 °C. $^1$H NMR (DMSO-d$_6$): δ = 8.48 − 8.47 (m, 4H), 7.15 − 7.14 (m, 4H), 3.88 (m, 6H). $^{13}$C NMR (DMSO-d$_6$): δ = 166.2, 152.4, 111.0, 55.7. Anal. Calc. for C$_{12}$H$_{14}$AgF$_6$N$_2$O$_2$P: C, 30.60; H, 3.00; N, 5.95%. Found: C, 30.51; H, 2.98; N 5.93%.

**Bis(4-methoxypyridine)silver(I) hexafluoroantimonate [Ag(MeO-Py)₂] (2.11e).**

Prepared by procedure E. Yield: 0.22 g (78%). $^1$H NMR (DMSO-d$_6$): δ = 8.47 − 8.46 (m, 4H), 7.13 − 7.12 (m, 4H), 3.88 (m, 6H). $^{13}$C NMR (DMSO-d$_6$): δ = 166.2, 152.3, 111.0, 55.7. Anal. Calc. for C$_{12}$H$_{14}$AgF$_6$N$_2$O$_2$Sb: C, 25.65; H, 2.51; N, 4.99%. Found: C, 26.15; H, 2.61; N, 5.04%.
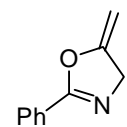
**Bis(4-methoxypyridine)silver(I) trifluoroacetate [Ag(MeO-Py)₂]CF₃CO₂ (2.11f).**

Prepared by procedure E. Yield: 0.20 g (91%). $^1$H NMR (CDCl$_3$): δ = 8.45 − 8.43 (m, 4H), 6.85 − 6.83 (m, 4H), 3.85 (m, 6H). $^{13}$C NMR (CDCl$_3$): δ = 166.5, 152.8, 110.7, 55.4. Anal. Calc. for C$_{13}$H$_{14}$AgF$_3$N$_2$O$_5$S: C, 32.86; H, 2.97; N, 5.90%. Found: C, 38.45; H, 2.82; N, 6.36%.
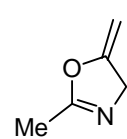
**General procedure for the Ag(I)-catalyzed cycloisomerization of propargyl amides (Procedure L):**

The propargyl amide substrate (2.0 mmol, 1 eq.) was dissolved in $CH_2Cl_2$ (5.0 mL) at room temperature and $[Ag(MeO\text{-}Py)_2]PF_6$ (1-15 mol%) was added. After the prescribed reaction time, the reaction mixture was filtered, and the filtrate concentrated *in vacuo*. The residue was purified by column chromatography (petroleum ether/ethyl acetate).

**2-Phenyl-5-methylene-4,5-dihydrooxazole (3.2a).**[156]

Prepared by procedure L, purified by column chromatography (petroleum ether/ethyl acetate, 1:1). Yield: 0.30 g (94%). Yellow oil. ^{1}H NMR (CDCl$_3$): δ = 8.05 – 7.91 (m, 2H, C*H*-aromatic), 7.56 – 7.47 (m, 1H, C*H*-aromatic), 7.48 – 7.40 (m, 2H, C*H*-aromatic), 4.82 (q, *J* = 2.9, 1H, =C*H*), 4.65 (t, *J* = 2.9, 2H, NC*H*$_2$), 4.36 (q, *J* = 2.6, 1H, =C*H*). ^{13}C NMR (CDCl$_3$): δ = 163.7 (N*C*O), 158.8 (*C*=CH$_2$), 131.8 (*C*H-aromatic), 128.5 (*C*H-aromatic), 128.0 (*C*H-aromatic), 126.7 (*C*H-aromatic), 83.7 (=*C*H$_2$), 57.7 (N*C*H$_2$). HRMS (ESI) calcd for C$_{10}$H$_9$NO [M+H]$^+$: 160.0757; found 160.0751. $v_{max}$/cm$^{-1}$: 1692 (C=C), 1647 (C=N).

**2-Methyl-5-methylene-4,5-dihydrooxazole (3.2b).**

Prepared by procedure L, but too volatile to be isolated. ^{1}H NMR (CD$_2$Cl$_2$): δ = 4.73 – 4.71 (m, 1H, =C*H*), 4.47 – 4.44 (m, 2*H*, C*H*$_2$), 4.34 – 4.33 (m, 1H, =C*H*), 2.12 (t, *J* = 1.5, 3H, C*H*$_3$).

**2-*tert*-Butyl-5-methylene-4,5-dihydrooxazole (3.2c).**[154]
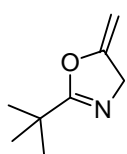
Prepared by procedure L, but too volatile to be isolated. ^{1}H NMR (CD$_2$Cl$_2$): δ = 4.52 (dt, $J$ = 3.0, 2.4, 1H, =C$H$), 4.29 (dd, $J$ = 2.4, 2H, C$H_2$), 4.14 (dt, $J$ = 3.0, 2.4, 1H, =C$H$), 1.13 (s, 9H, C(C$H_3$)$_3$).

**(*E*)-5-Methylene-2-styryl-4,5-dihydrooxazole (3.2d).**[154]
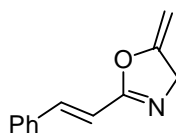
Prepared by procedure L, purified by column chromatography (petroleum ether/ethyl acetate, 2:1). Yield: 0.31 g (84%). White solid. ^{1}H NMR (CDCl$_3$): δ = 7.60 – 7.30 (m, 6H, C$H$-aromatic, C$_6$H$_5$C$H$=), 6.63 (d, $J$ = 16.3, 1H, C$_6$H$_5$CH=C$H$), 4.76 (q, $J$ = 2.9, 1H, =C$H$), 4.58 (t, $J$ = 2.8, 2H, NC$H_2$), 4.32 (q, $J$ = 2.7, 1H, =C$H$). ^{13}C NMR (CDCl$_3$): δ = 163.5 (N$C$O), 158.5 ($C$=CH$_2$), 140.8 (C$_6$H$_5$$C$H=), 134.9 ($C$H-aromatic), 129.7 ($C$H-aromatic), 128.9 ($C$H-aromatic), 127.6 ($C$H-aromatic), 114.1 (C$_6$H$_5$CH=$C$H), 83.3 (=$C$H$_2$), 57.7 (N$C$H$_2$). HRMS (ESI) calcd for C$_{12}$H$_{11}$NO [M+H]$^+$: 186.0913; found 186.0916. ν$_{max}$/cm$^{-1}$: 1687 (C=C), 1656 (C=N).

**Ethyl-(5-methylene-4,5-dihydro-1,3-oxazol-2-yl)acetate (3.2h).**[154]
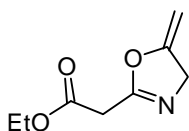
Prepared by procedure L. Due to the low yield of this compound (*ca.* 10% by NMR) and difficulties in separation from unreacted starting material, this compound was not isolated. ^{1}H NMR (CDCl$_3$): δ = 4.70 (q, $J$ = 3.0, 1H, =C$H$), 4.46 (td, $J$ = 2.8, 1.4, 2H, NC$H_2$), 4.30 (q, $J$ = 2.7, 1H, =C$H$), 4.22 (q, $J$ = 7.1, 2H, C$H_2$CH$_3$), 3.43 (s, 2H, COC$H_2$), 1.28 (t, $J$ = 7.1, 3H, CH$_2$C$H_3$).

**4,4-Dimethyl-5-methylene-2-phenyl-4,5-dihydrooxazole (3.2i).**[157]
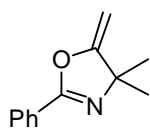
Prepared by procedure L, purified by column chromatography (petroleum ether/ethyl acetate, 6:1). Yield: 0.36 g (96%). Colorless oil. $^1$H NMR (CDCl$_3$): $\delta$ = 8.00 – 7.98 (m, 2H, C*H*-aromatic), 7.54 – 7.47 (m, 1H, C*H*-aromatic), 7.47 – 7.40 (m, 2H, C*H*-aromatic), 4.74 (d, $J$ = 2.8, 1H, =C*H*), 4.25 (d, $J$ = 2.9, 1H, =C*H*), 1.45 (s, 6H, C(C*H*$_3$)$_2$). $^{13}$C NMR (CDCl$_3$): $\delta$ = 167.9 (N*C*O), 159.8 (*C*=CH$_2$), 131.6 (*C*H-aromatic), 128.4 (*C*H-aromatic), 128.1 (*C*H-aromatic), 127.0 (*C*H-aromatic), 82.3 (=*C*H$_2$), 69.1 (*C*(CH$_3$)$_2$), 29.7 (C(*C*H$_3$)$_2$). HRMS (ESI) calcd for C$_{12}$H$_{13}$NO [M+H]$^+$: 188.1070; found 188.1074. $\nu_{max}$/cm$^{-1}$: 1694 (C=C), 1645 (C=N).

**2,2'-Pentane-3,3-diylbis(5-methylene-4,5-dihydro-1,3-oxazole) (3.2j).**[154]
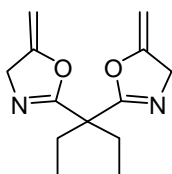
Prepared by procedure L, purified by column chromatography (petroleum ether/ethyl acetate, 6:1). Yield: 0.13 g (28%). White solid. $^1$H NMR (CDCl$_3$): $\delta$ = 4.64 (q, $J$ = 3.0, 2H, =C*H*), 4.45 (t, $J$ = 2.9, 4H, NC*H*$_2$), 4.24 (q, $J$ = 2.6, 2H, =C*H*), 2.00 (q, $J$ = 7.5, 4H, C*H*$_2$CH$_3$), 0.83 (t, $J$ = 7.5, 6H, CH$_2$C*H*$_3$). $^{13}$C NMR (CDCl$_3$): $\delta$ = 166.8 (N*C*O), 158.6 (*C*=CH$_2$), 83.8 (=*C*H$_2$), 57.1 (N*C*H$_2$), 47.2 (*C*(CH$_2$CH$_3$)$_2$), 25.1 (*C*H$_2$CH$_3$), 8.2 (CH$_2$*C*H$_3$). HRMS (ESI) calcd for C$_{13}$H$_{18}$N$_2$O$_2$ [M+H]$^+$: 234.1369; found 234.1360. $\nu_{max}$/cm$^{-1}$: 1692 (C=C), 1660 (C=N).

**1,3-Bis(5-methylene-4,5-dihydrooxazol-2-yl)benzene (3.2k).**
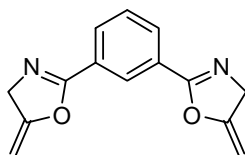
Prepared by procedure L, purified by column chromatography (petroleum ether/ethyl acetate, 2:3).

Yield: 0.13 g (42%). White solid. mp 107 – 109 °C. $^1$H NMR (CDCl$_3$): δ = 8.52 (d, $J$ = 1.8, 1H, C*H*-aromatic), 8.11 (dd, $J$ = 7.8, 1.8, 2H, C*H*-aromatic), 7.51 (t, $J$ = 7.8, 1H, C*H*-aromatic), 4.83 (q, $J$ = 3.0, 2H, =C*H*), 4.65 (t, $J$ = 2.9, 4H, NC*H$_2$*), 4.37 (q, $J$ = 2.7, 2H, =C*H*). $^{13}$C NMR (CDCl$_3$): δ = 162.9 (N*C*O), 158.6 (*C*=CH$_2$), 131.1 (*C*H-aromatic), 128.8 (*C*H-aromatic), 127.6 (*C*H-aromatic), 127.3 (*C*H-aromatic), 84.2 (=*C*H$_2$), 57.8 (N*C*H$_2$). HRMS (ESI) calcd for C$_{14}$H$_{12}$N$_2$O$_2$ [M+H]$^+$: 241.0972; found 241.0976. $\nu_{max}$/cm$^{-1}$: 1693 (C=C), 1646 (C=N). Anal. Calc. for C$_{14}$H$_{12}$N$_2$O$_2$: C, 69.99; H, 5.03; N, 11.66%. Found: C, 70.07; H, 5.06; N, 11.59%.

**(5*E*)-5-Pentylidene-4-(4-methoxyphenyl)-2-phenyl-4,5-dihydro-1,3-oxazole (*E*-3.2l).**
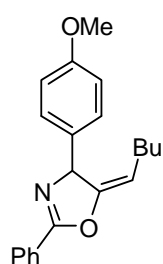
Prepared by procedure L. This compound decomposes on silica and was not isolated. $^1$H NMR (CDCl$_3$): δ = 8.01 – 7.99 (m, 2H, C*H*-aromatic), 7.42 – 7.37 (m, 3H, C*H*-aromatic), 7.30 – 7.27 (m, 2H, C*H*-aromatic), 6.90 – 6.88 (m, 2H, C*H*-aromatic), 5.19 (d, 1H, $J$ = 2.8, =C*H*), 4.84 (d, 1H, $J$ = 2.8, NC*H*), 3.80 (s, 3 H, OC*H$_3$*), 2.23 (t, 2H, $J$ = 7.5, =CHC*H$_2$*), 1.63 – 1.56 (m, 2H, C*H$_2$*CH$_2$), 1.50 – 1.43 (m, 2H, C*H$_2$*CH$_3$), 0.95 (t, 3H, $J$ = 7.3, CH$_2$C*H$_3$*).

**(5*Z*)-5-Pentylidene-4-(4-methoxyphenyl)-2-phenyl-4,5-dihydro-1,3-oxazole (*Z*-3.2l).**
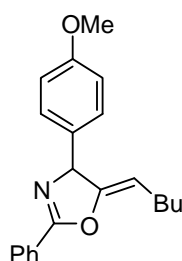
Prepared by procedure L. This compound decomposes on silica and was not isolated. $^1$H NMR (CDCl$_3$): δ = 8.08 –

8.06 (m, 2H, C*H*-aromatic), 7.47 − 7.44 (m, 3H, C*H*-aromatic), 7.25 − 7.23 (m,

2H, C*H*-aromatic), 6.90 − 6.88 (m, 2H, C*H*-aromatic), 5.68 (d, *J* = 2.5, 1H,

NC*H*), 4.54 (td, *J* = 7.5, 2.5, 1H, =C*H*), 3.80 (s, 3H, OC*H*₃), 2.32 − 2.17 (m,

2H, =CHC*H*₂), 1.40 − 1.33 (m, 4H, C*H*₂C*H*₂CH₃), 0.91 (t, *J* = 7.1, 3H,

CH₂C*H*₃).

**2-Phenyl-6-trimethylsilyl-4H-1,3-oxazine (3.4m).**
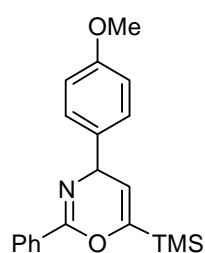
Prepared by procedure L. This compound decomposes on silica and was not isolated. $^{1}$H NMR (CDCl₃): δ = 7.79 − 7.77 (m, 2H, C*H*-aromatic), 7.52 − 7.48 (m, 3H, C*H*-aromatic), 7.42 (t, *J* = 7.4, 2H, C*H*-aromatic), 6.90 − 6.88 (m, 2H, C*H*-aromatic), 6.58 (d, *J* = 8.5, 1H, =C*H*), 6.22 (d, *J* = 8.5, 1H, NC*H*), 3.80 (s, 3H, OC*H*₃), 0.21 (s, 9H, Si(C*H*₃)₃).

**(5*E*)-5-(Cyclopropylmethylene)-4-(4-methoxyphenyl)-2-phenyl-4,5-dihydro-1,3-oxazole (*E*-3.2n).**
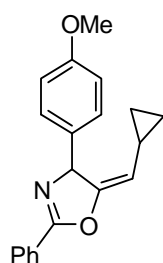
Prepared by procedure L. This compound decomposes on silica and was not isolated. $^{1}$H NMR (CDCl₃): δ = 7.95 − 7.93 (m, 2H, C*H*-aromatic), 7.43 − 7.36 (m, 3H, C*H*-aromatic), 7.29 − 7.27 (m, 2H, C*H*-aromatic), 6.90 − 6.88 (m, 2H, C*H*-aromatic), 5.19 (d, *J* = 3.0, 1H, =C*H*), 4.91 (d, *J* = 3.0, 1H, NC*H*), 3.79 (s, 3H, OC*H*₃), 1.58 − 1.51 (m, 1H, cyclopropyl C*H*), 0.90 − 0.86 (m, 2H, cyclopropyl C*H*₂), 0.78 − 0.72 (m, 2H, cyclopropyl C*H*₂).

**(5Z)-5-(Cyclopropylmethylene)-4-(4-methoxyphenyl)-2-phenyl-4,5-dihydro-1,3-oxazole (Z-3.2n).**
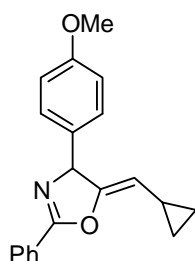
Prepared by procedure L. This compound decomposes on silica and was not isolated. $^1$H NMR (CDCl$_3$): δ = 8.10 − 8.08 (m, 2H, C*H*-aromatic), 7.55 − 7.51 (m, 1H, C*H*-aromatic), 7.47 − 7.43 (m, 2H, C*H*-aromatic), 7.24 − 7.22 (m, 2H, C*H*-aromatic), 6.90 − 6.87 (m , 2H, C*H*-aromatic), 5.70 (d, 1H, *J* = 2.4, NC*H*), 4.07 (dd, 1H, *J* = 9.5, 2.4, =C*H*), 3.79 (s, 3H, OC*H*$_3$), 1.85 − 1.76 (m, 1H, cyclopropyl C*H*), 0.84 − 0.73 (m, 2H, cyclopropyl C*H*$_2$), 0.42 − 0.32 (m, 2H, cyclopropyl C*H*$_2$).

**(5E)-5-(1-Cyclohexenylmethylene)-4-(4-methoxyphenyl)-2-phenyl-4,5-dihydro-1,3-oxazole (E-3.2o).**
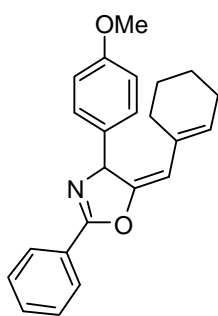
Prepared by procedure L. This compound decomposes on silica and was not isolated. $^1$H NMR (CDCl$_3$): δ = 8.07 − 8.04 (m, 2H, C*H*-aromatic), 7.48 − 7.39 (m, 3H, C*H*-aromatic), 7.32 − 7.28 (m, 2H, C*H*-aromatic), 6.91 − 6.88 (m, 2H, C*H*-aromatic), 6.49 (t, 1H, *J* = 4.0, cyclohexenyl C*H*), 5.27 (d, 1H, *J* = 3.4, NC*H*), 5.08 (d, 1H, *J* = 3.4, =C*H*), 3.80 (s, 3H, OC*H*$_3$), 2.27 − 2.21 (m, 2H, cyclohexenyl C*H*$_2$), 2.20 − 2.12 (m, 2H, cyclohexenyl C*H*$_2$), 1.75 − 1.62 (m, 4H, cyclohexenyl C*H*$_2$).

**(5Z)-5-(1-Cyclohexenylmethylene)-4-(4-methoxyphenyl)-2-phenyl-4,5-dihydro-1,3-oxazole (Z-3.2o).**
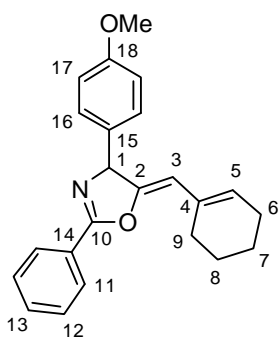
Prepared by procedure L, purified by preparative TLC (petroleum ether/ethyl acetate, 4:1). Yield: 0.34 g (49%). White solid. mp 116 – 120 °C. ^{1}H NMR (CDCl$_3$): δ = 8.09 – 8.02 (m, 2H, H-11), 7.59 – 7.51 (m, 1H, H-13), 7.50 – 7.44 (m, 2H, H-12), 7.26 – 7.21 (m, 2H, H-16), 6.93 – 6.86 (m, 2H, H-17), 5.77 (br s, 1H, H-3), 5.71 (br s, 1H, H-1), 5.05 (br s, 1H, H-5), 3.80 (s, 2H, OC$H_3$), 2.54 (s, 2H, H-9), 2.12 (s, 2H, H-6), 1.78 – 1.67 (m, 2H, H-8), 1.64 – 1.56 (m, 2H, H-7). ^{13}C NMR (CDCl$_3$): δ = 162.65 (C-10), 159.30 (C-2), 152.43 (C-14), 133.31 (C-18), 133.15 (C-15), 131.90 (C-13), 128.52 (C-11), 128.29 (C-12), 126.94 (C-16), 126.77 (C-1), 114.17 (C-17), 106.13 (C-5), 73.16 (C-3), 55.29 (OC$H_3$), 27.79 (C-9), 25.86 (C-6), 22.96 (C-8), 22.03 (C-7). HRMS (ESI) calcd for C$_{23}$H$_{23}$NO$_2$ [M+H]$^+$: 346.1818; found 346.1807. ν$_{max}$/cm$^{-1}$: 1686 (C=C), 1646 (C=N). Anal. Calc. for C$_{23}$H$_{23}$NO$_2$: C, 79.97; H, 6.71; N, 4.05%. Found: C, 79.92; H, 6.64; N, 4.03%.

**(5Z)-5-Benzylidene-4-(4-methoxyphenyl)-2-phenyl-4,5-dihydro-1,3-oxazole (Z-3.2p).**
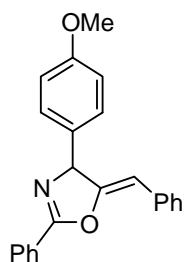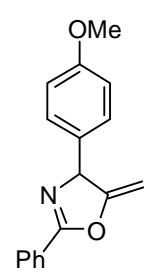
Prepared by procedure L, purified by column chromatography (petroleum ether/ethyl acetate, 4:1). Yield = 0.56 g (82%). White solid. X-ray diffraction quality single crystals were grown from CH$_2$Cl$_2$/hexane at -20 °C. mp 160 – 163 °C. ^{1}H NMR (CDCl$_3$): δ = 8.17 – 8.15 (m, 2H, C$H$-aromatic), 7.62 –

7.54 (m, 3H, C*H*-aromatic), 7.54 − 7.52 (m, 2H, C*H*-aromatic), 7.40 − 7.38 (m, 2H, C*H*-aromatic), 7.31 − 7.28 (m, 2H, C*H*-aromatic), 6.94 − 6.90 (m, 1H, C*H*-aromatic), 6.94 − 6.90 (m, 2H, C*H*-aromatic), 5.93 (d, 1H, $J$ = 2.4, =C*H*), 5.52 (d, 1H, $J$ = 2.4, NC*H*), 3.81 (s, 3H, OC*H*$_3$). $^{13}$C NMR (CDCl$_3$): δ = 162.6 (N*C*O), 159.5 (O*C*=C), 155.7 (*C*H-aromatic), 134.8 (*C*H-aromatic), 132.5 (*C*H-aromatic), 132.2 (*C*H-aromatic), 128.9 (*C*H-aromatic), 128.6 (*C*H-aromatic), 128.5 (*C*H-aromatic), 128.4 (*C*H-aromatic), 128.0 (*C*H-aromatic), 127.0 (*C*H-aromatic), 126.4 (*C*H-aromatic), 114.3 (*C*H-aromatic), 102.8 (=*C*H), 73.7 (N*C*H), 55.3 (O*C*H$_3$). HRMS (ESI) calcd for C$_{23}$H$_{19}$NO$_2$ [M+H]$^+$: 342.1494; found 342.1500. ν$_{max}$/cm$^{-1}$: 1692 (C=C), 1650 (C=N). Anal. Calc. for C$_{23}$H$_{19}$NO$_2$: C, 80.92; H, 5.61; N, 4.10%. Found: C, 81.13; H, 5.56; N, 4.05%.

**4-(4-Methoxyphenyl)-5-methylene-2-phenyl-4,5-dihydro-1,3-oxazole (3.2q).**

Prepared by procedure L, purified by column chromatography (petroleum ether/ethyl acetate, 4:1). Yield = 0.48 g (90%). White solid. mp 75 − 81 °C. $^1$H NMR (CDCl$_3$): δ = 8.10 − 8.03 (m, 2H, C*H*-aromatic), 7.58 − 7.51 (m, 1H, C*H*-aromatic), 7.50 − 7.42 (m, 2H, C*H*-aromatic), 7.29 − 7.23 (m, 2H, C*H*-aromatic), 6.94 − 6.87 (m, 2H, C*H*-aromatic), 5.74 (t, $J$ = 2.8, 1H, =C*H*), 4.91 (t, $J$ = 2.9, 1H, =C*H*), 4.27 (t, $J$ = 2.7, 1H, NC*H*), 3.80 (s, 3H, OC*H*$_3$). $^{13}$C NMR (CDCl$_3$): δ = 162.7 (N*C*O), 162.6 (*C*=CH$_2$), 159.3 (*C*H-aromatic), 132.7 (*C*H-aromatic), 132.0 (*C*H-aromatic), 128.5 (*C*H-aromatic), 128.5 (*C*H-aromatic), 128.3 (*C*H-aromatic), 126.6 (*C*H-aromatic), 114.2 (*C*H-aromatic), 85.0 (=*C*H$_2$), 71.8 (N*C*H), 55.3

(O$CH_3$). HRMS (ESI) calcd for $C_{17}H_{15}NO_2$ [M+H]$^+$: 342.1494; found 342.1500. $\nu_{max}$/cm$^{-1}$: 1695 (C=C), 1645 (C=N). Anal. Calc. for $C_{17}H_{15}NO_2$: C, 76.96; H, 5.70; N, 5.28%. Found: C, 76.80; H, 5.64; N, 5.20%.

**General procedure for trapping of organosilver(I) intermediates with electrophiles (Procedure M):**

To a solution of propargyl amide **3.1** (1.0 mmol, 1.0 equiv.) in acetone (10 mL) was added *N*-bromosuccinimide (0.21 g, 1.2 mmol, 1.2 equiv) or *N*-iodosuccinimide (0.27 g, 1.2 mmol, 1.2 equiv.). The resulting mixture was cooled to 0 °C before the addition of silver(I) trifluoromethanesulfonate (25.7 mg, 0.1 mmol, 0.1 eq.). The reaction mixture was allowed to rise to room temperature, and stirred for another 1 h. The solvent was removed *in vacuo*, and the residue purified by column chromatography.

**2-Phenyl-5-bromomethylene-4,5-dihydrooxazole (3.7a).**
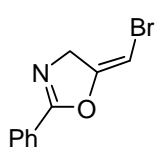


Prepared by procedure M from **3.1a** (0.16 g) and *N*-bromosuccinimide (0.21 g). Purified by column chromatography on silica (petroleum ether/ethyl acetate, 8:1). Yield: 0.20 g (84%). White solid. mp 95 – 98 °C. $^1$H NMR (CDCl$_3$): δ = 7.99 – 7.91 (m, 2H, C*H*-aromatic), 7.60 – 7.50 (m, 1H, C*H*-aromatic), 7.45 (t, *J* = 7.7, 2H, C*H*-aromatic), 6.01 (t, *J* = 3.2, 1H, =C*H*Br), 4.67 (d, *J* = 3.2, 2H, C*H$_2$*). $^{13}$C NMR (CDCl$_3$): δ = 163.6 (N*C*O), 155.6 (*C*=CHBr), 132.1 (*C*H-aromatic), 128.6 (*C*H-aromatic), 128.1 (*C*H-aromatic), 126.3 (*C*H-aromatic), 80.1 (=*C*HBr), 59.2 (N*C*H$_2$). HRMS (ESI) calcd for $C_{10}H_8BrNO$ [M+H]$^+$: 237.9862; found 237.9861. $\nu_{max}$/cm$^{-1}$: 1685 (C=C), 1652 (C=N).

**2-Phenyl-5-iodomethylene-4,5-dihydrooxazole (3.7b).**
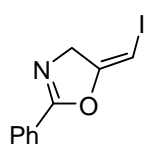
Prepared by procedure M from **3.1a** (0.16 g) and *N*-iodosuccinimide (0.27 g). Purified by column chromatography on neutral alumina (petroleum ether/ethyl acetate, 20:1). Yield: 0.16 g (56%). White solid. mp 111 – 117 °C. $^1$H NMR (CDCl$_3$): δ = 8.01 – 7.90 (m, 2H, C*H*-aromatic), 7.59 – 7.49 (m, 1H, C*H*-aromatic), 7.48 – 7.41 (m, 2H, C*H*-aromatic), 5.77 (t, *J* = 3.3, 1H, =C*H*I), 4.62 (d, *J* = 3.3, 2H, C*H*$_2$). $^{13}$C NMR (CDCl$_3$): δ = 163.9 (N*C*O), 158.0 (*C*=CHI), 132.1 (*C*H-aromatic), 128.6 (*C*H-aromatic), 128.0 (*C*H-aromatic), 126.5 (*C*H-aromatic), 61.2 (=*C*HI), 47.1 (N*C*H$_2$). HRMS (ESI) calcd for C$_{10}$H$_8$INO [M+H]$^+$: 285.9723; found 285.9735. $\nu_{max}$/cm$^{-1}$: 1671 (C=C), 1643 (C=N).

**2-*tert*-Butyl-5-bromomethylene-4,5-dihydrooxazole (3.7c).** [154]
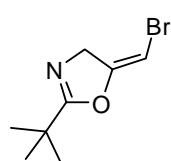
Prepared by procedure M from **3.1c** (0.14 g) and *N*-bromosuccinimide (0.21 g). Purified by column chromatography on silica (petroleum ether/ethyl acetate, 8:1). Yield: 0.14 g (64%). White solid. mp 48 – 55 °C. $^1$H NMR (CDCl$_3$): δ = 5.84 (t, *J* = 3.2, 1H, =C*H*Br), 4.42 (d, *J* = 3.2, 2H, C*H*$_2$), 1.25 (s, 9H, C(C*H*$_3$)$_3$). $^{13}$C NMR (CDCl$_3$): δ = 173.7 (N*C*O), 156.2 (*C*=CHBr), 80.0 (=*C*HBr), 58.8 (N*C*H$_2$), 33.6 (*C*(CH$_3$)$_3$), 27.3 (C(*C*H$_3$)$_3$). HRMS (ESI) calcd for C$_8$H$_{12}$BrNO [M+H]$^+$: 218.0181; found 218.0187. $\nu_{max}$/cm$^{-1}$: 1686 (C=C), 1658 (C=N).

### (*E,E*)-5-Bromomethylene-2-styryl-4,5-dihydrooxazole (3.7d).[154]
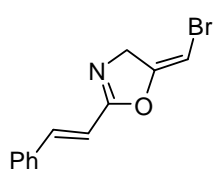
Prepared by procedure M from **3.1d** (0.19 g) and *N*-bromosuccinimide (0.21 g). Purified by column chromatography (petroleum ether/ethyl acetate, 8:1). Yield: 0.31 g (84%). White solid. X-ray diffraction quality single crystals were grown from petroleum ether/ethyl acetate (8:1) at -20 °C. mp 128 − 132 °C. $^1$H NMR (CDCl$_3$): δ = 7.55 − 7.45 (m, 3H, C*H*-aromatic, C$_6$H$_5$C*H*=), 7.42 − 7.37 (m, 3H, C*H*-aromatic), 6.63 (d, *J* = 16.3, 1H, C$_6$H$_5$CH=C*H*), 5.96 (t, *J* = 3.2, 1H, =C*H*Br), 4.60 (d, *J* = 3.2, 2H, C*H$_2$*). $^{13}$C NMR (CDCl$_3$): δ = 163.4 (N*C*O), 155.2 (*C*=CHBr), 141.5 (C$_6$H$_5$*C*H=), 134.6 (*C*H-aromatic), 130.1 (*C*H-aromatic), 129.0 (*C*H-aromatic), 127.7 (*C*H-aromatic), 113.5 (C$_6$H$_5$CH=*C*H), 80.7 (=*C*HBr), 59.1 (N*C*H$_2$). HRMS (ESI) calcd for C$_{12}$H$_{10}$BrNO [M+H]$^+$: 264.0024; found 264.0014. $v_{max}$/cm$^{-1}$: 1686 (C=C), 1653 (C=N).
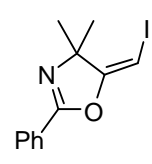
### 4,4-Dimethyl-5-bromomethylene-2-phenyl-4,5-dihydrooxazole (3.7e).
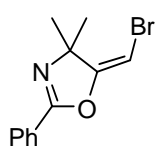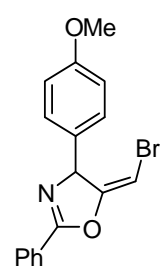
Prepared by procedure M from **3.1i** (0.19 g) and *N*-bromosuccinimide (0.21 g) in the absence of AgOTf. Purified by column chromatography (petroleum ether/ethyl acetate, 8:1). Yield: 0.24 g (90%). Colorless oil. $^1$H NMR (CDCl$_3$): δ = 7.96 − 7.93 (m, 2H, C*H*-aromatic), 7.53 − 7.49 (m, 1H, C*H*-aromatic), 7.45 − 7.41 (m, 2H, C*H*-aromatic), 6.00 (s, 1H, =C*H*Br), 1.68 (s, 6H, C(C*H$_3$*)$_2$). $^{13}$C NMR (CDCl$_3$): δ = 161.9 (N*C*O), 158.8 (*C*=CHBr), 131.9 (*C*H-aromatic), 128.5 (*C*H-aromatic), 128.1 (*C*H-aromatic), 126.3 (*C*H-aromatic), 81.0 (=*C*HBr), 71.3 (*C*(CH$_3$)$_2$),

25.4 (C(CH$_3$)$_2$). ). HRMS (ESI) calcd for C$_{12}$H$_{12}$BrNO [M+H]$^+$: 266.0175; found 266.0170. $\nu_{max}$/cm$^{-1}$: 1678 (C=C), 1649 (C=N).

### 4,4-Dimethyl-5-iodomethylene-2-phenyl-4,5-dihydrooxazole (3.7f).

Prepared by procedure M from **3.1i** (0.19 g) and *N*-iodosuccinimide (0.27 g) in the absence of AgOTf. Purified by column chromatography on neutral alumina (petroleum ether/ethyl acetate, 30:1). Yield: 0.30 g (96%). Colorless oil. $^1$H NMR (CDCl$_3$): δ = 7.95 − 7.93 (m, 2H, C*H*-aromatic), 7.55 − 7.48 (m, 1H, C*H*-aromatic), 7.48 − 7.39 (m, 2H, C*H*-aromatic), 5.76 (s, 1H, =C*H*I), 1.69 (s, 6H, C(C*H$_3$*)$_2$). $^{13}$C NMR (CDCl3): δ = 163.4 (N*C*O), 158.5 (*C*=CHI), 131.8 (*C*H-aromatic), 128.5 (*C*H-aromatic), 128.1 (*C*H-aromatic), 126.2 (*C*H-aromatic), 71.3 (=*C*HI), 48.4 (*C*(CH$_3$)$_2$), 25.8 (C(*C*H$_3$)$_2$). HRMS (ESI) calcd for C$_{12}$H$_{12}$INO [M+H]$^+$: 314.0042; found 314.0050. $\nu_{max}$/cm$^{-1}$: 1668 (C=C), 1645 (C=N).

### 5-Bromomethylene-4-(4-methoxyphenyl)-2-phenyl-4,5-dihydro-1,3-oxazole (3.7g).

Prepared by procedure M from **3.1q** (0.27 g) and *N*-bromosuccinimide (0.21 g). Purified by column chromatography on neutral alumina (petroleum ether/ethyl acetate, 30:1). Yield: 0.34 g (98%). mp 83 − 88 °C. $^1$H NMR (CDCl$_3$): δ = 8.05 − 7.97 (m, 2H, C*H*-aromatic), 7.57 − 7.50 (m, 1H, C*H*-aromatic), 7.49 − 7.40 (m, 2H, C*H*-aromatic), 7.25 (dd, *J* = 6.5, 2.2, 2H, C*H*-aromatic), 6.92 − 6.85 (m, 2H, C*H*-aromatic), 6.16 (d, *J* = 2.8, 1H, =C*H*Br),

5.80 (d, $J$ = 2.8, 1H, NC$H$), 3.79 (s, 3H, OC$H_3$). ^{13}C NMR (CDCl$_3$): δ = 161.7 (N$C$O), 159.4 ($C$=CHBr), 158.0 ($C$H-aromatic), 132.2 ($C$H-aromatic), 129.2 ($C$H-aromatic), 128.6 ($C$H-aromatic), 128.3 ($C$H-aromatic), 126.6 ($C$H-aromatic), 126.1 ($C$H-aromatic), 114.0 ($C$H-aromatic), 84.0 (=$C$HBr), 73.1 (N$C$H), 55.2 (O$C$H$_3$). HRMS (ESI) calcd for C$_{17}$H$_{14}$BrNO$_2$ [M+H]$^+$: 334.0286; found 334.0269. ν$_{max}$/cm$^{-1}$: 1687 (C=C), 1648 (C=N).

## 6.3 Compounds used in Chapter 4

*N,N′*-Bis(2,6-diisopropylphenyl)-1,4-diaza-1,3-butadiene.[266]
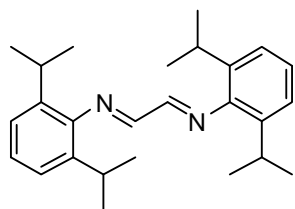


2,4,6-diisopropylaniline (5.6 mL, 40 mmol) was dissolved in 20 mL of methanol, and glyoxal (40% w/w aqueous solution, 2.9 mL, 20 mmol) was added, followed by a few drops of formic acid. The reaction mixture was stirred for 15 h at room temperature, and the resulting yellow precipitate was collected by filtration and washed with 3 × 5 mL of methanol. Yield: 6.37 g (85%). Yellow solid. ^{1}H NMR (CDCl$_3$): δ = 8.12 (s, 2H, =C$H$), 7.22 – 7.15 (m, 6H, C$H$-aromatic), 2.96 (sept, $J$ = 6.9, 4H, C$H$(CH$_3$)$_2$), 1.23 (d, $J$ = 6.9, 24H, C$H_3$). ^{13}C NMR (CDCl$_3$): δ = 163.1 ($C$H-aromatic), 148.0 ($C$H-aromatic), 136.7 ($C$H-aromatic), 125.1 ($C$H-aromatic), 123.2 (=$C$H), 28.0 ($C$H(CH$_3$)$_2$), 23.4 ($C$H$_3$).

*N,N'*-Bis(2,6-diisopropylphenyl)-ethylenediamine.[267]
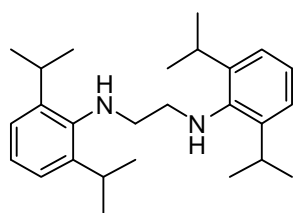


To a solution of *N,N′*-bis(2,6-diisopropylphenyl)-1,4-diaza-1,3-butadiene (6.02 g, 20.6 mmol) in THF

(41 mL) was cooled to 0 °C, and a 2.0 M solution of LiAlH$_4$ in THF (22.5 mL) was added. The mixture was warmed slowly to room temperature and stirred overnight. The reaction mixture was the cooled to 0 °C and quenched by the addition of ice water until the evolution of gas ceased. 10 mL of 3.0 M KOH solution was added, and the organic layer extracted with 100 mL of ethyl acetate. Removal of the solvent *in vacuo* gave a pale yellow solid, which was recrystallized from hot isopropanol to give colorless crystals of the desired product. Yield: 5.21 g (66%). Colorless crystals. $^1$H NMR (CDCl$_3$): δ = 7.20 – 7.07 (m, 6H, C*H*-aromatic), 3.40 (sept, *J* = 6.9, 4H, C*H*(CH$_3$)$_2$), 3.20 (s, 4H, C*H*$_2$) and 1.30 (d, *J* = 6.9, 24H, C*H*$_3$). $^{13}$C NMR (CDCl$_3$): δ = 143.2 (*C*H-aromatic), 142.4 (*C*H-aromatic), 123.9 (*C*H-aromatic), 123.6 (*C*H-aromatic), 52.3 (*C*H$_2$), 27.8 (*C*H(CH$_3$)$_2$), 24.2 (*C*H$_3$).

### 1,3-Bis-(2,6-diisopropylphenyl)imidazolium chloride (IPr·HCl).[266]
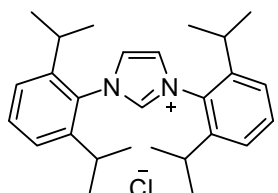
*N,N′*-bis(2,6-diisopropylphenyl)-1,4-diaza-1,3-butadiene (6.37 g, 16.9 mmol, 1.0 eq.) was dissolved in ethyl acetate (34 mL), and a solution of paraformaldehyde (0.55 g, 18.4 mmol, 1.09 eq.) in HCl (4.0 M in dioxane, 6.3 mL, 25.4 mmol, 1.5 eq.) was added slowly whilst maintaining a gentle heating of the reaction mixture over 1 h. The reaction mixture was stirred overnight at room temperature. The resulting precipitate was filtered off and washed with 3 × 10 mL of ethyl acetate to obtain a light pink powder. The powder was dissolved in a minimal amount of saturated aqueous NaHCO$_3$ solution, and extracted with 3 × 10 mL of ethyl acetate to remove the colored impurities. The aqueous layer was further extracted with 3

× 10 mL of dichloromethane. The organic extracts were dried over MgSO$_4$, and the solvent removed *in vacuo*. The residue was redissolved in a minimal amount of CH$_2$Cl$_2$, and ethyl acetate was added to precipitate the product. Filtration and washing with ethyl acetate afforded the product as colorless crystals. Yield: 1.51 g (21%). Colorless crystals. ^{1}H NMR (CDCl$_3$): δ = 10.02 (s, 1H, NC*H*N), 8.15 (s, 2H, C*H*-aromatic), 7.57 (t, *J* = 7.8, 2H, imidazole C*H*), 7.34 (d, *J* = 7.8, 4H, C*H*-aromatic), 2.44 (sept, *J* = 6.8, 4H, C*H*(CH$_3$)$_2$), 1.27 (d, 12H, *J* = 6.7, CH(C*H*$_3$)$_2$), 1.24 (d, 12H, *J* = 6.7, CH(C*H*$_3$)$_2$). ^{13}C NMR (DMSO-d$_6$): δ = 144.8 (NC*H*N), 139.4 (*C*H-aromatic), 131.8 (*C*H-aromatic), 130.1 (*C*H-aromatic), 126.2 (*C*H-aromatic), 124.6 (imidazole *C*H), 28.6 (*C*H(CH$_3$)$_2$), 24.1 (CH(*C*H$_3$)$_2$), 23.1 (CH(*C*H$_3$)$_2$).

**1,3-Bis-(2,6-diisopropylphenyl)imidazolium          tetrafluoroborate (IPr·HBF$_4$).**[266]
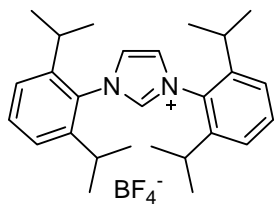


IPr·HCl (3.55 mmol, 1.51 g) was dissolved in a minimal amount of water, and HBF$_4$ (50% w/w aqueous solution, 3.9 mmol, 0.6 mL) was added. The white precipitate that formed instantly was filtered off, washed with 5 mL of water, and dried *in vacuo*. Yield: 1.36 g (98%). White powder. ^{1}H NMR (DMSO-d$_6$): 10.16 (s, 1H, NC*H*N), 8.57 (s, 2H, C*H*-aromatic), 7.70 (t, *J* = 7.8, 2H, imidazole C*H*), 7.54 (d, *J* = 7.8, 4H, C*H*-aromatic), 2.36 (sept, *J* = 6.8, 4H, C*H*(CH$_3$)$_2$), 1.27 (d, *J* = 6.7, 12H, CH(C*H*$_3$)$_2$), 1.17 (d, *J* = 6.8, 12H, CH(C*H*$_3$)$_2$). ^{13}C NMR (DMSO-d$_6$): δ = 144.8 (NC*H*N), 139.2 (*C*H-aromatic), 131.9 (*C*H-aromatic), 130.0 (*C*H-aromatic), 126.2 (*C*H-aromatic), 124.6 (imidazole *C*H), 28.6 (*C*H(CH$_3$)$_2$), 24.1 (CH(*C*H$_3$)$_2$), 23.1 (CH(*C*H$_3$)$_2$).

**1,3-Bis(2,6-diisopropylphenyl)-4,5-dihydroimidazolium tetrafluoroborate (SIPr·HBF₄).**[268]
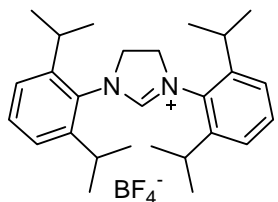
Triethyl orthoformate (25 mmol, 4.2 mL) and NH₄BF₄ (10 mmol, 1.05 g) were added to *N,N'*-bis(2,6-diisopropylphenyl)-ethylenediamine (10 mmol, 3.81 g) and the resulting slurry was heated to 120 °C for 2 h. The excess triethylorthoformate and ethanol formed during the reaction mixture were removed by distillation, leaving behind a light yellow solid. Recrystallization of the residue from hot ethanol afforded the desired product as colourless crystals. Yield: 2.30 g (48%). Colorless crystals. $^1$H NMR (DMSO-d₆): δ = 9.44 (s, 1H, NC*H*N), 7.56 (t, *J* = 7.8, 2H, C*H*-aromatic), 7.44 (d, *J* = 7.8 , 4H, C*H*-aromatic), 4.53 (s, 4H, imidazole C*H₂*), 3.08 (sept, *J* = 6.8, 4H, C*H*(CH₃)₂), 1.36 (d, *J* = 6.8, 12H, CH(C*H₃*)₂), 1.21 (d, *J* = 6.8, 12H, CH(C*H₃*)₂). $^{13}$C NMR (DMSO-d₆): δ = 160.1 (N*C*HN), 146.1 (*C*H-aromatic), 131.1 (*C*H-aromatic), 129.9 (*C*H-aromatic), 124.8 (*C*H-aromatic), 53.7 (imidazole *C*H), 28.3 (*C*H(CH₃)₂), 25.0 (CH(*C*H₃)₂), 23.3 (CH(*C*H₃)₂).


**General procedure for the synthesis of silver(I) carboxylates Ag(O₂CR) (Procedure N).**[269]

The corresponding carboxylic acid (2.0 mmol) was added to a 0.2 M aqueous solution of NaOH (12 mL, 2.4 mmol) with stirring. After the carboxylic acid has dissolved (gentle heating may be needed), a saturated aqueous solution of AgNO₃ (2.0 mmol, 0.34 g) acidified with a few drops of acetic acid was added.

The white precipitate that formed immediately was collected by filtration, washed with water, and dried *in vacuo*.

**Silver(I) benzoate (AgOBz).**

Prepared by procedure N, from benzoic acid (0.24 g). Yield: 0.27 g (59%). White solid. $^1$H NMR (DMSO-d$_6$): δ = 7.97 − 7.95 (m, 2H), 7.46 − 7.36 (m, 3H). $^{13}$C NMR (DMSO-d$_6$): δ = 170.1, 136.8, 130.2, 129.5, 127.7. $\nu_{max}$/cm$^{-1}$: 1512.8 (C=O), 1379.3 (C=O).

**Silver(I) 4-methylbenzoate (Ag(4-MeC$_6$H$_4$CO$_2$)).**

Prepared by procedure N, from 4-toluic acid (0.27 g). Yield: 0.42 g (86%). White solid. $^1$H NMR (DMSO-d$_6$): δ = 7.85 (d, $J$ = 7.6, 2H), 7.18 (d, $J$ = 7.9, 2H), 2.33 (s, 3H). $^{13}$C NMR (DMSO-d$_6$): δ = 170.2, 139.8, 134.0, 129.6, 128.3, 21.0. $\nu_{max}$/cm$^{-1}$: 1510.3 (C=O), 1379.3 (C=O).

**Silver(I) 4-chlorobenzoate (Ag(4-ClC$_6$H$_4$CO$_2$)).**

Prepared by procedure N, from 4-chlorobenzoic acid (0.31 g). Yield: 0.43 g (81%). White solid. Yield: 0.43 g (81%). $^1$H NMR (DMSO-d$_6$): δ = 7.93 (d, $J$ = 7.9, 2H), 7.42 (d, $J$ = 7.9, 2H). $^{13}$C NMR (DMSO-d$_6$): δ = 169.1, 135.9, 134.9, 131.3, 127.8. $\nu_{max}$/cm$^{-1}$: 1508.8 (C=O), 1371.1 (C=O).

**General procedure for the synthesis of silver(I) NHC carboxylate complexes (Procedure O).**

A mixture of NHC·HBF$_4$ (0.2 mmol, 1 eq.) and Ag(O$_2$CR) (0.24 mmol, 1.2 eq.) in CH$_2$Cl$_2$ (5 or 10 mL) was stirred for 15 min and K$_2$CO$_3$ (4.0 mmol, 20 eq.)

was added. After *x* h (indicated separately below), the mixture was filtered through Celite and solvent was removed *in vacuo*. The residue was washed with 5 mL of Et$_2$O to obtain the crude product as a white solid. Recrystallization from CH$_2$Cl$_2$/hexane at 0 °C afforded the desired product as colourless crystals.

**[(IPr)AgOAc] (4.19a).**[190]

Prepared by procedure O from IPr·HBF$_4$ (0.2 mmol, 95.3 mg), AgOAc (0.24 mmol, 40.0 mg), K$_2$CO$_3$ (4.0 mmol, 0.55 g) and CH$_2$Cl$_2$ (10 mL); *x* = 1. Yield: 53.3 mg (48%). $^1$H NMR (CDCl$_3$): δ = 7.51 (t, *J* = 7.8, 2H, C*H*-aromatic), 7.31 (d, *J* = 7.8, 4H, C*H*-aromatic), 7.23 (d, *J* = 2.0, 2H, imidazole C*H*), 2.57 (sept, *J* = 6.9, 4H, C*H*(CH$_3$)$_2$), 1.86 (s, 3H, C*H*$_3$CO$_2$), 1.31 (d, *J* = 6.9, 12H, CH(C*H*$_3$)$_2$), 1.24 (d, *J* = 6.9, 12H, CH(C*H*$_3$)$_2$). $^{13}$C NMR (CDCl$_3$): δ = 184.5 (dd, *J*($^{109}$Ag, $^{13}$C) = 288, *J*($^{107}$Ag, $^{13}$C) = 249, NCN), 178.1 (CO), 145.6 (C*H*-aromatic), 134.7 (C*H*-aromatic), 130.6 (C*H*-aromatic), 124.2 (C*H*-aromatic), 123.5 (d, *J*($^{107}$Ag, $^{13}$C) = 8.1, imidazole C*H*), 28.7 (CH(CH$_3$)$_2$), 24.6 (CH(C*H*$_3$)$_2$), 24.0 (CH(C*H*$_3$)$_2$), 22.6 (CH$_3$CO$_2$). MS [ESI]: *m/z* (%) = 536.22 [(IPr)Ag(MeCN)]$^+$ (100). ν$_{max}$/cm$^{-1}$: 1588.3 (C=O), 1326.1 (C=O). Anal. Calc. for C$_{29}$H$_{39}$AgN$_2$O$_2$: C, 62.70; H, 7.08; N, 5.04%. Found: C, 62.70; H, 7.08; N, 5.00%.

**[(IPr)AgOBz] (4.19b).**

Prepared by procedure O from IPr·HBF$_4$ (0.2 mmol, 95.3 mg), AgOBz (0.24 mmol, 55.0 mg), K$_2$CO$_3$ (4.0 mmol, 0.55 g) and CH$_2$Cl$_2$ (10 mL); *x* = 1. Yield: 55.6 mg (45%). $^1$H NMR (CDCl$_3$): δ = 7.90 (d, *J* = 6.9, 2H, benzoate C*H*),

7.49 (t, $J$ = 7.8, 2H, C*H*-aromatic), 7.32 – 7.22 (m, 7H, benzoate C*H*, C*H*-aromatic), 7.22 (d, $J$ = 2.1, 2H, imidazole C*H*), 2.60 (sept, $J$ = 6.9, 4H, C*H*(CH$_3$)$_2$), 1.34 (d, $J$ = 6.9, 12H, CH(C*H*$_3$)$_2$), 1.23 (d, $J$ = 6.9, 12H, CH(C*H*$_3$)$_2$). $^{13}$C NMR (CDCl$_3$): δ = 184.4 (dd, $J$($^{109}$Ag, $^{13}$C) = 290, $J$($^{107}$Ag, $^{13}$C) = 251, N*C*N), 172.8 (*C*O), 145.6 (*C*H-aromatic), 136.1 (*C*H-aromatic), 134.7 (*C*H-aromatic), 130.6 (*C*H-aromatic), 129.8 (*C*H-aromatic), 129.7 (*C*H-aromatic), 127.4 (*C*H-aromatic), 124.3 (*C*H-aromatic), 123.6 (d, $J$($^{107}$Ag, $^{13}$C) = 8.0 , imidazole *C*H), 28.7 (*C*H(CH$_3$)$_2$), 24.7 (CH(*C*H$_3$)$_2$), 24.1 (CH(*C*H$_3$)$_2$). MS [ESI]: $m/z$ (%) = 536.22 [(IPr)Ag(MeCN)]$^+$ (100). $v_{max}$/cm$^{-1}$: 1611.7 (C=O), 1346.2 (C=O). Anal. Calc. for C$_{34}$H$_{41}$AgN$_2$O$_2$: C, 66.12; H, 6.69; N, 4.54%. Found: C, 66.26; H, 6.79; N, 4.58%.

## [(IPr)Ag(4-MeC$_6$H$_4$CO$_2$)] (4.19c).

Prepared by procedure O from IPr·HBF$_4$ (0.2 mmol, 95.3 mg), Ag(4-MeC$_6$H$_4$CO$_2$) (0.24 mmol, 58.3 mg), K$_2$CO$_3$ (4.0 mmol, 0.55 g) and CH$_2$Cl$_2$ (10 mL); $x$ = 2. Product contained [Ag(IPr)$_2$]X as an impurity. Crude yield: 65.8 mg (52%). $^1$H NMR (CDCl$_3$): δ = 7.79 (d, $J$ = 7.9, 2H, benzoate C*H*), 7.40 (t, $J$ = 7.8, 2H, C*H*-aromatic), 7.30 (d, $J$ = 7.6, 4H, C*H*-aromatic), 7.22 (d, $J$ = 2.1, 2H, imidazole C*H*), 7.04 (d, $J$ = 7.9, 2H, benzoate C*H*), 2.60 (sept, $J$ = 6.8, 4H, C*H*(CH$_3$)$_2$), 2.28 (s, 3H, benzoate C*H*$_3$), 1.33 (d, $J$ = 6.9, 12H, CH(C*H*$_3$)$_2$), 1.23 (d, $J$ = 6.9, 12H, CH(C*H*$_3$)$_2$). $^{13}$C NMR (CDCl$_3$): δ = 184.5 (dd, $J$($^{109}$Ag, $^{13}$C) = 289 , $J$($^{107}$Ag, $^{13}$C) = 250 , N*C*N), 172.9 (*C*O), 145.6 (*C*H-aromatic), 139.8 (*C*H-aromatic), 134.7 (*C*H-aromatic), 133.2 (*C*H-aromatic), 130.6 (*C*H-aromatic), 129.8 (*C*H-aromatic), 128.1 (*C*H-aromatic), 124.3 (*C*H-aromatic), 123.6 (d, $J$($^{107}$Ag, $^{13}$C) = 8.0, imidazole *C*H), 28.7 (*C*H(CH$_3$)$_2$), 24.7

(CH(CH$_3$)$_2$), 24.1 (CH(CH$_3$)$_2$), 21.3 (benzoate CH$_3$). MS [ESI]: *m/z* (%) = 536.22 [(IPr)Ag(MeCN)]$^+$ (100). ν$_{max}$/cm$^{-1}$: 1602.7 (C=O), 1359.2 (C=O).

### [(IPr)Ag(4-ClC$_6$H$_4$CO$_2$)] (4.19d).

Prepared by procedure O from IPr·HBF$_4$ (0.2 mmol, 95.3 mg), Ag(4-ClC$_6$H$_4$CO$_2$) (0.24 mmol, 63.2 mg), K$_2$CO$_3$ (4.0 mmol, 0.55 g) and CH$_2$Cl$_2$ (10 mL); *x* = 2. Product contained [Ag(IPr)$_2$]X as an impurity. Crude yield: 87.5 mg (67%). $^1$H NMR (CDCl$_3$): δ = 7.85 − 7.82 (m, 2H, benzoate C*H*), 7.49 (t, *J* = 7.8, 2H, C*H*-aromatic), 7.30 (d, *J* = 7.8, 4H, C*H*-aromatic), 7.23 − 7.18 (m, 4H, imidazole C*H*, benzoate C*H*), 2.59 (sept, *J* = 6.9, 4H, C*H*(CH$_3$)$_2$), 1.32 (d, *J* = 6.9, 12H, CH(C*H*$_3$)$_2$), 1.23 (d, *J* = 6.9, 12H, CH(C*H*$_3$)$_2$). $^{13}$C NMR (126 MHz, CDCl$_3$): δ = 184.1 (dd, *J*($^{109}$Ag, $^{13}$C) = 291, *J*($^{107}$Ag, $^{13}$C) = 252, N*C*N), 171.8 (*C*O), 145.6 (*C*H-aromatic), 145.1 (*C*H-aromatic), 135.8 (*C*H-aromatic), 134.7 (*C*H-aromatic), 131.2 (*C*H-aromatic), 130.6 (*C*H-aromatic), 127.5 (*C*H-aromatic), 124.3 (*C*H-aromatic), 123.6 (d, *J*($^{107}$Ag, $^{13}$C) = 8.1, imidazole *C*H), 28.7 (*C*H(CH$_3$)$_2$), 24.7 (CH(*C*H$_3$)$_2$), 24.0 (CH(*C*H$_3$)$_2$). MS [ESI]: *m/z* (%) = 536.22 [(IPr)Ag(MeCN)]$^+$ (100). ν$_{max}$/cm$^{-1}$: 1606.6 (C=O), 1365.9 (C=O).

### [(SIPr)AgOAc] (4.20a).[190]

Prepared by procedure O from SIPr·HBF$_4$ (0.2 mmol, 95.7 mg), AgOAc (0.24 mmol, 40.0 mg), K$_2$CO$_3$ (4.0 mmol, 0.55 g) and CH$_2$Cl$_2$ (10 mL); *x* = 2. Yield: 62.5 mg (56%). $^1$H NMR (CDCl$_3$): δ = 7.40 (t, *J* = 7.8, 2H, C*H*-aromatic), 7.24 (d, *J* = 7.8, 4H, C*H*-aromatic), 4.06 (s, 4H, imidazole C*H*$_2$), 3.06 (sept, *J* = 6.9, 4H, C*H*(CH$_3$)$_2$), 1.80 (s, 3H, C*H*$_3$CO$_2$), 1.36 (d, *J* = 6.9, 12H,

CH(C$H_3$)$_2$), 1.34 (d, $J$ = 6.9, 12H, CH(C$H_3$)$_2$). $^{13}$C NMR (126 MHz, CDCl$_3$): δ

= 207.9 (dd, $J$($^{109}$Ag, $^{13}$C) = 271, $J$($^{107}$Ag, $^{13}$C) = 234, N$C$N), 178.2 ($C$O),

146.6 ($C$H-aromatic), 134.6 ($C$H-aromatic), 129.9 ($C$H-aromatic), 124.6 ($C$H-

aromatic), 53.8 (d, $J$($^{107}$Ag, $^{13}$C) = 9.2, imidazole $C$H$_2$), 28.9 ($C$H(CH$_3$)$_2$), 25.3

($C$H(CH$_3$)$_2$), 24.0 (CH($C$H$_3$)$_2$), 22.5 ($C$H$_3$CO$_2$). MS [ESI]: $m/z$ (%) = 538.24

[(SIPr)Ag(MeCN)]$^+$ (100). ν$_{max}$/cm$^{-1}$: 1587.2 (C=O), 1326.1 (C=O). Anal.

Calc. for C$_{29}$H$_{41}$AgN$_2$O$_2$: C, 62.48; H, 7.41; N, 5.02%. Found: C, 62.62; H,

7.50; N, 5.14%.


**[(SIPr)AgOBz] (4.20b).**

Prepared by procedure O from IPr·HBF$_4$ (0.2 mmol, 95.7 mg), AgOBz (0.24

mmol, 63.2 mg), K$_2$CO$_3$ (4.0 mmol, 0.55 g) and CH$_2$Cl$_2$ (10 mL); $x$ = 1. Yield:

68.2 mg (55%). $^1$H NMR (CDCl$_3$): δ = 7.87 − 7.84 (m, 2H, benzoate C$H$),

7.40 (t, $J$ = 7.8, 2H, C$H$-aromatic), 7.27 − 7.19 (m, 7H, benzoate C$H$, C$H$-

aromatic), 4.08 (s, 4H, imidazole C$H_2$), 3.11 (sept, $J$ = 6.8, 4H, C$H$(CH$_3$)$_2$),

1.41 (d, $J$ = 6.9, 12H, CH(C$H_3$)$_2$), 1.35 (d, $J$ = 6.8, 12H, CH(C$H_3$)$_2$). $^{13}$C NMR

(126 MHz, CDCl$_3$): δ = 207.9 (dd, $J$($^{109}$Ag, $^{13}$C) = 271 , $J$($^{107}$Ag, $^{13}$C) = 235,

N$C$N), 172.9 ($C$O), 146.6 ($C$H-aromatic), 136.0 ($C$H-aromatic), 134.7 ($C$H-

aromatic), 129.9 ($C$H-aromatic), 129.8 ($C$H-aromatic), 129.7 ($C$H-aromatic),

127.3 ($C$H-aromatic), 124.7 ($C$H-aromatic), 53.9 (d, $^1J$($^{107}$Ag, $^{13}$C) = 9.4 ,

imidazole $C$H$_2$), 28.9 ($C$H(CH$_3$)$_2$), 25.4 (CH($C$H$_3$)$_2$), 24.1 (CH($C$H$_3$)$_2$). MS

[ESI]: $m/z$ (%) = 538.24 [(SIPr)Ag(MeCN)]$^+$ (100). ν$_{max}$/cm$^{-1}$: 1606.7 (C=O),

1364.5 (C=O). Anal. Calc. for C$_{34}$H$_{43}$AgN$_2$O$_2$: C, 65.91; H, 7.00; N, 4.52%.

Found: C, 65.85; H, 7.09; N, 4.60%.

**[(SIPr)Ag(4-MeC₆H₄CO₂)] (4.20c).**

Prepared by procedure O from IPr·HBF₄ (0.2 mmol, 95.7 mg), Ag(4-MeC₆H₄CO₂) (0.24 mmol, 58.3 mg), K₂CO₃ (4.0 mmol, 0.55 g) and CH₂Cl₂ (10 mL); $x = 4$. Yield: 60.9 mg (54%). $^1$H NMR (CDCl₃): δ = 7.75 (d, $J$ = 7.9, 2H, benzoate C*H*), 7.40 (t, $J$ = 7.8, 2H, C*H*-aromatic), 7.25 (d, $J$ = 7.6, 4H, C*H*-aromatic), 7.01 (d, $J$ = 7.9, 2H, benzoate C*H*), 4.07 (s, 4H, imidazole C*H*₂), 3.10 (sept, $J$ = 6.8, 4H, C*H*(CH₃)₂), 2.27 (s, 3H, C*H*₃C₆H₄CO₂), 1.41 (d, $J$ = 6.9, 12H, CH(C*H*₃)₂), 1.35 (d, $J$ = 6.9, 12H, CH(C*H*₃)₂). $^{13}$C NMR (126 MHz, CDCl₃): δ = 207.9 (dd, $J(^{109}\text{Ag}, ^{13}\text{C})$ = 271, $J(^{107}\text{Ag}, ^{13}\text{C})$ = 235, N*C*N), 172.9 (*C*O), 146.6 (*C*H-aromatic), 139.7 (*C*H-aromatic), 134.7 (*C*H-aromatic), 133.2 (*C*H-aromatic), 129.9 (*C*H-aromatic), 129.7 (*C*H-aromatic), 128.0 (*C*H-aromatic), 124.6 (*C*H-aromatic), 53.8 (d, $^1J(^{107}\text{Ag}, ^{13}\text{C})$ = 9.3, imidazole *C*H₂), 28.9 (*C*H(CH₃)₂), 25.4 (CH(*C*H₃)₂), 24.1 (CH(*C*H₃)₂), 21.3 (*C*H₃C₆H₄CO₂). MS [ESI]: $m/z$ (%) = 538.24 [(SIPr)Ag(MeCN)]⁺ (100). $\nu_{max}$/cm⁻¹: 1603.6 (C=O), 1360.2 (C=O). Anal. Calc. for C₃₅H₄₅AgN₂O₂: C, 66.35; H, 7.16; N, 4.42%. Found: C, 63.64; H, 7.49; N, 4.27%.


**[(SIPr)Ag(4-ClC₆H₄CO₂)] (4.20d).**

Prepared by procedure O from IPr·HBF₄ (0.2 mmol, 95.7 mg), Ag(4-ClC₆H₄CO₂) (0.24 mmol, 63.2 mg), K₂CO₃ (4 mmol, 0.55 g) and CH₂Cl₂ (10 mL); $x = 4$. Product contained [Ag(SIPr)₂]X as an impurity. Crude yield: 85.9 mg (66%). $^1$H NMR (CDCl₃): δ = 7.80 – 7.77 (m, 2H, benzoate C*H*), 7.40 (t, $J$ = 7.8, 2H, C*H*-aromatic), 7.25 (d, $J$ = 7.8, 4H, C*H*-aromatic), 7.18 – 7.15 (m, 2H, benzoate C*H*), 4.08 (s, 4H, imidazole C*H*₂), 3.10 (sept, $J$ = 6.8, 4H, C*H*(CH₃)₂), 1.39 (d, $J$ = 6.8, 12H, CH(C*H*₃)₂), 1.35 (d, $J$ = 6.8, 12H,

CH(C$H_3$)$_2$). $^{13}$C NMR (126 MHz, CDCl$_3$): δ = 207.6 (dd, $J$($^{109}$Ag, $^{13}$C) = 273, $J$($^{107}$Ag, $^{13}$C) = 236, N$C$N), 171.8 ($C$O), 146.6 ($C$H-aromatic), 146.1 ($C$H-aromatic), 135.8 ($C$H-aromatic), 134.6 ($C$H-aromatic), 131.2 ($C$H-aromatic), 129.9 ($C$H-aromatic), 127.5 ($C$H-aromatic), 124.7 ($C$H-aromatic), 53.9 (d, $^{1}J$($^{107}$Ag, $^{13}$C) = 9.3, imidazole $C$H$_2$), 28.9 ($C$H(CH$_3$)$_2$), 25.4 (CH($C$H$_3$)$_2$), 24.1 (CH($C$H$_3$)$_2$). MS [ESI]: $m/z$ (%) = 538.24 [(SIPr)Ag(MeCN)]$^+$ (100). $\nu_{max}$/cm$^{-1}$: 1606.6 (C=O), 1365.9 (C=O).

## [(IPent)AgOAc] (4.44a).

Prepared by procedure O from IPent·HBF$_4$ (0.2 mmol, 117.7 mg), AgOAc (0.24 mmol, 40.0 mg), K$_2$CO$_3$ (4 mmol, 0.55 g) and CH$_2$Cl$_2$ (5 mL); $x$ = 1.5. Purification by recrystallization was unnecessary. Yield: 82.9 mg (62%). $^1$H NMR (500 MHz, CDCl$_3$): δ = 7.47 (t, $J$ = 7.8, 2H, C$H$-aromatic), 7.20 (d, $J$ = 7.8, 4H, C$H$-aromatic), 7.09 (d, $J$ = 1.9, 2H, imidazole C$H$), 2.16 − 2.09 (m, 4H, Et$_2$C$H$), 1.80 (s, 3H, C$H_3$CO$_2$), 1.78 − 1.59 (m, 12H, CH$_3$C$H_2$), 1.48 (m, 4H, CH$_3$C$H_2$), 0.90 (t, $J$ = 7.4, 12H, C$H_3$CH$_2$), 0.77 (t, $J$ = 7.4 12H, C$H_3$CH$_2$). $^{13}$C NMR (126 MHz, CDCl$_3$): δ = 184.3 (dd, $J$($^{109}$Ag, $^{13}$C) = 288, $J$($^{107}$Ag, $^{13}$C) = 250, N$C$N), 177.8 ($C$O), 143.2 ($C$H-aromatic), 137.5 ($C$H-aromatic), 130.2 ($C$H-aromatic), 124.6 ($C$H-aromatic), 124.1 (d, $J$($^{107}$Ag, $^{13}$C) = 8.3, imidazole $C$H), 42.7 (Et$_2$$C$H), 29.3 ($C$H$_2$), 28.5 ($C$H$_2$), 22.6 ($C$H$_3$CO$_2$), 12.8 ($C$H$_3$), 12.6 ($C$H$_3$). MS [ESI]: $m/z$ (%) = 648.34 [(IPent)Ag(MeCN)]$^+$ (100). $\nu_{max}$/cm$^{-1}$: 1599.9 (C=O), 1375.8 (C=O). Anal. Calc. for C$_{37}$H$_{55}$AgN$_2$O$_2$: C, 66.56; H, 8.30; N, 4.20%. Found: C, 66.46; H, 8.23; N, 4.13%.

**[(IPent)AgOBz] (4.44b).**

Prepared by procedure O from IPent·HBF$_4$ (0.2 mmol, 117.7 mg), AgOBz (0.24 mmol, 63.2 mg), K$_2$CO$_3$ (4 mmol, 0.55 g) and CH$_2$Cl$_2$ (5 mL); $x$ = 1.5. Purification by recrystallization was unnecessary. Yield: 102.3 mg (70%). ^{1}H NMR (CDCl$_3$): δ = 7.85 (d, $J$ = 6.9, 2H, benzoate C*H*), 7.48 (t, $J$ = 7.8, 2H, C*H*-aromatic), 7.29 – 7.19 (m, 6H, C*H*-aromatic, benzoate C*H*), 7.10 (d, $J$ = 1.9, 2H, imidazole C*H*), 2.21 – 2.14 (m, 4H, Et$_2$C*H*), 1.84 – 1.59 (m, 12H, CH$_3$C*H$_2$*), 1.51 (m, 4H, CH$_3$C*H$_2$*), 0.93 (t, $J$ = 7.3, 12H, C*H$_3$*CH$_2$), 0.79 (t, $J$ = 7.3, 12H, C*H$_3$*CH$_2$). ^{13}C NMR (CDCl$_3$): δ = 184.2 (dd, $J$([109]Ag, ^{13}C) = 289, $J$([107]Ag, ^{13}C) = 250, N*C*N), 172.5 (*C*O), 143.3 (*C*H-aromatic), 137.5 (*C*H-aromatic), 136.8 (*C*H-aromatic), 130.2 (*C*H-aromatic), 129.6 (*C*H-aromatic), 129.5 (*C*H-aromatic), 127.2 (*C*H-aromatic), 124.7 (*C*H-aromatic), 124.2 (d, $J$([107]Ag, ^{13}C) = 8.3, imidazole *C*H), 42.8 (Et$_2$*C*H), 29.3 (*C*H$_2$), 28.6 (*C*H$_2$), 12.9 (*C*H$_3$), 12.6 (*C*H$_3$). MS [ESI]: $m/z$ (%) = 648.34 [(IPent)Ag(MeCN)]$^+$ (100). $\nu_{max}$/cm$^{-1}$: 1606.7 (C=O), 1364.5 (C=O). Anal. Calc. for C$_{42}$H$_{57}$AgN$_2$O$_2$: C, 69.12; H, 7.87; N, 3.84%. Found: C, 68.94; H, 7.74; N, 3.90%.


**[(IPent)Ag(4-ClC$_6$H$_4$CO$_2$)] (4.44d).**

Prepared by procedure O from IPent·HBF$_4$ (0.2 mmol, 117.7 mg), Ag(4-ClC$_6$H$_4$CO$_2$) (0.24 mmol, 63.2 mg), K$_2$CO$_3$ (4 mmol, 0.55 g) and CH$_2$Cl$_2$ (5 mL); $x$ = 2.5. Purification by recrystallization was unnecessary. Yield: 79.6 mg (52%). ^{1}H NMR (500 MHz, CDCl$_3$): δ = 7.80 – 7.77 (m, 2H, benzoate C*H*), 7.49 (t, $J$ = 7.8, 2H, C*H*-aromatic), 7.22 (m, $J$ = 7.8, 4H, C*H*-aromatic), 7.19 – 7.14 (m, 2H, benzoate C*H*), 7.11 (d, $J$ = 1.9, 2H, imidazole C*H*), 2.20 – 2.14 (m, 4H, Et$_2$C*H*), 1.82 – 1.61 (m, 12H, CH$_3$C*H$_2$*), 1.50 (m, 4H, CH$_3$C*H$_2$*),

0.9 (t, $J$ = 7.4, 12H, C$H_3$CH$_2$), 0.79 (t, $J$ = 7.4, 12H, C$H_3$CH$_2$). $^{13}$C NMR (126 MHz, CDCl$_3$): δ = 183.9 (dd, $J$($^{109}$Ag, $^{13}$C) = 291, $J$($^{107}$Ag, $^{13}$C) = 252, N$C$N), 171.4 ($C$O), 143.2 ($C$H-aromatic), 137.5 ($C$H-aromatic), 135.5 ($C$H-aromatic), 135.3 ($C$H-aromatic), 131.1 ($C$H-aromatic), 130.2 ($C$H-aromatic), 127.4 ($C$H-aromatic), 124.7 ($C$H-aromatic), 124.2 (d, $J$($^{107}$Ag, $^{13}$C) = 8.4, imidazole $C$H), 42.8 (Et$_2$$C$H), 29.3 ($C$H$_2$), 28.6 ($C$H$_2$), 12.9 ($C$H$_3$), 12.6 ($C$H$_3$). MS [ESI]: $m/z$ (%) = 648.34 [(IPent)Ag(MeCN)]$^+$ (100). $\nu_{max}$/cm$^{-1}$: 1607.5 (C=O), 1369.6 (C=O). Anal. Calc. for C$_{42}$H$_{56}$AgClN$_2$O$_2$: C, 66.01; H, 7.39; N, 3.67%. Found: C, 66.08; H, 7.26; N, 3.82%.


## [(IAd)AgOAc] (4.45a).

Prepared by procedure O from IAd·HBF$_4$ (0.2 mmol, 117.7 mg), AgOAc (0.24 mmol, 40.0 mg), K$_2$CO$_3$ (4 mmol, 0.55 g) and CH$_2$Cl$_2$ (5 mL); $x$ = 1.5. Purification by recrystallization results in decomposition. Yield: 59.4 mg (59%). $^1$H NMR (CDCl$_3$): δ = 7.10 (d, $J$ = 1.9, 2H, imidazole C$H$), 2.37 – 2.36 (m, 12H, adamantyl C$H_2$), 2.26 (br s, 6H, adamantyl C$H$), 2.12 (s, C$H_3$CO$_2$), 1.81 – 1.73 (m, 12H, adamantyl C$H_2$). MS [ESI]: $m/z$ (%) = 337.27 [IAd+H]$^+$ (100). $\nu_{max}$/cm$^{-1}$: 1595.0 (C=O), 1372.2 (C=O).


## [(IAd)AgOBz] (4.45b).

Prepared by procedure O from IPent·HBF$_4$ (0.2 mmol, 117.7 mg), AgOBz (0.24 mmol, 63.2 mg), K$_2$CO$_3$ (4 mmol, 0.55 g) and CH$_2$Cl$_2$ (5 mL); $x$ = 1.5. Purification by recrystallization results in decomposition. Yield: 48.2 mg (48%). $^1$H NMR (CDCl$_3$): δ = 8.16 – 8.13 (m, 2H, benzoate C$H$), 7.40 – 7.37 (3H, benzoate C$H$), 7.12 (d, $J$ = 1.9, 2H, imidazole C$H$), 2.41 (m, 12H,

adamantyl C$H_2$), 2.26 (br s, 6H, adamantyl C$H$), 1.82 – 1.73 (m, 12H, adamantyl C$H_2$). MS [ESI]: $m/z$ (%) = 337.27 [IAd+H]$^+$ (100). $\nu_{max}$/cm$^{-1}$: 1597.8 (C=O), 1368.3 (C=O).

**Ag$_4$(SIMes)$_2$(CF$_3$CO$_2$)$_4$ (4.43).**

SIMes·HCl (1.0 mmol, 0.34 g) was added to a solution of potassium *tert*-butoxide (1.0 mmol, 0.11 g) in THF (20 mL) at room temperature. The mixture was stirred for 4 h at room temperature, and the white KCl precipitate was filtered off. The filtrate was evaporated, and the oily residue was extracted with dry *n*-hexane. The combined extracts were evaporated, leaving an off-white solid, which was dissolved in THF (10 mL). Silver(I) trifluoroacetate (0.75 mmol, 0.17 g) was added, and the resulting light brown solution stirred overnight at room temperature. The reaction mixture was filtered and evaporation of the filtrate gave a yellow oil, which was triturated with *n*-hexane to give an off-white solid. X-ray diffraction quality single crystals were obtained from a saturated solution of the crude product using MeOH:Et$_2$O (1:1). $^1$H NMR (CDCl$_3$): δ = 6.97 (s, 4H, C$H$-aromatic), 4.02 (s, 4H, imidazole C$H_2$), 2.31 (s, 18H, C$H_3$). $^{13}$C NMR (CDCl$_3$): δ = 139.0 (s, $C$H-aromatic), 135.4 (s, $C$H-aromatic), 135.0 (s, $C$H-aromatic), 129.9 (s, $C$H-aromatic), 51.2 (s, imidazole $C$H$_2$), 21.0 (s, $C$H$_3$), 17.9 (s, $C$H$_3$). $^{19}$F NMR (CDCl$_3$): δ = −74.3 (s, CF$_3$CO$_2^-$). MS [ESI]: $m/z$ (%) = 456.14 [(SIMes)Ag(MeCN)]$^+$ (100).

**[(SIMes)AgCl].**[270]

SIMes·HCl (0.5 mmol, 171.5 mg) was dissolved in 15 mL of $CH_2Cl_2$ and silver(I) oxide (0.25 mmol, 57.9 mg) was added. The resulting mixture was stirred at room temperature for 24 h, filtered through Celite, and concentrated *in vacuo*. Recrystallization from $CH_2Cl_2$/*n*-hexane gave the desired complex as colorless crystals. Yield: 157 mg (70%). Colorless crystals. $^1$H NMR (CDCl$_3$): $\delta$ = 6.94 (s, 4H, C*H*-aromatic), 4.00 (s, 4H, imidazole C*H*$_2$), 2.29 (s, 18H, C*H*$_3$). $^{13}$C NMR (CDCl$_3$): $\delta$ = 207.5 (dd, $J(^{109}$Ag, $^{13}$C) = 256, $J(^{109}$Ag, $^{13}$C) = 222, N*C*N), 139.0 (s, *C*H-aromatic), 135.7 (s, *C*H-aromatic), 135.3 (s, *C*H-aromatic), 130.0 (s, *C*H-aromatic), 51.3 (s, imidazole *C*H$_2$), 21.2 (s, *C*H$_3$), 18.1 (s, *C*H$_3$).

**[(IPr)AgCl].**[191]

IPr·HCl (0.5 mmol, 212.5 mg) was dissolved in 5 mL of $CH_2Cl_2$ and silver(I) oxide (0.3 mmol, 69.5 mg) was added. The resulting mixture was stirred at room temperature for 12 h, filtered through Celite, and concentrated *in vacuo*. Pentane was added to precipitate a white solid, which was washed further with pentane (3 × 5 mL) and dried *in vacuo*. Yield: 125 mg (47%). White powder. $^1$H NMR (CDCl$_3$): $\delta$ = 7.50 (m, 2H, C*H*-aromatic), 7.30 (m, 4H, C*H*-aromatic), 7.21 (s, 2H, imidazole C*H*), 2.54 (septet, $J$ = 6.8, 4H, C*H*(CH$_3$)$_2$), 1.28 (d, $J$ = 6.8, 12H, CH(C*H*$_3$)$_2$), 1.22 (d, $J$ = 6.8, 12H, CH(C*H*$_3$)$_2$). $^{13}$C NMR (CDCl$_3$): $\delta$ = 184.6 (dd, $J(^{109}$Ag, $^{13}$C) = 271, $J(^{109}$Ag, $^{13}$C) = 235, N*C*N), 145.6 (*C*H-aromatic), 130.8 (*C*H-aromatic), 124.4 (*C*H-aromatic), 123.7 (*C*H-aromatic), 123.6 (imidazole *C*H), 28.7 (*C*H(CH$_3$)$_2$), 24.7 (CH(*C*H$_3$)$_2$), 24.0 (CH(*C*H$_3$)$_2$).

**[Ag(IPr)$_2$]$_2$[PF$_6$].**[229]

A mixture of [(IPr)AgCl] (0.2 mmol, 106.4 mg) and NH$_4$PF$_6$ (0.25 mmol, 40.8 mg) in methanol (10 mL) were stirred at room temperature for 2 days. All volatiles were then evaporated, and CH$_2$Cl$_2$ (10 mL) was added to give a pale yellow suspension that was filtered through Celite. The filtrate was concentrated and addition of *n*-hexane (10 mL) precipitated an off-white powder that was collected and dried *in vacuo*. Yield: 144 mg (70%). Off-white powder. $^1$H NMR (CDCl$_3$): δ 9.94 (t, 4H, *J* = 7.8, C*H*-aromatic), 7.13 (d, 8H, *J* = 7.8, C*H*-aromatic), 7.07 (d, 4H, *J* = 1.8, imidazole C*H*), 2.27 (sept, 8H, *J* = 6.9, C*H*(CH$_3$)$_2$), 1.06 (d, 24H, *J* = 6.9, CH(C*H$_3$*)$_2$), 0.77 (d, 24H, *J* = 6.9, CH(C*H$_3$*)$_2$). $^{13}$C NMR (CDCl$_3$): δ = 183.6 (dd, *J*($^{109}$Ag, $^{13}$C) = 211, *J*($^{109}$Ag, $^{13}$C) = 183, N*C*N), 145.3 (*C*H-aromatic), 134.6 (*C*H-aromatic), 129.9 (*C*H-aromatic), 125.0 (*C*H-aromatic), 123.8 (d, *J*($^{107}$Ag, $^{13}$C) = 6.0, imidazole *C*H), 28.7 (*C*H(CH$_3$)$_2$), 24.7 (CH(*C*H$_3$)$_2$), 24.0 (CH(*C*H$_3$)$_2$).

**General procedure for Ag(I)-NHC catalyzed conversion of 2.1 to 2.2 or 2.8 to 2.9 (Procedure M):**

The substrate (0.2 mmol) and the 1,3,5-trimethoxybenzene internal standard (ca. 6.8 mg) were dissolved in CD$_2$Cl$_2$ (0.5 mL) at room temperature, followed by the catalyst (0.01 or 0.05 equiv.). The solution was transferred to an NMR tube, and the reaction progress was monitored by $^1$H NMR spectroscopy. The yields and conversions were calculated by comparison of the integrals of the product and substrate resonances to that of the internal standard.

**5-methylene-2-vinyl-4,5-dihydrooxazole (3.2e).**
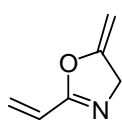
This compound was previously reported[271] but no spectroscopic data was given. $^1$H NMR (CD$_2$Cl$_2$): δ 6.33 (dd, $J$ = 17.6, 10.9, 1H, C$H$=CH$_2$), 6.16 (d, $J$ = 17.6, 1H, CH=C$H$), 5.81 (d, $J$ = 10.9, 1H, CH=C$H$), 4.73 (q, $J$ = 2.9, 1H, OC=C$H$), 4.55 (t, $J$ = 2.9, 2H, NC$H_2$), 4.33 (q, $J$ = 2.6, 1H, OC=C$H$).

**2-carboethoxy-5-methylene-4,5-dihydrooxazole (3.2g).**
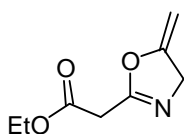
$^1$H NMR (CD$_2$Cl$_2$): δ 4.88 (q, $J$ = 3.2, 1H, =C$H$), 4.67 (t, $J$ = 3.0, 2H, NC$H_2$), 4.44 (q, $J$ = 3.2, 1H, =C$H$), 4.35 (q, $J$ = 7.5, 2H, C$H_2$), 1.39 – 1.36 (m, 5H, C$H_2$C$H_3$).

# Appendix

**Table A1.** Bond lengths (Å), bond angles (deg), and $\delta C_{carbene}$ resonance of Ag(I) NHC carboxylate complexes

| Complex | $\delta C_{carbene}$ / ppm | $^1J(^{13}C-^{107,109}Ag)$ / Hz | NMR solvent | Ag1-C1 / Å | Ag1-O1 / Å | C1-Ag1-O1 / ° | Ag–Ag | Ref. |
|---------|------|------|------|------|------|------|------|------|
| 4.1a | 186.2 | – | DMSO-d$_6$ | 2.067(3) | 2.1198(19) | 168.19(9) | – | [1] |
| 4.1b | 186.5 | – | DMSO-d$_6$ | 2.072(4) | 2.118(3) | 175.9(1) | 3.199 | [2] |
| 4.1c | 187.4 | – | DMSO-d$_6$ | 2.068(2) | 2.112(2) | 174.78(9) | – | [3] |
| 4.1d | 186.5 | – | DMSO-d$_6$ | 2.022(7) | 2.064(5) | 178.2(2) | – | [4] |
| 4.2 | 173.0 | – | CD$_2$Cl$_2$ | 2.064(6) | 2.115(5) | 165.2(2) | 3.2181 | [5] |
| 4.3 | 178.6 | – | DMSO-d$_6$ | 2.064(5) | 2.117(3) | 176.0(2) | – | [6] |
| 4.4 | 182.0 | – | DMSO-d$_6$ | 2.061(6) | 2.129(5) | 167.3(2) | – | [6] |
| 4.5a | 177.0 | – | CDCl$_3$ | 2.065(1) | 2.131(1) | 172.76(5) | – | [7] |
| 4.5b | 177.8 | – | CDCl$_3$ | – | – | – | – | [7] |
| 4.5c | 179.8 | – | DMSO-d$_6$ | 2.077(5) | 2.165(3) | 163.4(1) | 3.0050(5) | [8] |
| 4.5d | 180.2 | – | CDCl$_3$ | 2.067(2) | 2.156(1) | 171.80(7) | – | [9] |
| 4.5e | 179.0 | – | CDCl$_3$ | 2.065 | 2.438 | 153.2 | – | [10] |
| 4.6a | 188.1 | – | CDCl$_3$ | – | – | – | – | [11] |
| 4.6b | 178.4 | – | CDCl$_3$ | – | – | – | – | [11] |
| 4.6c | 178.3 | – | CDCl$_3$ | – | – | – | – | [11] |
| 4.7a | 178.9 | – | CDCl$_3$ | 2.090(2) | 2.159(2) | 163.40(6) | 2.9107(2) | [12], [13] |
| 4.7b | 178.6 | – | CDCl$_3$ | – | – | – | – | [13] |
| 4.7c | 178.6 | – | CDCl$_3$ | – | – | – | – | [13] |
| 4.7d | 206.9 | – | CDCl$_3$ | 2.060(2) | 2.101(1) | 178.76(8) | – | [13] |

| | | | | | | | | |
|---|---|---|---|---|---|---|---|---|
| **4.7e** | 178.9 | – | CDCl$_3$ | 2.059(2) | 2.116(2) | 174.69(6) | – | [13] |
| **4.8a** | 199.0 | – | CDCl$_3$ | 2.055(2) | 2.110(1) | 178.18(6) | – | [14] |
| **4.8b** | 177.2 | – | CDCl$_3$ | – | – | – | – | [14] |
| **4.8c** | 178.6 | – | CDCl$_3$ | – | – | – | – | [14] |
| **4.8d** | 179.1 | – | CDCl$_3$ | 2.049(2) | 2.110(2) | 170.37(9) | – | [14] |
| **4.8e** | 179.1 | – | CDCl$_3$ | – | – | – | – | [14] |
| **4.9a** | 178.7 | – | CDCl$_3$ | – | – | – | – | [15] |
| **4.9b** | 178.5 | – | CDCl$_3$ | 2.085(2) | 2.164(1) | 163.71(5) | – | [15] |
| **4.9c** | 159.2 | – | CDCl$_3$ | – | – | – | – | [15] |
| **4.9d** | 164.5 | – | CDCl$_3$ | 2.069(1) | 2.120(1) | 170.07(5) | 3.1265 | [15] |
| **4.9e** | 166.5 | – | CDCl$_3$ | – | – | – | – | [15] |
| **4.10a** | 170.3 | – | CDCl$_3$ | – | – | – | – | [13] |
| **4.10b** | 178.9 | – | CDCl$_3$ | – | – | – | – | [13] |
| **4.10c** | 178.9 | – | CDCl$_3$ | 2.087(2) 2.073(2) | 2.158(2) 2.120(2) | 173.89(7) 167.77(8) | – | [13] |
| **4.10d** | 179.2 | – | CDCl$_3$ | – | – | – | – | [13] |
| **4.10e** | 178.9 | – | CDCl$_3$ | – | – | – | – | [13] |
| **4.11a** | 178.8 | – | CDCl$_3$ | – | – | – | – | [15] |
| **4.11b** | 178.0 | – | CDCl$_3$ | 2.071(1) | 2.130(1) | 165.07(7) | 3.0791(2) | [15] |
| **4.11c** | – | – | – | – | – | – | – | [15] |
| **4.11d** | 176.7 | – | CDCl$_3$ | – | – | – | – | [15] |
| **4.12a** | 179.9 | – | CDCl$_3$ | – | – | – | – | [8] |
| **4.12b** | 179.2 | – | DMSO-d$_6$ | – | – | – | – | [12] |
| **4.12c** | 180.5 | – | CDCl$_3$ | 2.067(3) | 2.137(2) | 176.10(9) | – | [9] |
| **4.12d** | 180.1 | – | CDCl$_3$ | – | – | – | – | [10] |

| | | | | | | | | |
|---|---|---|---|---|---|---|---|---|
| **4.13a** | 179.7 | – | DMSO-d$_6$ | 2.030(8) | 2.154(5) 2.715(5) | N.A. | – | [6], [16] |
| **4.13b** | 186.3 | – | DMSO-d$_6$ | – | – | – | – | [17], [18] |
| **4.14a** | 177.5 | – | CDCl$_3$ | 2.064(4) | 2.278(4) 2.503(5) | N.A. | – | [7] |
| **4.14b** | 176.1 | – | CDCl$_3$ | – | – | – | – | [7] |
| **4.14c** | 185.6 | – | DMSO-d$_6$ | 2.062(2) | 2.118(2) | 174.89(7) | – | [8] |
| **4.14d** | 179.9 | – | CDCl$_3$ | – | – | – | – | [9] |
| **4.14e** | 183.3 | – | DMSO-d$_6$ | – | – | – | – | [10] |
| **4.15a** | 180.1 | – | CDCl$_3$ | – | – | – | – | [8] |
| **4.15b** | 181.4 | – | DMSO-d$_6$ | 2.069(4) | 2.140(3) | 173.86(14) | – | [12] |
| **4.15c** | 176.2 | – | CDCl$_3$ | 2.060(8) | 2.127(7) | 177.9(3) | – | [4] |
| **4.15d** | 180.9 | – | CDCl$_3$ | 2.040(9) | 2.173(7) 2.687(8) | N.A. | 3.1412 | [10] |
| **4.16** | 179.7 | – | DMSO-d$_6$ | 2.070(9) 2.053(8) | 2.125(6) 2.138(5) 2.713(7) | 175.0(3) N.A. | 3.22669 | [3] |
| **4.17** | 150.4 | – | CDCl$_3$ | – | – | – | – | [15] |
| **4.18** | – | – | CD$_2$Cl$_2$ | 2.084(6) | 2.196(5) | 170.8(2) | 3.171(1) | [19] |
| **4.19** | 207.9 | 234, 271 | CDCl$_3$ | 2.058(7) to 2.060(7) | 2.151(6) to 2.338(7) and 2.300(7) to 2.590(8) | N.A. | – | [20] |
| **4.20** | 184.5 | 249, 288 | CD$_2$Cl$_2$ | 2.064(5) | 2.113(3) | 176.8(1), 177.6(2) | – | [21] |
| **4.21** | 179.41 | – | CDCl$_3$ | 2.070(6) | 2.120(7) | 167.0(3) | – | [22] |

| | | | | | | | | |
|---|---|---|---|---|---|---|---|---|
| **4.22** | – | – | CDCl$_3$ | 2.160(3) 2.156(3) | 2.568(2) | – | – | [22] |
| **4.23a** | 175.7 | – | DMSO-d$_6$ | 2.059(3) | 2.250(3) 2.475(4) | 164.2(1) 141.6(1) | – | [7] |
| **4.23b** | 180.0 | – | DMSO-d$_6$ | 2.072(6) | 2.085(5) | 170.1(2) | – | [8] |
| **4.23c** | 180.2 | – | CDCl$_3$ | 2.055(2) | 2.093(2) | 171.1(1) | – | [9] |
| **4.23d** | 190.5 | – | DMSO-d$_6$ | – | – | – | – | [10] |
| **4.24** | 178.9 | – | CDCl$_3$ | 2.072(5) | 2.1206 2.612(2) | 170.1 | – | [7] |
| **4.25a** | 189.21 | – | CDCl$_3$ | – | – | – | – | [11] |
| **4.25b** | 179.1 | – | CDCl$_3$ | 2.060(2) | 2.1088(14) | 170.76(7) | – | [11] |
| **4.25c** | 178.8 | – | CDCl$_3$ | – | – | – | – | [11] |
| **4.25d** | 179.3 | – | CDCl$_3$ | – | – | – | – | [11] |
| **4.26a** | 180.0 181.4 | – – | CDCl$_3$ DMSO-d$_6$ | 2.049(4) | 2.097(3) | 176.8(1) | – | [8], [12] |
| **4.26b** | 182.4 | – | CDCl$_3$ | – | – | – | – | [9] |
| **4.26c** | 179.0 | – | CDCl$_3$ | – | – | – | – | [10] |
| **4.26d** | 185.9 | – | DMSO-d$_6$ | – | – | – | – | [12] |
| **4.27a** | 185.9 | – | DMSO-d$_6$ | 2.073(4) | 2.171(3) | 165.38(15) | – | [12] |
| **4.27b** | 181.7 | – | DMSO-d$_6$ | 2.052(3) | 2.113(2) | 170.49(10) | 3.1818(2) | [12] |
| **4.28a** | 179.2 | – | DMSO-d$_6$ | 2.079(6) | 2.154(4) | 172.3(2) | – | [23] |
| **4.28b** | 197.0 | – | DMSO-d$_6$ | 2.072(4) | 2.105(4) | 169.5(2) | 3.249 | [23] |
| **4.28c** | 197.5 | – | DMSO-d$_6$ | 2.069(2) | 2.122(2) | 176.68(8) | 3.266 | [23] |

**Table A2.** Bond lengths (Å), bond angles (deg), and $\delta C_{carbene}$ resonance of bis(NHC) and (NHC)AgX (X = halide) complexes

| Complex | $\delta C_{carbene}$ / ppm | $^1J(^{13}C\text{-}^{107,109}Ag)$ / Hz | NMR solvent | Ag-C / Å | Ag-X / Å | C-Ag-C or C-Ag-X / ° | Ag–Ag | Ref. |
|---------|---------|---------|---------|---------|---------|---------|---------|---------|
| **4.29** | 151.2[a] | – | CDCl$_3$ | 2.091(2) | 2.3695 | 163.09 | – | [24] |
| **4.30** | 184.6[a] | 235, 271 | CDCl$_3$ | 2.056(7) | 2.313(2) | 175.2(2) | – | [25] |
| **4.31** | 207.7[a] | 253, 219 | CDCl$_3$ | 2.081(9) | 2.320(2) | 173.3(2) | – | [25] |
| **4.32** | 181.2[a] | – | CDCl$_3$ | 2.087(4) | 2.347(1) | 175.3(1) | 3.281 | [19] |
| **4.33** | 180.7[a] | – | CDCl$_3$ | – | – | – | – | [26] |
| **4.34** | 185.4[a] | – | CDCl$_3$ | 2.094(3) | 2.4873(6) | 161.03(9) | – | [27] |
| **4.35** | 186.7[b] | – | DMSO-d$_6$ | 2.068 | – | 171.4 | – | [28] |
| **4.36** | 181.0[b] | – | DMSO-d$_6$ | 2.086 | – | 180.0 | – | [29] |
| **4.37** | 183.6[a] | – | CDCl$_3$ | 2.129 | – | 180.0 | – | [20], [30] |
| **4.38** | 205.8[c] | 178, 155 | CD$_2$Cl$_2$ | – | – | – | – | [31] |
| **4.39** | 181.3[b] | – | DMSO-d$_6$ | 2.082 | – | 176.4(2) | – | [32] |
| **4.40** | 180.7[b] | – | DMSO-d$_6$ | 2.092 | – | 180.0 | – | [30] |
| **4.41** | 177.6[b] | – | DMSO-d$_6$ | – | – | – | – | [33] |
| **4.42** | 136.7[b] | – | DMSO-d$_6$ | 2.089(3) | – | 177.88(10) | – | [34] |

**References for Tables A1 and A2**

[1]     Kascatan-Nebioglu, A.; Melaiye, A.; Hindi, K.; Durmus, S.; Panzner, M. J.; Hogue, L. A.; Mallett, R. J.; Hovis, C. E.; Coughenour, M.; Crosby, S. D.; Milsted, A.; Ely, D. L.; Tessier, C. A.; Cannon, C. L.; Youngs, W. J. *J. Med. Chem.* **2006**, *49*, 6811−6818.

[2]     Panzner, M. J.; Hindi, K. M.; Wright, B. D.; Taylor, J. B.; Han, D. S.; Youngs, W. J.; Cannon, C. L. *Dalton Trans.* **2009**, 7308−7313.

[3]     Panzner, M. J.; Deeraksa, A.; Smith, A.; Wright, B. D.; Hindi, K. M.; Kascatan-Nebioglu, A.; Torres, A. G.; Judy, B. M.; Hovis, C. E.; Hilliard, J. K.; Mallett, R. J.; Cope, E.; Estes, D. M.; Cannon, C. L.; Leid, J. G.; Youngs, W. J. *Eur. J. Inorg. Chem.* **2009**, 1739−1745.

[4]     Knapp, A. R.; Panzner, M. J.; Medvetz, D. A.; Wright, B. D.; Tessier, C. A.; Youngs, W. J. *Inorg. Chim. Acta* **2010**, *364*, 125−131.

[5]     Chung, M. *Bull. Korean Chem. Soc.* **2002**, *23*, 1160−1162.

[6]     Hindi, K. M.; Siciliano, T. J.; Durmus, S.; Panzner, M. J.; Medvetz, D. A.; Reddy, D. V.; Hogue, L. A.; Hovis, C. E.; Hilliard, J. K.; Mallet, R. J.; Tessier, C. A.; Cannon, C. L.; Youngs, W. J. *J. Med. Chem.* **2008**, *51*, 1577−1583.

[7]     Patil, S.; Claffey, J.; Deally, A.; Hogan, M.; Gleeson, B.; Méndez, L. M. M.; Müller-Bunz, H.; Paradisi, F.; Tacke, M. *Eur. J. Inorg. Chem.* **2010**, 1020−1031.

[8]     Patil, S.; Dietrich, K.; Deally, A.; Gleeson, B.; Müller-Bunz, H.; Paradisi, F.; Tacke, M. *Appl. Organomet. Chem.* **2010**, *24*, 781−793.

[9]     Patil, S.; Dietrich, K.; Deally, A.; Gleeson, B.; Müller-Bunz, H.; Paradisi, F.; Tacke, M. *Helv. Chim. Acta* **2010**, *93*, 2347−2364.

[10]    Patil, S.; Dietrich, K.; Deally, A.; Gleeson, B.; Hackenberg, F.; Müller-Bunz, H.; Paradisi, F.; Tacke, M. *Z. Anorg. Allg. Chem.* **2011**, *637*, 386−396.

[11]    Hackenberg, F.; Deally, A.; Lally, G.; Malenke, S.; Müller-Bunz, H.; Paradisi, F.; Patil, S.; Quaglia, D.; Tacke, M. *Int. J. Inorg. Chem.* **2012**, 121540.

[12]    Patil, S.; Deally, A.; Gleeson, B.; Hackenberg, F.; Müller-Bunz, H.; Paradisi, F.; Tacke, M. *Metallomics* **2011**, *3*, 74−88.

[13]    Hackenberg, F.; Lally, G.; Müller-Bunz, H.; Paradisi, F.; Quaglia, D.; Streciwilk, W.; Tacke, M. *J. Organomet. Chem.* **2012**, *717*, 123−134.

[14]    Hackenberg, F.; Lally, G.; Müller-Bunz, H.; Paradisi, F.; Quaglia, D.; Streciwilk, W.; Tacke, M. *Inorg. Chim. Acta* **2013**, *395*, 135−144.

[15]    Streciwilk, W.; Cassidy, J.; Hackenberg, F.; Müller-Bunz, H.; Paradisi, F.; Tacke, M. *J. Organomet. Chem.* **2014**, *749*, 88−99.

[16]    Medvetz, D. A.; Hindi, K. M.; Panzner, M. J.; Ditto, A. J.; Yun, Y. H.; Youngs, W. J. *Met.-Based Drugs*, **2008**, 384010.

[17]    Ornelas-Megiatto, C.; Shah, P. N.; Wich, P. R.; Cohen, J. L.; Tagaev, J. A.; Smolen, J. A.; Wright, B. D.; Panzner, M. J.; Youngs, W. J.; Fréchet, J. M. J.; Cannon, C. L. *Mol. Pharmaceutics* **2012**, *9*, 3012−3022.

[18]    Leid, J. G.; Ditto, A. J.; Knapp, A.; Shah, P. N.; Wright, B. D.; Blust, R.; Christensen, L.; Clemons, C. B.; Wilber, J. P.; Young, G. W.; Kang, A. G.; Panzner, M. J.; Cannon, C. L.; Yun, Y. H.; Youngs, W. J.; Seckinger, N. M.; Cope, E. K. *J. Antimicrob. Chemother.* **2012**, *67*, 138–148.

[19]     Powell, A. B.; Bielawski, C. W.; Cowley, A. H. *J. Am. Chem. Soc.*
         **2010**, *132*, 10184–10194.

[20]     Partyka, D. V.; Deligonul, N. *Inorg. Chem.* **2009**, *48*, 9463–9475.

[21]     Partyka, D. V.; Robilotto, T. J.; Updegraff III, J. B.; Zeller, M.; Hunter,
         A. D.; Gray, T. G. *Organometallics* **2009**, *28*, 795−801.

[22]     Humenny, W. J.; Mitzinger, S.; Khadka, C. B.; Najafabadi, B. K.;
         Vieiraa, I.; Corrigan, J. F. *Dalton Trans.* **2012**, *41*, 4413–4422.

[23]     Wright, B. D.; Shah, P. N.; McDonald, L. J.; Shaeffer, M. L.; Wagers,
         P. O.; Panzner, M. J.; Smolen, J.; Tagaev, J.; Tessier, C. A.; Cannon, C.
         L.; Youngs, W. J. *Dalton Trans.* **2012**, 6500–6506.

[24]     Newman, C. P.; Clarkson, G. J.; Rourke, J. P. *J. Organomet. Chem.*
         **2007**, *692*, 4962–4968.

[25]     de Frémont, P.; Scott, N. M.; Stevens, E. D.; Ramnial, T.; Lightbody,
         O. C.; Macdonald, C. L. B.; Clyburne, J. A. C.; Abernethy, C. D.;
         Nolan, S. P. *Organometallics* **2005**, *24*, 6301−6309.

[26]     Maishal, T. K.; Basset, J.-M.; Boualleg, M.; Copéret, C.; Veyre, L.;
         Thieuleux, C. *Dalton Trans.* **2009**, 6956−6959.

[27]     Ray, L.; Katiyar, V.; Barman, S.; Raihan, M. J.; Nanavati, H.; Shaikh,
         M. M.; Ghosh, P. *J. Organomet. Chem.* **2007**, 692, 4259–4269.

[28]     Kascatan-Nebioglu, A.; Panzner, M. J.; Garrison, J. C.; Tessier, C. A.;
         Youngs, W. J. *Organometallics* **2004**, *23*, 1928−1931.

[29]     Kriechbaum, M.; Hölbling, J.; Stammler, H.-G.; List, M.; Berger, R. J.
         F.; Monkowius, U. *Organometallics* **2013**, *32*, 2876−2884.

[30]     Yu, X.-Y.; Patrick, B. O.; James, B. R. *Organometallics* **2006**, *25*,
         2359–2363.

298

[31]    Tate, B. K.; Wyss, C. M.; Bacsa, J.; Kluge, K.; Gelbauma, L.; Sadighi, J. P. *Chem. Sci.* **2013**, *4*, 3068–3074.

[32]    Siciliano, T. J.; Deblock, M. C.; Hindi, K. M.; Durmus, S.; Panzner, M. J.; Tessier, C. A.; Youngs, W. J. *J. Organomet. Chem.* **2011**, *696*, 1066–1071.

[33]    Chianese, A. R.; Zeglis, B. M.; Crabtree, R. H. *Chem. Commun.* **2004**, 2176–2177.

[34]    Kishore, R.; Das. S. K. *J. Mol. Struct.* **2013**, *1053*, 38–47.

**Table A3.** Crystal data and structure refinement for compounds **2.6**, **2.9i**, **2.9j** and **2.10d**

| Compound | 2.6 | 2.9i | 2.9j | 2.10d |
|---|---|---|---|---|
| Formula | $C_{20}H_{16}AgN_4$, $CF_3O_3S$ | $C_6H_5BrCl_3NO$ | $C_6H_5Cl_4NO$ | $C_{14}H_{14}AgN_2O_2$, $F_6P$, $C_2H_3N$ |
| Formula weight | 569.31 | 293.37 | 248.91 | 536.16 |
| Temperature | 173 K | 173 K | 173 K | 173 K |
| Diffractometer, wavelength | Agilent Xcalibur 3 E, 0.71073 Å | Agilent Xcalibur 3 E, 0.71073 Å | Agilent Xcalibur 3 E, 0.71073 Å | Agilent Xcalibur 3 E, 0.71073 Å |
| Crystal system, space group | Monoclinic, $P\,2_1/n$ | Monoclinic, $P\,2_1/n$ | Monoclinic, $P\,2_1/n$ | Monoclinic, $P\,2_1/c$ |
| Unit cell dimensions | $a = 25.7088(13)$ Å<br>$b = 7.0984(3)$ Å<br>$c = 25.7377(13)$ Å<br>$\alpha = 90°$<br>$\beta = 114.318(6)°$<br>$\gamma = 90°$ | $a = 8.5246(4)$ Å<br>$b = 6.3768(3)$ Å<br>$c = 17.6623(10)$ Å<br>$\alpha = 90°$<br>$\beta = 98.355(5)°$<br>$\gamma = 90°$ | $a = 8.5068(5)$ Å<br>$b = 6.2672(4)$ Å<br>$c = 17.5265(12)$ Å<br>$\alpha = 90°$<br>$\beta = 97.924(6)°$<br>$\gamma = 90°$ | $a = 8.0009(4)$ Å<br>$b = 25.1137(8)$ Å<br>$c = 10.2433(4)$ Å<br>$\alpha = 90°$<br>$\beta = 105.046(5)°$<br>$\gamma = 90°$ |
| Volume, Z | 4280.2(4) Å$^3$, 8 | 949.93(9) Å$^3$, 4 | 925.48(10) Å$^3$, 4 | 1987.66(15) Å$^3$, 4 |
| Density (calculated) | 1.767 Mg/m$^3$ | 2.051 Mg/m$^3$ | 1.786 Mg/m$^3$ | 1.792 Mg/m$^3$ |
| Absorption coefficient | 1.098 mm$^{-1}$ | 5.120 mm$^{-1}$ | 1.226 mm$^{-1}$ | 1.167 mm$^{-1}$ |
| F(000) | 2272 | 568 | 496 | 1064 |
| Crystal color / morphology | Pale yellow needles | Colorless blocks | Colorless blocks | Colorless tablets |
| Crystal size | 0.52 x 0.17 x 0.10 mm$^3$ | 0.40 x 0.37 x 0.23 mm$^3$ | 0.54 x 0.19 x 0.10 mm$^3$ | 0.38 x 0.28 x 0.08 mm$^3$ |
| θ range for data collection | 2.239 to 27.288° | 2.524 to 27.859° | 2.346 to 28.075° | 2.621 to 27.943° |

| Index ranges | -33 ≤ h ≤ 32, -6 ≤ k ≤ 8, -33 ≤ l ≤ 32 | -5 ≤ h ≤ 11, -4 ≤ k ≤ 8, -21 ≤ l ≤ 22 | -7 ≤ h ≤ 10, -8 ≤ k ≤ 7, -21 ≤ l ≤ 22 | -10 ≤ h ≤ 9, -29 ≤ k ≤ 32, -13 ≤ l ≤ 7 |
|---|---|---|---|---|
| Reflns collected / unique | 22003 / 8460 [R(int) = 0.0273] | 3191 / 1879 [R(int) = 0.0229] | 4884 / 1918 [R(int) = 0.0227] | 6519 / 3902 [R(int) = 0.0191] |
| Reflns observed [F>4σ(F)] | 7759 | 1606 | 1687 | 3072 |
| Absorption correction | Analytical | Analytical | Analytical | Analytical |
| Max. and min. transmission | 0.901 and 0.705 | 0.460 and 0.248 | 0.908 and 0.726 | 0.912 and 0.751 |
| Refinement method | Full-matrix least-squares on $F^2$ | Full-matrix least-squares on $F^2$ | Full-matrix least-squares on $F^2$ | Full-matrix least-squares on $F^2$ |
| Data / restraints / parameters | 8460 / 0 / 596 | 1879 / 0 / 110 | 1918 / 0 / 109 | 3902 / 941 / 325 |
| Goodness-of-fit on $F^2$ | 1.043 | 1.097 | 1.116 | 1.081 |
| Final R indices [F>4σ(F)] | $R_1$ = 0.0296, $wR_2$ = 0.0583 | $R_1$ = 0.0362, $wR_2$ = 0.0658 | $R_1$ = 0.0319, $wR_2$ = 0.0754 | $R_1$ = 0.0430, $wR_2$ = 0.0726 |
| R indices (all data) | $R_1$ = 0.0348, $wR_2$ = 0.0609 | $R_1$ = 0.0468, $wR_2$ = 0.0708 | $R_1$ = 0.0388, $wR_2$ = 0.0822 | $R_1$ = 0.0606, $wR_2$ = 0.0790 |
| Largest diff. peak, hole | 0.423, -0.427 e$Å^{-3}$ | 0.709, -0.427 e$Å^{-3}$ | 0.481, -0.275 e$Å^{-3}$ | 0.365, -0.438 e$Å^{-3}$ |
| Mean and maximum shift/error | 0.000 and 0.002 | 0.000 and 0.000 | 0.000 and 0.001 | 0.000 and 0.003 |

**Table A4.** Crystal data and structure refinement for compounds **2.11d**, **3.2p** and **3.7d**

| Compound | 2.11d | 3.2p | 3.7d |
|---|---|---|---|
| Formula | $C_{12}H_{14}AgN_2O_2$, $F_6P$, $C_2H_3N$ | $C_{23}H_{19}NO_2$ | $C_{12}H_{10}BrNO$ |
| Formula weight | 512.14 | 341.39 | 264.12 |
| Temperature | 173 K | 173 K | 173 K |
| Diffractometer, wavelength | Agilent Xcalibur 3 E, 0.71073 Å | Agilent Xcalibur PX Ultra A, 1.54184 Å | Agilent Xcalibur 3 E, 0.71073 Å |
| Crystal system, space group | Monoclinic, P $2_1$/c | Monoclinic, P $2_1$/c | Monoclinic, P $2_1$/c |
| Unit cell dimensions | a = 11.0252(4) Å | a = 18.6869(5) Å | a = 6.0878(3) Å |
|  | b = 12.6897(4) Å | b = 5.69862(12) Å | b = 9.6230(5) Å |
|  | c = 14.2634(4) Å | c = 17.4008(4) Å | c = 18.6612(10) Å |
|  | $\alpha$ = 90° | $\alpha$ = 90° | $\alpha$ = 90° |
|  | $\beta$ = 107.351(3)° | $\beta$ = 106.219(3)° | $\beta$ = 94.192(5)° |
|  | $\gamma$ = 90° | $\gamma$ = 90° | $\gamma$ = 90° |
| Volume, Z | 1904.74(11) $Å^3$, 4 | 1779.26(7) $Å^3$, 4 | 1090.31(10) $Å^3$, 4 |
| Density (calculated) | 1.786 $Mg/m^3$ | 1.274 $Mg/m^3$ | 1.609 $Mg/m^3$ |
| Absorption coefficient | 1.213 $mm^{-1}$ | 0.643 $mm^{-1}$ | 3.741 $mm^{-1}$ |
| F(000) | 1016 | 720 | 528 |
| Crystal color / morphology | Colorless blocks | Colorless blocky needles | Colorless blocky needles |
| Crystal size | 0.58 x 0.40 x 0.28 $mm^3$ | 0.23 x 0.20 x 0.11 $mm^3$ | 0.72 x 0.23 x 0.14 $mm^3$ |
| $\theta$ range for data collection | 2.614 to 27.814° | 5.179 to 73.739° | 3.045 to 27.969° |

| | | | |
|---|---|---|---|
| Index ranges | $-13 \leq h \leq 14$, $-8 \leq k \leq 16$, $-18 \leq l \leq 9$ | $-20 \leq h \leq 23$, $-6 \leq k \leq 5$, $-17 \leq l \leq 21$ | $-7 \leq h \leq 6$, $-12 \leq k \leq 11$, $-14 \leq l \leq 22$ |
| Reflns collected / unique | 6325 / 3772 [R(int) = 0.0172] | 5634 / 3396 [R(int) = 0.0157] | 3779 / 2180 [R(int) = 0.0206] |
| Reflns observed [$F>4\sigma(F)$] | 3081 | 2935 | 1589 |
| Absorption correction | Analytical | Analytical | Analytical |
| Max. and min. transmission | 0.751 and 0.650 | 0.943 and 0.902 | 0.616 and 0.399 |
| Refinement method | Full-matrix least-squares on $F^2$ | Full-matrix least-squares on $F^2$ | Full-matrix least-squares on $F^2$ |
| Data / restraints / parameters | 3772 / 0 / 248 | 3396 / 49 / 262 | 2180 / 0 / 137 |
| Goodness-of-fit on $F^2$ | 1.031 | 1.052 | 1.022 |
| Final R indices [$F>4\sigma(F)$] | $R_1 = 0.0322$, $wR_2 = 0.0669$ | $R_1 = 0.0362$, $wR_2 = 0.0868$ | $R_1 = 0.0350$, $wR_2 = 0.0691$ |
| R indices (all data) | $R_1 = 0.0434$, $wR_2 = 0.0723$ | $R_1 = 0.0433$, $wR_2 = 0.0912$ | $R_1 = 0.0599$, $wR_2 = 0.0786$ |
| Largest diff. peak, hole | 0.370, -0.339 e$\text{Å}^{-3}$ | 0.137, -0.129 e$\text{Å}^{-3}$ | 0.437, -0.529 e$\text{Å}^{-3}$ |
| Mean and maximum shift/error | 0.000 and 0.002 | 0.000 and 0.000 | 0.000 and 0.001 |

**Table A5.** Crystal data and structure refinement for compounds **4.19a-d**

| Compound | 4.19a | 4.19b | 4.19c | 4.19d |
|---|---|---|---|---|
| Formula | $C_{29}H_{39}AgN_2O_2$ | $C_{34}H_{41}AgN_2O_2$ | $C_{35}H_{43}AgN_2O_2$ | $C_{34}H_{40}AgClN_2O_2$ |
| Formula weight | 555.49 | 617.56 | 631.58 | 652.00 |
| Temperature | 173 K | 173 K | 173 K | 173 K |
| Diffractometer, wavelength | Agilent Xcalibur PX Ultra A, 1.54184 Å | Agilent Xcalibur PX Ultra A, 1.54184 Å | Agilent Xcalibur 3 E, 0.71073 Å | Agilent Xcalibur 3 E, 0.71073 Å |
| Crystal system, space group | Orthorhombic, $P\,2_1\,2_1\,2_1$ | Monoclinic, $P\,2_1/n$ | Monoclinic, $P\,2_1/n$ | Monoclinic, $P\,2_1/n$ |
| Unit cell dimensions | a = 15.51926(11) Å | a = 22.27585(13) Å | a = 9.4763(2) Å | a = 9.4950(3) Å |
| | b = 17.13766(12) Å | b = 12.57197(8) Å | b = 14.6677(3) Å | b = 14.7260(4) Å |
| | c = 21.90834(15) Å | c = 22.83708(14) Å | c = 24.1576(8) Å | c = 24.0880(7) Å |
| | $\alpha = 90°$ | $\alpha = 90°$ | $\alpha = 90°$ | $\alpha = 90°$ |
| | $\beta = 90°$ | $\beta = 104.8537(6)°$ | $\beta = 100.000(3)°$ | $\beta = 100.841(3)°$ |
| | $\gamma = 90°$ | $\gamma = 90°$ | $\gamma = 90°$ | $\gamma = 90°$ |
| Volume, Z | 5826.83(7) $\text{Å}^3$, 8 | 6181.84(7) $\text{Å}^3$, 8 | 3306.79(16) $\text{Å}^3$, 4 | 3307.95(17) $\text{Å}^3$, 4 |
| Density (calculated) | 1.266 $\text{Mg/m}^3$ | 1.327 $\text{Mg/m}^3$ | 1.269 $\text{Mg/m}^3$ | 1.309 $\text{Mg/m}^3$ |
| Absorption coefficient | 5.737 $\text{mm}^{-1}$ | 5.466 $\text{mm}^{-1}$ | 0.640 $\text{mm}^{-1}$ | 0.720 $\text{mm}^{-1}$ |
| F(000) | 2320 | 2576 | 1320 | 1352 |
| Crystal color / morphology | Colorless blocky needles | Colorless blocky needles | Colorless blocks | Colorless blocks |
| Crystal size | 0.36 x 0.12 x 0.09 $\text{mm}^3$ | 0.35 x 0.12 x 0.07 $\text{mm}^3$ | 0.37 x 0.26 x 0.24 $\text{mm}^3$ | 0.37 x 0.25 x 0.15 $\text{mm}^3$ |
| θ range for data collection | 3.274 to 73.663° | 2.472 to 73.732° | 2.587 to 27.867° | 2.494 to 27.467° |
| Index ranges | -13 ≤ h ≤ 18, -21 ≤ k ≤ | -18 ≤ h ≤ 27, -15 ≤ k ≤ 8, | -11 ≤ h ≤ 12, -18 ≤ k ≤ | -12 ≤ h ≤ 5, -16 ≤ k ≤ 17, |

| | | | | |
|---|---|---|---|---|
| | 19, $-27 \leq l \leq 26$ | $-27 \leq l \leq 22$ | 11, $-31 \leq l \leq 18$ | $-25 \leq l \leq 29$ |
| Reflns collected / unique | 12787 / 9409 [R(int) = 0.0241] | 20665 / 11932 [R(int) = 0.0190] | 11054 / 6522 [R(int) = 0.0223] | 10067 / 6391 [R(int) = 0.0367] |
| Reflns observed [F>4$\sigma$(F)] | 9063 | 10774 | 5385 | 5359 |
| Absorption correction | Analytical | Analytical | Analytical | Analytical |
| Max. and min. transmission | 0.649 and 0.296 | 0.724 and 0.331 | 0.895 and 0.843 | 0.908 and 0.829 |
| Refinement method | Full-matrix least-squares on $F^2$ | Full-matrix least-squares on $F^2$ | Full-matrix least-squares on $F^2$ | Full-matrix least-squares on $F^2$ |
| Data / restraints / parameters | 9409 / 52 / 642 | 11932 / 0 / 704 | 6522 / 0 / 370 | 6391 / 0 / 369 |
| Goodness-of-fit on $F^2$ | 1.020 | 1.030 | 1.053 | 1.049 |
| Final R indices [F>4$\sigma$(F)] | $R_1$ = 0.0300, $wR_2$ = 0.0754 | $R_1$ = 0.0253, $wR_2$ = 0.0612 | $R_1$ = 0.0345, $wR_2$ = 0.0661 | $R_1$ = 0.0382, $wR_2$ = 0.0799 |
| R indices (all data) | $R_1$ = 0.0317, $wR_2$ = 0.0777 | $R_1$ = 0.0290, $wR_2$ = 0.0637 | $R_1$ = 0.0475, $wR_2$ = 0.0723 | $R_1$ = 0.0487, $wR_2$ = 0.0865 |
| Largest diff. peak, hole | 0.604, -0.680 e$\text{Å}^{-3}$ | 0.434, -0.513 e$\text{Å}^{-3}$ | 0.390, -0.452 e$\text{Å}^{-3}$ | 0.400, -0.552 e$\text{Å}^{-3}$ |
| Mean and maximum shift/error | 0.000 and 0.002 | 0.000 and 0.002 | 0.000 and 0.002 | 0.000 and 0.001 |

**Table A6.** Crystal data and structure refinement for compounds **4.20a-d**

| Compound | 4.20a | 4.20b | 4.20c | 4.20d |
|---|---|---|---|---|
| Formula | $C_{29}H_{41}AgN_2O_2$, $CH_2Cl_2$ | $C_{34}H_{43}AgN_2O_2$, $2(CH_2Cl_2)$ | $C_{35}H_{45}AgN_2O_2$, $CH_2Cl_2$ | $C_{34}H_{42}AgClN_2O_2$, $CH_2Cl_2$ |
| Formula weight | 642.43 | 789.42 | 718.52 | 738.94 |
| Temperature | 173 K | 173 K | 173 K | 173 K |
| Diffractometer, wavelength | Agilent Xcalibur 3 E, 0.71073 Å | Agilent Xcalibur 3 E, 0.71073 Å | Agilent Xcalibur 3 E, 0.71073 Å | Agilent Xcalibur 3 E, 0.71073 Å |
| Crystal system, space group | Triclinic, P -1 | Orthorhombic, P b c a | Monoclinic, P $2_1$/n | Monoclinic, P $2_1$/n |
| Unit cell dimensions | a = 10.8480(3) Å | a = 16.3671(4) Å | a = 12.2083(4) Å | a = 12.2174(4) Å |
| | b = 18.7829(6) Å | b = 20.2854(6) Å | b = 14.4921(5) Å | b = 14.4354(5) Å |
| | c = 31.9648(10) Å | c = 22.7391(8) Å | c = 20.5457(6) Å | c = 20.4824(6) Å |
| | $\alpha$ = 92.691(3)° | $\alpha$ = 90° | $\alpha$ = 90° | $\alpha$ = 90° |
| | $\beta$ = 91.406(3)° | $\beta$ = 90° | $\beta$ = 91.067(3)° | $\beta$ = 90.863(3)° |
| | $\gamma$ = 96.524(3)° | $\gamma$ = 90° | $\gamma$ = 90° | $\gamma$ = 90° |
| Volume, Z | 6460.8(3) Å$^3$, 8 | 7549.7(4) Å$^3$, 8 | 3634.4(2) Å$^3$, 4 | 3611.9(2) Å$^3$, 4 |
| Density (calculated) | 1.321 Mg/m$^3$ | 1.389 Mg/m$^3$ | 1.313 Mg/m$^3$ | 1.359 Mg/m$^3$ |
| Absorption coefficient | 0.816 mm$^{-1}$ | 0.850 mm$^{-1}$ | 0.733 mm$^{-1}$ | 0.812 mm$^{-1}$ |
| F(000) | 2672 | 3264 | 1496 | 1528 |
| Crystal color / morphology | Colorless blocky needles | Colorless platy needles | Colorless blocks | Colorless blocks |
| Crystal size | 0.58 x 0.12 x 0.08 mm$^3$ | 0.53 x 0.16 x 0.05 mm$^3$ | 0.54 x 0.29 x 0.20 mm$^3$ | 0.58 x 0.47 x 0.31 mm$^3$ |
| $\theta$ range for data collection | 2.347 to 27.988° | 2.527 to 28.020° | 2.430 to 27.987° | 2.410 to 27.881° |

| Index ranges | $-13 \leq h \leq 14$, $-22 \leq k \leq 15$, $-41 \leq l \leq 40$ | $-12 \leq h \leq 20$, $-9 \leq k \leq 24$, $-29 \leq l \leq 16$ | $-15 \leq h \leq 15$, $-18 \leq k \leq 11$, $-26 \leq l \leq 15$ | $-15 \leq h \leq 15$, $-18 \leq k \leq 18$, $-26 \leq l \leq 14$ |
|---|---|---|---|---|
| Reflns collected / unique | 37872 / 25031 [R(int) = 0.0447] | 15203 / 7445 [R(int) = 0.0238] | 11761 / 7136 [R(int) = 0.0235] | 12031 / 7122 [R(int) = 0.0199] |
| Reflns observed [F>4σ(F)] | 16416 | 5353 | 5688 | 5668 |
| Absorption correction | Analytical | Analytical | Analytical | Analytical |
| Max. and min. transmission | 0.946 and 0.761 | 0.963 and 0.836 | 0.876 and 0.760 | 0.842 and 0.737 |
| Refinement method | Full-matrix least-squares on $F^2$ | Full-matrix least-squares on $F^2$ | Full-matrix least-squares on $F^2$ | Full-matrix least-squares on $F^2$ |
| Data / restraints / parameters | 25031 / 119 / 1390 | 7445 / 0 / 406 | 7136 / 25 / 402 | 7122 / 25 / 401 |
| Goodness-of-fit on $F^2$ | 1.131 | 1.033 | 1.042 | 1.048 |
| Final R indices [F>4σ(F)] | $R_1 = 0.1054$, $wR_2 = 0.1847$ | $R_1 = 0.0412$, $wR_2 = 0.0857$ | $R_1 = 0.0376$, $wR_2 = 0.0752$ | $R_1 = 0.0337$, $wR_2 = 0.0643$ |
| R indices (all data) | $R_1 = 0.1528$, $wR_2 = 0.2095$ | $R_1 = 0.0695$, $wR_2 = 0.0993$ | $R_1 = 0.0539$, $wR_2 = 0.0831$ | $R_1 = 0.0509$, $wR_2 = 0.0726$ |
| Largest diff. peak, hole | 1.271, -2.460 e$\text{Å}^{-3}$ | 0.868, -0.659 e$\text{Å}^{-3}$ | 0.542, -0.549 e$\text{Å}^{-3}$ | 0.458, -0.465 e$\text{Å}^{-3}$ |
| Mean and maximum shift/error | 0.000 and 0.001 | 0.000 and 0.002 | 0.000 and 0.001 | 0.000 and 0.003 |

**Table A7.** Crystal data and structure refinement for compounds **4.43**, **4.44a, b** and **d**

| Compound | 4.43 | 4.44a | 4.44b | 4.44d |
|---|---|---|---|---|
| Formula | $C_{50}H_{52}Ag_4F_{12}N_4O_8$ | $C_{37}H_{55}AgN_2O_2$, $0.5(C_6H_{14})$ | $C_{42}H_{57}AgN_2O_2$ | $C_{42}H_{56}AgClN_2O_2$ |
| Formula weight | 1496.43 | 710.78 | 729.76 | 764.20 |
| Temperature | 173 K | 173 K | 173 K | 173 K |
| Diffractometer, wavelength | Agilent Xcalibur 3 E, 0.71073 Å | Agilent Xcalibur 3 E, 0.71073 Å | Agilent Xcalibur 3 E, 0.71073 Å | Agilent Xcalibur 3 E, 0.71073 Å |
| Crystal system, space group | Triclinic, P -1 | Monoclinic, P $2_1$/n | Monoclinic, P $2_1$/n | Monoclinic, C 2/c |
| Unit cell dimensions | a = 12.1972(4) Å | a = 12.0395(4) Å | a = 23.0097(8) Å | a = 23.2721(12) Å |
| | b = 22.3935(6) Å | b = 15.7310(4) Å | b = 15.6891(4) Å | b = 15.7814(4) Å |
| | c = 31.4990(9) Å | c = 20.5650(6) Å | c = 23.5011(8) Å | c = 23.8030(10) Å |
| | $\alpha$ = 82.629(2)° | $\alpha$ = 90° | $\alpha$ = 90° | $\alpha$ = 90° |
| | $\beta$ = 81.319(2)° | $\beta$ = 97.511(3)° | $\beta$ = 113.686(4)° | $\beta$ = 114.313(6)° |
| | $\gamma$ = 75.828(3)° | $\gamma$ = 90° | $\gamma$ = 90° | $\gamma$ = 90° |
| Volume, Z | 8208.7(4) $Å^3$, 6 | 3861.4(2) $Å^3$, 4 | 7769.2(5) $Å^3$, 8 | 7966.7(7) $Å^3$, 8 |
| Density (calculated) | 1.816 $Mg/m^3$ | 1.223 $Mg/m^3$ | 1.248 $Mg/m^3$ | 1.274 $Mg/m^3$ |
| Absorption coefficient | 1.506 $mm^{-1}$ | 0.556 $mm^{-1}$ | 0.554 $mm^{-1}$ | 0.609 $mm^{-1}$ |
| F(000) | 4440 | 1516 | 3088 | 3216 |
| Crystal color / morphology | Colorless blocks | Colorless blocks | Colorless blocks | Colorless blocks |
| Crystal size | 0.35 x 0.27 x 0.15 $mm^3$ | 0.59 x 0.36 x 0.24 $mm^3$ | 0.57 x 0.45 x 0.22 $mm^3$ | 0.52 x 0.43 x 0.33 $mm^3$ |
| $\theta$ range for data collection | 2.230 to 27.992° | 2.590 to 28.257° | 2.295 to 28.264° | 2.747 to 28.243° |

| | | | | |
|---|---|---|---|---|
| Index ranges | $-15 \leq h \leq 13, -26 \leq k \leq 26, -27 \leq l \leq 37$ | $-10 \leq h \leq 15, -12 \leq k \leq 20, -26 \leq l \leq 26$ | $-26 \leq h \leq 30, -12 \leq k \leq 19, -30 \leq l \leq 17$ | $-28 \leq h \leq 19, -21 \leq k \leq 12, -30 \leq l \leq 29$ |
| Reflns collected / unique | 45329 / 31759 [R(int) = 0.0232] | 13536 / 7687 [R(int) = 0.0224] | 27109 / 15510 [R(int) = 0.0247] | 14414 / 7979 [R(int) = 0.0299] |
| Reflns observed [$F>4\sigma(F)$] | 17629 | 6262 | 10823 | 6058 |
| Absorption correction | Analytical | Analytical | Analytical | Analytical |
| Max. and min. transmission | 0.851 and 0.676 | 0.897 and 0.850 | 0.904 and 0.806 | 0.861 and 0.815 |
| Refinement method | Full-matrix least-squares on $F^2$ | Full-matrix least-squares on $F^2$ | Full-matrix least-squares on $F^2$ | Full-matrix least-squares on $F^2$ |
| Data / restraints / parameters | 31759 / 728 / 2314 | 7687 / 82 / 434 | 15510 / 22 / 856 | 7979 / 9 / 451 |
| Goodness-of-fit on $F^2$ | 1.093 | 1.049 | 1.032 | 1.021 |
| Final R indices [$F>4\sigma(F)$] | $R_1 = 0.0607$, $wR_2 = 0.1213$ | $R_1 = 0.0442$, $wR_2 = 0.0982$ | $R_1 = 0.0565$, $wR_2 = 0.1158$ | $R_1 = 0.0455$, $wR_2 = 0.1059$ |
| R indices (all data) | $R_1 = 0.1120$, $wR_2 = 0.1524$ | $R_1 = 0.0591$, $wR_2 = 0.1062$ | $R_1 = 0.0916$, $wR_2 = 0.1340$ | $R_1 = 0.0660$, $wR_2 = 0.1184$ |
| Largest diff. peak, hole | 2.351, -1.475 e$\text{Å}^{-3}$ | 1.210, -0.402 e$\text{Å}^{-3}$ | 2.340, -1.336 e$\text{Å}^{-3}$ | 0.910, -0.569 e$\text{Å}^{-3}$ |
| Mean and maximum shift/error | 0.000 and 0.001 | 0.000 and 0.001 | 0.000 and 0.002 | 0.000 and 0.001 |

**Table A8.** Crystal data and structure refinement for compounds **4.45a** and **b**

| Compound | 4.45a | 4.45b |
|---|---|---|
| Formula | $C_{25}H_{35}AgN_2O_2$, $CH_2Cl_2$ | $C_{30}H_{37}AgN_2O_2$ |
| Formula weight | 588.34 | 565.48 |
| Temperature | 173 K | 173 K |
| Diffractometer, wavelength | Agilent Xcalibur 3 E, 0.71073 Å | Agilent Xcalibur 3 E, 0.71073 Å |
| Crystal system, space group | Monoclinic, P $2_1$/c | Monoclinic, P $2_1$/n |
| Unit cell dimensions | a = 11.0188(5) Å | a = 11.6913(3) Å |
| | b = 11.8584(4) Å | b = 11.8435(3) Å |
| | c = 19.6802(7) Å | c = 18.6475(5) Å |
| | $\alpha$ = 90° | $\alpha$ = 90° |
| | $\beta$ = 99.173(4)° | $\beta$ = 102.744(3)° |
| | $\gamma$ = 90° | $\gamma$ = 90° |
| Volume, Z | 2538.62(17) $\text{Å}^3$, 4 | 2518.45(12) $\text{Å}^3$, 4 |
| Density (calculated) | 1.539 $\text{Mg/m}^3$ | 1.491 $\text{Mg/m}^3$ |
| Absorption coefficient | 1.031 $\text{mm}^{-1}$ | 0.831 $\text{mm}^{-1}$ |
| F(000) | 1216 | 1176 |
| Crystal color / morphology | Colorless blocks | Colorless blocks |
| Crystal size | 0.62 x 0.46 x 0.45 $\text{mm}^3$ | 0.56 x 0.35 x 0.18 $\text{mm}^3$ |
| $\theta$ range for data collection | 2.541 to 28.256° | 2.479 to 28.226° |
| Index ranges | $-9 \le h \le 14$, $-9 \le k \le 15$, $-26 \le l \le 19$ | $-15 \le h \le 14$, $-13 \le k \le 15$, $-14 \le l \le 24$ |
| Reflns collected / unique | 8735 / 5115 [R(int) = 0.0214] | 9081 / 5084 [R(int) = 0.0220] |
| Reflns observed [F>4$\sigma$(F)] | 4185 | 4349 |
| Absorption correction | Analytical | Analytical |
| Max. and min. transmission | 0.701 and 0.650 | 0.877 and 0.729 |
| Refinement method | Full-matrix least-squares on $F^2$ | Full-matrix least-squares on $F^2$ |
| Data / restraints / parameters | 5115 / 0 / 299 | 5084 / 0 / 316 |
| Goodness-of-fit on $F^2$ | 1.057 | 1.076 |
| Final R indices [F>4$\sigma$(F)] | $R_1$ = 0.0403, $wR_2$ = 0.0821 | $R_1$ = 0.0369, $wR_2$ = 0.0879 |
| R indices (all data) | $R_1$ = 0.0547, $wR_2$ = 0.0886 | $R_1$ = 0.0465, $wR_2$ = 0.0930 |
| Largest diff. peak, hole | 0.754, -0.580 $\text{eÅ}^{-3}$ | 0.856, -0.444 $\text{eÅ}^{-3}$ |
| Mean and maximum shift/error | 0.000 and 0.001 | 0.000 and 0.001 |

# References

1 Hashmi, A. S. K., Toste, F. D., Eds. *Modern Gold-Catalyzed Synthesis*; Wiley VCH: Weinheim, 2012.

2 Jiménez-Núñez, E.; Echavarren, A. M. *Chem. Rev.* **2008**, *108*, 3326–3350.

3 Gorin, D. J.; Sherry, B. D.; Toste, F. D. *Chem. Rev.* **2008**, *108*, 3351–3378.

4 Muuronen, M.; Perea-Buceta, J. E.; Nieger, M.; Patzschke, M.; Helaja, J. *Organometallics* **2012**, *31*, 4320–4330.

5 Weber, D.; Tarselli, M. A.; Gagné, M. R. *Angew. Chem., Int. Ed.* **2009**, *48*, 5733–5736.

6 Weber, D.; Gagné, M. R. *Org. Lett.* **2009**, *11*, 4962–4965.

7 Ghosh, N.; Nayak, S.; Sahoo, A. *J. Org. Chem.* **2011**, *76*, 500−511.

8 Wang, D.; Cai, R; Sharma, S.; Jirak, J.; Thummanapelli, S. K.; Akhmedov, N. G.; Zhang, H.; Liu, X.; Petersen, J. L.; Shi, X. *J. Am. Chem. Soc.* **2012**, *134*, 9012−9019.

9 Weber, S. G.; Rominger, F.; Straub, B. F. *Eur. J. Inorg. Chem.* **2012**, 2863–2867.

10 Zhu, Y.; Day, C. S.; Zhang, L.; Hauser, K. J.; Jones, A. C. *Chem.–Eur. J.* **2013**, 12264−12271.

11 Mézailles, N.; Ricard, L.; Gagosz, F. *Org. Lett.* **2005**, *7*, 4133–4136.

12 Ricard, L.; Gagosz, F. *Organometallics* **2007**, *26*, 4704 –4707.

13 Herrero-Gómez, E.; Nieto-Oberhuber, C.; López, S.; Benet-Buchholz, J.; Echavarren, A. M. *Angew. Chem., Int. Ed.* **2006**, *45*, 5455−5459.

14    De Frémont, P.; Stevens, E. D.; Fructos, M. R.; Díaz-Requejo, M. M.; Perez, P. J.; Nolan, S. P. *Chem. Commun.* **2006**, 2045−2047.

15    Amijs, C. H. M.; López-Carrillo, V.; Raducan, M.; Pérez-Galán, P.; Ferrer, C.; Echavarren, A. M. *J. Org. Chem.* **2008**, *73*, 7721−7730.

16    Yang, Y.; Ramamoorthy, V.; Sharp, P. R. *Inorg. Chem.* **1993**, *32*, 1946–1950.

17    Sherry, B. D.; Toste, F. D. *J. Am. Chem. Soc.* **2004**, *126*, 15978–15979.

18    Duan, H.; Sengupta, S.; Petersen, J. L.; Akhmedov, N. G.; Shi, X. *J. Am. Chem. Soc.* **2009**, *131*, 12100−12102.

19    Teles, J. H.; Brode, S.; Chabanas, M. *Angew. Chem., Int. Ed.* **1998**, *37*, 1415−1418.

20    Lambert, J. B.; Zhang, S.; Stern, C. L.; Huffman, J. C. *Science* **1993**, *260*, 1917–1918.

21    Reed, C. A. *Acc. Chem. Res.* **1998**, *31*, 325–332.

22    Lavallo, V.; Frey, G. D.; Kousar, S.; Donnadieu, B.; Bertrand, G. *Proc. Natl. Acad. Sci. U.S.A.* **2007**, *104*, 13569–13573.

23    Guérinot, A.; Fang, W.; Sircoglou, M.; Bour, C.; Bezzenine-Lafollée, S.; Gandon, V. *Angew. Chem., Int. Ed.* **2013**, *52*, 5848−5852.

24    Fang, W.; Presset, M.; Guérinot, A.; Bour, C.; Bezzenine-Lafollée, S.; Gandon, V. *Chem.−Eur. J.* **2014**, *20*, 5439−5446.

25    Fang, W.; Presset, M.; Guérinot, A.; Bour, C.; Bezzenine-Lafollée, S.; Gandon, V. *Org. Chem. Front.* **2014**, *1*, 608−613.

26    Gaillard, S.; Slawin, A. M. Z.; Nolan, S. P. *Chem. Commun.* **2010**, *46*, 2742−2744.

27     Gaillard, S.; Bosson, J.; Ramon, R. S.; Nun, P.; Slawin, A. M. Z.; Nolan, S. P. *Chem.−Eur. J.* **2010**, *16*, 13729−13740.

28     Ramón, R. S.; Gaillard, S.; Poater, A.; Cavallo, L.; Slawin, A. M. Z.; Nolan, S. P. *Chem.−Eur. J.* **2011**, *17*, 1238−1246.

29     Harmata, M., Ed. *Silver in Organic Chemistry*; John Wiley & Sons: New Jersey, 2010.

30     For recent reviews on metal-catalyzed synthesis of heterocycles, see: (a) Yamamoto, Y. *Chem. Soc. Rev.* **2014**, *43*, 1575−1600. (b) Gulevich, A. V.; Dudnik, A. S.; Chernyak, N.; Gevorgyan, V. *Chem. Rev.* **2013**, *113*, 3084−3213. (c) Wu, X.-F.; Neumann, H.; Beller, M. *Chem. Rev.* **2013**, *113*, 1−35. (d) Wolfe, J. P., Ed. *Synthesis of Heterocycles via Metal-Catalyzed Reactions that Generate One or More Carbon-Heteroatom Bonds*; Topics in Heterocyclic Chemistry Vol. 32; Springer-Verlag: Berlin Heidelberg, 2013. (e) Stokes, B. J.; Driver, T. G. *Eur. J. Org. Chem.* **2011**, 4071−4088.

31     Yamamoto, Y. *J. Org. Chem.* **2007**, *72*, 7817−7831.

32     Weibel, J.-M.; Blanc, A.; Pale, P. *Chem. Rev.* **2008,** *108,* 3149–3173.

33     Álvarez-Corral, M.; Muñoz-Dorado, M.; Rodríguez-García, I. *Chem. Rev.* **2008,** *108,* 3174–3198.

34     Wen, J.-J.; Zhu, Y.; Zhan, Z. P. *Asian J. Org. Chem.* **2012**, *1*, 108–129.

35     Patil, N. T.; Kavthe, R. D.; Shinde, V. S. *Tetrahedron* **2012**, *68*, 8079−8146.

36     Pale, P.; Chuche, J. *Tetrahedron Lett.* **1987**, *28*, 6447−6448.

37     Pale, P.; Chuche, J. *Eur. J. Org. Chem.* **2000**, 1019−1025.

38      Dalla, V.; Pale, P. *New J. Chem.* **1999**, *23*, 803−805.

39      Harkat, H.; Weibel, J.-M.; Pale, P. *Tetrahedron Lett.* **2007**, *48*, 1439–1442.

40      Marshall, J. A.; Sehon, C. A. *J. Org. Chem.* **1995**, *60*, 5966−5968.

41      Arimitsu, S.; Hammond, G. B. *J. Org. Chem.* **2007**, *72*, 8559–8561.

42      Oh, C. H.; Yi, H. J.; Lee, J. H. *New J. Chem.* **2007**, *31*, 835–837.

43      Kern, N.; Blanc, A.; Miaskiewicz, S.; Robinette, M.; Weibel, J.-M.; Pale, P. *J. Org. Chem.* **2012**, *77*, 4323–4341.

44      Alcaide, B.; Almendros, P.; Martinez del Campo, T.; Carrascosa, R. *Eur. J. Org. Chem.* **2010**, 4912–4919.

45      Jong, T. T.; Leu, S. J. *J. Chem. Soc., Perkin Trans. 1* **1990**, 423–424.

46      Harkat, H.; Blanc, A.; Weibel, J.-M.; Pale, P. *J. Org. Chem.* **2008**, *73*, 1620−1623.

47      Castaner, J.; Pascual, J. *J. Chem. Soc.* **1958**, 3962–3964.

48      Belil, C.; Pascual, J.; Serratosa, F. *Tetrahedron* **1964**, *20*, 2701–2708.

49      Anastasia, L.; Xu, C.; Negishi, E. *Tetrahedron Lett.* **2002**, *43*, 5673–5676.

50      Ogawa, Y.; Mamno, M.; Wakamatsu, T. *Heterocycles* **1995**, *41*, 2587−2599.

51      Negishi, E.; Kotora, M. *Tetrahedron* **1997**, *53*, 6707−6738.

52      Marchal, E.; Uriac, P.; Legouin, B.; Toupet, L.; van de Weghe, P. *Tetrahedron* **2007**, *63*, 9979−9990.

53      Rammah, M. M.; Othman, M.; Ciamala, K.; Strohmann, C.; Rammah, M. B. *Tetrahedron* **2008**, *64*, 3505–3516.

54 Tomás-Mendivil, E.; Toullec, P. Y.; Díez, J.; Conejero, S.; Michelet, V.; Cadierno, V. *Org. Lett.* **2012**, *14*, 2520–2523.

55 Yamada, W.; Sugawara, Y.; Cheng, H. M.; Ikeno, T.; Yamada, T. *Eur. J. Org. Chem.* **2007**, 2604–2607.

56 Yamada, W.; Sugawara, Y.; Cheng, H. M.; Ikeno, T.; Yamada, T. *Eur. J. Org. Chem.* **2007**, 2604–2607.

57 Ugajin, R.; Kikuchi, S.; Yamada, T. *Synlett* **2014**, *25*, 1178–1180.

58 Yoshida, S.; Fukui, K.; Kikuchi, S.; Yamada, T. *J. Am. Chem. Soc.* **2010**, *132*, 4072–4073.

59 Peng, A.-Y.; Ding, Y.-X. *Org. Lett.* **2005**, *7*, 3299–3301.

60 Godet, T.; Vaxelaire, C.; Michel, C.; Milet, A.; Belmont, P. *Chem. –Eur. J.* **2007**, *13*, 5632–5641.

61 Patil, N. T.; Pahadi, N. K.; Yamamoto, Y. *J. Org. Chem.* **2005**, *70*, 10096–10098.

62  Harmata, M.; Huang, C. *Synlett* **2008**, 1399–1401.

63  Beesley, R. M.; Ingold, C. K.; Thorpe, J. F. *J. Chem. Soc., Trans.* **1915**, *107*, 1080 –1106.

64  Aucagne, V.; Amblard, F.; Agrofoglio, L. A. *Synlett* **2004**, 2406–2408.

65 Amblard, F.; Aucagne, V.; Guenot, P.; Schinazi, R. F.; Agrofoglio, L. A. *Biorg. Med. Chem.* **2005**, *13*, 1239–1248.

66 Robins, M. J.; Barr, P. J. *J. Org. Chem.* **1983**, *48*, 1854–1862.

67 Müller, T. E.; Pleier, A. K. *J. Chem. Soc., Dalton Trans.* **1999**, 583–587.

68    Müller, T. E.; Grosche, M.; Herdtweck, E.; Pleier, A. K.; Walter, E.; Yan, Y.-K. *Organometallics* **2000**, *19*, 170−183.

69    Carney, J. M.; Donoghue, P. J.;Wuest,W. M.; Wiest, O.; Helquist, P. *Org. Lett.* **2008**, *10*, 3903−3906.

70    Beeren, S. R.; Dabb, S. L.; Messerle, B. A. *J. Organomet. Chem.* **2009**, *694*, 309−312.

71    Van Esseveldt, B. C. J.; Vervoort, P. W. H.; Van Delft, F. L.; Rutjes, F. P. J. T. *J. Org. Chem.* **2005**, *70*, 1791−1795.

72    Agarwal, S.; Knölker, H. J. *Org. Biomol. Chem.* **2004**, *2*, 3060−3062.

73    Robinson, R. S.; Dovey, M. C.; Gravestock, D. *Tetrahedron Lett.* **2004**, *45*, 6787−6789.

74    Robinson, R. S.; Dovey, M. C.; Gravestock, D. *Eur. J. Org. Chem.* **2005**, 505−511.

75    Ding, Q.; Ye, Y.; Fan, R.; Wu, J. *J. Org. Chem.* **2007**, 72, 5439−5442.

76    Prasad, J. S.; Liebeskind, L. S. *Tetrahedron Lett.* **1988**, *29*, 4253−4256.

77    Koseki, Y.; Kuano, S.; Nagasaka, T. *Tetrahedron Lett.* **1998**, *39*, 3517−3520.

78    Kimura, M.; Kure, S.; Yoshida, Z.; Tanaka, S.; Fugami, K.; Tamaru, Y. *Tetrahedron Lett.* **1990**, *31*, 4887−4890.

79    Ritter, S.; Horino, Y.; Lex, J.; Schmalz, H.-G. *Synlett* **2006**, 3309−3313.

80    Barange, D. K.; Nishad, T. C.; Swamy, N. K.; Bandameedi, V.; Kumar, D.; Sreekanth, B. R.; Vyas, K.; Pal, M. *J. Org. Chem.* **2007**, *72*, 8547−8550.

81    Susanti, D.; Koh, F.; Kusuma, J. A.; Kothandaraman, P.; Chan, P. W. H. *J. Org. Chem.* **2012**, *77*, 7166−7175.

82    Kothandaraman, P.; Rao, W.; Foo, S. J.; Chan, P. W. H. *Angew. Chem., Int. Ed.* **2010**, *49*, 4619−4623.

83    Mothe, S. R.; Kothandaraman, P.; Lauw, S. J. L.; Chin, S. M. W.; Chan, P. W. H. *Chem. − Eur. J.* **2012**, *18*, 6133−6137.

84    Huang, Q.; Hunter, J. A.; Larock, R. C. *J. Org. Chem.* **2002**, *67*, 3437−3444.

85    Asao, N.; Yudha, S.; Nogami, T.; Yamamoto, Y. *Angew. Chem., Int. Ed.* **2005**, *44*, 5526−5528.

86    Harrison, T. J.; Kozak, J. A.; Corbella-Pane, M.; Dake, G. R. *J. Org. Chem.* **2006**, *71*, 4525−4529.

87    Lee, Y. T.; Chung, Y. K. *J. Org. Chem.* **2008**, *73*, 4698−4701.

88    Chen, Z.; Yang, X.; Wu, J. *Chem. Commun.* **2009**, 3469−3471.

89    Lok, R.; Leone, R. E.; Williams, A. J. *J. Org. Chem.* **1996**, *61*, 3289−3297.

90    Zhang, X.; Zhou, Y.; Wang, H.; Guo, D.; Ye, D.; Xu, Y.; Jiang, H.; Liu, H.; *Green Chem.* **2011**, *13*, 397−405.

91    Seregin, I. V.; Schammel, A. W.; Gevorgyan, V. *Org. Lett.* **2007**, *9*, 3433−3436.

92    Chioua, M.; Soriano, E.; Infantes, L.; Jimeno, M. L.; Marco-Contelles, J.; Samadi, A. *Eur. J. Org. Chem.* **2013**, 35−39.

93    Prajapati, R. K.; Kumar, J.; Verma, S. *Chem. Commun.* **2010**, *46*, 3312−3314.

94   Ermolat'ev, D. S.; Bariwal, J. B.; Steenackers, H. P. L.; De Keersmaecker, S. C. J.; Van der Eycken, E. V. *Angew. Chem. Int. Ed.* **2010**, *49*, 9465 –9468.

95   Gainer, M. J.; Bennett, N. R.; Takahashi, Y.; Looper, R. E. *Angew. Chem. Int. Ed.* **2011**, *50*, 684 –687.

96   Clegg, W.; Collingwood, S. P.; Golding, B. T.; Hodgson, S. M. *J. Chem. Soc., Chem. Commun.* **1988**, 1175–1176.

97   Peshkov, V. A.; Pereshivko, O. P.; Sharma, S.; Meganathan, T.; Parmar, V. S.; Ermolat'ev, D. S.; Van der Eycken, E. V. *J. Org. Chem.* **2011**, *76*, 5867–5872.

98   Pereshivko, O. P.; Peshkov, V. A.; Peshkov, A. A.; Jacobs, J.; Van Meervelt, L.; Van der Eycken, E. V. *Org. Biomol. Chem.* **2014**, *12*, 1741−1750.

99   Pereshivko, O. P.; Peshkov, V. A.; Jacobs, J.; Van Meervelt, L.; Van der Eycken, E. V. *Adv. Synth. Catal.* **2013**, *355*, 781–789.

100  Niu, Y.-N.; Yan, Z.-Y; Gao, G.-L.; Wang, H.-L.; Shu, X.-Z.; Ji, K.-G.; Liang, Y.-M. *J. Org. Chem.* **2009**, *74*, 2893–2896.

101  Hayes, J.; Knight, D. W.; O'Halloran, M.; Pickering, S. R. *Synlett* **2008**, 2188−2190.

102  Arduengo III, A. G.; Dias, H. V. R.; Calabrese, J. C. Davidson, F. *Organometallics* **1993**, *12*, 3405−3409.

103  Wang, H. M. J.; Lin, I. J. B. *Organometallics* **1998**, *17*, 972−975.

104  Lin, I. J. B.; Vasam, C. S. *Coord. Chem. Rev.* **2007**, *251*, 642−670.

105    Díez-González, S.; Marion, N.; Nolan, S. P. *Chem. Rev.* **2009**, *109*, 3612−3676.

106    Marion, N. NHC-Copper, Silver and Gold Complexes in Catalysis. In *N-Heterocyclic Carbenes: From Laboratory Curiosities to Efficient Synthetic Tools*; Díez-González, S. Ed.; RSC Catalysis Series No. 6; Royal Society of Chemistry: Cambridge, 2011; pp 326−328.

107    Baker, R. T.; Nguyen, P.; Marder, T. B.; Westcott, S. A. *Angew. Chem., Int. Ed.* **1995**, *34*, 1336−1338.

108    Ramírez, J.; Corberán, R.; Sanaú, M.; Peris, E.; Fernández, E. *Chem. Commun.* **2005**, 3056−3058.

109    Corberán, R.; Ramírez, J.; Poyatos, M.; Peris, E.; Fernández, E. *Tetrahedron: Asymmetry* **2006**, *17*, 1759−1762.

110    Iglesias-Sigüenza, J.; Ros, A.; Díez, E.; Magriz, A.; Vázquez, A.; Álvarez, A.; Fernández, R.; Lassaletta, J. M. *Dalton Trans.* **2009**, 8485−8488.

111    Prieto, A.; Fructos, M. R.; Díaz-Requejo, M. M.; Pérez, P. J.; Pérez-Galán, P.; Delpont, N.; Echavarren, A. M. *Tetrahedron* **2009**, *65*, 1790−1793.

112    Biffis, A.; Lobbia, G. G.; Papini, G.; Pellei, M.; Santini, C.; Scattolin, E.; Tubaro, C. *J. Organomet. Chem.* **2008**, *693*, 3760−3766.

113    Li, P.; Wang, L. *Synlett* **2006**, 2261−2265.

114    Fujii, Y.; Terao, J.; Kambe, N. *Chem. Commun.* **2009**, 1115−1117.

115    Fu, X.-P.; Liu, L.; Wang, D.; Chen, Y.-J.; Li, C.-J. *Green Chem.* **2011**, *13*, 549−553.

116    Li, P.; Wang, L.; Zhang, Y.; Wang, M. *Tetrahedron Lett.* **2008**, *49*, 6650−6654.

117    He, Y.; Lv, M.-F.; Cai, C. *Dalton Trans.* **2012**, *41*, 12428−12433.

118    Li, Y.; Chen, X.; Song, Y.; Fang, L.; Zou, G. *Dalton Trans.* **2011**, 40, 2046−2052.

119    Chen, M.-T.; Landers, B.; Navarro, O. *Org. Biomol. Chem.* **2012**, *10*, 2206−2208.

120    Cheng, C.-H.; Chen, D.-F.; Song, H.-B.; Tang, L.-F. *J. Organomet. Chem.* **2013**, *726*, 1−8.

121    Li, Q.; Xie, Y.-F.; Sun, B.-C.; Yang, J.; Song, H.-B.; Tang, L.-F. *J. Organomet. Chem.* **2013**, *745-746*, 106−114.

122    Li, Q.; Li, X.; Yang, J.; Song, H.-B.; Tang, L.-F. *Polyhedron* **2013**, *59*, 29−37.

123    Tang, X.; Qi, C.; He, H.; Jiang, H.; Ren, Y.; Yuan, G. *Adv. Synth. Catal.* **2013**, 355, 2019−2028.

124    Yoshida, H.; Kageyuki, I.; Takaki, K. *Org. Lett.* **2014**, 16, 3512−3515.

125    Wile, B. M.; Stradiotto, M. *Chem. Commun.* **2006**, 4104−4106.

126    Wang, D.; Zhang, B.; He, C.; Wu, P.; Duan, C. *Chem. Commun.* **2010**, *46*, 4728−4730.

127    Arbour, J. L.; Rzepa, H. S.; Contreras-García, J.; Adrio, L. A.; Barreiro, E. M.; Hii, K. K. *Chem.−Eur. J.* **2012**, *18*, 11317−11324.

128    Overman, L. E.; Tsuboi, S.; Angle, S. *J. Org. Chem.* **1979**, *44*, 2323−2325.

129    Kang, J.-E.; Kim, H.-B.; Lee, J.-W.; Shin, S. *Org. Lett.* **2006**, *8*, 3537–3540.

130    Hashmi, A. S. K.; Rudolph, M.; Schymura, S.; Visus, J.; Frey, W. *Eur. J. Org. Chem.* **2006**, 4905–4909.

131    Brown, H. C.; McDaniel, D. H.; Häfliger, O. Dissociation Constants. In *Determination of Organic Structures by Physical Methods*; Braude, E.A., Nachod F.C., Eds.; Academic Press: New York, 1955; Vol. 1, pp 567−662.

132    Kolthoff, I. M., Elving, P. J., Eds. *Treatise on Analytical Chemistry*; Interscience Encyclopedia: New York, 1959.

133    Guthrie, J. P. *Can. J. Chem.* **1978**, *56*, 2342−2354.

134    Biffis, A.; Gazzola, L.; Gobbo, P.; Buscemi, G.; Tubaro, C.; Basato, M. *Eur. J. Org. Chem.* **2009**, 3189−3198.

135    Mori, S.; Ue, M.; Ida, K. (Mitsubishi Petrochemical Co., Ltd.). Electrolyte for Aluminum Electrolytic Capacitor. US Patent 4,774,011, September 27, 1988.

136    Kirk-Othmer. *Encyclopedia of Chemical Technology*, 4th ed.; Wiley: USA, 2001, Vol. 23.

137    Dewick, P. M. *Essentials of Organic Chemistry: For Students of Pharmacy, Medicinal Chemistry and Biological Chemistry*; John Wiley and Sons: England, 2006.

138    Schwarzenbach, G.; Meier, J. *J. Inorg. Nucl. Chem.* **1958**, *8*, 302−312.

139    Lettko, L.; Wood, J. S.; Rausch, M. D. *Inorg. Chim. Acta* **2000**, *308*, 37−44.

140   Di Nicola, C.; Effendy, Marchetti, F.; Nervi, C.; Pettinari, C.; Robinson, W. T.; Sobolev, A. N.; White, A. H. *Dalton Trans.* **2010**, *39*, 908−922.

141   Bowmaker, G. A; Effendy; Marfuah, S.; Skelton, B. W.; White A. H. *Inorg. Chim. Acta* **2005**, *358*, 4371−4388.

142   Cooney, R. P.; Howard, M. W.; Mahoney, M. R.; Mernagh, T. P. *Chem. Phys. Lett.* **1981**, *79*, 459−464.

143   Leschke, M.; Rheinwald, G.; Lang, H. *Z. Anorg. Allg. Chem.* **2002**, *628*, 2470−2477.

144   Inoguchi, Y.; Milewski-Mahrla, B.; Neugebauer, D.; Jones, P. G.; Schmidbaur H.*Chem. Ber.* **1983**, *116*, 1487−1493.

145   Skapski, A. C.; Sutcliffe, V. F.; Young, G. B. *J. Chem. Soc., Chem. Commun.* **1985**, 609−611.

146   McKay, M. J.; Nguyen, H. M. *ACS Catal.* **2012**, *2*, 1563−1595.

147   Chen, C. Y.; Zeng, J. Y.; Lee, H. M. *Inorg. Chim. Acta* **2007**, *360*, 21−30.

148   Lin, J. C. Y.; Tang, S. S.; Vasam, C. S.; You, W. C.; Ho, T. W.; Huang, C. H.; Sun, B. J.; Huang, C. Y.; Lee, C. S.; Hwang, W. S.; Chang, A. H. H.; Lin, I. J. B. *Inorg. Chem.* **2008**, *47*, 2543−2551.

149   Bondi, A. *J. Phys. Chem.* **1964**, *68*, 441−451.

150   See for example: (a) Suen, M. C.; Yeh, C. W.; Ho, Y. W.; Wang, J. C. *New J. Chem.* **2009**, *33*, 2419−2425. (b) Desmarets, C.; Azcarate, I.; Gontard, G.; Amouri, H. *Eur. J. Inorg. Chem.* **2011**, 4558−4563.

151   Nilsson, B. M.; Hacksell, U. *J. Heterocycl. Chem.* **1989**, *26*, 269−275.

152 (a) Arcadi, A.; Cacchi, S.; Cascia, L.; Fabrizi, G.; Marinelli, F. *Org. Lett.* **2001**, *3*, 2501−2504. (b) Bacchi, A.; Costa, M.; Gabriele, B.; Pelizzi, G.; Salerno, G. *J. Org. Chem.* **2002**, *67*, 4450−4457. (c) Merkul, E.; Müller, T. J. J. *Chem. Commun.* **2006**, 4817−4819. (d) Merkul, E.; Grotkopp, O.; Müller, T. J. J. *Synthesis* **2009**, 502−507. (e) Beccalli, E. M.; Borsini, E.; Broggini, G.; Palmisano, G.; Sottocor-nola, S. *J. Org. Chem.* **2008**, *73*, 4746−4749. (f) Yasuhara, S.; Sasa, M.; Kusakabe, T.; Takayama, H.; Kimura, M.; Mochida, T.; Kato, K. *Angew. Chem. Int. Ed.* **2011**, *50*, 3912−3915.

153 Hashmi, A. S. K.; Weyrauch, J. P.; Frey, W. Bats, J. W. *Org. Lett.* **2004**, *6*, 4391−4394.

154 Weyrauch, J. P.; Hashmi, A. S. K.; Schuster, A.; Hengst, T.; Schetter, S.; Littmann, A.; Rudolph, M.; Hamzic, M.; Visus, J.; Rominger, F.; Frey, W.; Bats, J. W. *Chem.−Eur. J.* **2010**, *16*, 956−963.

155 Hashmi, A. S. K.; Schuster, A. M.; Schmuck, M.; Rominger, F. *Eur. J. Org. Chem.* **2011**, 4595−4602.

156 Meng, X.; Kim, S. *Org. Biomol. Chem.* **2011**, *14*, 4429−4431.

157 Senadi, G. C.; Hu, W.-P.; Hsiao, J.-S.; Vandavasi, J. K.; Chen, C.-Y.; Wang, J. -J. *Org. Lett.* **2012**, *14*, 4478−4481.

158 Alhalib, A.; Moran, W. J. *Org. Biomol. Chem.*, **2014**, *12*, 795−800.

159 Nishibayashi, Y.; Milton, M. D.; Inada, Y.; Yoshikawa, M.; Wakiji, I.; Hidai, M.; Uemura, S. *Chem.−Eur. J.* **2005**, *11*, 1433−1451.

160 Zhan, Z.-P.; Yu, J.-L.; Liu, H.-J.; Cui, Y.-Y.; Yang, R.-F.; Yang, W.-Z.; Li, J.-P. *J. Org. Chem.* **2006**, *71*, 8298−8301.

161 Reddy, C. R.; Madhavi, P. P.; Reddy, A. S. *Tetrahedron Lett.* **2007**, **48**, 7169–7172.

162 Georgy, M.; Boucard, V.; Debleds, O.; Dal Zotto, C.; Campagne, J.-M. *Tetrahedron* **2009**, *65*, 1758–1766.

163 Pennell, M. N.; Turner, P. G.; Sheppard, T. D. *Chem.–Eur. J.* **2012**, *18*, 4748–4758.

164 Zhan, Z.-P.; Yang, W.-Z.; Yang, R.-F.; Yu, J.-L.; Li, J.-P.; Liu. H.-J. *Chem. Commun.* **2006**, 3352–3354.

165 Qin, H.; Yamagiwa, N.; Matsunaga, S.; Shibasaki, M. *Angew. Chem., Int. Ed.* **2007**, *46*, 409 –413.

166 Gohain, M.; Marais, C.; Bezuidenhoudt, B. C. B. *Tetrahedron Lett.* **2012**, *53*, 1048–1050.

167 Masuyama, Y.; Hayashi, M.; Suzuki, N. *Eur. J. Org. Chem.* **2013**, 2914–2921.

168 Gujarathi, S.; Hendrickson, H. P.; Zheng, G. *Tetrahedron Lett.* **2013**, *54*, 3550–3553.

169 Díez-González, S. *et al.* unpublished results.

170 Milton, M. D.; Inada, Y.; Nishibayashi, Y.; Uemura, S. *Chem. Commun.* **2004**, 2712– 2713.

171 Kumar, M. P.; Liu, R.-S. *J. Org. Chem.* **2006**, 71, 4951–4955.

172 Pan, Y.-M.; Zheng, F.-J. ; Lin, H.-X.; Zhan, Z.-P. *J. Org. Chem.* **2009**, *74*, 3148–3151.

173 Zhang, X.; Teo, W. T.; Chan, P. W. H. *J. Organomet. Chem.* **2011**, *696*, 331–337.

174    Haynes, W. M.; Lide, D. R.; Bruno, T. J. *CRC Handbook of Chemistry and Physics*, 93rd Ed.; CRC Press: USA, 2012.

175    Harmata, M.; Huang, C. *Synlett* **2014**, *25*, 1190.

176    Meyer, G.; Sehabi, M.; Pantenburg, I. Coordinative Flexibility of Monovalent Silver in $[Ag^I{\leftarrow}L_1]L_2$ Complexes. In *Design and Construction of Coordination Polymers*; Hong, M.-C., Chen, L., Eds.; John Wiley & Sons: Hoboken, 2009; pp 1−23.

177    Smith, G.; Cloutt, B. A.; Lynch, D. E.; Byriel, K. A.; Kennard, C. H. L. *Inorg. Chem.* **1998**, *37*, 3236−3242.

178    Cote, A. P.; Shimizu, G. K. H. *Inorg. Chem.* **2004**, *43*, 6663−6673.

179    Awaleh, M. O.; Badia, A.; Brisse, F. *Inorg. Chem.* **2007**, *46*, 3185−3191.

180    Omary, M. A.; Webb, T. R.; Assefa, Z.; Shankle, G. E.; Patterson, H. H. *Inorg. Chem.* **1998**, *37*, 1380−1386.

181    Brammer, L. *Chem. Soc. Rev.* **2004**, *33*, 476–489.

182    Robinand, A. Y.; Fromm, K. Y. *Coord. Chem. Rev.* **2006**, *250*, 2127–2157.

183    Brammer, L.; Burgard, M. D.; Rodger, C. S.; Swearingen, J. K.; Rath, N. P. *Chem. Commun.* **2001**, 2468–2469.

184    Brammer, L.; Burgard, M. D.; Eddleston, M. D.; Rodger, C. S.; Rath, N. P.; Adams, H. *CrystEngComm* **2002**, *4*, 239−248.

185    For example, see Yang, J. H.; Zheng, S. L.; Yu, X.-L.; Chen, X.-M. *Cryst. Growth Des.* **2004**, *4*, 831−836.

186    Kascatan-Nebioglu, A.; Panzner, M. J.; Tessier, C. A.; Cannon, C. L.; Youngs, W. J. *Coord. Chem. Rev.* **2007**, *251*, 884−895.

187    Teyssot, M. L.; Jarrousse, A.-S.; Manin, M.; Chevry, A.; Roche, S.; Norre, F.; Beaudoin, C.; Morel, L.; Boyer, D.; Mahioue, R.; Gautier, A. *Dalton Trans.* **2009**, 6894−6902.

188    Hindi, K. M.; Panzner, M. J.; Tessier, C. A.; Cannon, C. L.; Youngs, W. J. *Chem. Rev.* **2009**, *109*, 3859−3884.

189    Powell, A. B.; Bielawski, C. W.; Cowley, A. H. *J. Am. Chem. Soc.* **2010**, *132*, 10184−10194.

190    Partyka, D. V.; Deligonul, N. *Inorg. Chem.* **2009**, *48*, 9463−9475.

191    Partyka, D. V.; Robilotto, T. J.; Updegraff III, J. B.; Zeller, M.; Hunter, A. D.; Gray, T. G. *Organometallics* **2009**, *28*, 795−801.

192    Humenny, W. J.; Mitzinger, S.; Khadka, C. B.; Najafabadi, B. K.; Vieiraa, I.; Corrigan, J. F. *Dalton Trans.* **2012**, *41*, 4413−4422.

193    Chung, M. *Bull. Korean Chem. Soc.* **2002**, *23*, 1160−1162.

194    Kascatan-Nebioglu, A.; Melaiye, A.; Hindi, K.; Durmus, S.; Panzner, M. J.; Hogue, L. A.; Mallett, R. J.; Hovis, C. E.; Coughenour, M.; Crosby, S. D.; Milsted, A.; Ely, D. L.; Tessier, C. A.; Cannon, C. L.; Youngs, W. J. *J. Med. Chem.* **2006**, *49*, 6811−6818.

195    Medvetz, D. A.; Hindi, K. M.; Panzner, M. J.; Ditto, A. J.; Yun, Y. H.; Youngs, W. J. *Met.-Based Drugs* **2008**, 384010.

196    (a) Arnold, P. L. *Heteroat. Chem.* **2002**, *13*, 534−539. (b) Lin, I. J. B.; Vasam, C. S. *Comments Inorg. Chem.* **2004**, *25*, 75−129. (c) Garrison, J. C.; Youngs, W. J. *Chem. Rev.* **2005**, *105*, 3978−4008. (d) Lin, I. J. B.;

Vasam, C. S. *Coord. Chem. Rev.* **2007**, *251*, 642−670. (e) Lin, J. C. Y.; Huang, R. T. W.; Lee, C. S.; Bhattacharyya, A.; Hwang, W. S.; Lin, I . J. B. *Coord. Chem. Rev.* **2009**, *109*, 3561. (f) Díez-González, S.; Marion, N.; Nolan, S. P. *Chem. Rev.* **2009**, *109*, 3612−3676.

197    Chen, M.-T.; Landers, B.; Navarro, O. *Org. Biomol. Chem.* **2012**, *10*, 2206−2208.

198    Panzner, M. J.; Hindi, K. M.; Wright, B. D.; Taylor, J. B.; Han, D. S.; Youngs, W. J.; Cannon, C. L. *Dalton Trans.* **2009**, 7308−7313.

199    Panzner, M. J.; Deeraksa, A.; Smith, A.; Wright, B. D.; Hindi, K. M.; Kascatan-Nebioglu, A.; Torres, A. G.; Judy, B. M.; Hovis, C. E.; Hilliard, J. K.; Mallett, R. J.; Cope, E.; Estes, D. M.; Cannon, C. L.; Leid, J. G.; Youngs, W. J. *Eur. J. Inorg. Chem.* **2009**, 1739−1745.

200    Knapp, A. R.; Panzner, M. J.; Medvetz, D. A.; Wright, B. D.; Tessier, C. A.; Youngs, W. J. *Inorg. Chim. Acta* **2010**, *364*, 125−131.

201    Hu, J. J.; Bai, S.-Q.; Yeh, H. H.; Young, D. J.; Chi, Y.; Hor, T. S. A. *Dalton Trans.* **2011**, *40*, 4402−4406.

202    Patil, S.; Deally, A.; Gleeson, B.; Hackenberg, F.; Müller-Bunz, H.; Paradisi, F.; Tacke, M. *Metallomics* **2011**, *3*, 74−88.

203    Hindi, K. M.; Siciliano, T. J.; Durmus, S.; Panzner, M. J.; Medvetz, D. A.; Reddy, D. V.; Hogue, L. A.; Hovis, C. E.; Hilliard, J. K.; Mallet, R. J.; Tessier, C. A.; Cannon, C. L.; Youngs, W. J. *J. Med. Chem.* **2008**, *51*, 1577−1583.

204    Patil, S.; Dietrich, K.; Deally, A.; Gleeson, B.; Müller-Bunz, H.; Paradisi, F.; Tacke, M. *Appl. Organomet. Chem.* **2010**, *24*, 781−793.

205    Hackenberg, F.; Lally, G.; Müller-Bunz, H.; Paradisi, F.; Quaglia, D.; Streciwilk, W.; Tacke, M. *J. Organomet. Chem.* **2012**, *717*, 123−134.

206    Khramov, D. M.; Lynch, V. M.; Bielawski, C. W. *Organometallics* **2007**, *26*, 6042−6049.

207    Tornatzky, J.; Kannenberg, A.; Blechert, S. *Dalton Trans.* **2012**, *41*, 8215−8225.

208    Clavier, H.; Nolan, S. P. *Chem. Commun.* **2010**, *46*, 841−861.

209    Hillier, A. C.; Sommer, W. J.; Yong, B. S.; Petersen, J. L.; Cavallo, L.; Nolan, S. P. *Organometallics* **2003**, *22*, 4322−4326.

210    Poater, A.; Cosenza, B.; Correa, A.; Giudice, S.; Ragone, F.; Scarano, V.; Cavallo, L. *Eur. J. Inorg. Chem.* **2009**, 1759−1766.

211    Patil, S.; Dietrich, K.; Deally, A.; Gleeson, B.; Müller-Bunz, H.; Paradisi, F.; Tacke, M. *Helv. Chim. Acta* **2010**, *93*, 2347−2364.

212    Hocking, R. K.; Hambley, T. W. *Inorg. Chem.* **2003**, *42*, 2833−2835.

213    Hocking, R. K.; Hambley, T. W. *Dalton Trans.* **2005**, 969−978.

214    Patil, S.; Dietrich, K.; Deally, A.; Gleeson, B.; Hackenberg, F.; Müller-Bunz, H.; Paradisi, F.; Tacke, M. *Z. Anorg. Allg. Chem.* **2011**, *637*, 386−396.

215    Patil, S.; Claffey, J.; Deally, A.; Hogan, M.; Gleeson, B.; Méndez, L. M. M.; Müller-Bunz, H.; Paradisi, F.; Tacke, M. *Eur. J. Inorg. Chem.* **2010**, 1020−1031.

216    Penner, G. H.; Liu, X. *Prog. Nucl. Magn. Reson. Spectrosc.* **2006**, *49*, 151−167.

217    Wang, H. M. J.; Lin, I. J. B. *Organometallics* **1998**, *17*, 972−975.

218  Su, H.-L.; Pérez, L. M.; Lee, S.-J.; Reibenspies, J. H.; Bazzi, H. S.; Bergbreiter, D. E. *Organometallics* **2012**, *31*, 4063−4071.

219  Caytan, E.; Roland, S. *Organometallics* **2014**, *33*, 2115−2118.

220  Herrmann, W. A.; Runte, O.; Artus, G. *J. Organomet. Chem.* **1995**, 501, C1−C4.

221  de Fremont, P.; Singh, R.; Stevens, E. D.; Petersen, J. L.; Nolan, S.P. *Organometallics* **2007**, *26*, 1376−1385.

222  Ray, R; Shaikh, M. M.; Ghosh, P. *Inorg. Chem.* **2008**, 47, 230−240.

223  Kriechbaum, M.; Hölbling, J.; Stammler, H.-G.; List, M.; Berger, R. J. F.; Monkowius, U. *Organometallics* **2013**, *32*, 2876−2884.

224  Hu, X. L.; Tang, Y. J.; Gantzel, P.; Meyer, K. *Organometallics* **2003**, *22*, 612−614.

225  Hu, X. L.; Castro-Rodriguez, I.; Olsen, K.; Meyer, K.; *Organometallics* **2004**, *23*, 755−764.

226  Bourissou, D.; Guerret, O.; Gabbaï, F. P.; Bertrand, G. *Chem. Rev.* **2000**, *100*, 39−91.

227  Caytan, E.; Roland, S. *Organometallics* **2014**, *33*, 2115−2118.

228  de Frémont, P.; Scott, N. M.; Stevens, E. D.; Ramnial, T.; Lightbody, O. C.; Macdonald, C. L. B.; Clyburne, J. A. C.; Abernethy, C. D.; Nolan, S. P. *Organometallics* **2005**, *24*, 6301−6309.

229  Yu, X.-Y; Patrick, B. O.; James, B. R. *Organometallics* **2006**, *25*, 2359−2363.

230  Collado, A.; Gómez-Suárez, A.; Martin, A. R.; Slawin, A. M. Z.; Nolan, S. P. *Chem. Commun.* **2013**, *49*, 5541−5543.

231 Santoro, O.; Collado, A.; Slawin, A. M. Z.; Nolan, S. P.; Cazin, C. S. J. *Chem. Commun.* **2013**, *49*, 10483−10485.

232 Visbal, R.; Laguna, A.; Gimeno, M. C. *Chem. Commun.* **2013**, *49*, 5642−5644.

233 Penner, G. H.; Liu, X. *Prog. Nucl. Magn. Reson. Spectrosc.* **2006**, *49*, 151-167.

234 Herrmann, W. A.; Schneider, S. K.; Öfele, K.; Sakamoto, M.; Herdtweck, E. *J. Organomet. Chem.* **2004**, *689*, 2441−2449.

235 Nakamoto, K. *Infrared and Raman Spectra of Inorganic and Coordination Compounds*, 5th ed.; Wiley: New York, 1997, pp 59−62.

236 Deacon, G. B.; Phillips, R. J. *Coord. Chem. Rev.* **1980**, *33*, 227−250.

237 Gibson, D. H.; Ding, Y.; Miller, R. L.; Sleadd, B. A.; Mashuta, M. S.; Richardson, J. F. *Polyhedron* **1999**, *18*, 1189−1200.

238 Alcock, N. W.; Culver, J.; Roe, S. M. *J. Chem. Soc., Dalton Trans.* **1992**, 1477−1484.

239  Organ, M. G.; Çalimsiz, S.; Sayah, M.; Hoi, K. H.; Lough, A. J. *Angew. Chem., Int. Ed.* **2009**, *48*, 2383−2387.

240 Collado, A.; Balogh, J.; Meiries, S.; Slawin, A. M. Z.; Falivene, L.; Cavallo, L.; Nolan, S. P. *Organometallics* **2013**, *32*, 3249−3252.

241 Altenhoff, G.; Goddard, R.; Lehmann, C. W.; Glorius, F. *J. Am. Chem. Soc.* **2004**, *126*, 15195−15201.

242 Lavallo, V.; Canac, Y.; DeHope, A.; Donnadieu, B.; Bertrand, G. *Angew. Chem., Int. Ed.* **2005**, *44*, 7236−7239.

243    Würtz, S.; Lohre, C.; Fröhlich, R.; Bergander, K.; Glorius, F. *J. Am. Chem. Soc.* **2009**, *131*, 8344–8345

244    Berthon-Gelloz, G.; Siegler, M. A.; Spek, A. L.; Tinant, B.; Reek, J. N. H.; Marko, I. E. *Dalton Trans.* **2010**, *39*, 1444−1446.

245    Giner, X.; Nájera, C.; Kovács, J., Lledós, A.; Ujaque, G. *Adv. Synth. Catal.* **2011**, *353*, 3451−3466.

246    See for example: Bates, R. W.; Sa-Ei, K. *Tetrahedron* **2002**, *58*, 5957−5978.

247    Lait, S. M.; Rankic, D. A.; Keay, B. A. *Chem. Rev.* **2007**, *107*, 767−796.

248    Detz, R. J.; Delville, M. M. E.; Hiemstra, H.; van Maarseveen, J. H. *Angew. Chem., Int. Ed.* **2008**, *47*, 3777–3780.

249    Martin, D. B. C.; Nguyen, L. Q.; D. Vanderwal, C. *J. Org. Chem.* **2012**, *77*, 17–46.

250    Viola, A.; MacMillan, J. H. *J. Am. Chem. Soc.* **1968**, *90*, 6141–6145.

251    O'Rourke, N. F.; Davies, K. A.; Wulff, J. E. *J. Org. Chem.* **2012**, *77*, 8634–8647.

252    Hensarling, R. M.; Doughty, V. A.; Chan, J. W.; Patton, D. L. *J. Am. Chem. Soc.* **2009**, *131*, 14673–14675.

253    Jiang, Y.; Khong, V. Z. Y.; Lourdusamy, E.; Park, C.-M. *Chem. Commun.* **2012**, *48*, 3133–3135.

254    Zhao, Y.; Wang, G.; Li, Y.; Wang, S.; Li, Z. *Chin. J. Chem.* **2010**, *28*, 475–479.

255    Hediger, M. E. *Bioorg. Med. Chem.* **2004**, *12*, 4995–5010.

256    Marcoux, D.; Charette, A. B. *Angew. Chem. Int. Ed.* **2008**, *47*, 10155−10158.

257    Toke, L.; Hell, Z.; Szabo, G. T.; Toth, G.; Bihari, M.; Rockenbauer, A. *Tetrahedron* **1993**, *49*, 5133−5146.

258    Capozzi, G.; Caristi, C.; Gattuso, M.; D'Alcontres, G. S. *Tetrahedron Lett.* **1981**, *22*, 3325−3328.

259    Wipf, P.; Aoyama, Y.; Benedum, T. E. *Org. Lett.* **2004**, *6*, 3593–3595.

260    Wipf, P.; Hopkins, C. R. *J. Org. Chem.* **1999**, *64*, 6881−6887.

261    Welser, K.; Perera, M. D. A.; Aylott, J. W.; Chan, W. C. *Chem. Commun.* **2009**, 6601 − 6603.

262    Xu, Y.; Smith, M. D.; Geer, M. F.; Pellechia, P. J.; Brown, J. C.; Wibowo, A. C.; Shimizu, L. S. *J. Am. Chem. Soc.* **2010**, *132*, 5334–5335.

263    Yamabe, H.; Mizuno, A.; Kusama, H.; Iwasawa, N. *J. Am. Chem. Soc.* **2005**, *127,* 3248–3249.

264    Ali, S.; Ji, K.-G.; Liang, Y.-M.; Liu, X.-Y.; Wang, L.-J.; Yang, F.; Zhao, S.-C.; Zhu, H.-T. *Org. Lett.* **2011**, *13*, 684–687.

265    Pacholska-Dudziak, E.; Szterenberg, L.; Latos-Grażyński, L. *Chem.−Eur. J.* **2011**, *17*, 3500 − 3511.

266    Bantreil, X.; Nolan, S. P. *Nat. Protoc.* **2011**, *6*, 69−77.

267    Thomson, J. E.; Campbell , C. D.; Concellón , C.; Duguet, N.; Rix, K.; Slawin , A. M. Z.; Smith, A. D. *J. Org. Chem.* **2008**, *73*, 2784–2791.

268    Higgins, E. M.; Sherwood, J. A.; Lindsay, A. G.; Armstrong, J.; Massey, R. S.; Alder, R. W.; O'Donoghue, A. C. *Chem. Commun.* **2011**, *47*, 1559–1561.

269    Stromnova, T. A.; Paschenko, D. V.; Boganova, L. I.; Daineko, M. V.; Katser, S. B.; Churakov, A. V.; Kuz'mina, L. G.; Howard, J. A. K. *Inorg. Chim. Acta* **2003**, *350*, 283–288.

270    Paas, M.; Wibbeling, B.; Fröhlich, R.; Hahn, F. E. *Eur. J. Inorg. Chem.* **2006**, 158–162.

271    Aguilar, D.; Contel, M.; Navarro, R.; Soler, T.; Urriolabeitia, E. P. *J. Organomet. Chem.* **2009**, *694*, 486–493.